1 DEVELOPMENT AND BASIC TERMS OF PHOTOCHEMISTRY OF COORDINATION COMPOUNDS

For many years mankind knew of phenomena such as the fading of dyes, the necessity of sunlight for the growth of plants and the darkening of certain silver salts due to exposure to light, which were connected with the interaction of light and chemical substances. The ever increasing knowledge of the properties of light and matter has led to a gradual change from the qualitative recording of photochemical changes of substances to the study of the quantitative aspects of the interaction between radiation and matter.

The theory, frequently in close contact with practical needs, has dealt with both the questions of the proper interaction between light and matter and the chemical consequences of this interaction. The quantitative aspects of light absorption were solved in 1729 by Bouguer, who formulated the light absorption law which is now known as the Lambert–Beer law.

In 1817, Grotthüs realized that photochemical changes were not due to the passage of light through a system, its diffusion or reflection, but that they were due to light absorption. This fact is essential for the *first law of photochemistry* (the Grotthüs–Draper law), which states that only the light absorbed by the reacting system can be effective in producing a chemical change. This law expressed the qualitative aspects of photochemical changes.

Understanding of the quantitative aspects of light-induced chemical changes was conditioned by the knowledge of quantum physics. Starting from the fact that light is emitted in discrete quanta, called photons, with an energy proportional to the frequency of the light, and that absorption corresponds to the capture of a photon by the molecule (atom or ion), Einstein and Stark formulated the *second law of photochemistry*: each light quantum absorbed activates one molecule. It should be noted that there have been no demonstrations of the simultaneous excitation of two or more molecules by one photon; on the other hand, with the advent of high-intensity lasers, multiphoton excitations of one molecule have been detected.

It is worth keeping in mind that several decades have passed since the discovery of the first two fundamental laws of photochemistry, during which a substantial amount of new information has been obtained. The importance of these laws, however, has not decreased, their validity has not been disproved and "the third law of photochemistry" is still expected.

Chemistry has been dealing with the terms complex, coordination compound, central atom and ligand since the last century, particularly as a result of the systematic studies of Werner.

Along with the study of structure, composition and spontaneous (dark) reactions of coordination compounds, attention has also been focused on the effect of light on the properties and reactivity of these compounds.

The particular studies which not only recorded but, within the frame of the given theoretical and experimental possibilities, also purposefully investigated the effect of light on chemical transformations of complexes started to be published in scientific journals more regularly in the 1920s (photosubstitution and photoredox processes); papers on photoisomerization were published in the 1930s.

In the 1950s and 1960s, the approach of crystal field and later ligand field theory was applied to the interpretation of the electronic absorption spectra of coordination compounds, and experimental techniques were developed (equipment for continuous photolysis, monochromatization of radiation, development of UV and visible light sources, improvement of the quality of spectral methods and increase in their number) that stimulated the development of photochemistry in general, and that of coordination compounds particularly. Knowledge of the mechanisms of photochemical reactions has been expanding.

Naturally, the quantitative increase in knowledge and information resulted in the 1960s in attempts to classify photochemical reactions, and to formulate generalizations and laws or rules based on which it would be possible not only to elucidate but also predict the photochemical properties of coordination compounds.

The first review classifying the data from approximately 250 papers was published by Szychliński in Wiadomości Chemiczne [1] in 1962. At the end of the 1960s other papers [2–5] on similar topics were published, and in 1967 Adamson formulated [6] the first rules of photochemical reactivity applicable to the photosubstitution reactions of most Cr(III) complexes. Attempts to summarize and classify all data on the photochemistry of coordination compounds culminated in an excellent monograph by Balzani and Carassiti entitled *Photochemistry of Coordination Compounds* published in 1970 [7].

The 1970s and 1980s have been characterized by the development and application of new techniques (e.g., nano-, pico- and femtosecond flash photolysis and laser techniques), improvements in older research methods (e.g., application of Raman, infrared and electronic absorption spectroscopy to particles in their excited states; utilization of EPR spin trapping) and the orientation of photochemical research to the solution of important practical problems (synthesis of new compounds; photocatalysis; solar energy utilization).

The photochemistry of coordination compounds has exploited and stimulated the development of theoretical chemistry (particularly in the field of thermodynamics and kinetics) and an intensive transfer of information has taken place between the photochemistry of coordination compounds and other scientific disciplines (organic photochemistry, catalysis, biochemistry, electrochemistry, etc.).

As the rate of growth of information during the above period has excluded the possibility of processing all available data (except for the photochemistry of organometallics [9]), review papers have been devoted either to selected types of compounds, or to theoretical, practical and methodical phenomena of the photochemistry of complexes. A successful attempt to express the new directions in this field can be exemplified by the book *Concepts of Inorganic Photochemistry* by Adamson and Fleischauer [8]. Several books on photochemistry of complexes [7–13] can be included among essential monographs on topics such as molecular and electronic structures and the reactivity of coordination compounds [14–16]. These monographs [7–13] not only complete the existing system of knowledge but also develop and extend the views on coordination compounds by presenting details of new aspects such as the dimension of electronically excited states.

In this review, the terms generally accepted in photochemistry are used, being defined where necessary. With the development of the photochemistry and chemistry of coordination compounds its terminology has also been developing, and it can be assumed that the terms and their meanings will be extended and gradually made more precise as the available knowledge deepens. In spite of this, it seemed to be useful to give the meanings of at least the essential terms used in this review. *Photochemistry* is a branch of chemistry that deals with the study of causes and courses of chemical deactivation processes of particles from their electronically excited states, usually with the participation of UV, visible or near-infrared radiation. Chemical changes of particles that are the consequence of the electronic excitation of the set of these particles in the system due to external energy effects are called *photochemical reactions.* Photochemical reactions differ from spontaneous (dark) reactions, which denote chemical changes without previous electronic excitation induced by external effects. Here, it should be noted, that electronic and molecular structures of the particles from which the given chemical change takes place (thexi state for photochemical reactions and the transition state for spontaneous reactions) need not differ, only the way they are generated is different [8]. Sometimes, reactions resulting from vibrationally excited but electronically ground state are also called photochemical reactions in the literature.

Complex denotes a multiatom particle containing at least one central atom chemically bonded with a number of atoms of other elements that is larger than the absolute value of its oxidation number. A complex can be an electronically neutral molecule, ion or polymer fragment, the composition of which corresponds to the empirical formula. The substance consisting (at least partially) of the complex particles is a *coordination compound.*

The review is divided into six chapters. The contents of the chapters and their sections has been elaborated so as to correspond with the individual processes in the sequence of a photochemical reaction. In accordance with this, Chapter 2 deals with the modes of formation and with the properties of electronically excited complexes. Photophysical deactivations are discussed in Chapter 3. The "centre of gravity" of the work lies in Chapter 4, in which the specific types of photochemical reactions are classified and discussed, and the rules of the photochemical reactivity of complexes are presented. Chapter 5 summarizes practical applications of the knowledge in the field of the photochemistry of coordination compounds. Chapter 6 concludes the review with general remarks and prospects for the development of the photochemistry of coordination compounds.

Because of the limited extent of the review, thermal reactions and necessary information on the structure of coordination compounds are not presented separately (for details see, e.g., [13–16]) but they are adequately discussed in the various sections where required.

The photochemistry and photophysics of coordination compounds are characterized by an enormous growth of publications, and it was impossible to list them all. Therefore, in References mainly works of a review character and monographs are presented. The original papers are cited only in special cases (e.g., presentation of numerical data, data for the figures).

The current state of knowledge in the field of the photochemistry of coordination compounds documented in later chapters indicates that the research on different types of compounds and their properties and reactions is rather uneven and the state of knowledge is heterogeneous. The aim of this book is to emphasize the chemical aspects of photoprocesses and to point to the broad extent of knowledge being achieved in the photochemistry of coordination compounds. The objectives chosen might stimulate photochemists towards the transfer of knowledge between the individual fields of photochemical research and to focus their attention on "blank" areas. Emphasizing chemical rather than physical aspects of photoprocesses should point to the analogy between spontaneous (dark) and photochemical reactions, and thus to generally valid regularities in the chemical changes of complexes.

Chapters 2 and 3 and Sections 4.1, 4.2, 4.3, 4.5, 4.6 and 5.4 were produced by J. Šima and Sections 4.4, 4.7, 5.1, 5.2, 5.3 and 5.5 by J. Sýkora. Chapters 1 and 6 were written by both authors.

2 FORMATION AND PROPERTIES OF COORDINATION COMPOUNDS IN EXCITED STATES

2.1 Introduction

The essential problem in the photochemistry of coordination compounds is the study of relationships between the composition and electronic and molecular structures of complexes in excited states, and the course of their chemical and physical deactivation processes. From this point of view, a photochemist is interested especially in:

— the distribution of electron density in different electronically excited states of a complex;
— the molecular structure of complexes in excited states;
— the thermodynamic properties of complexes in excited states;
— the relationship between the above properties and deactivation processes, especially the photochemical reactivity of complexes in excited states.

With respect to the chronology of the processes, the first step is the formation of an electronically excited state of the complex. The individual modes of the transition of the complex from the ground state to the excited states (photoexcitation, energy transfer, chemical reactions, effects of mechanical energy) are covered in Section 2.2. The electronic structures of the complexes in excited states and their impact on the electronic absorption spectra are presented in Section 2.3. The data on molecular structure and spectral properties of complexes in excited states are presented in Section 2.4. The last Section, 2.5, deals with thermodynamic properties of the complexes in excited states.

2.2 Physical conditions of the formation of complexes in excited states

2.2.1 Photoexcitation

In the study of most photochemical processes, excitation takes place by interaction of radiation with the complex, i.e., by photoexcitation:

$$A + h\nu \rightarrow A^* \tag{2.1}$$

where A is a complex in the ground state (acceptor of photon energy $h\nu$) and A* a complex in an excited state (an asterisk will be used for labelling the excited state throughout this book).

The term photoexcitation designates the electric dipole transition. Other types of transitions (magnetic dipole or electric quadrupole transitions) are not of interest from the photochemistry viewpoint. Photoexcitation is a resonance process which can take place if:

— the difference between the energy of any of the excited states (the state described by the wavefunction Ψ_{ES}) and that of the ground state (the state described by the function Ψ_{GS}) is equal to the energy of a photon interacting with the complex, i.e.,

$$E_{\mathrm{ES}} - E_{\mathrm{GS}} = h\nu \tag{2.2}$$

— a specific interaction takes place between the electric vector of radiation and the electron system.

The rules determining the probability of the formation of excited states by photoexcitation are based on the following postulates:

— the total wavefunction can be factored into electronic, Ψ_{e}, vibrational, Ψ_{v}, and rotational, Ψ_{r}, components, which are mutually independent owing to the different rate of electronic transition (ca 10^{-15} s), vibrational (ca 10^{-12} s) and rotational motions (ca 10^{-8} s):

$$\Psi = \Psi_{\mathrm{e}}\Psi_{\mathrm{v}}\Psi_{\mathrm{r}} \tag{2.3}$$

— the electronic component, Ψ_{e}, of the total wavefunction can be expressed as follows:

$$\Psi_{\mathrm{e}} = \Psi_{\mathrm{o}}\Psi_{\mathrm{s}} \tag{2.4}$$

where Ψ_{o} and Ψ_{s} denote the orbital and spin parts, respectively, of Ψ_{e}, as Ψ_{o} is a function of the spatial coordinates, and Ψ_{s} is not;

— one-electron functions Ψ_{e} (molecular orbitals) are the same for the ground state and excited states of a molecule (frozen orbitals).

The probability of light absorption is expressed by means of the oscillator strength, f:

$$f = \frac{8\pi^2 m\nu g}{3he^2}\left(\int \Psi_{GS}\hat{R}\Psi_{ES}\,\mathrm{d}\tau\right)^2 \tag{2.5}$$

where h is Planck's constant, ν the frequency of radiation, g a number referring to the degeneracies of the states Ψ_{GS} and Ψ_{ES}, $\hat{R}$ the dipole moment operator and e and m are the charge and mass of an electron, respectively.

It results from a detailed analysis of eqn. 2.5 that the transition moment (integral in eqn. 2.5) has a zero value for certain transitions, and such transitions are forbidden. Conditions under which the transition moment reaches the zero value are expressed by selection rules:

- electric dipole transitions between states of equal parity are forbidden (orbitally forbidden transitions);
- transitions between states of different multiplicity are forbidden (spin-forbidden transitions);
- transitions involving the simultaneous excitation of two or more electrons are forbidden.

In general, a molecule is electronically excited with simultaneous excitation of an appropriate odd vibration, which is known as vibronic coupling. It results from group theory that if a transition is to be vibronically allowed, the product of Ψ_e for the ground and excited states involved and the component of the dipole moment operator $\hat{R}$ must be of the same representation as an odd vibration of the molecule. If this condition is not fulfilled, the transition is vibronically forbidden.

As the postulates considered for deriving the selection rules are not strictly valid in the electronic absorption spectra of coordination compounds, the bands of forbidden transitions can also be found. For the allowed transitions the oscillator strength is $f \approx 10^{-3} - 10^{-1}$; that for orbitally forbidden, spin-allowed transitions is $f \approx 10^{-4} - 10^{-3}$ and that for spin-forbidden transitions is $f \approx 10^{-8}$–10^{-4} [17].

In spectroscopy and photochemistry, the experimentally measurable spectral characteristics (absorbance, molar absorption coefficient, band width) are used more frequently than the theoretical value (oscillator strength). Between the oscillator strength f and experimental quantities, the following relationship is approximately valid:

$$f \approx 4.6 \times 10^{-9} \varepsilon_{\max} \Delta \nu_{1/2} \tag{2.6}$$

where $\Delta \nu_{1/2}$ is the half-width of the absorption band (frequency difference at which $\varepsilon = 0.5\varepsilon_{\max}$) and $\varepsilon_{\max}$ is the molar absorption coefficient (in l mol^{-1} cm^{-1}) in the absorption band maximum.

Let us consider as an example [18] the spectrum of the $[Co(NH_3)_6]^{3+}$ complex. To the orbitally and spin-forbidden transition $^1A_{1g} \rightarrow {}^3T_{1g}$ corresponds an f value of 4×10^{-6}, $\varepsilon_{770\,nm} = 0.23$ l mol^{-1} cm^{-1}; for orbitally forbidden, spin-allowed transitions $^1A_{1g} \rightarrow {}^1T_{1g}$ and $^1A_{1g} \rightarrow {}^1T_{2g}$, $f = 9 \times 10^{-4}$ and 8×10^{-4}, $\varepsilon_{472\,nm} = 56$ l mol^{-1} cm^{-1} and $\varepsilon_{339\,nm} = 46$ l mol^{-1} cm^{-1}, respectively. For orbitally and spin-allowed LMCT transitions, $f = 0.8$ and $\varepsilon_{200\,nm} = 20\,000$ l mol^{-1} cm^{-1}.

The relationship between the molar absorption coefficient, ε_λ, absorbance, A_λ, intensity of incident light, $I_{0.\lambda}$ and intensity of light absorbed, $I_{a.\lambda}$ at a given wavelength is expressed by the equation

$$A_\lambda = \varepsilon_\lambda c d = \log\left(\frac{I_{0.\lambda}}{I_{0.\lambda} - I_{a.\lambda}}\right) \tag{2.7}$$

where c is the molar concentration of a solute (a complex in our case) and d the path length (cm). In most photochemical experiments, the electronic absorption spectra of coordination compounds were measured in their solutions (and also in frozen solutions).

If more species absorbing radiation of a given wavelength are present in a system, the amount of radiation absorbed by one of them (jth species), $I_{a,j}$, bears the following relationship to the total amount of absorbed radiation, $I_{a.\lambda}$:

$$I_{a,j} = I_{a.\lambda}\,\frac{\varepsilon_{j.\lambda} c_j}{\sum_i \varepsilon_{i.\lambda} c_i} \tag{2.8}$$

where c_i are the molar concentrations of the individual components of the system and $\varepsilon_{i.\lambda}$ are molar absorption coefficients of these species at the wavelength λ. Equations 2.7 and 2.8 are used especially for the study of the course of photochemical reactions of kinetically labile complexes.

The spectral line shape depends on the Franck–Condon factors $\Psi_{v(\mathrm{GS})}\,\Psi_{v'(\mathrm{ES})}$, where v and v' are vibrational quantum numbers. As v and v' refer to different electronic states, the changes in the vibrational quantum number on electronic transitions are not limited by the selection rules. In general, the greater the difference between the force constants of bonds in the ground and excited states of a complex, the more distinct the difference between equilibrium internuclear distances in both states and the higher the value of $\Delta\nu_{1/2}$ of the band of the corresponding transition in the spectrum. For examples, see Section 2.3.

2.2.2 Formation of complexes excited by energy transfer

The thermodynamic condition of energy transfer between a donor in the excited state D* and an acceptor in the ground state A,

$$\mathrm{D}^* + \mathrm{A} \rightarrow \mathrm{D} + \mathrm{A}^* \tag{2.9}$$

is expressed by

$$(E_{\mathrm{ES}} - E_{\mathrm{GS}})_{\mathrm{D}} \geqslant (E_{\mathrm{ES}} - E_{\mathrm{GS}})_{\mathrm{A}} \tag{2.10}$$

Energy transfer is the simultaneous deactivation of the originally excited molecule D* to its ground state and the promotion of the acceptor molecule A to an electronically excited state.

Energy transfer may occur via a radiative or a non-radiative mechanism [19]. Radiative energy transfer can be described as the emission of a photon by D* which is followed by absorption of the emitted photon by A. This mode of formation of excited complexes is very uncommon in the photochemistry of coordination compounds.

Non-radiative energy transfer may occur by a long-range resonance mechanism or by an exchange mechanism. In the former instance the interaction takes place via the electromagnetic field and physical contact between the interacting partners D* and A is not required. The resonance dipole–dipole interaction may take place if $\Psi_{GS} \rightleftharpoons \Psi_{ES}$ transitions of the donor and acceptor are allowed, and if the acceptor absorption spectrum and donor emission spectrum overlap. This scarce mode of energy transfer in photochemistry is not limited by the spin selection rules (spin correlation, suggested by Wigner) [9]. The resonance mechanism cannot be excluded, at least when the medium is a rigid glass and the donor and acceptor are on average ca 5000 pm or more apart.

The exchange mechanism of energy transfer requires a collision between the partners D* and A as orbital overlap is needed. The efficient energy transfer and excited A* formation are conditioned by the validity of the Wigner rule of spin conservation, which means that at least one of the spin states formed by the interaction of D* and A in the pair D*/A must be identical with some of the spin states of the pair D/A*. From this point of view, for example, the triplet excited state of the organic donor {and also of a complex, e.g., triplet MLCT state of Ru(II) complexes [20]} can be quenched by the Cr(III) complex, which results in the production of both quartet excited and doublet excited LF states of the Cr(III) complex. For the pair $^3D^*/^4A$ the states 5/2, 3/2 and 1/2 exist, for the pair $^1D/^4A^*$ the states 3/2 and 1/2 exist and for the pair $^1D/^2A^*$ the state 1/2 exists. For some Cr(III) complexes as acceptors, it has been observed experimentally [21] that, depending on the triplet energy of the organic donor, either a quartet or a doublet excited LF state was produced by energy transfer.

Provided that D and A are complexes, not every encounter results in energy transfer [22] and the rate constant of energy transfer does not reach the limiting diffusion-controlled rate constant value, which is approximately 5×10^9 l mol^{-1} s^{-1} for water at room temperature, whereas for glycerine, for example, it is about 5×10^6 l mol^{-1} s^{-1}. For example [21], the rate constant of energy transfer between $[Cr(NN)_3]^{3+}$(NN = 2,2′-bipyridine or 1,10-phenanthroline) in the doublet excited state and $[M(H_2O)_6]^{n+}$ ions [M = Cr(III), Fe(III), Co(II), Mn(II), Ni(II) and Cu(II)] in the ground state varies within the range from 4×10^3 to 3.7×10^6 l mol^{-1} s^{-1} in aqueous media.

2.2.3 Formation of excited complexes as products of a chemical reaction

A complex in the excited state can be a product of chemical (electrochemical) reaction provided that

$$|-\Delta G_r| \geqslant |(E_{ES} - E_{GS})| \tag{2.11}$$

where ΔG_r is the change in the Gibbs reaction energy. If the products and reactants of the reaction are complexes, the selection rules have in fact negligible influence on the course of the reaction. If at least one of the reactants is a complex, the chemical reaction through which the complex excited state is produced is a redox reaction

$$B^- + A^+ \rightarrow A^* + B \tag{2.12}$$

or

$$B^+ + A^- \rightarrow A^* + B \tag{2.13}$$

Experimentally, the formation of A* is followed by measuring the emission spectra of A*, and the processes are called chemiluminescent reactions. As an example [23], the reaction of the $[Cr(phen)_3]^{2+}$ complex with $S_2O_8^{2-}$ anions, for which $\Delta G_r = -3.65$ eV, can be considered. As the energy of the doublet excited LF state of the $[Cr(phen)_3]^{3+}$ complex is 1.70 eV, the reaction product may be an excited complex, which has been confirmed by investigation of its phosphorescence. For the reaction

$$[Cr(phen)_3]^{2+} + [Ru(bpy)_3]^{3+} \rightarrow [Cr(phen)_3]^{3+} + [Ru(bpy)_3]^{2+} \tag{2.14}$$

$\Delta G_r = -1.51$ eV. The Gibbs reaction energy change is sufficient for the production of both $^*[Ru(bpy)_3]^{2+}$ in the triplet excited MLCT state (with an emission maximum at 607 nm) and $^*[Cr(phen)_3]^{3+}$ in the doublet LF state (with an emission maximum at 727 nm). It resulted from emission spectra measurements that in reaction 2.14 both complexes are produced in the excited states quoted above.

Study [24] of the chemiluminescent reactions of Ru(III) and Co(I) complexes has shown that the yield of the MLCT excited state of poly(pyridine)ruthenium(II) complexes increases with the exergonicity of the reaction. For example, for the reaction of $[Ru(bpy)_3]^{3+}$ with $[Co(4,4\text{-}Me_2bpy)_3]^+$ the yield is 31 ± 4% ($\Delta G_r = -0.29$ eV); for the least exergonic system studied (the reaction of $[Ru(4,7\text{-}Me_2phen)_3]^{3+}$ with $[Co(bpy)_3]^+$, where $\Delta G_r \approx 0$ eV, the yield of the excited ruthenium(II) complex is 7 ± 2%.

2.2.4 *Formation of excited complexes caused by application of mechanical energy*

The application of mechanical energy to a solid can cause emission of light, a phenomenon known as triboluminescence. The fact that a triboluminescent spectrum is frequently almost identical with the photoluminescent spectrum has led to the conclusion that triboluminescence takes place from electronically excited state; in other words, the excited states of substances (and also of complexes) may also be formed as a result of mechanical energy applied to solid substances (coordination compounds).

It has been suggested [25] that triboluminescence should take place at the surface of newly created fracture surfaces by electron-impact excitation or electron-hole pair recombination. The detailed mechanism of electronic excitation is not yet clearly understood.

A comparison of triboluminescent and photoluminescent spectra of Mn(II) and UO_2^{2+} compounds has shown [26] that in the former instance Mn(II) complexes were formed in a forbidden quartet LF state owing to the effects of mechanical energy, and in the latter instance UO_2^{2+} complexes were formed in the triplet $^3\pi_u$ state.

The study of the photochemical properties of complexes in excited states achieved by the application of mechanical energy has not yet been carried out. Research in this field is focused rather on the elucidation of mechanisms for the formation of excited complexes by the application of mechanical energy than on the chemically possible deactivation processes.

2.3 Electronic structure of complexes in excited states

2.3.1 *Electron density transfer during excitation*

In Section 2.1, conditions for the achievement of excited states of complexes were presented without a description of the properties of these states. As the differences in chemical reactivity of complexes in the ground and excited states are connected especially with different distributions of electron density, we prefer to characterize the processes of excitation $A \rightarrow A^*$ according to localization of the electron density transfer in the complexes. Such transfers can take place within a complex, or exchange of an electron may occur between the complex and its environment. Here, it should be emphasized that even when talking about the electron transfer between molecular orbitals to achieve the spectroscopic excited state (i.e., a state in which the population of vibration levels is determined by quantum-chemical Franck–Condon factors), the whole electron system of the complex is always changed (interelectronic repulsion is changed, in addition to degenerations of levels, energy of orbitals, etc.).

The extent of electron transfer in the case of spectral transition is not the same in all instances and it is not necessarily equal to unity. Its calculation based on the experimental study of the complexes in their ground and excited states has been considered only rarely. For example [27], from the frequencies in the time-resolved resonance Raman spectra of Os(I), Ru(II) and Re(I) complexes with 2,2-bipyridine in their ground and MLCT excited states, it has been calculated that the extent of electron transfer, x, within the transition

$$[\mathrm{M}^{n}(\mathrm{bpy})^{0}]_{\mathrm{GS}} \xrightarrow{h\nu} [\mathrm{M}^{n+x}(\mathrm{bpy})^{x-}]^{*}_{\mathrm{MLCT}} \tag{2.15}$$

is in the range $x = 0.74-0.91$.

Much valuable information on changes in the electronic structure during excitation was obtained by the study of single-crystal spectra with application of polarized radiation, by the study of circular dichroism and magnetic circular dichroism and by other spectral techniques. In the following sections, attention is focused particularly on such knowledge, which is of great importance in the photochemistry of coordination compounds.

Despite the fact that the absorption spectra of complexes reflect the complexity of their electronic structure, from the photochemical point of view it is convenient to classify the electronic transitions according to the localization of the molecular orbitals involved. Specifically, four fundamental types of electronic transitions may be identified:

(a) Transitions between MOs predominantly localized on the central atom (polymetal moiety in cases of polynuclear complexes containing at least one metal–metal bond). Such transitions can be divided into LF transitions (electron density transfer between *d*-orbitals or *f*-orbitals of the same principal quantum number), Rydberg transitions (transfer between orbitals differing in principal quantum number) and IVCT transitions (transfer from one to the other central atom in polynuclear bridged complexes).

(b) Transitions between MOs localized predominantly on ligands. These are usually called IL transitions (electron density transfer between MOs localized on one ligand) or LLCT transitions (electron transfer from one ligand's HOMO to the other ligand's LUMO).

(c) Transitions between MOs of different localization. Depending on the direction of electron density transfer, there are MLCT transitions (displacement of negative charge from the central atom to the ligands) and LMCT transitions (opposite flow of negative charge).

(d) Transfer of an electron between the complex and an environmental particle. These transitions can be divided into CTTS (an electron is ejected from the complex to an unspecified molecule in its environment) and IPCT (exchange of an electron between the complex and usually ionic component of its secondary coordination sphere).

These types of transitions will be discussed in more detail in the following sections.

2.3.2 *Transfer of electron density between orbitals localized predominantly on the central atom*

Depending on the character of molecular orbitals taking part in transitions of the above type, they are conventionally classified into ligand field (LF) transitions (*d–d* and *f–f* LF transitions in the complexes of transition and inner transition elements, respectively) and Rydberg transitions connected with a change in the principal quantum number of the orbitals involved [for instance, $(n-2)f \rightarrow (n-1)d$ transitions in the complexes of lanthanoids and actinoids].

LF transitions are orbitally forbidden and can also be spin-forbidden. The bands of such transitions are usually present in the visible and near-IR regions of the spectrum. Their position, intensity and shape are very sensitive (for *d–d* transitions) to the character of the coordinated ligands and the symmetry of the chromophore (Table 1). The bands with values of $\varepsilon_{\max} \approx 10^1$–$10^2$ l mol^{-1} cm^{-1} correspond to the spin-allowed *d–d* transitions, and the bands with $\varepsilon_{\max} \approx 10^{-3}$–$10^0$ l mol^{-1} cm^{-1} correspond to the spin-forbidden transitions. For example [28], in the spectrum of the $[Mn(H_2O)_6]^{2+}$ complex, eight bands of spin-forbidden transitions from the sextet ground state $^6A_{1g}$ into the quartet excited states are present. The bands are in the range 530–245 nm and the $\varepsilon_{\max}$ values range from 0.0145 to 0.0783 l mol^{-1} cm^{-1}.

TABLE 1

LF transitions in electronic absorption spectra of chromium(III) complexes [36]

Complex	^4E_g	$^4B_{2g}$	$^4A_{2g}$		^4E_g
		$\lambda_{\max}$ (nm)	($\varepsilon_{\max}$) (l mol^{-1} cm^{-1})		
trans-$[Cr(en)_2F_2]^+$	525(19.0)	466(24.0)	350(18.0)		430(16.1)
trans-$[Cr(en)_2Cl_2]^+$	578(24.5)	453(22.9)	396(33.9)		367(22.9)
trans-$[Cr(en)_2Br_2]^+$	607(33.7)	460(24.0)		418(30.9)	
	^4E		$^4A_2(+^4E)$		
cis-$[Cr(en)_2F_2]^+$	516(75.0)		375(37.9)		
cis-$[Cr(en)_2Cl_2]^+$	528(70.6)		402(68.5)		
cis-$[Cr(en)_2Br_2]^+$	544(89.4)		415(83.0)		

Spectral bands of *f–f* transitions have been measured for several compounds of lanthanoids and actinoids [18, 29]. These bands have a small half-width and values of $\varepsilon_{\max} \approx 10^{-1}$–$10^1$ l mol^{-1} cm^{-1}; for example [30], the bands of the *f–f* transitions for the $[Pr(H_2O)_9]^{3+}$ cation have $\varepsilon_{597\,\mathrm{nm}} = 1.9$, $\varepsilon_{483\,\mathrm{nm}} = 4.0$, $\varepsilon_{469\,\mathrm{nm}} = 4.6$ and $\varepsilon_{446\,\mathrm{nm}} = 10.5$ l mol^{-1} cm^{-1}. The bands of the *f–f* transitions are less sensitive to the environment of the central atom as the *f*-orbitals are shielded from the environment. Albin and Horocks [31] presented the results of a study of the spectra of 36 Eu(III) compounds in which the maximum of the band of the $^7F_0 \rightarrow {}^5D_0$ transition ranged from 581 to 579 nm and the half-width of the band did not exceed $10\,\mathrm{cm}^{-1}$.

The Rydberg transition bands are present in the visible and UV regions of the spectrum, with $\varepsilon_{\mathrm{max}} \approx 10^1$–$10^2\,\mathrm{l\,mol^{-1}\,cm^{-1}}$. For the ion $[\mathrm{Pr(H_2O)_9}]^{3+}$ the band with $\varepsilon_{215\,\mathrm{nm}} = 50\ \mathrm{l\,mol^{-1}\,cm^{-1}}$ has been assigned to the $4f \rightarrow 5d$ transition. The bands of Rydberg transitions depend on the structure and symmetry of the coordination sphere of complexes, and on interaction of the complex with its environment. For example [32], the band of the $5d_{z^2} \rightarrow 6p_z$ transition in $[\mathrm{PtCl_4}]^{2-}$ and $[\mathrm{Pt(NH_3)_4}]^{2+}$ can be found in "isolated" complexes at 215 and 196 nm, but at 280 nm for $[\mathrm{Pt(NH_3)_4}][\mathrm{PtCl_4}]$. If the interaction between the platinum atoms is stronger (even if the formation of Pt–Pt bonds is not considered), the band of the $5d_{z^2} \rightarrow 6p_z$ transition occurs in the visible part of the spectrum, for example, for $[\mathrm{Pt(bpy)_2}][\mathrm{Pt(CN)_4}] \cdot 2\mathrm{H_2O}$ at 485 nm.

The electron density distribution between the central atom and ligands in the excited LF and Rydberg states is similar to those of the ground state of the complex. Excitation is not accompanied by a more significant change in the radial distribution of the negative charge and hence the redox properties of complexes in the ground state and the above-presented excited states do not differ very much. Owing to the changes in the force constants of the central atom–ligand bonds in LF transitions (the changes are not the same for all bonds, as they depend on the ligand properties), the tendency of the excited complexes to undergo substitution reactions is greater than for complexes in the ground state. The relationships between the changes in the force constants of particular bonds between the central atom and ligands and the course of photosubstitution reactions have been intensively studied and resulted in the formulation of several "rules of photochemical reactivity of complexes" (for details, see Section 4.4.4).

The group of transitions localized on the central atom can also involve the transitions between MOs formed by combination of d-orbitals of central atoms

TABLE 2
Metal–metal moiety localized transitions in electronic absorption spectra of $[\mathrm{Tc_2Cl_8}]^{3-}$ [35]

Complex	Transition	λ_{max} (nm)	$\varepsilon_{\mathrm{max}}$ ($\mathrm{l\,mol^{-1}cm^{-1}}$)
$[\mathrm{Tc_2Cl_8}]^{3-}$	$\delta \rightarrow \delta^*$	1695	630
	$\pi \rightarrow \delta^*$	735	35
	$\delta^* \rightarrow \pi^*$	637	172
	$\delta^* \rightarrow \sigma^*$	500	10
	$\delta^* \rightarrow \pi^*$		
	$\delta^* \rightarrow d_{x^2-y^2}$		
	$\delta \rightarrow d_{x^2-y^2}$		
	$\pi \rightarrow \pi^*$	318	3900
	$\pi \rightarrow a_{x^2-y^2}$		

in bi- and polynuclear complexes with metal–metal bonds [17, 33]. The transitions may be orbitally allowed, which is evident from the values of $\varepsilon_{\max}$, which are ca 10^2–10^4 l mol^{-1} cm^{-1}. The bands of such transitions are found especially in the visible and UV regions of the spectrum, and are sensitive to the properties of the environment of central atoms. For example [34], the spin-allowed singlet–singlet $d\sigma \rightarrow d\sigma^*$ transition occurs in the spectra of $[Pt_2(P_2O_5H_2)_4X_2]^{4-}$ as a band with $\varepsilon_{282\,nm} = 4840$ l mol^{-1} cm^{-1} for X = Cl, $\varepsilon_{305\,nm} = 55\,420$ l mol^{-1} cm^{-1} for X = Br and $\varepsilon_{338\,nm} = 42\,930$ l mol^{-1} cm^{-1} for X = I.

By measuring the polarized electronic absorption spectra of single-crystal compounds at low temperature and by theoretical analysis of the spectra, the bands have been assigned to several transitions involving MOs formed by interaction of *d*-orbitals in binuclear complexes. For example [35], Table 2 presents an interpretation of the spectrum of the $[Tc_2Cl_8]^{3-}$ ion for which the derived MOs are $a_{1g}(\sigma)^2$, $e_u(\pi)^4$, $b_{2g}(\delta)^2$, $b_{1u}(\delta^*)^1$, $e_g(\pi^*)^0$, $b_{1g}(d_{x^2-y^2})^0$ and $a_{2u}(\sigma^*)^0$ in the ground state.

2.3.3 *Electron density transfer between orbitals localized predominantly on ligands*

Transitions of this type, when localized on one ligand, are called intraligand or internal ligand transitions, and are designated IL transitions.

IL transitions are found with complexes that contain organic ligands with a multiple bond (bonds), such as pyridine, 2,2-bipyridine, 1,10-phenanthroline, phthalocyanine and porphyrin. The IL transitions are usually orbitally and spin-allowed, and they occur in the spectra as intense bands in the visible and UV regions with values of $\varepsilon_{\max} \approx 10^3$–$10^5$ l mol^{-1} cm^{-1}. In contrast to the bands of MLCT and LMCT transitions (Section 2.3.4), with which they frequently

TABLE 3
IL and LLCT transitions in electronic absorption spectra of coordination compounds

Compound	$\lambda_{\max}$ (nm)	$\varepsilon_{\max}$ (l mol^{-1} cm^{-1})
	IL transitions [37]	
Pc	698	162200
MgPc	675	87100
ZnPc	672	281800
CrPc	689	83200
CuPc	678	218800
PtPc	650	72400
AlPcCl	680	125900
	LLCT transitions [38]	
[Zn(phen)(tdt)]	475	80
[Zn(bpy)(tdt)]	465	65
[Zn(biqu)(tdt)]	590	40

overlap in the spectra, the bands of IL transitions depend only slightly on the character of the central atom and on the presence of other ligands in the coordination sphere. This is supported [37] by data on the most intense IL transitions in phthalocyanine (Pc) and its complexes, listed in Table 3.

The electron density distribution between the central atom and ligands remains in fact unchanged in IL transitions. Complexes in the IL states frequently undergo analogous chemical changes to the ligand itself in the particular excited state.

In closed-shell compounds containing both a good π-acceptor ligand (such as 1,10-phenanthroline or 2,2-bipyridine) and a good π-donor ligand (such as an aromatic thiol), a new kind of transition was observed which was named interligand transmetallic charge transfer [38] or ligand-to-ligand charge transfer [39, 40] (LLCT). Electron density transfer from HOMO localized on a certain ligand (thiol) into LUMO localized on another ligand (*N*-donor heterocycle) mediated by the central atom is manifested in the spectra by a broad band in the visible region. LLCT transitions are orbitally allowed and may also be spin-allowed, in the band maxima with $\varepsilon_{max} \approx 10^1$–$10^3$ l mol^{-1} cm^{-1}. The LLCT transition bands are markedly influenced by the properties of the environment in which the complex is present. For example [39], the LLCT band in the spectrum of the [Pt(bpy)(tdt)] complex in ethanol has $\varepsilon_{610\,nm} = 4100$ l mol^{-1} cm^{-1} and in chloroform $\varepsilon_{558\,nm} = 3900$ l mol^{-1} cm^{-1}. The spectral characteristics of LLCT transitions in some Zn(II) complexes are presented in Table 3.

As a significant redistribution of the negative charge takes place in the LLCT transition, a photochemical consequence of such a transition may be a redox process.

2.3.4 *Electron density transfer between molecular orbitals localized predominantly on the central atom and ligands*

Depending on the direction of electron density transfer, we can recognize LMCT (ligand-to-metal charge transfer) and MLCT (metal-to-ligand charge transfer) transitions, i.e., electron transfer from an MO localized on a ligand into an MO localized on the central atom, and vice versa [17, 18]. In such transitions radial redistribution of the charge takes place. The transitions are usually orbitally and spin-allowed, and they are represented by intense bands in the visible and UV regions with values of $\varepsilon_{max} \approx 10^3$–$10^5$ l mol^{-1} cm^{-1}. The energy of LMCT transitions increases with increasing oxidation state of the central atom and with ionization energy of the ligand involved. For the given central atom M and ligand L, the energy of LMCT transition is not remarkably influenced by the other ligands in the coordination sphere, chromophore symmetry and environment of the complex. For example [17, 41], the energetically lowest band of the transition $Cl^- \rightarrow Cu(II)$ in chlorocopper(II) complexes can be found in the spectra from 370 to 525 nm (Table 4).

An increase in the electron density on the central atom in an LMCT transition (and thus in fact reduction of the central atom and an equivalent decrease in the electron density on the ligands) markedly influence the capability of the complex to undergo inner-sphere redox processes. The population of the antibonding orbitals localized on the central atom in the complex lowers the strength of central atom–ligand bonds and complexes in an LMCT state are deactivated by substitution processes, too. For example [41, 42], it has been found that during irradiation of chlorocopper(II) complexes in non-aqueous media, both photoreduction of Cu(II) to Cu(I) and photosubstitution reactions take place simultaneously.

TABLE 4
Energetically lowest LMCT transition in some copper(II), iron(III) and iron(II) halogeno complexes [17]

Complex	Chromophore	λ_{max} (LMCT) (nm)
$[Cu(Me_4en)Cl_2]_2$	square-pyramidal CuN_2Cl_3	392
$CuCl_2$ (gaseous)	linear $CuCl_2$	526
$Cs_2[CuCl_4]$	tetrahedral $CuCl_4$	435
$(MeNH_3)_2[CuCl_4]$	square-planar $CuCl_4$	417
$[Co(NH_3)_6][CuCl_5]$	trigonal-bipyramidal $CuCl_5$	370
$Cs_2NaY(Fe)Cl_6$	octahedral $FeCl_6$	446
$(NH_4)_2In(Fe)Cl_5(H_2O)$	octahedral $FeOCl_5$	434
$(Et_4N)[FeCl_4]$	tetrahedral $FeCl_4$	364
$(Et_4N)[FeBr_4]$	tetrahedral $FeBr_4$	472
$(Et_4N)[FeI_4]$	tetrahedral FeI_4	699
$(Et_4N)_2[FeCl_4]$	tetrahedral $FeCl_4$	220
$(Et_4N)_2[FeBr_4]$	tetrahedral $FeBr_4$	256

MLCT transitions are expected when the ligand possesses low-lying empty orbitals (usually π^* LUMO) and the central atom is easily oxidizable. MLCT transitions lie at lower energies than IL $\pi \rightarrow \pi^*$ transitions of the ligand itself. The energy of an MLCT transition (and also the value of the molar absorption coefficient) depends on the properties of the solvent (or, in general, the environment), especially on its polarity (Table 5). MLCT transitions decrease in energy as the ligand becomes more reducible, and/or the central atom becomes more easily oxidizable, and the bands of these transitions are usually found in visible spectra with $\varepsilon_{max} \approx 10^2$–$10^4$ l mol^{-1} cm^{-1}.

A study [27] of excited complexes of some central atoms with two or three molecules of 2,2′-bipyridine (or 1,10-phenanthroline) by time-resolved resonance Raman spectroscopy confirmed that the transferred electron density is localized in the lowest π^* orbital of one ligand rather than delocalized over the π^* orbitals of the all available ligands on the vibrational time scale.

TABLE 5

Solvent dependence of MLCT transition in $[Ru^{II}(NH_3)_5(Me\text{-}4,4'\text{-}bpy)]^{3+}$ (I) and of LMCT transition in $[Ru^{III}(NH_3)_5(dmapy)]^{3+}$ (II) [43]

Solvent	DN (solvent)	λ_{max} (MLCT, I) (nm)	λ_{max} (LMCT, II) (nm)
nitromethane	2.7	561	610
benzonitrile	11.9	600	583
acetonitrile	14.1	584	589
acetone	17.0	605	577
dimethylformamide	26.6	658	537
dimethylacetamide	27.8	670	527
dimethyl sulphoxide	29.8	672	532
hexamethylphosphoramide	38.8	729	439

In comparison with the ground state of the complex, the electrostatic attraction between the central atom and ligands is stronger in MLCT excited states, which results in a reduction in the probability of deactivation by substitution processes. The reactivity of ligands to electrophilic agents in MLCT states increases. The reactivity of the central atom to nucleophilic agents also increases, but to a lesser extent because of steric hindrance.

2.3.5 Electron density transfer between central atoms in bridged polynuclear complexes

The interaction of a reducing and an oxidizing metal centre, mediated by a bridging ligand, leads to the appearance of an intervalence charge transfer (IVCT) absorption band in the electronic absorption spectrum. The electron is transferred from the reducing to the oxidizing central atom by an intramolecular or inner-sphere process.

The IVCT bands are broad and appear in the visible and near-IR regions. They are sensitive to the structure of the coordination sphere; molar absorption coefficients in the maxima of IVCT band reach values of $\varepsilon_{max} \approx 10^1\text{–}10^3$ l mol^{-1} cm^{-1}.

TABLE 6

IVCT transitions in electronic absorption spectra of binuclear bridged complex [17, 44]

Binuclear complex	λ_{max} (nm)	ε_{max} (l mol^{-1} cm^{-1})
$[(NH_3)_5Co^{III}\text{–}NC\text{–}Ru^{II}(CN)_5]^-$	375	690
$[(NC)_5Co^{III}\text{–}NC\text{–}Ru^{II}(CN)_5]^{6-}$	312	460
$[(NC)_5Co^{III}\text{–}NC\text{–}Fe^{II}(CN)_5]^{6-}$	385	630
$[(NC)_5Co^{III}\text{–}NC\text{–}Os^{II}(CN)_5]^{6-}$	360	734
$[(H_2O)(NH_3)_4Cr^{III}\text{–}NC\text{–}Fe^{II}(CN)_5]^-$	376	2500
$[(NH_3)_5Ru^{III}\text{–}pyr\text{–}Ru^{II}Cl(bpy)_2]^{4+}$	960	530
$[(NC)_5Fe^{III}\text{–}CN\text{–}Fe^{II}(CN)_5]^{6-}$	1300	3180
$[(NC)_5Fe^{III}\text{–}pyr\text{–}Fe^{II}(CN)_5]^{5-}$	1205	2200

IVCT transitions have been studied for Ru^{II}–Ru^{III}, Fe^{II}–Fe^{III}, Pt^{II}–Pt^{IV} and heteronuclear complexes (such as Co^{III}–Ru^{II} and Cr^{III}–Fe^{II}); examples are presented in Table 6. The spectra of such complexes (and also others, e.g., electrochemical properties) are not only the sum of the spectra of the related mononuclear complexes. A classical example is the intense blue colour of Prussian Blue (due to the IVCT $Fe^{II} \rightarrow CN^- \rightarrow Fe^{III}$ transition), whereas hexacyanoFe(II) and -Fe(III) complexes absorb mainly in the UV region.

In contrast to other types of excited states, the consequence of IVCT transitions is the creation of a redox isomer of the complex in a vibrationally and not electronically excited state. Owing to the radial redistribution of electron density in an IVCT transition, a change in the redox properties is observed, particularly in non-symmetric heteronuclear complexes.

2.3.6 Electron transfer between the complex and a component of its secondary coordination sphere

If an ion complex interacts with an oppositely charged ion, an electron transfer can take place from an MO localized on the complex into an MO localized on the counter-ion, or vice versa. This type of transition is called OSCT (outer-sphere charge transfer) or IPCT (ion-pair charge transfer).

The bands of IPCT transitions have been observed for systems containing an ion pair in which one ion is a complex, and also for the systems in which both components of the ion pair are complexes. Analogously to bridged complexes (Section 2.3.5), the presence of the ion pair is evident from the new spectral band(s) which is (are) not present in the spectra of separated solutions of the ions given. For example [45], the bands of IPCT transitions for $[Co(NH_3)_6]^{3+} . I^-$ and $[Ru(en)_3]^{3+} . I^-$ ion pairs and others are present in the visible region of the spectrum, with $\varepsilon_{max} \approx 10^2$–$10^4$ $l\ mol^{-1}\ cm^{-1}$.

TABLE 7

IPCT transitions in electronic absorption spectra of ion-pair systems [44–47]

Ion pair	λ_{max} (nm)	ε_{max} ($l\ mol^{-1} cm^{-1}$)
$[Eu(oac)]^{3+}/[Fe(CN)_6]^{4-}$	530	110
$[Eu(oac)]^{3+}/[Ru(CN)_6]^{4-}$	434	120
$[Eu(oac)]^{3+}/[Os(CN)_6]^{4-}$	450	110
$[Ru(NH_3)_5Cl]^{2+}/[Ru(CN)_6]^{4-}$	520	20
$[Ru(NH_3)_5py]^{3+}/[Ru(CN)_6]^{4-}$	643	38
$[Ru(NH_3)_5py]^{3+}/[Os(CN)_6]^{4-}$	654	40
$[Ru(NH_3)_5py]^{3+}/[Fe(CN)_6]^{4-}$	910	33
$[Ru(NH_3)_5(4\text{-Cl-py})]^{3+}/[Fe(CN)_6]^{4-}$	940	32
$[Ru(NH_3)_5(4\text{-Br-py})]^{3+}/[Fe(CN)_6]^{4-}$	932	29
$[Ru(NH_3)_5(4\text{-Me-py})]^{3+}/[Fe(CN)_6]^{4-}$	898	33
$UO_2^{2+}/[Ru(CN)_6]^{4-}$	344	5750
$VO^{2+}/[Ru(CN)_6]^{4-}$	317	3500

If a system contains kinetically inert, oppositely charged complexes of an oxidizable and a reducible central atom, these preserve their identity in the system and the central atoms are not bonded by a bridging ligand. In such systems, light-induced electron transfer can take place between the complexes [44]. Some examples [17, 44, 46, 47] of IPTC transitions for such systems are presented in Table 7.

IPCT transitions are connected with a change in the oxidation state of the ion-pair components, with a change in electrostatic interactions between them and change in solvation of the interacting particles. Formation of the IPCT state frequently results in a redox process.

2.3.7 *Electron transfer from the complex to the environment*

The type of transitions known as CTTS [18, 48] (charge transfer to solvent) can take place if the oxidation number of the complex central atom is low, if with an increase in the oxidation number of the central atom the structure of the coordination sphere is unchanged, and if the complex with a central atom with a higher oxidation number is stable. An electron emitted from the complex in a CTTS transition is solvated by the solvent molecules. In the next step, influenced by the reduction properties of the solvent molecules, the electron enters an MO localized in the solvent molecule, which usually results in secondary thermal reactions.

CTTS transitions are usually allowed. The CTTS transition bands appear in the UV region of the spectrum, and are characterized by $\varepsilon_{\mathrm{max}} \approx 10^1$–$10^3\,\mathrm{l\,mol^{-1}\,cm^{-1}}$. The positions of the bands and the values of $\varepsilon_{\mathrm{max}}$ are markedly influenced by the solvent reduction potential. The easier the reduction of the solvent molecule, the lower is the transition energy. For example [49], the CTTS band in the spectrum of $[\mathrm{Fe(CO)(Cp)}]_4$ has its maximum in $\mathrm{CCl_4}$ at 316 nm ($E^{\mathrm{red}}_{1/2} = -0.78$ V vs. SCE), in $\mathrm{CHCl_3}$ at 299 nm ($E^{\mathrm{red}}_{1/2} = -1.67$ V) and in $\mathrm{CH_2Cl_2}$ at 294 nm ($E^{\mathrm{red}}_{1/2} = -2.33$ V). The effect of the solvent on the value of $\varepsilon_{\mathrm{max}}$ can be exemplified [50], by the CTTS transition of ferrocene, for which $\varepsilon_{\mathrm{max}} = 49.3\ \mathrm{l\,mol^{-1}\,cm^{-1}}$ in cyclohexane, $147\ \mathrm{l\,mol^{-1}}$ in 1,2-dibromomethane and $960\ \mathrm{l\,mol^{-1}\,cm^{-1}}$ in tetrabromomethane.

CTTS transitions result in the oxidation of the central atom.

2.4 Molecular structure of complexes in excited states

The electronic and molecular structures of compounds are mutually conditioned. There are many references to the crystal and molecular structures of coordination compounds in their ground state. The molecular structure of excited complexes is estimated from the absorption and emission spectra, quantum-chemical calculations, the time-resolved resonance Raman and IR spectra, and electronic absorption of excited complexes.

Theoretically based considerations on different equilibrium geometries of Cr(III) complexes in the ground and excited LF states have been postulated by Adamson [6, 51], who stated on comparing absorption and emission spectra that vibrational relaxation of the quartet excited states must be accompanied by both considerable radial and angular distortions, that is, excited complexes have both different bond lengths and different symmetries with respect to the ground-state structure. These excited-state distortions can be evaluated by using Franck–Condon analysis when a highly resolved spectrum including vibronic progression is available. Unfortunately, the electronic emission and absorption spectra of inorganic molecules in condensed media typically contain broad, featureless bands, or their individual vibronic components are not well resolved.

The study of the absorption and emission spectra of Pt(II) complexes and of the *cis-trans* photoisomerization of such square-planar complexes has resulted in the assumption [17] of a tetrahedral-like configuration distorted towards the square-planar arrangement (transoid and cisoid configuration) in the energetically lowest LF state, which was assigned to the lowest triplet with D_{2d} (distorted tetrahedron) molecular geometry. On the other hand, from recent results [52] based on Franck–Condon analysis of the single-crystal polarized luminescence spectra of $K_2[PtX_4]$, where X = Cl or Br, the following conclusions were drawn:

— the emitting state is significantly distorted along the totally symmetric stretching coordinate;

— the excited state is assumed to retain D_{4h} symmetry.

However, it should be noted that the differing results [7, 52] may be due to the different environments of the complex when studying its properties.

Theoretical quantum chemical studies have also contributed to the classification of the structures of excited complexes. For example, an ab initio study of the $[Re_2Cl_8]^{2-}$ complex in its ground state and $\delta \rightarrow \delta^*$ excited state has shown [53] that excitation is accompanied by torsional distortion from D_{4h}(GS) towards D_{4d}(ES) geometry. For the $[Co(CO)_3(NO)]$ complex, which has a tetrahedral configuration and a linear Co–N–O fragment in its ground state, a planar structure of the chromophore and a bent structure of the given fragment are assumed in the MLCT state [54], derived from calculations [MLCT means the transition $Co^{-I}–(NO^+) \rightarrow Co^{I}–(NO^-)$].

One of the fields of application of pulsed laser flash photolysis within the range of nanoseconds to picoseconds is the study of the spectral properties of electronically excited complexes. Information on the electron system of the excited complexes and on the kinetics of deactivation is provided by ESA (excited-state absorption) spectra. Moreover, time-resolved resonance Raman spectra (preresonance Raman spectra) have significantly contributed to the determination of the molecular structure of excited complexes.

The conditions for the study of ESA spectra and their changes with time are a sufficiently long lifetime of the excited particles (excluding the duration of spectrum measurement) and different spectral properties of the particles in the ground and excited states studied, expressed in terms of the molar absorption coefficients, ε_λ(GS) and ε_λ(ES).

Possibilities offered by ESA spectra can be exemplified [55] by the study of an aqueous solution of the $[Ru(bpy)_3]^{2+}$ complex. Excitation of the complex by flashes at $\lambda = 265$, 353 or 530 nm results in the same ESA spectrum of the excited complex with a band at 360 nm [$\varepsilon_{360}(ES) > \varepsilon_{360}(GS)$]. $^3O_2$ quenches the excited state of the complex with a rate constant $k_q = 3.3 \times 10^9$ l mol^{-1} cm^{-1}, which means that the complex is in the triplet state. Based on the changes in the ESA spectrum with time at 360 nm (the absorbance decreases with time) and 453 nm [the absorbance increases with time as $\varepsilon_{453}(ES) < \varepsilon_{453}(GS)$], the rate constant of the transition from the excited to ground state was calculated. Its value in both instances (for calculations based on the change in absorbance at both of the above wavelengths) was the same ($k = 1.5 \times 10^6$ s^{-1}). Also, the value of $\varepsilon_{360}(ES) = 2730$ l mol^{-1} cm^{-1} was calculated; its magnitude indicates that the band in the ESA spectrum corresponds to the spin-allowed transition. The complex in the excited triplet state also emits radiation with a maximum at 610 nm and a rate constant of emission quenching of 1.5×10^6 s^{-1}.

Similarly, it has been found [56] (by a comparison of the phosphorescence rate constant and the ESA spectra changes) that the bands in the ESA spectra of Cr(III) complexes correspond to LF transitions between the energetically lowest and higher doublet states. The band in the ESA spectrum of $[Pt_2(P_2O_5H_2)_4]^{4-}$ at 325 nm was assigned [57] to the $5d\sigma \rightarrow 5d\sigma^*$ transition in the excited $^3A_{2u}$ state; four bands in the ESA spectrum of $[PtCl_4]^{2-}$ were attributed [52] to LF transitions in the $^3E_g(^3A_{2g})$ state of the complex, based on theoretical analysis of the possibilities of spectral transitions (maxima of the bands at 1190, 551, 377 and 333 nm, $\varepsilon_{max} \approx 10^2$–$10^3$ l mol^{-1} cm^{-1}).

Recently, together with Franck–Condon analysis of vibrational progressions observed (unfortunately very rarely) in absorption and emission spectra, the study of excited complexes by time-resolved resonance Raman spectroscopy has been widely used, which offers experimental data for the calculation of the structure of these complexes. For the calculations of the bond length displacement between the ground-state bond lengths and those of the excited state, Badger's rule [27] or Zink's method [58] is employed. A description of the continuously developing methods for the determination of molecular structure of excited complexes is beyond the scope of this book; here we present a few results achieved by a comprehensive study of the properties of selected complexes in excited states.

The ground state of complexes with a metal–metal bond, $[Pt_2(P_2O_5H_2)_4]^{4-}$ and $[Rh_2(1,3\text{-}(CN)_2pn)_4]^{2+}$, is $^1A_{1g}$ with HOMO $(d\sigma)^2\ (d\sigma^*)^2$. During excitation with formation of the energetically lowest excited state, $^3A_{2u}$, the metal–metal bond energy increases as the electron is transferred from the $d_{z^2}(\sigma^*)$ orbital to the bonding $p_z(\sigma)$ orbital. The ratio of the metal–metal bond energy in the excited state to that in the ground state is approximately 3 for the rhodium(I) complex [59] and about 1.8 for the platinum(II) complex [57]. The increase in the order of the metal–metal bond in the transition from the ground to the excited state is also demonstrated by a reduced metal–metal distance from 292.5 to 271 pm for the platinum complex and from 324.4 to 293 pm for the rhodium complex. On the other hand, with $[Mo_2^{II}(RCO)_4]$ complexes the $\delta \rightarrow \delta^*$ transition causes a change from a quadruple to triple bond between the molybdenum atoms, which results [60] (for R = CF_3) in an increase in the Mo–Mo distance by 7 pm in comparison with the ground state. The $\delta \rightarrow \pi^*$ transition in this complex [58] results in an increase in the Mo–Mo distance by 4.5 pm.

The energetically lowest excited state of $[W(CO)_5py]$ and $[W(CO)_5pip]$ complexes is the triplet state ^3E. In this state, the metal–ligand distances related to those in the ground state increased as follows: for $[W(CO)_5py]$, $\Delta(W\text{–}N) = 18$ pm, $\Delta(W\text{–}C_z) = 12$ pm and $\Delta(W\text{–}C_{x,y}) = 4$ pm; and for $[W(CO)_5pip]$, $\Delta(W\text{–}N) = 30$ pm, $\Delta(W\text{–}C_z) = 25$ pm and $\Delta(W\text{–}C_{x,y}) = 5$ pm. In both complexes the *N*-donor ligand was coordinated along the *z* axis. The most marked increase in internuclear distances on this axis is due to the fact that during excitation (d_{xz}, $d_{yz} \rightarrow d_{z^2}$), the electron density is increased to the greatest extent just along the *z* axis.

For calculations of distortions in $[Cr(CN)_5(NO)]^{3-}$ in the excited MLCT state towards the structure of the ground state, resonance Raman overtone intensities in addition to the intensities of fundamentals in the Raman spectra were taken into account [58]. Displacements assuming uncoupled normal modes are as follows: $\Delta(Cr\text{–}C) = 7$ pm; $\Delta(Cr-N) = 10$ pm; $\Delta(C-N) = 3$ pm and $\Delta(N-O) = 1$ pm.

Theoretical analysis of the resonance Raman spectra of $[Os(bpy)_x(P_2)_{3-x}]^{2+}$ complexes where $P_2 = cis\text{-}(C_6H_5)_2PCH{=}CHP(C_6H_5)_2$ and $x = 1, 2, 3$ in the ground-state and time-resolved Raman spectra of these complexes in the ^{3}MLCT excited state has shown [27] that on excitation the electron from the central atom Os(II) moves to an antibonding π^* orbital localized in one 2,2-bipyridine ligand to form bpy^-. Application of Badger's rule to the Raman data and Franck–Condon analysis of the emission data led to two independent determinations of average bond lenght displacements in the ^{3}MLCT state (vs. the ground state), which are 1.26 pm for $[Os(bpy)_3]^{2+}$; 1.84 pm for $[Os(bpy)_2(P_2)]^{2+}$ and 1.99 for $[Os(bpy)(P_2)_2]^{2+}$. The two approaches yielded displacement values that agreed within 0.1–0.3 pm.

With regard to the efforts to obtain the most comprehensive information on the properties of complexes in their excited states, one can expect even wider application of methods devoted to the study of the spectral and molecular structures of such complexes, and a search for relationships with their photochemical reactivity.

2.5 Thermodynamic properties of coordination compounds in excited states

Changes in the electronic and molecular structures of a complex accompanying electronic excitation result in changed thermodynamic properties. The change in energy content on excitation is commonly described by ΔG values (ergonicity of a process). It should be noted that in numerous instances ΔG values are presented without a knowledge of the ΔS values, or they are neglected. The differences in entropy on going from the ground to some of the excited states of the complex may be due to the changes in dipole moment, solvation, the internal degrees of freedom, orbital and spin degeneracies, etc. An exact determination of the values of entropy changes on excitation has not been elaborated so far either experimentally or theoretically; the changes in ΔS are estimated from the Stokes shift (energy difference between the maxima of the bands in absorption and emission spectra corresponding to the transitions between the same states). If the differences in solvation, shape and size of the complex in the ground and excited states are not too high, the Stokes shift is usually small (up to 5000 cm^{-1}), and in such instances the changes in ΔS can be neglected. Therefore, the relationships between thermodynamic quantities in this section are presented with application of this approximation.

The distribution of vibrational levels on transition from the ground to an excited state is determined by quantum-chemical quantities, i.e., values of Franck–Condon factors. Within several vibrations (for 10^{-13}–10^{-12} s), the set of complex particles reaches from the spectroscopic state a thermal equilibrium with the environment. The state in which the set of excited particles is in thermodynamic equilibrium with the environment is called [63] a *thexi* state (*th*ermally *e*quilibrated e*x*c*i*ted state). The energy of the thexi state is significantly higher than that of the ground state (by as much as 500 kJ mol^{-1}) and generally leads to markedly higher reactivity of a complex in the excited than in the ground state. In the following chapters on using the terms of equilibrium thermodynamics we assume that the lifetime of excited particles is sufficiently long to achieve a Boltzmann distribution of vibrational and rotational levels, i.e., the thexi state.

The relationships between the changes in some thermodynamic quantities due to electronic excitation of the molecules and the energy of photons corresponding to $0 \rightarrow 0$ transitions have been elaborated in a general form by Grabowski [61, 62]. Their qualitative form for equilibrium constants of acid–base processes (p*K*) and redox potentials (*E*) is illustrated in Fig. 1, where Ox, Red are oxidized and reduced forms of the Brönsted base B (acid A), respectively, and *hν* are 0 → 0 transition energies between the complex in question (for the sake of simplicity charges are not presented).

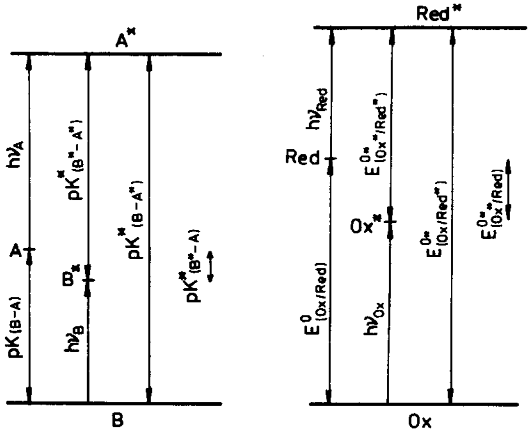

Fig. 1. Schematic representation of relationships between the energies of 0 → 0 transitions (*hν*), acid–base equilibrium constants (p*K*) and redox potentials (E^0) for complexes in their ground and excited states.

From the fundamental relationships of thermodynamics, quantitative relationships between particular quantities were derived. Thus, for example, for a change in the equilibrium constant of an acid–base reaction of a particle in the ground and excited states, the following equation is valid:

$$\mathrm{p}K^* - \mathrm{p}K = \frac{h\nu_\mathrm{B} - h\nu_\mathrm{A}}{2.303kT} \tag{2.16}$$

where pK^* and pK are values for the acid–base equilibrium in the excited and ground states of acid A and base B, respectively, and $h\nu_\mathrm{A}$ and $h\nu_\mathrm{B}$ are energies of 0 → 0 transitions of the acid and base. As an example [64] of the application of the above relationship to coordination compounds, the acid–base equilibrium between [Ru(bpy)$_2$(CN)$_2$] complex as the Brönsted base and the H_3O^+ ion can be considered. For the ground state of the complex the reaction equilibrium constant $K = 0.75 \pm 0.1$ and for the complex in MLCT excited triplet state $K^* = 5 \times 10^5$.

For the difference in redox potentials of a particle in the ground and excited states under standard conditions, the following relationship has been derived:

$$E^{*0} - E^0 = \frac{(h\nu_\mathrm{Ox} - h\nu_\mathrm{Red})N}{nF} \tag{2.17}$$

where N and F are the Avogadro and Faraday constants, respectively, and n is the number of exchanged electrons. The potential E^{*0} relates to the electron exchange between both the oxidized and reduced forms of the particle in excited states. In the study of the photochemical properties of coordination compounds, the reactions of electron exchange between one form of the complex (e.g., reduced) in the excited state and another form (oxidized) in the ground state are usually followed. The change in question can be expressed by the following equation [48]:

$$E^{*0}_{(\mathrm{Ox/Red}^*)} - E^{0}_{(\mathrm{Ox/Red})} = h\nu_{\mathrm{Red}}\,\frac{N}{nF} \tag{2.18}$$

In the opposite case (the oxidized form of the complex is excited), the following equation is valid:

$$E^{*0}_{(\mathrm{Ox}^*/\mathrm{Red})} - E^{0}_{(\mathrm{Ox/Red})} = h\nu_{\mathrm{Ox}}\,\frac{N}{nF} \tag{2.19}$$

Provided that the values $h\nu$ are expressed in eV (1000 cm^{-1} correspond to 0.1245 eV), the difference in the redox potentials is identical with $h\nu$ energy.

As an example [48], the changes in the oxidation and reduction properties of the $[\mathrm{Ru(bpy)_3}]^{2+}$ complex during its transition from the ground to the energetically lowest triplet MLCT state (the energy of the 0 → 0 transition is 2.12 eV) are presented in Fig. 2.

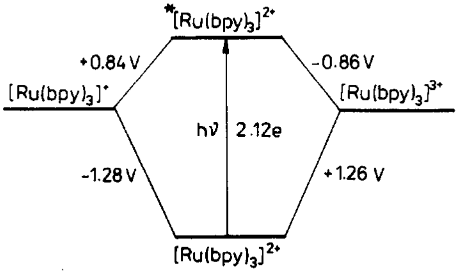

Fig. 2. Redox potentials of $[\mathrm{Ru(bpy)_3}]^{2+}$ in its ground and ^{3}MLCT excited states.

It is obvious that the accuracy of the E^{*0} value determination depends on the exactness of the determination of 0 → 0 transition energy. For emitting complexes one can find the value of $h\nu$ corresponding to 0 → 0 transition from the vibrational structure of the bands, or a point of intersection of the bands of corresponding transitions in the absorption and emission spectra (provided the same conditions are used). Commonly, the values of E^{*0} are determined from experimental data obtained from the study of electronic transitions between an excited complex and a series of quenchers with different redox potentials in the ground state. Direct electrochemical measurements in irradiated solutions with the use of semiconductor electrodes has occasionally been employed [65].

The changes in the redox properties of complexes due to excitation are connected with the increase in their electron affinity and the decrease in their ionization potential. Thus, the excited complex will be a stronger oxidizing agent and at the same time a stronger reducing agent than the complex in the ground state.

Of other quantities, the so-called threshold energy of reaction (E_{th}) is used in photochemistry, defined as the energy of radiation at which the quantum yield of the given reaction approaches zero [66]. This quasi-thermodynamic quantity is determined experimentally from the dependence of the quantum yield of a certain chemical reaction vs. the energy of excitating monochromatic radiation initiating the reaction in question. It should be noted that even if a chemical change often takes place in the complex fragment (for example, with substitution of one of the ligands), the E_{th} value is significantly determined by the composition and structure of the whole complex, in addition to the properties of the medium in which the complex is present. For example [67], the threshold energies of photooxidation of ligands $X^- = Cl^-$, Br^- and N_3^- in $[Fe([15]pydieneN_5)X_2]^+$ (369, 311 and 276 kJ mol^{-1}) are significantly lower than those of photooxidation of the same ligands in $[Fe([15]pyaneN_5)X_2]^+$ complexes (469, 410 and 364 kJ mol^{-1}).

Some experimental results and theoretical approaches indicate that photochemical reactions (or photophysical transitions between two excited states) can also take place from vibrationally non-relaxed states, i.e., before the thexi state is achieved. A reaction that is in competition with vibrational equilibration requires a rate constant for the processes forming products of $k > 10^{11}$ s^{-1}.

In this way the results of the study of photophysical and photoaquation processes of $[Cr(bpy)_3]^{3+}$ [68], $[Co(NH_3)_5Cl]^{2+}$ and others were rationalized (for details, see Section 4.4).

Such processes, from the viewpoint of their kinetics, cannot be treated in transition-state theory language. In the light of thermodynamics, the approach of non-equilibrium thermodynamics should be employed for their description.

3 PHOTOPHYSICAL DEACTIVATION PROCESSES

3.1 Deactivation modes of the excited states of coordination compounds

The term deactivation designates the formation of an energetically lower electronic state from a complex in a particular excited state [8, 22]. Possible modes of deactivation of a complex in the *i*th excited state are shown in the following Scheme 1. Monomolecular processes 3.1 to 3.3 and bimolecular processes 3.4 to 3.6 are photophysical deactivation processes; processes 3.7 and 3.8 are photochemical reactions.

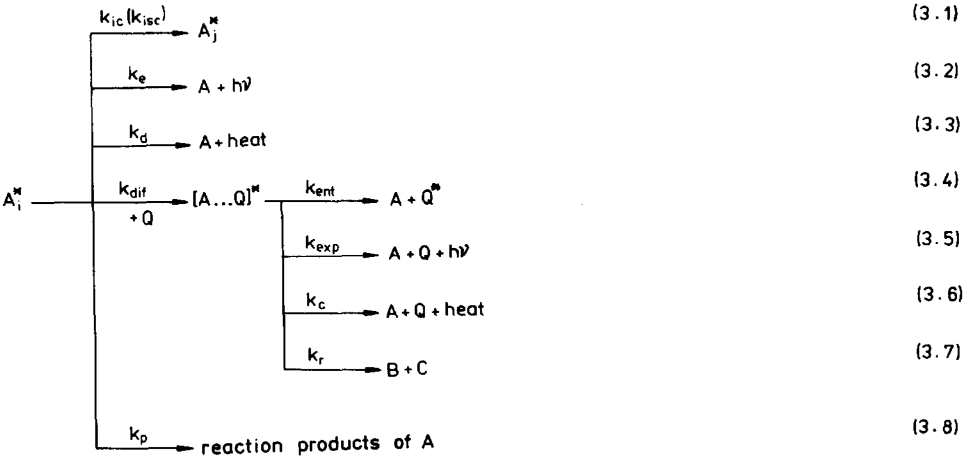

Scheme 1

Considerable attention has been paid to the study of photophysical deactivations in the photochemistry of coordination compounds [8, 22], as the results frequently determine the correct interpretation of the photochemical properties of complexes. Process 3.1, expressing the transition between two excited states of a complex, can be either the internal conversion (both states have identical multiplicity) or the process of intersystem crossing (the states differ in their multiplicity). In the literature, appropriate rate constants are represented by k_{ic}

(internal conversion) and k_{isc} (intersystem crossing). The radiative deactivation (process 3.2) results in the ground state of the complex and is divided into fluorescence (multiplicities A_i^* and A are identical) and phosphorescence (multiplicities A_i^* and A differ). In the non-radiative deactivation of A_i^* energy is released into the environment in the form of heat (process 3.3).

Interaction of A_i^* with another particle of the medium, Q, can result in energy transfer with the formation of Q* (process 3.4), non-radiative deactivation (process 3.6) and, in the case of exciplex formation, also in exciplex radiative deactivation (process 3.5). It should be mentioned that, in general, *(A... Q) designates a state formed by interaction between A* and Q, and a chemical bond between A* and Q need not necessarily be formed.

The lifetime of a complex in certain excited state A_i^* is defined by the following relationship:

$$\tau_i^0 = \frac{1}{\sum_a k_{i,a}} \tag{3.9}$$

where the superscript ^{0} designates the quantities in the absence of quenchers (Q) and $k_{i,a}$ are rate constants of the given monomolecular deactivation processes. The statistical probability of the realization of a certain deactivation pathway is expressed by the value of the quantum yield, defined as

$$\Phi_b^0 = \frac{k_{i,b}}{\sum_a k_{i,a}} = \tau_i^0 k_{i,b} \tag{3.10}$$

As the particle in the excited state must be deactivated, the following relationship is valid:

$$\sum_a \Phi_a^0 = 1 \tag{3.11}$$

In the presence of a quencher Q, interactions between particles A_i^* and Q take place. The possibility of collision depends on the temperature and viscosity of the medium, and is expressed by a rate constant of diffusion, k_{dif}, for which the following equation has been derived:

$$k_{dif} = \frac{2kT}{3000\eta}\left(2 + \frac{r_A}{r_Q} + \frac{r_Q}{r_A}\right) \tag{3.12}$$

where r_A and r_Q are the radii of the A and Q particles. For aqueous media at room temperature, the diffusion rate constant has a value of $k_{dif} \approx 5 \times 10^9$

l mol^{-1} s^{-1}. For the rate constant of bimolecular quenching, k_q, the following relationship can be derived:

$$k_q = k_{dif}\,\frac{k_{ent} + k_{exp} + k_c + k_r}{k_{-dif} + k_{ent} + k_{exp} + k_c + k_r} \tag{3.13}$$

where k_{-dif} expresses the rate constant of reversible decay of *(A . . . Q). In the presence of a quencher, the number of A* deactivation modes increases and, therefore, the lifetime decreases:

$$\tau_i = \frac{1}{k_q[Q] + \sum_a k_{i,a}} \tag{3.14}$$

The relationship between τ_i^0 and τ_i, derived as the ratio of eqns. 3.9 and 3.14, is called the Stern–Volmer equation:

$$\frac{\tau_i^0}{\tau_i} = 1 + k_q[Q]\tau_i^0 = 1 + K_{SV}[Q] \tag{3.15}$$

and the quantity K_{SV} is called the Stern–Volmer quenching constant. Equation 3.15 can be written in other forms depending on the type of the study, whether it is photochemical or photophysical. Usually, instead of the lifetime ratio, the ratio of quantum yields of a certain deactivation mode or the ratio of emission intensities (fluorescence, phosphorescence) in the absence and presence of the quencher Q is expressed. The slope K_{SV} is evaluated from the graphical illustration of eqn. 3.15 and, after the experimental determination of τ_i (e.g., by flash photolysis), the value of k_q can be calculated.

3.2 Monomolecular non-radiative deactivation processes

The energy of an excited complex can be dissipated by three possible non-radiative deactivation modes, during which no chemical reaction takes place and no electronically excited particles of the medium are formed [8, 22]:

(a) vibrational relaxation of the excited particles with the particles of the medium while the electronic state does not change (in condensed media thermal equilibrium with the environment takes place within 10^{-11}–10^{-13} s);

(b) spin-allowed internal conversion with $k_{ic} \approx 10^{12}\,s^{-1}$.

(c) spin-forbidden intersystem crossing with $k_{isc} \approx 10^9$—$10^{13}\,s^{-1}$.

If light is absorbed by complex A, we expect the transition A → A* to be a vertical one, that is, electronic rearrangement is not accompanied by appreciable simultaneous nuclear motion. The consequence is that excited complexes A* are not produced in an excited-state equilibrium geometry but in the ground-state geometry. If a coordination compound is present in a solution, the ground-state solvation sphere remains unchanged during electronic excitation also. From a spectroscopic, Franck–Condon collection of complexes, A^*_{FC}, relaxation takes place within few picoseconds, which is reflected in a decrease in vibrational A* energy due to interactions with the particles of the neighbouring medium, in achieving the excited-state equilibrium geometry and the formation of a new solvation sphere. The above process is called thermal equilibration. An ensemble of excited complexes A* with a Boltzmann distribution of vibrational states is at ambient temperature with respect to vibrations, and is called the thexi state [69].

From such a thermodynamic state, an electronically excited complex A* usually undergoes photophysical or photochemical deactivation processes. Cases when this does not happen (prompt processes occurring from highly vibrational levels) will be exemplified later.

Internal conversion:

$$ {}^{X}A_i^* \xrightarrow{k_{ic}} {}^{X}A_j^* \qquad (3.16) $$

intersystem crossing (X = Y ± 2):

$$ {}^{X}A_i^* \xrightarrow{k_{isc}} {}^{Y}A_j^* \qquad (3.17) $$

or reverse (back) intersystem crossing:

$$ {}^{Y}A_j^* \xrightarrow{k_{bisc}} {}^{X}A_i^* \qquad (3.18) $$

can take place if the energy surfaces of the states do not cross, and in centrosymmetric particles no parity change occurs during transition. The processes themselves (13.16 to 3.18) are not processes of total energy content lowering the excited complex, as they take place only within the isoenergetic states of the complex.

The energy decrease occurs only in the case of collisions with the particles of the medium. Back intersystem crossing (process 3.18) is the more probable the lower is the energy difference of the thexi states ${}^{Y}A_j^*$ and ${}^{X}A_i^*$. Until the energy of these states is very close (a difference of a few kT), both states can be in equilibrium owing to simultaneous processes 3.17 and 3.18.

Spin forbiddenness for the intersystem crossing, which is markedly observed in organic substances without a heavy atom (usually for organic substances $k_{ic}/k_{isc} \approx 10^3$–$10^6$), does not apply with complexes and from the kinetic viewpoint both processes are often indistinguishable [22].

Values of rate constants and quantum yields of the internal conversion and intersystem crossing are determined from studies of luminescence kinetics, time dependence of ESA spectra, consequences of chemical reactions and investigation of the energy transfer of A*.

As an example [59, 70] of the calculated k_{ic} and k_{isc} values, the results obtained by the study of lifetime and quantum yields of phosphorescence of the complex $[Rh_2(1,3\text{-}(NC)_2pn)_4]^{2+}$ and by the study of dependences of the ESA spectra on the excitation wavelength are presented in Fig. 3. The given complex undergoes from an excited state ^1E_u localized in a binuclear moiety, both internal conversion to the state $^1A_{2u}$ ($\Phi_{ic} = 0.15$) and intersystem crossing ($k_{isc} \approx 10^{13}\ s^{-1}$), which mutually compete. However, usually in the absence of upper excited state chemistry, $\Phi_{ic} = 1$.

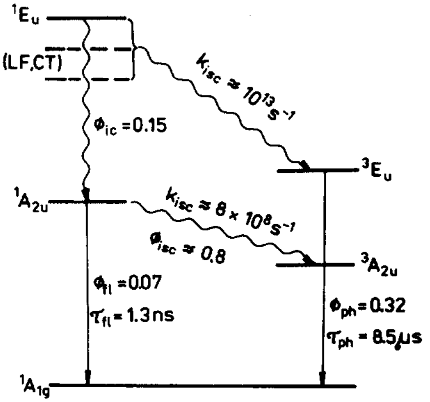

Fig. 3. Values of parameters of photophysical deactivation modes for $[Rh_2(1,3\text{-}(NC)_2pn)_4]^{2+}$ in its singlet and triplet excited states.

Internal conversion can also take place from atoms other than the central atom(s)-localized excited state. In connection with the study of solar-to-chemical energy conversion, photophysical properties of the complex $[Ru(bpy)_3]^{2+}$ and its analogues have been studied in detail [48]. Based on the finding that the emission quantum yield (^{3}MLCT → ^{1}GS) is invariant on excitation to $^1(\pi \rightarrow \pi^*)$ and ^{1}MLCT states (the former in the UV and the latter in the visible region), it has been determined that $\Phi_{ic} = 1.0$ for the process $^1\pi\pi^* \xrightarrow{ic} {}^1$(MLCT). From luminescence measurements (study of the intensity of phosporescence on excitation to an ^{1}MLCT or ^{3}MLCT state) and determinations of the quantum yield Φ_{isc}, it follows that for crossing ^{1}MLCT → ^{3}MLCT, $1.0 \geqslant \Phi_{isc} \geqslant 0.85$.

The effect of the central atom on the ligand-localized $^1(\pi \rightarrow \pi^*) \rightarrow {}^3(\pi \rightarrow \pi^*)$ intersystem crossing was considered [71] for the complexes of lanthanides with methyl salicylate, $M(Me\text{-}sal)_3$, where M = La, Gd and Lu. The chelates were investigated by measurements of picosecond fluorescence, ESA spectroscopy and quantum yield measurements. From the experimental results, rate constants $k_{isc} = 5 \times 10^7$, 7.5×10^8 and 7.9×10^7 s^{-1} were calculated, in addition to quantum yields $\Phi_{isc} = 0.12$, 0.18 and 0.19, for La(III), Gd(III) and Lu(III) chelates, respectively.

Photochemical experimental techniques were also utilized for the investigation of intersystem crossing dynamics of spin-crossover complexes, for which both high- and low-spin electronic ground states are accessible thermally. For $[Fe(byim)_3]^{2+}$ and $[Fe(phenmethoxa)_3]^{2+}$ complexes, lifetimes of first-order quintet → singlet relaxation of 45 ns for the former complex and 110 ns for the latter in acetone [72] at 298 K were determined by pulse flash photolysis.

The process 3.3, in the course of which a complex in the ground electronic state A_{GS} is formed from the excited complex $^{X}A_j^*(^{Y}A_i^*)$, also belongs to the monomolecular photophysical non-radiative deactivations. If the excited complex is deactivated by monomolecular photophysical processes only, the values of non-radiative deactivation rate constants, k_d, can be calculated from the following equation:

$$k_d = k_e \frac{(1 - \Phi_e)}{\Phi_e} \tag{3.19}$$

Determination of the rate constant, k_e, and quantum yield, Φ_e, of radiation deactivation is presented in Section 3.3. Of the values of Φ_e and k_e determined for phosphorescence $^2E \rightarrow {}^4A_2$ of Cr(III) complexes, the values $k_d \approx 10^1$–10^4 s^{-1} were calculated [73], and for phosphorescence $^3T_1 \rightarrow {}^1A_1$ of Rh(III) complexes the values [74–76] $k_d \approx 10^3$–10^5 s^{-1} and for the transition ^{3}MLCT → $^1A_1$ of Ru(II) complexes the values $k_d \approx 10^4$–10^6 s^{-1} were determined [77]. In these examples, phosphorescence was measured at 77 K.

In non-radiative deactivation, energy is dissipated into the environment in the form of heat. The marked effect of temperature on non-radiative deactivation (k_d increases exponentially with temperature) becomes manifest in lowered parameters of competing deactivation processes (e.g., intensity and luminescence lifetime). From the thermal dependence of k_d the Arrhenius parameters can be calculated. Thus, for example, for $[Rh_2(Me_2(CN)_2hx)_4]^{2+}$ in different media, values of the activation energies ($E_a = 0.248$–0.409 eV) and the frequency factor for activated non-radiative decay ($A = 2 \times 10^{11}$–3×10^{13} s^{-1}) were calculated [78].

3.3 Monomolecular radiative deactivation processes

Monomolecular radiative deactivations in general can take place from all types of excited states of complexes. Until now they have been intensively studied for the complexes of transition metals in the LF excited states with d^2–d^8 configurations, complexes of rare earth-metals with f^1–f^{13} configurations, and complexes with an aromatic ligand(s) in IL, MLCT and LLCT excited states.

Luminescence is expressed by the luminescence (emission) yield, Φ_e, which is the number of photons that are emitted per photon absorbed by the system. It results from Scheme 1 that the following equation is valid for the complex A_i^*

$$\Phi_e(A_i^*) = \frac{k_e}{k_e + k_{ic} + k_{isc} + k_d + k_p + k_{dif}[Q]} \tag{3.20}$$

In practice, the $\Phi_e(A_i^*)$ value is determined in such a way that under identical conditions the number of emitted photons of $I(A_i^*)$ and $I(L^*)$ is calculated from emission spectra of the investigated A_i^* complex and a standard L^*, and the value of $\Phi_e(A_i^*)$ is evaluated from the relationship

$$\Phi_e(A_i^*) = \frac{I(A_i^*)}{I(L^*)}\Phi_e(L^*) \tag{3.21}$$

As a standard Rhodamine B is usually used [79], for which $\Phi_e = 0.69$.

Another quantity of great importance in photochemistry and photophysics is the lifetime of an excited complex A_i^*. It is generally measured by pulse techniques in such a way that luminescence decay following termination of the flash is monitored and analysed. From a semilogarithmic plot of intensity versus time, the value of the lifetime is obtained [80].

The shape of a luminescence spectrum, i.e., the dependence of the number of emitted photons on their wavelength (frequency), is connected with changes in the bond force constants in excited and ground states of the complex and the measurement conditions (medium, temperature, pressure, excitation energy). The effects of these factors will be illustrated using radiative deactivation of complexes with d^3 and d^6 configurations of the central atom in LF and MLCT excited states, respectively.

Both modes of radiative deactivation, fluorescence and phosphorescence, usually take place from the energetically lowest excited spin-allowed, or spin-forbidden state, to the ground state, thus following the so-called Kasha rule. However, if the energy difference between the first (energetically lowest) excited state and other (energetically higher) excited states is high (analogy with azulene in organic photochemistry [85]), radiative deactivation from higher excited states can also occur.

According to current theories of radiative transitions, kinetic parameters and other properties of luminescence are not significantly influenced by the properties of the luminescent particle. The dependence of these properties on the environment (temperature, pressure, etc.) is connected with changes in parameters of other deactivation processes, e.g., non-radiative deactivation, chemical deactivations. Therefore, we shall present mainly kinetic parameters of luminescence, which should be regarded as values measured under particularly defined conditions.

Fluorescence:

$$ {}^{X}A_i^{*} \rightarrow {}^{X}A_{GS} + h\nu \qquad (3.22) $$

taking place from LF excited states of complexes of transition metals was studied particularly in the case of d^3 complexes of Cr(III) and Mn(IV). The oscillator strength for fluorescence reached values of $f \approx 10^{-5}$–10^{-3}.

The transition ${}^4T_2 \rightarrow {}^4A_2$ ($t_{2g}{}^2e_g^1 \rightarrow t_{2g}^3$ in the field of O_h symmetry) is connected with depopulation of an antibonding orbital, e_g, which evokes a significant increase in the force constants of central atom–ligand bonds and thus also a change in the equilibrium structure. Thus, from the Franck–Condon principle, levels with higher vibrational quantum numbers are populated on both absorption and emission of a photon. The bands in the absorption and emission spectra are wide (the half-width of a fluorescence band being $\nu_{1/2} > 1000\ \text{cm}^{-1}$) and the Stokes shift is very large ($> 2000\ \text{cm}^{-1}$), which is evident from the results in Table 8. The fluorescence bands do not exhibit vibrational structure, even at low temperatures.

TABLE 8

Stokes shifts for ${}^4T_2 \leftrightarrow {}^4A_2$ transition in some Cr^{3+}-doped compounds and complexes [8, 110, 111]

Compound	Stokes shift (cm^{-1})
Cr^{3+} in ruby Al_2O_3	3600
Cr^{3+} in $Be_3Al_3Si_6O_{18}$	3300
Cr^{3+} in $LiNbO_3$	5050
Cr^{3+} in $LiTaO_3$	4630
Cr^{3+} in borate glasses	>3000[a]
$CrCl_3$	2550
$CrBr_3$	2800
$(NH_4)_3[CrF_6]$	2240
$K_2[CrF_5(H_2O)]$	3200
$(NH_4)[Cr(en)F_4]$	3840
$[CrF_3(H_2O)_3]$	3920
$[CrF_3(H_2O)_3]\,.\,H_2O$	3540
$[CrF_3(H_2O)_3]\,.\,2H_2O$	3620
$[CrF_5(H_2O)](SiF_6)$	5490
$[Cr(H_2O)_6]F_3$	4170
$[Cr(urea)_6]^{3+}$ (solution)	3700

[a] Spectral properties influenced by the composition of the borate glass and temperature [53].

The spin-allowed quartet state of Cr(III) and Mn(IV) complexes can be achieved by photoexcitation during irradiation into the relevant LF bands, by transitions from energetically higher excited states (e.g., CT states) and by back (reverse) intersystem crossing (process 3.18). As the following equation is valid [8] (for $^4T_2$ and ^2E states of complexes with d^3 configuration):

$$\frac{k_{\mathrm{bisc}}}{k_{\mathrm{isc}}} = \frac{g(^4\mathrm{T}_2)}{g(^2E)} \exp\left(-\frac{\Delta E}{RT}\right) \tag{3.23}$$

the efficiency of the reverse intersystem crossing increases with increasing temperature. In eqn. 3.23, g are degeneracies of the states involved and ΔE is the energy difference between $^4T_2$ and ^2E states.

From the relationship between the ratio of quantum yields of fluorescence and phosphorescence and temperature:

$$\ln\frac{\Phi_{\mathrm{fl}}}{\Phi_{\mathrm{ph}}} = \ln\left[\frac{k_{\mathrm{fl}}g(^4T_2)}{k_{\mathrm{ph}}g(^2E)}\right] - \frac{\Delta E}{RT} \tag{3.24}$$

values of $\Delta E = 2900\,\mathrm{cm}^{-1}$ and $k_{\mathrm{fl}}/k_{\mathrm{ph}} = 6000$ were calculated. For $[\mathrm{Cr(NH_3)_6}]^{3+}$, $[\mathrm{Cr(NH_3)_5(NCS)}]^{2+}$ and *trans*-$[\mathrm{Cr(en)_2(NCS)_2}]^+$ complexes, the calculated values were $k_{\mathrm{bisc}} = 5\times10^3$, 10^4 and $5\times10^4\ \mathrm{s}^{-1}$, respectively, and $\Delta E \approx 4000\,\mathrm{cm}^{-1}$. The above type of thermally determined fluorescence is called delayed fluorescence [81].

In conjunction with the utilization of lanthanoid compounds for colour television and monitor screens, the luminescence of such compounds which could be the result of $f\rightarrow f$ transitions was investigated. Bands in emission spectra measured at low temperatures show vibrational structure and they are the consequence of not only electronic dipole transitions but also magnetic dipole transitions [82–84]. The Stokes shift is small (ca $10^2\ \mathrm{cm}^{-1}$) owing to shielding of f-orbitals from the environment and the bands are in the visible and IR regions. This can be exemplified [82] by the fluorescence of $[\mathrm{TmBr_6}]^{3-}$ (f^{12} configuration), for which the bands of the transitions $^3F_3 \rightarrow {}^3H_6$, $^3H_4 \rightarrow {}^3H_6$, and $^3H_5 \rightarrow {}^3H_6$ were centred in the regions of 710, 810 and 1200 nm, respectively.

Binuclear complexes with metal–metal bonds show fluorescence in addition to phosphorescence, not only at low temperature but also in solutions at room temperature. Thus, for example [24], the anion $[\mathrm{Pt_2(P_2O_5H_2)_4}]^{4-}$ deactivates from excited states by both phosphorescence ($^3A_{2u} \rightarrow {}^1A_{1g}$, $\lambda_{\max} = 520\,\mathrm{nm}$, $\tau = 10^4\,\mathrm{ns}$) and fluorescence ($^1A_{2u} \rightarrow {}^1A_{1g}$, $\lambda_{\max} = 410\,\mathrm{nm}$, $\tau = 2\,\mathrm{ns}$). With regard to the redistribution of electron density on deactivation, both processes can be expressed as the transition $(d\sigma^2 d\sigma^{*1} p\sigma^1) \rightarrow (d\sigma^2 d\sigma^{*2})$. Simultaneously occurring phosphorescence and fluorescence were observed [70] in a study of the photophysical properties of the $[\mathrm{Rh_2(1,3\text{-}(CN)_2pn)_4}]^{2+}$ complex. Fluorescence with a maximum at 656 nm was attributed to the transition ${}^1A_{2u} \rightarrow {}^1A_{1g}$ (the maximum of the corresponding absorption band is at 553 nm) and at 20°C in CH_3CN $\Phi_{fl} = 0.07, \tau = 1.3$ ns. Under the same conditions, the complex exhibits phosphorescence with a maximum at 825 nm, a quantum yield $\Phi_{ph} = 0.32$ and a lifetime of 8500 ns. Significant Stokes shifts (fluorescence 2800 cm^{-1}) are in agreement with the marked changes in the strength of the Rh–Rh bond during transition (see Section 3.2).

Fluorescence can also be due to intraligand transitions. Until the energy difference between the first and higher spin-allowed excited states is large, fluorescence can take place not only from the first (energetically lowest) but also from higher IL states. Such a phenomenon [86–88] was observed in closed–shell porphyrin complexes, for which $\Delta E(S_2–S_1) > 6500$ cm^{-1}. Together with fluorescence $S_1 \rightarrow S_0$ ($\Phi_{fl} \approx 10^{-4}–10^{-1}$), a band of $S_2 \rightarrow S_0$ ($\Phi \approx 10^{-6}–10^{-3}$) fluorescence is also present in the emission spectra. Data for some complexes are given in Table 9. The lifetime in the S_2 state (second singlet excited state) was determined to be $\tau^0 < 3$ ps and the rate constant of the deactivation $S_2 \rightarrow S_0$ was $k_{fl} \approx 10^9$ s^{-1}.

TABLE 9

Data on $S_1 \rightarrow S_0$ and $S_2 \rightarrow S_0$ fluorescence for some metalloporphyrins

Complex	Solvent	$\Phi(S_1 \rightarrow S_0)$	$\Phi(S_2 \rightarrow S_0)$	Ref.
Zn(TPP)	ethanol	2.2×10^{-2}	1.0×10^{-3}	[112]
Zn(TPP)	hexane	1.8×10^{-2}	9.0×10^{-4}	[112]
Zn(TPP)	ACN	3.3×10^{-2}	3.7×10^{-4}	[87]
Zn(TBP)	ACN	0.35	1.6×10^{-3}	[87]
Cd(TPP)	ACN	1.0×10^{-3}	1.1×10^{-4}	[87]
Al(TPP)Cl	ACN	0.14	6.7×10^{-4}	[87]
Lu(TBP)Cl	ethanol	2.1×10^{-3}	1.3×10^{-3}	[112]
Lu(TPP)(acac)	methanol	1×10^{-3}	1×10^{-3}	[86]
Y(TPP)(acac)	methanol	6×10^{-3}	1×10^{-3}	[86]
Th(TPP)(acac)$_2$	methanol	1×10^{-4}	4×10^{-4}	[86]
H_4TPP^{2+}	benzene		5.9×10^{-5}	[88]

Analogously to fluorescence, also phosphorescence:

$$ {}^{Y}A_i^* \rightarrow {}^{X}A_{GS} + h\nu \tag{3.25} $$

can take place from different types of excited states of the ${}^{Y}A_i^*$ complex. A type of spin-forbidden, energetically lowest excited state can be determined by coordination sphere composition for complexes of the particular central atom. As an example [89], phosphorescence accompanying the deactivation Y(triplet) → X(singlet) for Ir(III) complexes takes place from the ^{3}IL state for $[IrCl_2(5,6\text{-}Me_2phen)_2]^+$, from the ^{3}MLCT state for $[IrCl_2(phen)_2]^+$ and from the ^{3}LF state for $[IrCl_4(phen)]^-$. Differences between the equilibrium geometries of the given complexes in the emitting excited state and the ground state are seen in the emission spectra. For the first two complex cations there are four bands with a small half-width ($\Delta\nu_{1/2} < 1000\,\mathrm{cm}^{-1}$) in the range 454–624 nm; the emission spectrum of the third anion consists of one wide band ($\Delta\nu_{1/2} \approx 4000\,\mathrm{cm}^{-1}$) centred around 920 nm.

It follows from the above data (small energy differences between the particular types of excited states and significant differences in the Stokes shifts) that Ir(III) complexes are appropriate for the study of the mutual relationship between molecular and electronic structures of excited complexes. If under external force effects, e.g., pressure, the molecular structure changes (equilibrium internuclear distances), then the sequence of excited state energies should also change. After demonstrating the capability of changing molecular structure and electronic configuration [reversible change of a high-spin to a low-spin Fe(II) complex] of complex in their ground state, such changes for excited complex have also been investigated [72]. The population of σ^*_{ML} orbitals in the LF excited state of Ir(III) complexes results in the volume of, for instance, $[\mathrm{IrCl_2(bpy)_2}]^+$ in the ^{3}LF state, being greater by approximately $4\,\mathrm{cm}^3\,\mathrm{mol}^{-1}$ than its volume in the ^{3}MLCT state. The energetically lowest excited state at low pressure is ^{3}LF for the given complex and at a sufficiently high pressure it is the ^{3}MLCT state for a compressed complex. These principles were confirmed by investigating the dependence of the phosphorescence of the complex on pressure. With increasing pressure the intensity of emission from the ^{3}LF state decreased (the band at $14000\,\mathrm{cm}^{-1}$) and the intensity of phosphorescence from the ^{3}MLCT state increased (bands in the region of $17\,000$–$22\,000\,\mathrm{cm}^{-1}$). The dependence of the logarithm of the ratio of these intensities on pressure was linear.

The band width in emission spectra and the Stokes shifts depend on the changes in the electron density distribution in the complex on transitions analogous to those for the complexes deactivated by fluorescence. If this is unchanged, the position of the maxima in the absorption and emission spectra will correspond to a $0 \rightarrow 0$ transition, the bands will have a small half-width and the Stokes shift will be minimal. As an example [90] for the $[\mathrm{Cr(urea)_6}]^{3+}$ complex the Stokes shift is $110\,\mathrm{cm}^{-1}$; the bands in the emission and absorption spectra (Fig. 4) correspond to $^2E \leftrightarrow {}^4A_{2g}$ transitions with a change in the spin of one of the d-electrons only. The complex cation $[\mathrm{Cr(urea)_6}]^{3+}$ is one of a few complexes showing both fluorescence and phosporescence simultaneously.

During $t_{2g}^5 e_g^1 \rightarrow t_{2g}^6$ transitions ($^3T_1 \rightarrow {}^1A_1$ in the field of O_h symmetry), the electronic configuration of the central atom changes. Depopulation of the antibonding orbital e_g on deactivation results in strengthening of the bonds and in shortening of equilibrium distances between the central atom and the ligands. These changes are reflected in the emission spectrum as a wide band [8]. The determination of the Stokes shift is usually difficult as the band of the spin-forbidden transition $^1A_1 \rightarrow {}^3T_1$ is overlapped in the absorption spectrum by more intense bands of spin-allowed LF transitions, and it is not always easy to identify it.

Vibrational structure of the bands was only observed at very low temperatures. From the analysis [91] of the emission spectra of complexes with D_{4h} ($[RhX_2L_4]^+$ cations where X = Cl, Br and L = pyridine and its derivatives) and O_h symmetry ($[Co(CN)_6]^{3-}$ anion) measured at 2 K, it can be seen that the complexes have the same symmetry in both the ground state and triplet LF state. The differences in the equilibrium M–L distances for complexes in their ground and excited states are approximately 1 pm.

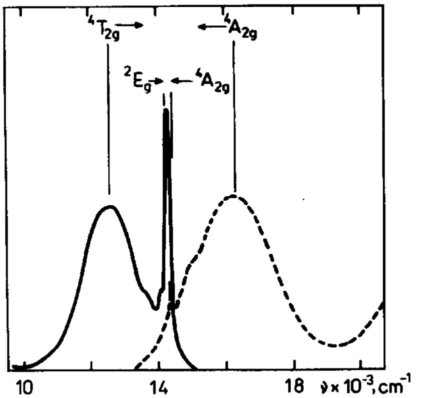

Fig. 4. Electronic absorption and emission spectra of $[Cr(urea)_6]^{3+}$.

Examples of binuclear complexes with metal–metal bonds which are deactivate simultaneously by both fluorescence and phosphorescence were considered above. Some polynuclear complexes exhibit only phosphorescence. For example [92], there are $[Pt_2(P_2O_5H_2)_4X_2]^{4-}$ complexes (X = Cl, Br, NCS) which exhibit strong red triplet → singlet phosphorescence at 77 K in an EtOH/MeOH glass (centred at 685, 715 and 754 nm, respectively). The phosphorescence is cation- and solvent-sensitive ($\tau \approx 10^4$ ns) and the emissive excited state has $d\sigma^*$ character and is strongly distorted along the Pt–Pt coordinate. Not only d^7–d^7 Pt(III) complexes, presented above, are deactivated by phosphorescence, but also d^8–d^8 Rh(I), Ir(I) and Pt(II) complexes. For example [93], $[Pt_2(P_2O_5H_4)]^{4-}$ exhibits green phosphorescence ($\lambda_{max} = 517$ nm, $\tau = 10^4$ ns). The emitting state is $^3A_{2u}(d\sigma^* p\sigma)$.

Phosphorescence can also be due to f–f transitions in the complexes of lanthanoids and actinoids. In the $[TmBr_6]^{3-}$ ion a vibrationally structured band of phosphorescence $^1G_4 \rightarrow {}^3H_6$ centred at 485 nm (the absorption maximum of $^3H_6 \rightarrow {}^1G_4$ is at 475 nm) is also present in the emission spectrum together with fluorescence [82]. Great attention was paid to the study of the luminescence of Eu(III) complexes in which the Eu(III) ion possesses non-degenerated ground ($^7F_0$) and emitting excited ($^5D_0$) states. The study of the spectral properties of thirty-six Eu(III) complexes has shown [31] that the $^7F_0 \rightarrow {}^5D_0$ transition exhibits a band with a very small half-width, the position of the emission maximum being in the range 17 226–17 275 cm^{-1}, depending on the types of ligands present and the experimental conditions.

Phosphorescence as a manifestation of intraligand $\pi^* \rightarrow \pi$ transitions was observed in some diamagnetic complexes with aromatic ligands. The kinetic parameters of IL phosphorescence depend on the properties of the central atom. For example [86], the lifetimes of phosphorescence for porphyrin Y(III), Lu(III) and Th(IV) complexes decrease as 29×10^{-3}, 2.8×10^{-3} and 3×10^{-4} s and the quantum yield increases to 0.01, 0.02 and 0.03. Reduction of the spin forbiddenness of triplet–singlet transitions due to spin–orbit coupling induced by the central atom results in a marked decrease in the excited coordinated ligand lifetime compared with a non-coordinated ligand. Under the same conditions, for example [94], the triplet IL state of non-coordinated 1,10-phenanthroline has a lifetime $\tau \approx 1.5$ s; on the other hand, when coordinated in the $[Rh(phen)_3]^{3+}$ ion a lifetime $\tau = 0.048$ s is observed.

An interesting situation occurs with some mixed ligand complexes, e.g., $[Rh(phen)_2(bpy)]^{3+}$ and $[Rh(phen)(bpy)_2]^{3+}$. For these complexes a definite non-exponential decay curve can be deconvoluted to give two lifetimes, τ(bpy) and τ(phen), the magnitudes of which are identical with those measured for the pure precursor complexes $[Rh(phen)_3]^{3+}$ and $[Rh(bpy)_3]^{3+}$. Apparently, the ligand localized phosphorescence from the mixed ligand complexes occurs from states essentially characteristic of a single chelate (phen or bpy) ring [95]. It is possible that also for complexes $[Rh(bpy)_3]^{3+}$ and $[Rh(phen)_3]^{3+}$ phosphorescence will be a consequence of the intraligand transition localized on one of the ligands, and not due to the transition between MO delocalized on the whole coordination sphere. The phenomenon of simultaneous emission from several energetically close excited states of one substance is called multiple state emission [95].

Multiple state emission is observed with some complexes with a low-lying LLCT excited state. Thus, for example [40], [Zn(4-Cl–PhS)] exhibits a prominent structured blue-green emission that decays in 0.76 s and originates from ^{3}IL(phen), in addition to a broad band with a maximum at 17 000 cm^{-1} ($\tau \approx 10^4$ ns) which originates from the ^{3}LLCT state of the complex. Other mixed ligand complexes of Zn(II) and Cd(II) are also deactivated by phosphorescence from the ^{3}LLCT state.

With d^6 complexes of the second and third transition-row elements with bipyridine and phenanthroline and their derivatives, radiative deactivation $^3T_{1u} \rightarrow {}^1A_{1g}(t_{2g}^5 t_{1u}^1 \rightarrow t_{2g}^6$, where t_{1u} is a π^* orbital localized on the ligand) has been followed in connection with the study of solar energy utilization. Considerable attention was, and still is being paid particularly to the $[Ru(bpy)_3]^{2+}$ complex. The emitting excited state is a state of ^{3}MLCT character. Interest in this complex and its derivatives was evoked by the fact that these complexes absorb radiation in the visible region and have long lifetime ($\tau \approx 10^{-9}$–10^{-6} s) in the excited emitting state, as well as at room temperature in solutions [48].

The effect of pressure on the equilibrium between the ^{3}MLCT and ^{3}LF excited states of the $[Ir(Mephen)_2Cl_2]^+$ complex has already been presented. Multiple-state emission covering the MLCT excited state was also observed [95] with other Ir(III) complexes. In the Re(I) and Cu(I) complexes phosphorescence from the MLCT state is accompanied by phosphorescence from the IL excited state.

In the introduction to this section, it was mentioned that fluorescence and phosphorescence are intramolecular deactivation processes. The effect of external factors (pressure, temperature, solvent, counter-ion) on luminescence can be considered with regard to (a) the effect on other deactivation processes and (b) the effect on the molecular and electronic structure of the emitting complex itself.

The first factor, for example, can be seen in the effect of temperature on excited state lifetimes when temperature influences the rate of non-radiative deactivation, and this is reflected in the kinetics of luminescence quenching (usually $1/\tau$ is inversely proportional to $1/T$). As an example [96], luminescence lifetimes of $[Ru(bpy)_3]^{2+}$ in CH_3CN are 1020 ns at 20°C, 730 ns at 30°C, 460 ns at 40°C and 270 ns at 50°C.

The counter-ion and solvent influence both non-radiative decay rate constants and the spectral characteristics of the absorption and emission of the complex (positions of band maxima, shape of the spectral line, radiative decay rates) as a consequence of changes in ion–dipole interactions with changes in the counter-ion or solvent. The solvent effect exhibits itself in luminescence analogously to that in absorption and it is mainly the result of the effect of the electric field of solvent molecules forming the secondary coordination sphere on the electronic system (HOMO and LUMO) of the complex.

In addition to the above interactions, the effects of the counter-ion can be realized by the formation of ion pairs. The tendency to form ion pairs for excited complexes depends on the charge of the complex, the type of excited state and the properties of the solvent. Of course, changes in the formation of ion pairs in the excited state versus the ground state of the complex can take place only if the lifetime of the excited complex is sufficiently long for reorganization of the secondary coordination sphere. Of the various solvent properties, its dielectric constant is particularly important. For example [97], the emission spectrum of $[Os(phen)_3]^{2+}$ ion in propylene carbonate (dielectric constant $\varepsilon_r = 65$ at 20°C) does not depend on the counter-ion X^-, but in CH_2Cl_2 (dielectric constant $\varepsilon_r = 9$) the position of the emission maximum from the ^{3}MLCT state changes depending on X^- from 694 nm ($X^- = BPh_4^-$) to 714 nm ($X^- = Cl^-$) the lifetime from 357 ns ($X^- = BPh_4^-$) to 245 ns ($X^- = Cl^-$) and the rate constant of non-radiative deactivation, k_d, from 2.8×10^6 s^{-1} ($X^- = BPh_4^-$) to 4.08×10^6 s^{-1} ($X^- = Cl^-$).

The change in the tendency to form an ion pair in the excited state versus the ground state depending on the type of excitation depends on the change in dipole moment (e.g., the dipole moments in the excited states $[Ru^{III}(bpy)_2(bpy^-)]^{2+}$ and $[Os^{III}(bpy)_2(bpy^-)]^{2+}$ have been estimated to be 14 ± 6 and 13 ± 6 D [97]), hence it will be larger in CT than, e.g., in LF excited states.

Studies of the effect of pressure on phosphorescence of the $[Ru(bpy)_3]^{2+}$ complex (the use of $[Ru(bpy)_3](PF_6)_2$ monocrystals ruled out solvent effects) have shown [98] that with increasing pressure the emission intensity decreases, in addition to the band half-width in the emission spectrum and the transition energy. These changes are due to a reduction in the volume and an increase in the rigidity of the complex under the action of pressure changes in the properties of the electronic system of the complex and changes in the non-radiative relaxation rate.

The effect of pressure on photochemical and photophysical properties has been investigated more widely for solutions of coordination complexes than for monocrystals. From the data obtained (activation volumes of particular processes), much valuable information on the mechanism of deactivation processes can be derived. For example, it has been found [99] that the effect of pressure on phosphorescence from the LF state of the $[Rh(NH_3)_5Cl]^{2+}$ complex depends on the solvent properties. If the solvent is DMF, the emission lifetime decreases with increasing pressure ($V^{\neq}_{em} = +1.2$ cm^3 mol^{-1}), whereas if the solvent is FMA or DMSO a reverse situation is observed ($V^{\neq}_{em} = -0.6$ and -0.5 cm^3 mol^{-1}, respectively). These data together with the parameters for photosubstitution deactivation processes, enabled in detail the energy changes on substitution of an NH_3 molecule or Cl^- anion in the complex to be evaluated.

Not only the dependence of activation parameters on pressure, but also the dependences of rate constants, quantum yields and lifetime on applied pressure have been investigated directly. For example [96], for $[Ru(bpy)_3]^{2+}$ in CH_3CN at 25°C the quantum yield of phosphorescence and the lifetime increase with increasing pressure (by 42% and 39%, respectively, at a pressure of 300 MPa when compared with normal pressure), the rate constant of radiative deactivation hardly changes with pressure (3% increase) and the rate constant of non-radiative deactivation decreases with pressure (by 30% at a pressure of 300 MPa). These changes concern specifically the given complex and are not applicable to the general trend for the other complexes. For example, a structurally similar complex of $[Os(phen)_3]^{2+}$ under analogous conditions changes its characteristics with pressure to a much lesser extent and with the opposite tendency (the quantum yield of luminescence decreases by 5%, the rate constant of non-radiative deactivation increases by 8% and the lifetime decreases by 7%).

In connection with the discussion of the effect of external factors on the characteristics of radiative deactivations, it should be mentioned that luminescence can be evoked by external force effects (see Section 2.2.4). The hitherto known [25, 26] triboluminescence cases of coordination compounds include phosphorescence [e.g., $^4T \rightarrow {}^6A$ in the LF excited compounds of Mn(II); $^3E_u(^3A_{1u}) \rightarrow {}^1A_{1g}$ in Pt(II) complexes; $^3\pi_u \rightarrow {}^1\Sigma_j$ in the LF excited salts of UO_2^{2+}]. It seems to be worth mentioning that also photoluminescence and temperature-induced spontaneous emission of UO_2^{2+} originate in the $^3\pi_u$ state [104].

In the study of possibilities of the conversion of solar energy into chemical and electric energy, properties of systems containing micelles have been and still are being studied. Investigation of the kinetic parameters of the phosphorescence of Ru(II) complexes with 1,10-phenanthroline and its derivatives in systems in the absence and presence of Triton X-100 and Triton X-114 micelles has shown [100] that binding of the complexes to the micelles has little effect on the phosphorescence lifetime. The ratio of τ_{CM} values (a system with a complex bonded to a micelle) to τ^0 (free complex in solution) was not higher than 1.9. The effect of micelles on the luminescence lifetime is thus similar to the effect of the solvent (for example [42], the $[Ru(bpy)_2(CN)_2]$ complex at 21°C has lifetimes of $\tau^0 = 220$ ns in DMF, 400 ns in CH_3OH and 270 ns in H_2O).

3.4 Energy transfer

Quantum chemical and thermodynamic conditions of energy transfer are explained in Section 2.2.2; relationships between thermodynamic and kinetic parameters of energy transfer are analogous to those of electron transfer (Section 4.2). The lifetime of an excited particle D* (determined by the rate constants of competing deactivation processes) must be sufficient for energy transfer within the observable range. Therefore, on energy transfer the excited donor of energy D* is usually in a longer-lived spin-forbidden state.

Quenching of donor D* with acceptor A usually suggests the process of energy transfer but it should be borne in mind that quenching can be due to other processes, e.g., redox processes or photochemical reactions of excited acceptor A.

When discussing eqn. 3.15, it was shown that the ratio τ^0/τ can be replaced by the ratio Φ^0/Φ, or I^0/I for luminescence. However, this is only true when no association between A and Q takes place (e.g., formation of ion pairs). If association (characterized by the value of the association constant K_{as}) does take place, the form of the Stern–Volmer equation of quenching is different for the ratio of lifetime and quantum yields of luminescence. This difference is illustrated [20] using the results of phosphorescence quenching from the triplet MLCT state of the $[Ru(phen)_2(CN)_2]$ complex with ions of Ni^{2+} in water; in this process the AQ associate does not emit radiation and does not decay on excitation forming A*. The dependences of τ^0/τ and Φ^0/Φ on Ni^{2+} concentration are shown in Fig. 5. From the slope of the linear dependence of τ^0/τ on Ni^{2+} concentration ($K_{SV} = 14.3$) and the triplet lifetime $\tau^0 = 710\,\mathrm{ms}$, a value of $k_q = 2 \times 10^7\,\mathrm{l\,mol^{-1}\,s^{-1}}$ was calculated. The dependence of Φ^0/Φ on $[Ni^{2+}]$ is non-linear. With dynamic and static quenching, provided that $[Q] \gg [A]$ and that the AQ pair does not emit radiation and does not decay on excitation forming A*, the following equation is valid:

$$\frac{\Phi^0}{\Phi} = 1 + K^{\Phi}_{SV}[Q] = 1 + [Q](K^{\tau}_{SV} + \beta K_{as} + [Q]K_{SV}\beta K_{as}) \qquad (3.26)$$

For solutions with absorbance lower than 0.1, $\beta = 1$; for optically concentrated solutions (absorbance higher than 2), β is equal to the ratio of the molar absorption coefficients of A and AQ associate at the excitation wavelength. For the above example, values of $K^{\Phi}_{SV} = 55$ and $K_{as} = 20\,\mathrm{l\,mol^{-1}}$ were calculated from the experimental data.

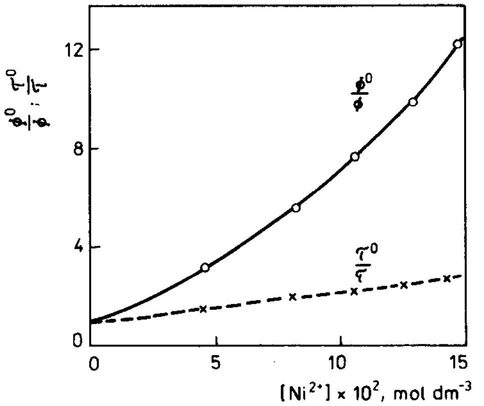

Fig. 5. Plots of Φ^0/Φ and τ^0/τ vs. the concentration of Ni^{2+} ions in the phosphorescence quenching of the $^*[Ru(bpy)_2(CN)_2]$ complex by Ni^{2+} ions in aqueous solution at 21°C.

Analogous to the energy transfer in the associate of donor A* with quencher Q is the energy transfer within the polynuclear complexes. As an example [101], energy transfer from LF excited states $^1T_{1g}$ and $^3T_{1g}$ localized on the $Co(III)C_6$ chromophore to the states of $^4T_{2g}$ and ^2E_g localized on the $Cr(III)N_6$ chromophore in the binuclear complex $[(NC)_5Co{-}CN{-}Cr(NH_3)_5]$ can be considered. If the spectral properties of this complex are compared with the photophysical and photochemical properties of the mononuclear complexes $[Cr(NH_3)_6]^{3+}$ and $[Co(CN)_6]^{3-}$ (the spectrum of a binuclear complex is almost identical with the superposition of the spectra of the mononuclear complexes) (some parameters are shown in Fig. 6), it can be seen from the photoexcited LF states localized on the CoC_6 chromophore that intramolecular energy transfer takes place with 75% efficiency on the CrN_6 chromophore.

So far, examples were presented in which energy transfer resulted in the formation of the energetically lowest excited state of acceptor A. According to the Rehm–Weller theory [102, 103], the value of the Gibbs activation energy of transfer (the theory was originally elaborated for electron-transfer processes), $\Delta G^{\neq}_{DA}$ asymptotically approaches zero with increasing ergonicity of the process (by a decrease in ΔG_{DA}) and the value of quenching rate constant, k_q, can be equal to that of the diffusion rate constant, k_{dif}.

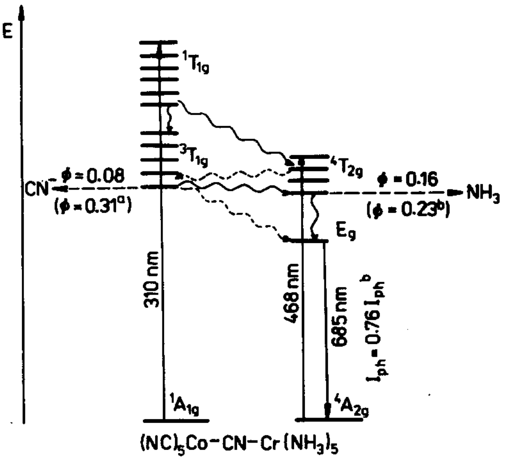

Fig. 6. Spectral properties and parameters of photophysical and photochemical deactivation processes of excited $[(NC)_5Co–CN–Cr(NH_3)_5]^*$. [a]Corresponding values for $[Co(CN_6)]^{3-}$ complex. [b]Values for the binuclear complex in the $^4T_{2g}$ excited state; the other values are for the binuclear complex in its $^1T_{1g}$ excited state.

In strongly non-adiabatic processes, at a point in the exoergonic region, the formation of energetically higher excited states of A may be expected [19]. This is manifested in a stepwise change in the dependence of log k_q on ΔG_{DA}. Such a dependence (Fig. 7) was observed for energy transfer between the triplet state of different organic donors, $^3D^*$, and the $[Cr(acac)_3]$ complex and other Cr(III) complexes [103]. The plateau region (log $k_q \approx 8$) corresponds to the process

$$ {}^3D_i^* + (GS)[Cr(acac)_3] \rightarrow {}^1D_i + ({}^2E_g)[Cr(acac)_3] \qquad (3.27) $$

where ^2E_g is the energetically lowest doublet of the Cr(III) complex, the triplet energy $^3D_i^*$ being lower than 2.5 eV. The following plateau (log $k_q \approx 9$) corresponds to the process

$$^3D_j^* + (\mathrm{GS})\,[\mathrm{Cr(acac)_3}] \rightarrow {}^1D_j + (^2T_1)\,[\mathrm{Cr(acac)_3}] \tag{3.28}$$

where $^2T_1$ represents an energetically higher LF state of the Cr(III) complex (depending on the ligand field symmetry, the states can be split). The process occurs if the donor triplet energy $^3D_j^*$ is larger than 2.5 eV.

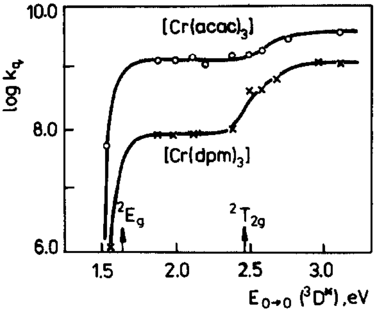

Fig. 7. Plot of log k_q vs. the triplet energy of organic donors for the redox quenching of excited donors by [Cr(acac)$_3$] and [Cr(dpm)$_3$]. The positions of the arrows indicate the energies of $^4A_{1g} \rightarrow {}^2E_g$ and $^4A_{1g} \rightarrow {}^2T_{2g}$ transitions for Cr(III) complexes.

All of the examples of energy-transfer processes discussed so far have included systems in which such processes can be followed by measurement of emission spectra. There are also non-emitting systems for which the occurrence of an energy-transfer process can only be deduced on the basis of chemical changes during irradiation. Systems containing Fe(II) and Fe(III) halogeno complexes in methanol/acetone mixtures irradiated with light absorbed by the Fe(III) complexes only ($\lambda_{\mathrm{irr}} \geqslant 365\,\mathrm{nm}$) may serve as an example.

A detailed investigation of the properties of above irradiated systems led to the conclusion that in addition to the spontaneous oxidation of Fe(II) by acetone due to the mutual influence of ligands via the central atom (the reaction denoted by the rate constant k_4 in (3.29) and the photoreduction of Fe(III) accompanied by the oxidation of methanol (step k_3), the oxidation of Fe(II) sensitized by the excited Fe(III)* complexes (steps k_5 and k_7) also occurred [105–109]:

$$\begin{tikzcd}
 & & & & \mathrm{Fe(II)} \\
\mathrm{Fe(III)} \arrow[r, "I(h\nu)", "k_2"'] & \mathrm{Fe(III)^*} \arrow[l, bend right=50, "k_1"'] \arrow[l, bend left=50] \arrow[d, "k_3"] & +\ \mathrm{Fe(II)} \arrow[d, "k_4"] \arrow[r, "k_5"] & \mathrm{Fe(III)} + \mathrm{Fe(II)^*} \arrow[urr, "k_6"] \arrow[drr, "k_7"'] & & \\
\mathrm{Fe(II)} & \mathrm{Fe(II)} & \mathrm{Fe(III)} & & \mathrm{Fe(III)}
\end{tikzcd} \tag{3.29}$$

In eqn. 3.29, Fe(II) and Fe(III) represent the respective Fe(II) and Fe(III) chloro or bromo complexes and I is the intensity of light absorbed by the Fe(III) complexes.

The limiting quantum yield of Fe(III) formed by the photosensitized oxidation of Fe(II)* was evaluated from the plot of $(\Phi_{\mathrm{Fe(III)}})^{-1}$ vs. $([\mathrm{Fe(II)}])^{-1}$ and reached values of 0.1–0.8, depending on the composition of the systems. Based on these values, it is obvious that both the energy-transfer (process k_5) and the Fe(II)* oxidation are very effective processes.

3.5 Exciplex and excimer formation

Changes in the electronic and molecular structures of a molecule A due to the formation of an excited state can result in chemical bonding between the excited molecule A* and another molecule Q of the system, yielding an excited adduct (A–Q)*. Such an adduct formed in a bimolecular dynamic adiabatic process:

$$\mathrm{A}^* + \mathrm{Q} \rightarrow (\mathrm{A{-}Q})^* \tag{3.30}$$

has been called an exciplex. It should be noted that A and Q can be ions or radicals (the term "molecule" will be used, however, in the following text), and the molecule Q may, in principle, also be in an excited state.

If both (or more, in general) molecules are identical in the ground state (A = Q) and at least one of them is in an excited state, their excited adduct (A–A)* has been named an excimer. The terms exciplex and excimer are usually used for cases when adduct formation between ground-state molecules does not occur.

Both exciples and excimers have their own properties (stability constant, lifetime, energy content, multiplicity, pathways of deactivation, etc.) and can thus be regarded as new chemical species.

The wavefunction of an exciplex (excimer), Ψ_{exc}, can be expressed as a combination of various excitation resonance and charge-transfer terms [113]:

$$\Psi_{\mathrm{exc}} = N(a\Psi_{(\mathrm{A}^* - \mathrm{Q})} + b\Psi_{(\mathrm{A} - \mathrm{Q}^*)} + c\Psi_{(\mathrm{A}^+ - \mathrm{Q}^-)} + d\Psi_{(\mathrm{A}^- - \mathrm{Q}^+)}) \tag{3.31}$$

Depending on the values of the coefficients *a*–*d*, exciplexes may be classified into two basic groups: charge-transfer exciplexes ($a, b < c$ or d) and non-polar (covalent) exciplexes ($c, d < a$ or b). In most instances both charge-transfer and excitation resonance contribute to the stability of exciplex, but to different extents.

For an exciplex (excimer) to be formed, some requirements must be fulfilled. Of the kinetic factors, a sufficiently long lifetime of the excited molecule A* is necessary, as the formation of an exciplex is a dynamic diffusion-limited process. In this connection, it is obvious that the concentration of excited A* must be high enough (usually powerful lasers must be used as the source of light). When discussing the possibility of the formation and stability of exciplexes from the viewpoint of thermodynamics, it is worth noting that both enthalpy and entropy contributions may be important. Of course, parameters such as redox potentials and electron-donating and -accepting ability depend strongly on the electronic structure of the molecules A* and Q.

Exciplexes and excimers are usually studied using laser flash photolysis, transient absorption and emission spectra measurements and studies of the kinetics of excited-state decay. There are experimental results which have been interpreted as being due to exciplex formation, but difficulties with the direct observation of the non-emitting exciplexes have been emphasized and often exciplex formation involving a coordination compound is speculative. With emitting exciplexes, the interpretation of experimental observations is simpler.

A complex can act in the process of exciplex (excimer) formation as an excited molecule A* or as quencher Q. The latter can be exemplified [114] by exciplex formation between a singlet excited 9,10-disubstituted anthracene, ^{1}(ANC)*, and singlet ground-state allyl- or benzylstannanes, $^1(SnR_4)$. The quenching of the fluorescence of substituted anthracenes by tin organometallics was proposed to occur via a charge-transfer stabilized exciplex-mediated bimolecular reaction mechanism. No new emision of the exciplexes $^1(ANC^- - SnR_4^+)$ was observed. Below the attention will be focused on exciplexes (excimers) formed by an excited complex.

The formation of exciplexes and excimers is well documented in the photochemistry of organic and polymeric compounds but it is not so common in the photochemistry of coordination compounds containing a metal atom as the central atom.

As can be seen in Table 10, most exciplexes involving complexes are those with a macrocyclic (porphyrin or phthalocyanine) ring. These complexes resemble organic compounds to a greater extent than inorganic complexes. The multiplicity of excited complexes A* is limited (with a few exceptions) to a singlet or triplet, as it is in organic systems. Moreover, in many instances the interaction of a quencher Q with an excited complex A* does not involve the central atom, and "organic fragments" of the exciplex-forming partners are directly bonded. The excited states of A* are predominantly intraligand in nature ($\pi - \pi^*$ triplet or singlet localized on a macrocycle ligand), but the formation of exciplexes by excited complexes in the MLCT excited state is also known.

A number of exciplex systems are given in Table 10, and those of excimers in Table 11. In this section only a few particular examples are introduced.

An emitting charge-transfer exciplex formation has been reported [117]. It was found that in the presence of *N*,*N*-dimethylaniline (DMA), the wavelength of phosphorescence of $^3[Re(dpphen)(CO)_3Cl]^*$ from its excited MLCT triplet state was shifted from 575 to 600 nm in non-polar media (alkanes). In acetonitrile the wavelength of emission was not changed but the emission was simply

TABLE 10

Examples of exciplexes (A–Q)* containing a coordination compound

Excited molecule A*	Excited state	Quencher Q	Solvent	Ref.
9,10-XY–anthracene X,Y = CN,CN; CN,H; Br,Br; Cl,Cl; H,H; CH_3,H; CH_3,CH_3	^{1}IL	[4-X–C_6H_4–CH_2–Sn(n-Bu)$_3$] X = H, F, Cl, CH_3, OCH_3 [C_6H_5–CH_2–SnL_3] L = Me, Ph [allyl–SnL_3] L = Br, Me [$SnMe_4$]	benzene, toluene, cyclohexane, ethanol, n-hexane, acetonitrile tetrahydrofuran	[114]
[Ir(C^3, N'-bpy)(bpy)$_2$]$^{2+}$	^{3}MLCT	Br^-[non-emitting(A–Q)]	water	[131]
[Ir(C^3, N'-bpy)(bpy)$_2$Br]$^+$	^{3}MLCT	Br^- [emitting(A–Q)]		
[Re(dpphen)(CO)$_3$Cl]	^{3}MLCT	DMA	decalin, isooctane	[117]
[Ru(bpy)$_3$]$^{2+}$	^{3}MLCT	O_2	water	[132]
[Cu(PPh_3)$_2$(BH_4)]^a		NBD	benzene	[133]
UO_2^{2+}	^{3}LMCT	H-atom (abstracted from H_2O or CH_3OH molecule) Tl^+, Ag^+, Pb^{2+}, Hg^{2+}, Cu^{2+}, Mn^{2+}	water water/methanol	[134–136]
$(UO_2H)^{2+}$		UO_2^{2+}	water	
[Pc–Ln–PcH] Ln = Nd, Lu, Y	^{3}IL	CH_2Cl_2	CH_3CN/CH_2Cl_2	[137]
[Ru(Pc)LL′] L,L′ = DMSO,DMSO; DMF,CO; py,CO; CH_3OH,Cl	^{3}IL	p-$(NO_2)_2C_6H_4$ paraquat diaquat	CH_2Cl_2 acetonitrile	[138]

TABLE 10 (continued)

Excited molecule A*	Excited state	Quencher Q	Solvent	Ref.
[Mg(TBPc)], [In(TBPc)OH], [Al(TBPc)Cl], [Al(TBPc)OH], [TiO(TBPc)], [Mg(TPP)], [In(TPP)OH], [Al(TPP)OH], [Al(TPP)Cl], [Ga(TPP)OH], [TiO(TPP)]	^{3}IL	benzoquinones, naphthoquinones, phenanthrenequinones, nitroaromatics, picryl chloride	toluene	[139, 140, 149]
[Chlorophyll *a*] [Chlorophyll *b*]	^{3}IL	nitroaromatics, benzaldehyde, benzoquinone, methylnaphthoquinone	benzene, toluene, hexane, dioxane, diethyl ether, DMF, alcohols	[141]
[Zn(Etio)], [Mg(Etio)], [Zn(TPP)]	^{3}IL	nitroaromatics, chloroalkanes, chloroaromatics	benzene	[125] [119]
	^{1}IL	nitrostilbenes	benzene, ethanol	[119]
[Zn(TMPyP)]	^{3}IL	methylviologen, MV^{2+}	water	[123]
[Pd(TPP)]	^{3}IL	dimethylaniline, DMA	benzene, pyridine, acetone, 2-propanol, isobutyronitrile	[121]
[In(TPP)]$^+$	^{3}IL	methylviologen, MV^{2+} triethanolamine, TEA	methanol	[124]
[In(TPP)(MV)]$^{3+}$		TEA		
[In(TPP)(TEA)]$^+$		MV^{2+}		
[Al(TPP)(OH)], [Mg(TPP)]	^{3}IL	quinones	toluene	[142]
[Mg(TPP)(py)]	^{3}IL	nitroaromatics	toluene	[118, 143]

TABLE 10 (continued)

Exctited molecule A*	Excited state	Quencher Q	Solvent	Ref.
[Zn(TPP)]	^{1}IL	*p*-benzoquinone, chloranil	dioxane, toluene, ethanol, DMF, acetone	
	^{3}IL	*p*-benzoquinone, chloranil *p*-X–$C_6H_4N_2^+$ X = H, Br, Cl, CH_3, OCH_3, $N(C_2H_5)_2$		[122, 144] [145]
$[Cu(dmphen)_2]^+$ $[Cu(PPh_3)_2(phen)]^+$	MLCT	methanol, acetone, acetonitrile, water, pyrazine	CH_2Cl_2	[146]
$[Ru(bpy)_3]^{2+}$ $[Ru(4,7\text{-}Me_2bpy)_3]^{2+}$	MLCT	Ag^+	water	[116]
$[Pt_2(P_2O_5H_2)_4]^{4-}$	$\sigma\sigma^*(Pt_2)$	Tl^+	water	[115]
$[Ru(bpz)_3]^{2+}$	MLCT	Ag^+	water	[150]

TABLE 11
Representative examples of excimers formed by metal-containing compounds

Excimer-forming molecules	Excimer	Solvent	Ref.
2 ${}^3[\mathrm{Zn(OEP)}]^*$	${}^1[\mathrm{Zn(OEP)\text{–}Zn(OEP)}]^*$	benzene	[129, 130]
2 ${}^3[\mathrm{Zn(TPP)}]^*$	${}^1[\mathrm{Zn(TPP)\text{–}Zn(TPP)}]^*$	benzene	
2 ${}^3[\mathrm{Al(Pc)Cl}]^*$	${}^1[\mathrm{Al(Pc)Cl\text{–}Al(Pc)Cl}]^*$	cyclohexane	
2 ${}^3[\mathrm{Si(Pc)(OEt)_2}]^*$	${}^1[\mathrm{Si(Pc)(OEt)_2\text{–}Si(Pc)(OEt)_2}]^*$	1-chloronaphthalene	
${}^3[\mathrm{Pd(TPP)}]^* + {}^1[\mathrm{Pd(TPP)}]$	${}^3[\mathrm{Pd(TPP)\text{–}Pd(TPP)}]^*$	toluene, THF mineral oil	[127, 147, 148]
${}^3[\mathrm{Pt(Etio)}]^* + {}^1[\mathrm{Pt(Etio)}]$ ${}^3[\mathrm{Zn(Etio)}]^* + {}^1[\mathrm{Zn(Etio)}]$	${}^3[\mathrm{Pt(Etio)\text{–}Pt(Etio)}]^*$ ${}^3[\mathrm{Zn(Etio)\text{–}Zn(Etio)}]^*$	mineral oil, THF	[127]
${}^2[\mathrm{Cr(phen)_3}]^{3+*} + {}^4[\mathrm{Cr(phen)_3}]^{3+} + \mathrm{X}^-$ $\mathrm{X}^- = \mathrm{ClO_4^-}, \mathrm{NO_3^-}, \mathrm{Br^-}, \mathrm{BrO_3^-}$, $\mathrm{SO_4^{2-}}, \mathrm{Cl^-}, \mathrm{HSO_4^-}$	$[\mathrm{Cr(phen)_3^{3+}\text{–}X^-\text{–}Cr(phen)_3^{3+}}]^*$	water	[128]
${}^3\mathrm{UO_2^{2+*}} + \mathrm{UO_2^{2+}} + \mathrm{H_2O}$	$[\mathrm{U_2O_4H}]^{4+*}$	water	[134, 135]

quenched obeying Stern–Volmer dependence. Based on experimental data, the enthalpy of formation of the exciplex $[Re(dpphen)(CO)_3Cl^- —DMA^+]^*$ was calculated to be $\Delta H_f = -239$ kJ mol^{-1} and the energy of the exciplex was evaluated as 2.08 eV.

The importance of the contribution of entropy to the stability of exciplexes has been pointed out [118]. A very detailed theoretical treatment of the formation of the triplet exciplexes $^3[Mg(TPP)(py)–XC_6H_4NO_2]^*$ (where X = 4-NO_2, 3-NH_2, 4-CH_3) led to the conclusion that high stability of the exciplex was due predominantly to the positive magnitude of ΔS values.

A number of complexes are able to form exciplexes in different excited states. It was shown [119] that singlet and triplet exciplexes of $[Zn(Etio)]^*$, $[Zn(TPP)]^*$ and $[Mg(Etio)]^*$ with nitrostilbenes did not interconvert and had different reactivities in producing *cis-trans* isomerization in nitrostilbenes (the triplet exciplexes were much more active).

On the other hand, other complexes of Zn(II) and Mg(II) (chlorophyll *a*, zinc(II) mesoporphyrin IX dimethyl ester [120]) form exciplexes with electron acceptors (nitro compounds, *p*-benzoquinone, chloranil) only when in their singlet excited state. Based on experimental observations, the absence of intersystem crossing in exciplexes seems to be a general phenomenon.

Exciplexes of porphyrin and phthalocyanine complex are usually characterized as being of the charge-transfer type, or at least with a significant charge-transfer contribution. The formation of the non-polar exciplex $^3[Pd(TPP)–DMA]^*$ has been described [121]. The stabilization energy of this exciplex does not exceed a few kJ mol^{-1} and the equilibrium constant for exciplex formation is $K \approx 10$ l mol^{-1}. The excitation within the exciplex is localized on the porphyrin ring, i.e., in the wavefunction in eqn. 3.31 for the exciplex $a \gg b, c, d$.

Of various medium effects on the formation and deactivation of exciplexes, the effects of solvent polarity and ionic strength have been investigated in detail.

It is believed that the polarity of the solvent should strongly influence the formation and stability of charge-transfer exciplexes but has only a small (or negligible) effect on non-polar exciplexes. A strong influence of the solvent on exciplex formation was demonstrated, for example [117], by investigating the properties of solutions of $^3[Re(dpphen)(CO)_3Cl]^*$ in the presence of DMA. However, when the sum of the absolute values of the charges localized on the particles forming an exciplex is not changed on exciplex formation (charge is only exchanged but not formed), solvents should not exhibit a strong influence on charge-transfer exciplex formation and such exciplexes could be found even in polar media.

Charge-transfer exciplex formation in a polar solvent (acetone) was reported [122] for a case of triplet $^3[Zn(TPP)]^*$. The excited neutral complex $^3[Zn(TPP)]^*$ interacts with a diazonium arene cation:

$$ {}^3[\mathrm{Zn(TPP)}]^* + 4\text{-X-}\mathrm{C_6H_4N_2^+} \rightarrow {}^3[\{\mathrm{Zn(TPP)}\}^+ - (4\text{-X-}\mathrm{C_6H_4N_2})^0]^* \qquad (3.32) $$

forming a charge-transfer exciplex that is subsequently decomposed:

$$ {}^3[\{\mathrm{Zn(TPP)}\}^+ - (4\text{-X-}\mathrm{C_6H_4N_2})^0]^* \rightarrow [\mathrm{Zn(TPP)}]^+ + \mathrm{N_2} + 4\text{-X-}\mathrm{C_6H_4} \qquad (3.33) $$

(X = H, Br, Cl, CH_3, CH_3O, $N(C_2H_5)_2$). It was found that the tendency of the respective exciplexes to undergo radiationless deactivation follows the Hammett parameters of the substituent X. It follows from reaction 3.32 that in exciplex formation an electron was trasferred from the excited donor to a diazonium cation.

The effect of ionic strength on exciplex deactivation was investigated [123] for aqueous solutions of the triplet excited ${}^3[\mathrm{Zn(TMPyP)}]^*$ and methylviologene, MV^{2+}. The exciplex ${}^3[\mathrm{Zn(TMPyP)(MV)}]^{2+}$ decomposes according to

$$ [\mathrm{Zn(TMPyP)}]_{\mathrm{GS}} + \mathrm{MV}^{2+} \leftarrow {}^3E \rightarrow [\mathrm{Zn(TMPyP)}]^+ + \mathrm{MV}^+ \qquad (3.34) $$

where ${}^3E$ denotes the exciplex. The yield of redox products decreases with increase in the ionic strength. Also in the presented example, the exciplex should be charge-transfer in nature and was formed in polar media.

The possibility of exciplex formation may depend not only on the electronic but also on the steric properties of molecules A and Q. Some interesting results have been published in this connection [124]. The excited triplet ${}^3[\mathrm{In(TPP)}]^+$ in methanol forms exciplexes with MV^{2+} (cation–cation interaction):

$$ {}^3[\mathrm{In(TPP)}]^+ + \mathrm{MV}^{2+} \rightleftharpoons {}^3[\mathrm{In(TPP)(MV)}]^{3+} \qquad (3.35) $$

as well as with triethanolamine:

$$ {}^3[\mathrm{In(TPP)}]^+ + \mathrm{TEA} \rightleftharpoons {}^3[\mathrm{In(TPP)(TEA)}]^+ \qquad (3.36) $$

MV^{2+} is assumed to interact with the porphyrin ring, whereas TEA is bonded to the central atom in the axial position of the excited complex.

Both ${}^3[\mathrm{In(TPP)(MV)}]^{3+}$ and ${}^3[\mathrm{In(TPP)(TEA)}]^+$ exciplexes form a three-component exciplex ${}^3[\mathrm{In(TPP)(TEA)(MV)}]^{3+}$ with TEA and MV^{2+} molecules, respectively. The excited analogous complex ${}^3[\mathrm{In(TPP)(TEA)_2}]^+$ with a pseudo-octahedral chromophore is also effectively quenched by MV^{2+}, but no exciplex is formed, owing to steric hindrance of two TEA molecules occupying both axial positions in the complex and preventing an MV^{2+} cation from interacting with active sites localized on the excited porphyrin ring.

Three-component exciplex formation was assumed [125] when interpreting the quenching of the excited triplet ${}^3[\mathrm{Zn(Etio)}]^*$ by *trans-p*-nitrostilbene or *p*-nitrotoluene in benzene. Based on the observed changes in lifetime with quencher concentration, in addition to two-component exciplexes $^3(A\text{–}Q)^*$, three-component exciplex formation was suggested ($^3A = {}^3[Zn(Etio)]^*$; $Q =$ *trans-p*-nitrostilbene or *p*-nitrobenzene):

$$^3A^* + {}^1Q \rightarrow {}^3(A\text{–}Q)^* \tag{3.37}$$

$$^1A_{(GS)} + {}^1Q \leftarrow {}^3(A\text{–}Q)^* \xrightarrow{Q} {}^3(Q\text{–}A\text{–}Q)^* \tag{3.38}$$

The excimer formation was believed to occur in cases when a parameter of the quenching process of A* depended either on the ground-state A concentration or on the concentration of A*. In the former instance the rate constant of an observed quenching process obeys the equation

$$k_{obs} = k_1 + k_2[A] \tag{3.39}$$

where k_1 is the first-order rate constant of decay ($k_1 = \tau_0^{-1}$) and k_2 is the second-order rate constant for ground-state quenching. It was found [127] that the experimental (observed) rate constant for phosphorescence quenching of $^3[Pt(Etio)]^*$ and $^3[Pd(TPP)]^*$, and also for delayed fluorescence quenching of $^1[Zn(Etio)]^*$, can be fitted by eqn. 3.39 and thus the process can be schematized as follows:

$$A^* + A_{(GS)} \rightleftharpoons (A\text{–}A)^* \rightarrow 2A_{(GS)} \tag{3.40}$$

The formation of the excimer (A–A)* occurs only in fluid solution (THF, mineral oil). In rigid solution [poly(methyl methacrylate)], the luminescence lifetime is independent of the ground-state complex concentration as the medium prevents collision of an excited A* with a ground-state molecule A.

Analogous but anion-mediated excimer formation has been described [128]. The emission lifetime of $(^2T_1/^2E)[Cr(phen)_3]^{3+}$ was found to depend on the ground-state $[Cr(phen)_3]^{3+}$ (obeying eqn. 3.46) and on the anion present (the k_2 values decreased in the order $ClO_4^- > NO_3^- > Br^- > BrO_3^- \approx SO_4^{2-} > Cl^- > HSO_4^-$). Anion mediation is suggested to arise from encounters of excited and ground-state complexes to form the ion-bridged excimer $^*[\{Cr(phen)_3\}^{3+}\text{–}X^-\text{–}\{Cr(phen)_3\}^{3+}]$. It follows from temperature studies that the enthalpy of excimer formation is $\Delta H_f \approx 17\,kJ\ mol^{-1}$.

The apparently first evidence of excimer formation by self-association of excited complexes was published in 1986 [129, 130]. Based on the results of an excited-state decay kinetics study and of the influence of solvent polarity and an external magnetic field, the following mechanism of triplet annihilation was proposed:

$$2\ {}^3\mathrm{A}^* \rightarrow {}^1(\mathrm{A{-}A})^* \rightarrow {}^1\mathrm{A}^* + {}^1\mathrm{A}_{\mathrm{GS}} \tag{3.41}$$

where A denotes [Zn(TPP)], [Zn(OEP)], [Al(Pc)Cl] and $[\mathrm{Si(Pc)(C_2H_5O)_2}]$; the triplet and singlet excited states are ${}^3E_u$ and ${}^1A_{1g}$, respectively. The bonding in singlet excimers is covalent in nature. The concentration of the excimers increased with increasing flash-light intensity.

At the beginning of this section it was stated that exciplexes and excimers are not very common in the photochemistry of coordination compounds. There is no reason, however, why their formation should not occur, particularly with long-lived excited complexes. It might be that weak exciplexes are frequent but hidden precursors to photoproducts. The lack of information on exciplexes and excimers in the photochemistry of coordination compounds might be due to the simple fact that they have not been systematically looked for.

4 PHOTOCHEMICAL REACTIONS OF COORDINATION COMPOUNDS

4.1 Chemical deactivation and classification of photochemical reactions

The term chemical deactivation (photochemical reaction) designates a process in which at least part of the energy difference of a complex in an excited and a ground state is used to produce a chemical change in the complex. A photochemical reaction can be either a monomolecular (process 3.22) or a bimolecular (process 3.21). The molecularity depends on the presence of the potential reaction partners and the values of the kinetic and thermodynamic parameters of the possible deactivation modes of the complex under given conditions.

Depending on the energy content of a reactant(s), R, and a product(s), P, the photochemical reactions can be in general divided into three groups [151] (Fig. 8).

In the first instance (Fig. 8a), the energy of absorbed radiation is utilized to overcome the energetic barrier $\Delta G^{\neq}$ of a spontaneously realizable reaction (from the viewpoint of thermodynamics). This means that absorption of radiation has in fact a catalytic effect on the course of reaction.

In the second instance (Fig. 8b), photochemical transformation of reactants with a low energy content to products with a high energy content takes place. This type of spontaneously forbidden reactions is being intensively studied in connection with the conversion of light to chemical energy (see Section 5.2).

An excited state can also be the product of a chemical reaction of reactants in the ground state (Fig. 8c). The possibility of such a process is determined by the ΔG value of the spontaneous reaction and the energy of the excited state. The process when the excited particle is also deactivated by photon emission is called chemiluminescence. In this book, reactions will be discussed in which the excited particle is a complex.

Compared with organic compounds [152, 153], the multiplicity of photoreactive excited states of complexes exhibits a wider range, but without always being exactly defined (owing to strong spin–orbit interactions). The energetically lowest excited state of a given multiplicity need not be photoreactive, but frequently only higher states are photoreactive, e.g., $[(CO)_2Rh(\mu\text{-TPP})Rh(CO)_2]$ undergoes photochemical decomposition from the third and higher excited singlets only [154]. Analogous to the photochemistry of organic compounds, where an intersystem crossing $S_1 \rightarrow T_1$ often precedes photoreaction, coordination compounds do not necessarily react chemically from that excited state which was achieved by photoexcitation (for examples, see Section 4.4).

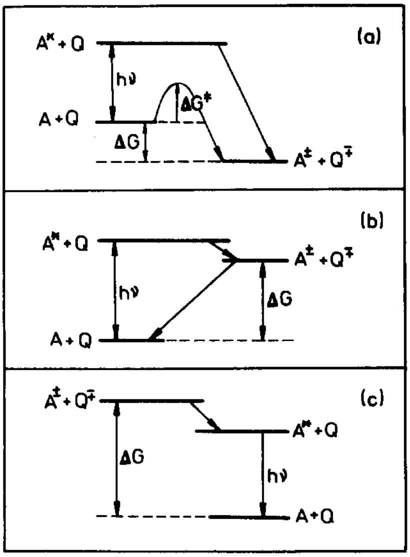

Fig. 8. Schematic diagram of the fundamental types of electron-transfer processes involving an excited state. (a) Photocatalysis; (b) conversion of light into chemical energy; (c) formation of an excited state and chemiluminescence.

Depending on the rate constants of vibrational relaxation, k_v (transition from the spectroscopic Franck–Condon to the thexi state), and of product formation, k_p, the photochemical reaction can run from the thexi state ($k_v > k_p$) and is designated as "slow", or from higher vibrational levels ($k_v \leqslant k_p$), designated "fast" [155]. A special case of fast reaction is a process taking place from higher vibrational levels of the ground electronic state (hot ground-state reaction) of the complex [156]. Individual types of photochemical reactions are discussed in more detail in the following sections.

As in thermal reactions, photochemical reactions of complexes can be classified according to various criteria.

In the first review on the photochemistry of coordination compounds, Szychliński [1] classified photochemical reactions into redox, substitution and isomerization. Balzani and Carassiti [7] classified the results of the study of photochemical reactions of complexes according to the central atoms, and

Geoffroy and Wrighton [9] classified the photochemical properties of organometallics according to ligands. In a book edited by Adamson and Fleischauer [8], various types of reactions and various types of inorganic compounds were discussed in the individual chapters.

According to the objectives and purposes of this review, photochemical reactions are classified on the basis of the knowledge of the changes in the oxidation number of the central atom and ligands in the complex, and the structure and composition of the complexes. Photoredox processes are dealt with in Section 4.2, non-redox processes during which only the structure of a complex is changed are discussed in Section 4.3 and Section 4.4 covers photosubstitution reactions. Section 4.5 is devoted to the photochemical non-redox reactions of coordinated ligands, while reactions of photoinsertion, photoelimination and photoaddition are discussed in Section 4.6.

Each of the above-mentioned types is documented using several carefully selected examples with the aim of pointing out the level of success achieved by the theoretical approach and experimental techniques used and prospects of the investigation in the field in question.

4.2 Photoredox reactions of coordination compounds

Photoredox reactions of complexes are classified as follows:

a) Reactions of an electron exchange between the complex and particles of the environment in which the complex composition and structure are preserved. This group includes photochemical reactions of solvated electron formation (Section 4.2.1) and outer-sphere reactions of the exchange of an electron between the complex and a certain particle of the secondary coordination sphere (Section 4.2.2).

b) Reactions of the complex producing changes in structure in which the composition of the complex is preserved. Such processes include photochemical reactions of inner-complex rearrangements with a change in the oxidation number of the central atom (Section 4.2.3).

c) Reactions of the complex producing changes in composition, divided into elimination and addition types (Section 4.2.4), inner-sphere electron-transfer decomposition reactions (Section 4.2.5), reactions of the formation and decomposition of polynuclear complexes (Section 4.2.6) and photoredox reactions of coordinated ligands (Section 4.2.7).

4.2.1 *Photochemical formation of solvated electrons*

The formation of solvated electrons can, in general, be expressed by the following equation:

$$^{*}[\mathrm{ML}_n]^{z-} \xrightarrow[\text{solvent}]{} [\mathrm{ML}_n]^{(1-z)} + \mathrm{e}^{-}_{\mathrm{solv}} \tag{4.1}$$

Most of the reactions of solvated electron formation are believed to be connected with the CTTS nature of the transition, and to result in oxidation of the central atom. Radial redistribution of electron density from the central atom to the periphery of the complex which is connected with the CTTS excited state formation can be due to photoexcitation in the region of the CTTS transition, or to internal conversion from short-lived energy-rich charge-transfer excited states.

Results obtained by the study of the photochemical properties of the anionic complexes $[Fe(CN)_6]^{4-}$, $[Ru(CN)_6]^{4-}$, $[Fe(CN)_5(PBu_3)]^{3-}$, $[Mo(CN)_8]^{4-}$ and others [48,157–159] have indicated that the efficiency (quantum yield) of solvated electron production depends on the wavelength of the excitation radiation and on the solvent properties. Quantum yields of solvated electrons for $[Fe(CN)_6]^{4-}$ as a function of excitation wavelength are summarized in Table 12. The electronic absorption spectrum of $[Fe(CN)_6]^{4-}$ consists of a mutually overlapping CTTS band (centred at 270 nm), an MLCT band at 218 nm and LF bands in the lower-energy UV region. The fact that the quantum yield at 228 nm is higher than that at 254 nm (although the CTTS state is reached directly at 254 nm) can be explained [48] by the hydrated electrons being formed with higher yields from higher excited CTTS levels. However, one cannot rule out the possibility that in the case of the internal conversion MLCT → CTTS, a thexi CTTS state with a higher energy content is formed compared with that obtained on direct irradiation into the CTTS band, and the difference in the energy content of the same excited CTTS state causes a different photoreactivity of the complex. This idea is also supported by the fact that solvated electrons obtained from the same substance by radiolysis and photolysis often do not have identical behaviour.

TABLE 12
Quantum yields of solvated electron, Φ_{e^-}, as a function of the wavelength of exciting light for $[Fe(CN)_6]^{4-}$ in aqueous solution [157]

λ(nm)	229	254	265	289	303	313	365
Φ_{e^-}	0.89	0.55	0.52	0.18	0.14	0.10	0.02

The determination of the concentration of solvated electrons produced by photolysis of the $[Fe(CN)_6]^{4-}$ complex in water–alcohol mixtures showed that the quantum yields of solvated electrons change with change in the composition of the mixture [159]. From the theoretical evaluation of the experimental data it followed that the thermalization length of the ejected electrons was about 3000 pm, independently of the solvent composition. The results cannot be interpreted in terms of a single parameter of the solvent (such as dielectric constant, relaxation time or diffusion coefficient), or explained by a cage effect of the solvent only. The viscosity of the solvent can, however, play an important role in the secondary thermal reactions of solvated electrons.

From the viewpoint of stoichiometry, the formation of a solvated electron (process 4.1) is the simplest redox process of an excited complex. The way in which the electron separates from its parent complex and the fate of the ejected electron have been the subject of much discussion, however. The release of an electron from an excited complex can evoke rapid structural changes in the solvent surrounding the oxidized complex. The primary products may recombine or undergo subsequent secondary thermal reactions.

The formation of solvated electrons is usually detected by measuring its absorption spectrum, or by the determination of the products of its reactions with solvated electron scavengers. A good specific scavenger is nitrous oxide (N_2O), which has a high rate constant for the reaction with solvated electrons ($k = 8.7 \times 10^9\ \mathrm{l\ mol^{-1}\ s^{-1}}$). The amount of nitrogen formed in the reaction

$$e^-_{solv} + N_2O + H^+ = N_2 + {}^\bullet OH \tag{4.2}$$

is directly related to the yield of solvated electrons.

Hydrated electrons have been produced [160] with a high quantum yield ($\Phi_{e^-} \approx 1$) on irradiation of the hydrated ions Co^+, Ni^+, Zn^+ and Cd^+ at $\lambda_{irr} \approx 300\,\mathrm{nm}$. It should be noted, however, that in the photooxidation of hydrated metal ions in their normal oxidation states (e. g. $[Fe(H_2O)_6]^{2+}$), the reaction can be described as an outer-sphere electron transfer though hydrated electrons have never been observed [48].

Electron transfer from the excited complex into the surrounding environment has also been postulated for some complexes in the LLTC state. For example [39], from studies of the electronic spectra and the ESR spectra, it has been found that on irradiating the [Pt(bpy)(tdt)] complex in $CHCl_3$ into the LLCT band ($\lambda = 577\,\mathrm{nm}$) at 77 K, the photon absorption not only results in electron transfer from the tdt^{2-} ligand through the Pt(II) central atom into the π^* orbital of the 2,2′-bipyridine ligand, but also a cationic complex with coordinated tdt^- anion is formed:

$$[Pt(bpy)(tdt)] + CHCl_3 \xrightarrow[LLCT]{h\nu} [Pt(bpy)(tdt^-)]^+ + Cl^- + CHCl_2^\bullet \tag{4.3}$$

The cationic complex undergoes subsequent thermal reactions.

From the viewpoint of sequence, a reverse process to the formation of a solvated electron is the reaction of a complex in the ground state with the solvated electron. In such reactions a complex in the excited state can be formed as, for example [48, 126], during the reaction

$$[Ru(bpy)_3]^{3+} + e^-_{solv} \rightarrow {}_{MLCT}^{\ \ 3}\!{}^{*}[Ru(bpy)_3]^{2+} \tag{4.4}$$

when triplet MLCT state formation was suggested from the emission spectra.

Also, the low-spin complex $[Co^{III}(NH_3)_5R^-]^+$, generated in the reaction of the $[Co^{III}(NH_3)_5R]^{2+}$ complex with a solvated electron (R = nitrobenzene ligand), can be considered [161] for the MLCT excited state of the high-spin $[Co^{II}(NH_3)_5R]^+$ complex, which is formed by inner-complex electron transfer from the reduced R^- ligand to the central atom.

4.2.2 Outer-sphere photoredox reactions of complexes

Outer-sphere electron-transfer processes are reactions in which no bonds are formed or broken, and only the charge of the reactants is changed. The reactions can, in general, be described by the following equation:

$$*A + Q = A^{\pm} + Q^{\mp} \tag{4.5}$$

where the excited particle, *A in our case, will be a complex and both *A and Q can be charged particles (for the sake of simplicity the original charges of *A and Q are omitted).

Simple kinetic treatment shows that only those excited complexes *A with lifetimes longer than about 10^{-10} s can be involved in outer-sphere electron-transfer reactions [151]. Lifetimes of complexes in their spin-allowed excited states are usually shorter (only ca 10^{-12} s). From a short-lived spin-allowed state via intersystem crossing ($k_{isc} \approx 10^9$–$10^{12}\,s^{-1}$), an energetically lower spin-forbidden state *A is obtained which can be deactivated in the presence of a quencher Q by reaction 4.5.

Reactions in which the oxidation number of the central atom increases are called oxidative quenchings and those in which the oxidation number of the central atom decreases are called reductive quenchings.

Thermodynamic conditions for oxidative and reductive quenching are expressed by the following relationships:

$$E^0(A^+/A^*) \leqslant E^0(Q/Q^-) \tag{4.6}$$

$$E^0(A^*/A^-) \geqslant E^0(Q^+/Q) \tag{4.7}$$

Elementary steps of the outer-sphere electron exchange during thermal and photochemical processes can be illustrated by the scheme in Fig. 9. The first step is the formation of precursor complex in which the reactants retain their identity. The rate of formation of the precursor complex is diffusion controlled. The next step is reorganization (changes of internuclear distances and of the bond angles) of the first coordination spheres and the solvent cage, producing an activated complex (not shown in the scheme), and conversion of the latter to the successor complex in which the particles have an electron structure corresponding to the products. The last step is the dissociation of the successor complex (the rate constant of the process is k_s) and solvation of the products by the solvent molecules. Exciplex formation is rare in the photochemistry of coordination compounds, and is not shown in Fig. 9. The rate constant of electron transfer, k_{et}, can generally be higher than, equal to or lower than the diffusion rate constant, k_{dif}. If $k_{et} > k_{dif}$, no thexi state of the A* complexes is achieved, and the electron exchange can take place only if the A complex and Q quencher were in contact at the moment of excitation (for details, see Section 4.2.6). The rate of such non-relaxed processes can decrease with increasing temperature. In the following sections such processes will be discussed for which $k_{et} < k_{dif}$ and to which the parameters of equilibrium thermodynamics and the kinetic transition-state theory can be applied.

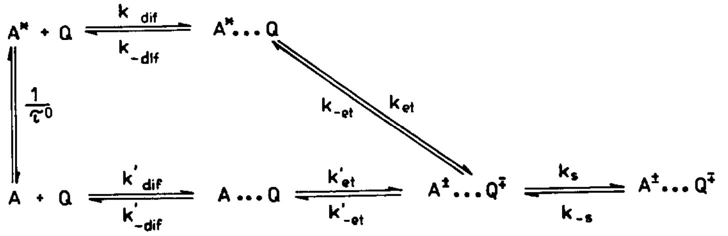

Fig. 9. Kinetic scheme for quenching by outer-sphere electron-transfer process.

In the most of the systems studied, the quenching process was not accompanied by permanent chemical changes, indicating that the back electron-transfer process is very fast and $k_{bet} > k_s$. These reactions, therefore, can be followed only by fast pulse techniques (flash photolysis in the nanosecond and picosecond regions).

Several authors [48, 151, 163, 164] have dealt with the problem of elaboration of a theoretical approach and its experimental verification when solving the relationships between the experimentally determinable rate constant of quenching process, k_q, and kinetic and thermodynamic parameters of the elementary steps involved in Fig. 9. Of various classical and quantum chemical approaches, those commonly used are the Marcus and empirical Rehm–Weller approaches.

A theoretical treatment of the kinetic and thermodynamic aspects of reversible outer-sphere electron-transfer processes illustrated in Fig. 9 led to the following equation under steady-state conditions (a detailed evaluation is beyond the scope of this book):

$$k_q = \frac{k_{dif}}{1 + \dfrac{k_{-dif}}{Z\exp(-\Delta G^{\ddagger}_{et}/RT)} + \dfrac{k_{-dif}\exp(\Delta G^0_{et}/RT)}{Z\exp(-\Delta G^{\ddagger}_{bet}/RT)}} \qquad (4.8)$$

where $\Delta G_i^{\ddagger}$ and ΔG^0_{et} are the activation free energy and free-energy change associated with the given step and Z is the frequency factor. Based on the assumption that the back electron transfer reaction leading to the ground-state precursor has no activation energy ($\Delta G^{\ddagger}_{\mathrm{bet}} = 0$, $K_{\mathrm{bet}} = Z$), Rehm and Weller [102] derived the simplified relationship

$$k_{\mathrm{q}} = \frac{k_{\mathrm{dif}}}{1 + \dfrac{k_{-\mathrm{dif}}}{Z}\left[\exp\left(\Delta G^{\ddagger}_{\mathrm{et}}/RT\right) + \exp\left(\Delta G^{0}_{\mathrm{et}}/RT\right)\right]} \tag{4.9}$$

The expression 4.9 is usually used to calculate the dependence of the experimental bimolecular quenching constant, k_{q}, on the overall free energy change, provided that a functional relationship between $\Delta G^{\ddagger}_{\mathrm{et}}$ and $\Delta G^{0}_{\mathrm{et}}$ is known. In this regard, two options are available.

According to the Marcus theory [165, 166], $\Delta G^{\ddagger}$ depends on ΔG^{0} as follows:

$$\Delta G^{\ddagger} = = \frac{\lambda}{4}\left(1 + \frac{\Delta G^{0}}{\lambda}\right)^{2} \tag{4.10}$$

where the reorganizational energy λ depends on the energies required to reorganize both the inner coordination shell of the reactants and the surrounding medium (outer shell of the reactants).

Rehm and Weller proposed the expression

$$\Delta G^{\ddagger} = \frac{\Delta G^{0}}{2} + \left[\left(\frac{\Delta G^{0}}{2}\right)^{2} + \left(\frac{\lambda}{4}\right)^{2}\right]^{0.5} \tag{4.11}$$

In the quenching of the excited state of A* by a homogeneous family of quenchers Q having variable redox potential, the values of λ, k_{dif}, $k_{-\mathrm{dif}}$ and Z are assumed to be constant. Hence, k_{q} is only a function of the free-energy change, which changes with the redox potential of the quenchers according to

$$\Delta G^{0} = E^{0}(\mathrm{A}^{+}/\mathrm{A}^{*}) - E^{0}(\mathrm{Q}/\mathrm{Q}^{-}) + w_{\mathrm{P}} - w_{\mathrm{R}} \tag{4.12}$$

where w_{R} and w_{P} are the energies required to bring the reactants and products from an infinite distance apart to their separation in the activated complex. Equation 4.12 is valid for oxidative quenching of A*, and an analogous equation may be written for reductive quenching of A*. It is worth bearing in mind that

$$-\left(\Delta G^{0}_{\mathrm{et}} + \Delta G^{0}_{\mathrm{bet}}\right) = E_{0\text{-}0} \tag{4.13}$$

where $E_{0\text{-}0}$ is zero-zero spectroscopic energy of the excited A*, provided that the entropy changes associated with excitation of A are negligible.

Depending on whether one uses the Marcus (eqn. 4.10) or the Rehm–Weller relationship (eqn. 4.11) to express the dependence of $\Delta G^{\ddagger}_{et}$ on ΔG^{0}_{et}, two different graphs are obtained for log k_q vs. ΔG^{0}_{et}. Both plots have an analogical Arrhenius-type portion in the endoergonic region and a plateau in the slightly exoergonic region, but a substantial difference in the highly exoergonic region. In this region, using the Rehm–Weller approach, the quenching constant k_q remains on the plateau, reaching the value of k_{dif}, whereas according to Marcus, a sharp drop in log k_q vs. ΔG^{0}_{et} is predicted. The available experimental results clearly show that the Rehm–Weller relationship is obeyed whereas no evidence for a decrease in k_q (the so-called Marcus inverted region) has been reported.

A very illustrative example comparing the experimental and calculated dependence of log k_q on ΔG^0 was provided by Balzani et al. [164], who studied the reductive quenching of LF excited $[Cr(bpy)_3]^{3+}$ by aromatic amines and methoxybenzenes. Results of the experiments and calculations (using a set of parameters $k_{dif} = 1 \times 10^{10}\,l\,mol^{-1}\,s^{-1}$, $k_{-dif} = 8.7 \times 10^{9}\,l\,mol^{-1}\,s^{-1}$, $Z = 1 \times 10^{11}\,s^{-1}$, $\lambda = 200\,kJ\,mol^{-1}$) are shown in Fig. 10.

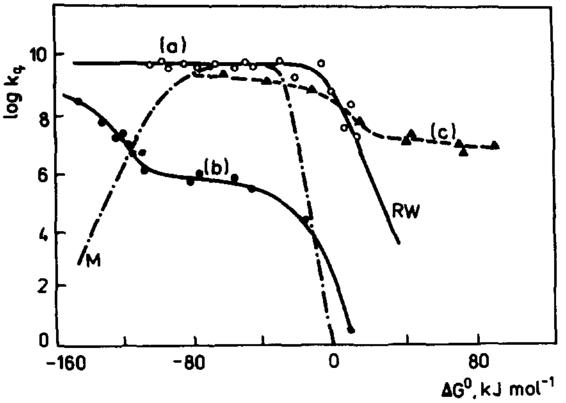

Fig. 10. Plots of log k_q vs. ΔG^0 for the following quenchings: (a) ○ — Redox quenching of $^*[Cr(bpy)_3]^{3+}$ by aromatic amines and methoxybenzenes [164]; curves RW and M represent the plots calculated according to the Rehm–Weller and Marcus relationships, respectively; (b) ● redox quenching of excited aromatics by aquated Eu^{2+} ions [151]; (c) ▲ — redox and energy-transfer quenching of $^*[Cu(dpp)_2]^{+}$ by aromatics and Cr(III) quenchers [175].

In principle, outer-sphere electron-transfer reactions can be adiabatic or non-adiabatic processes. The adiabaticity of a reaction depends on the electronic interaction energy, i.e., on the coupling between the precursor and successor. When the electronic interaction is strong (larger than about 0.1 eV), the reaction is said to be adiabatic and the probability of electron transfer from donor to acceptor is unity (or nearly unity). When the separation between the reactants is large, or when the reaction is spin- or symmetry-forbidden, the probability of electron transfer is proportional to the square of the interaction energy and may be much smaller than unity. Such reactions are called non-adiabatic (diabatic).

It is assumed that non-adiabaticity does not play an important role in outer-sphere electron-transfer processes of complexes. Some systems are known, however [for example [151], electron-transfer reactions of Eu(II) and Eu(III) complexes involving the transfer of an electron from a 4*f*-orbital], where a stepwise plot of log k_q vs. ΔG^0 suggests a non-adiabatic character of the process (Fig. 10).

In connection with the study of the properties of physiological redox protein pairs, mimicking highly efficient biological energy conversion, and with the verification of the validity of the theoretical approaches, various aspects of distance dependence of electron transfer have been intensively investigated [166–172]. In systems in which diffusion is negligible (rigid matrices), electron-transfer rates decrease exponentially with increasing donor–acceptor separation (up to a few nanometres), and depend on the exoergonicity of the reaction and on the lifetime of the excited state involved. As an example [169], a collisionless photoinduced electron transfer from excited $^*[RuL_3]^{2+}$ (where L are derivatives of bipyridine and phenanthroline) to methylviologen dication can be given. Depending on the ligand L (and thus on the free-energy change of the process), the reaction of electron transfer occurs at centre–to–centre distances of 122–155 nm, which are approximately equivalent to edge–edge distances of 2–5 nm. The electron pathway and the mechanism of collisionless long-distance electron-transfer processes are the subject of intensive investigation.

The k_q values are calculated from the Stern–Volmer relationship τ^0/τ vs. [Q]. The determination of the k_q values is demonstrated using the results of the study of the electron transfer between the excited $^*UO_2^{2+}$ ion and carbonyls of some metals [173]:

$$^*UO_2^{2+} + M(CO)_n \rightarrow UO_2^+ + M(CO)_n^+ \tag{4.14}$$

From the experimentally determined values (by means of flash photolysis) of the lifetime of $^*UO_2^{2+}$ in the absence (τ^0) and presence of carbonyl at known concentration (τ), a plot is made and the Stern–Volmer constant of quenching, K_{SV}, is calculated for each carbonyl (Fig. 11). A ratio between K_{SV} for the given carbonyl and τ^0 is the constant of redox quenching, k_q.The same values of k_q have also been obtained from a study of the changes in the luminescence intensity of $^*UO_2^{2+}$ and changes in the carbonyl concentration. The k_q values correlate with the values of the standard oxidation potentials of the particular carbonyls, and thus with the ΔG^0 values of reactions 4.14.

The oxidation ability of the $^*UO_2^{2+}$ ion [$E(^*UO_2^{2+}/UO_2^+) \approx 2.6\,V$] and the luminescence of this ion have been used [174] in the study of the mechanism of alcohol oxidation, where the primary process can be either the exchange of an electron between the alcohol molecule RH and $^*UO_2^{2+}$, producing an RH^+

alcohol cation that releases proton in the next step, or the abstraction of the H atom from the RH molecule producing UO_2H^{2+}. Based on the finding that the $\log k_q$ values for $^*UO_2^{2+}$ photoreduction are inversely proportional to the values of the dissociation energy of C–H bonds in alcohols and do not correlate with the ionization potentials of alcohols, the primary processes were postulated to be as follows:

$$^*UO_2^{2+} + RH \rightarrow UO_2H^{2+} + R^\bullet \qquad (4.15)$$

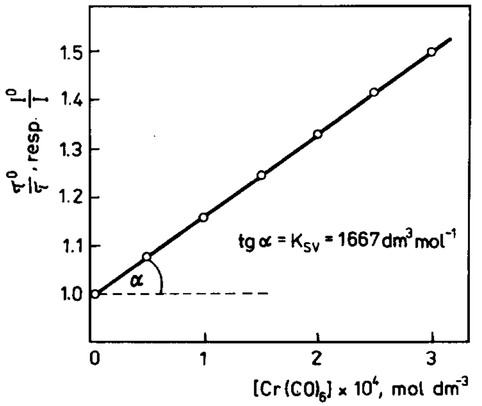

Fig. 11. Stern–Volmer dependence of the quenching of $^*UO_2^{2+}$ by $Cr(CO)_6$.

In several cases, together with the redox quenching, quenching by the energy transfer mechanism can also take place, as, for example [48], in the quenching of $^*[Ru(bpy)_3]^{2+}$ by hydrated Fe^{3+} cations. It results from the values of the redox potential of $E^0([Ru(bpy)_3]^{3+}/^*[Ru(bpy)_3]^{2+}) = -0.86\,V$ and $E^0(Fe^{3+}/Fe^{2+}) = +0.77\,V$ that the excited Ru(II) complex can be deactivated by electron transfer:

$$^*[Ru(bpy)_3]^{2+} + Fe^{3+} \rightarrow [Ru(bpy)_3]^{3+} + Fe^{2+} \qquad (4.16)$$

Based on the experimental data, the value $k_q = 2 \times 10^9\,l\,mol^{-1}\,s^{-1}$ has been calculated for reaction (4.16). It results from the values of the excitation energies of the $[Ru(bpy)_3]^{2+}$ complex (ca 2.2 eV) and the Fe^{3+} ion (ca 1.5 eV) that $^*[Ru(bpy)_3]^{2+}$ can also be quenched by Fe^{3+} via energy transfer:

$$^*[Ru(bpy)_3]^{2+} + Fe^{3+} \rightarrow [Ru(bpy)_3]^{2+} + {}^*Fe^{3+} \qquad (4.17)$$

As $E^0(^*Fe^{3+}/Fe^{2+}) \approx 2.3$ V, the $^*Fe^{3+}$ excited ion is an oxidizing agent toward $[Ru(bpy)_3]^{2+}$:

$$[\mathrm{Ru(bpy)_3}]^{2+} + {}^{*}\mathrm{Fe}^{3+} \rightarrow [\mathrm{Ru(bpy)_3}]^{3+} + \mathrm{Fe}^{2+} \qquad (4.18)$$

The products of reactions 4.16 and 4.17 provide a thermal reaction:

$$[\mathrm{Ru(bpy)_3}]^{3+} + \mathrm{Fe}^{2+} \rightarrow [\mathrm{Ru(bpy)_3}]^{2+} + \mathrm{Fe}^{3+} \qquad (4.19)$$

The experimentally determined rate constant of reaction 4.19 is $7.2 \times 10^5\,\mathrm{l\,mol^{-1}\,s^{-1}}$. This reaction has the result that during continuous photolysis no observable changes take place. Figure 12 shows the redox potentials, excitation energies and processes involved in the irradiated system of $[\mathrm{Ru(bpy)_3}]^{2+}$ and Fe^{3+} ions.

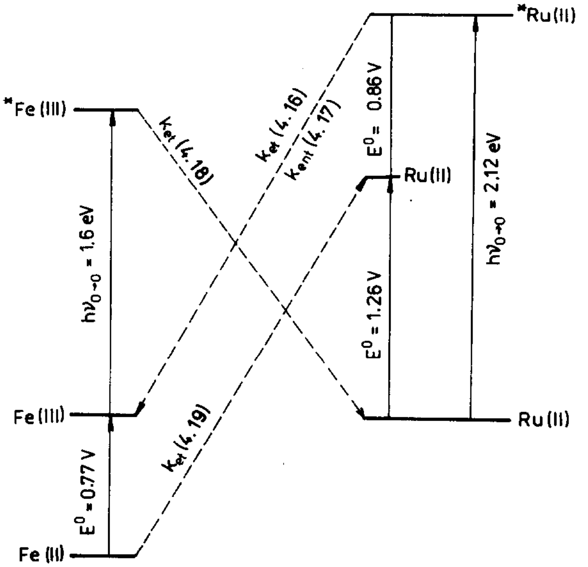

Fig. 12. Redox potentials, excitation energies and rate constants of energy-transfer and electron-transfer processes involved in irradiated systems containing $[\mathrm{Ru(bpy)_3}]^{2+}$ and Fe(III) ions.

It should be pointed out that simultaneously occurring electron-transfer and energy-transfer processes can result in a sigmoidal (or stepped) dependence of $\log k_q$ on ΔG^0, as was documented [175] for the quenching of $[\mathrm{Cu(dpp)_2}]^+$ by a series of $[\mathrm{Cr(acac)_3}]$ derivatives (Fig. 10c), where the plateau at $\log k_q \approx 9.5$ corresponded to an electron-transfer mechanism and the plateau at $\log k_q \approx 2 \times 10^7$ corresponded to quenching by energy transfer.

A typical outer-sphere electron transfer occurs on irradiating an ion-pair-containing system in the IPCT bands. In many instances the photoinduced electron-transfer reaction is followed by a fast back electron-transfer process which returns the system to its original state.This means that no net chemical change is observed. Such reactions are common not only for complexes with a cage-type ligand [176] but also for other ion pairs consisting of a "reversible" reductant and an oxidant. The mechanism of the reactions is simple, for example [176]:

$$[\mathrm{Co^{III}(sep)}]^{3+},\ \mathrm{I}^- \underset{\text{back electron transfer}}{\overset{h\nu\ (\text{IPCT})}{\rightleftharpoons}} [\mathrm{Co^{II}(sep)}]^{2+},\ \mathrm{I}^{\bullet} \tag{4.20}$$

If one (or both) of the counter-ions is an irreversible reductant (such as $C_2O_4^{2-}$) or oxidant (such as $[Co(NH_3)_6]^{3+}$), a net chemical change is usually observed. As an example, a photoredox decomposition reaction of the pair $[Co(NH_3)_5X]^{2+}$, $[B(C_6H_5)_4]^-$ may be considered [45]:

$$[\mathrm{Co(NH_3)_5X}]^{2+},\ [\mathrm{B(C_6H_5)_4}]^- \xrightarrow[\mathrm{CH_2Cl_2/CH_3OH}]{h\nu\,(\text{IPCT})} \mathrm{Co^{2+}_{solv}} + 5\mathrm{NH_3} + \mathrm{X}^- + [\mathrm{B(C_6H_5)_4}]^{\bullet} \tag{4.21}$$

The quantum yields of Co^{2+}($\Phi_{Co^{2+}} \approx 0.1$–$1.1$) decrease with increasing CH_3OH content, as with increasing polarity of the solvent the equilibrium constant of ion-pair formation decreases. The values of $\Phi_{Co^{2+}}$ depend on the acidoligand X^-, but there is no clear relationship between $\Phi_{Co^{2+}}$ and properties (as ionization potentials or optical electronegativity) of X^-.

It should be noted that a mechanism of electron-transfer quenching (dynamic or static) may depend on the experimental conditions of measurement. It was found [177] that the luminescence quenching of Eu(III) cryptate complex, $^*[Eu(oac)]^{3+}$, is a dynamic bimolecular process at low quencher concentration:

$$^*[\mathrm{Eu(oac)}]^{3+} + [\mathrm{M(CN)_6}]^{4-} \rightarrow [\mathrm{Eu(oac)}]^{2+} + [\mathrm{M(CN)_6}]^{3-} \tag{4.22}$$

At high concentrations of $[Eu(oac)]^{3+}$ and $[M(CN)_6]^{4-}$ even in aqueous solutions (high-polarity solvent!), the formation of an ion pair occurs, a new, low-energy IPCT broad absorption band in the visible region appears and IPCT excitation leads to a reversible electron-transfer reaction:

$$^*[\mathrm{Eu(oac)}]^{3+},\ [\mathrm{M(CN)_6}]^{4-} \underset{\text{back electron transfer}}{\overset{h\nu\ (\text{IPCT})}{\rightleftharpoons}} [\mathrm{Eu(oac)}]^{2+} + [\mathrm{M(CN)_6}]^{3-} \tag{4.23}$$

In contradistinction to the previous examples of ion pairs, there are many systems in which it is difficult to distinguish whether the counter-ions form an ion pair in it or if a binuclear bridged complex was formed. Such borderline systems can be exemplified by the systems of Mo(IV), Fe(II), W(IV) and Ru(II) cyano complexes containing solvated ions of Fe^{3+}, Cu^{2+} and others [178].

It is clear from the above examples that the outer-sphere electron-transfer reactions can involve a complex in various types of excited states. $^*[Cr(bpy)_3]^{3+}$ was quenched from the doublet LF state, $^*UO_2^{2+}$ from the LMCT triplet, $^*[Ru(bpy)_3]^{2+}$ from the MLCT triplet and ion pairs from the IPCT states. Although in most of the outer-sphere photoredox reactions of complexes the oxidation number of the central atom is changed, depending on the type and localization of HOMO and LUMO, the electron transfer can also result in oxidation (reduction) of the ligand without a change in the oxidation state of the central atom. Such processes are possible particularly for the complexes with macrocyclic unsaturated ligands, such as phthalocyanine. For example [179], on Q-band irradiation, $[Ru^{II}(Pc)L_2]$ complexes can be quantitatively photooxidized to stable π-cation radical species using either an irreversible electron acceptor at room temperature (such as CBr_4), or even a reversible one (2,3-dichloro-5,6-dicyanobenzoquinone) in a low-temperature experiment. The former process can be described by the following equation:

$$^*[Ru^{II}(Pc^{2-})L_2] + CBr_4 \rightarrow [Ru^{II}(Pc^{-})L_2]^+ + CBr_3^{\cdot} + Br^- \qquad (4.24)$$

where L = pyridine, CO, DMSO.

In the future we may expect increasing interest of photochemists in outer-sphere photoreduction reactions, not only in connection with the above-mentioned aspects (verification of the conclusions of the theory), but also in connection with the problems of solar energy conversion and its storage, and with the problems of the elucidation of photochemical reaction mechanisms taking place in living organisms (photosynthesis).

A significant contribution to the theory and practical application of the available knowledge results mainly from detailed studies of the relationships between the structure and photoreactivity of complexes (including their absolute configuration influencing the kinetics of electron-transfer reactions in the case of optically active substances [180], and localization of the charge transfer and photoreactivity (there are possibilities in the "tuning" of the properties of the excited state). Results of the study of photoredox reactions that take place in heterogeneous systems may also be of great value (study of membrane processes, effect of micelle formation on the course of photochemical reactions [38]). Of course, entirely new regions in the study of photoredox reactions of complexes cannot be ruled out.

4.2.3 Photoredox intramolecular rearrangements

Photoredox intramolecular rearrangements are redox isomerization photochemical reactions in which the composition of a complex is preserved, but the composition of individual ligands, the oxidation number of the central atom and in some instances also the coordination number of the central atom are changed. Thus, reactants and products can be considered to be coligand isomers [181].

A photoredox rearrangement reaction is frequently one of the steps in the mechanism of catalytic processes and syntheses of organic and organometallic compounds. As an example, the photochemical transformation of the π-complex $[(CO)_4Fe(CHBr=CHBr)]$ can be considered, in which the formation of a reactive Fe(II) intermediate can be expressed as follows [182]:

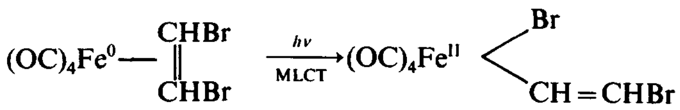

(4.25)

However, some other types of reactions exist during which an isolable product, a coligand isomer of the reactant, is formed. The first complex containing a $-C\equiv C-CN$ group as a ligand was prepared by continuous photolysis of $[Pt^0(PPh_3)_2(NCC_2CN)]$:

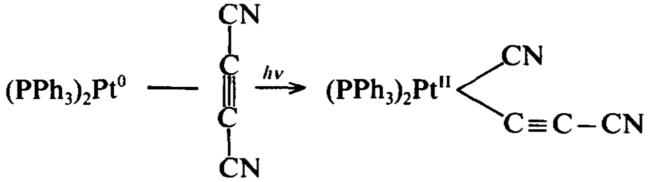

(4.26)

Irradiation of the related tetracyanoethylene π-complex of Pt(0) led [183] to the reaction

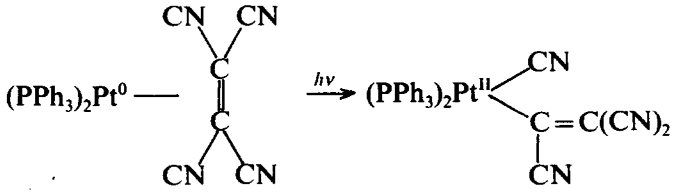

(4.27)

It was found that reaction 4.27 proceeded at least partially through the primary generation of a tetracyanoethylene anion radical.

The photochemical properties of $[Pt(PPh_3)_2(C_2H_4)]$ were strongly affected by the excitation wavelength and solvent [184]. Irradiation with 280-nm light in ethanol induced elimination of ethylene and the formation of orthometallated dimeric species. In $CHCl_3$ solution, the final product obtained was $[PtClH(PPh_3)_2]$. Continuous photolysis at 254 nm in CH_2Cl_2 led to no observable loss of ethylene and an orthometallated monomeric Pt(II) compound was formed according to the reaction involving a "pentacoordinated" π-complex:

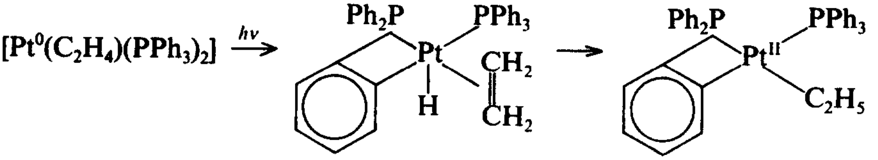

(4.28)

An alternative mechanism is possible, but not very likely.

The reactions of coligand isomer formation may be a consequence of migration or inversion processes. It should be noted, however, that not all of them represent redox processes localized on the central atom. Such reactions will be mentioned in Section 4.5.

For these and other reactions of this type, no relationship between the type of excited state of the complexes and the course of the reaction has been investigated. The studies were carried out with the aim of employing photochemistry as one of the synthetic methods in the chemistry of coordination compounds and organometallics. A knowledge of the photochemical generation of reactive intermediates (products of rearrangements) could potentially be applied to catalytic processes.

4.2.4 *Photoredox elimination and addition reactions*

Photoredox elimination and addition reactions are characterized by changes in the oxidation number of the central atom and in coordination number of the complex. Usually, an increase in the oxidation number is accompanied by an increase in the coordination number, and vice versa. The former reactions are called oxidative additions and the latter reductive eliminations. As components of reaction mechanisms, these reactions represent the formation of intermediates and only in a limited number of instances a stable product has been isolated and characterized.

Photoredox addition reactions may take place when the Lewis acidity of the central atom in the complexes is increased by excitation, and the reactive particle of the system is bonded to the vacant, unoccupied site with simultaneous oxidation of the central atom.

It was found from a detailed kinetic study [185] of the photoredox reaction between [Pt(Me)$_2$(phen)] and i-PrI that the triplet MLCT state of the complex abstracts the iodine atom from the isopropyl iodine molecule and the pentacoordinated Pt(III) complex reacts in the presence of the 4-methoxyphenol free-radical inhibitor by abstraction of the second iodine atom to produce the final [Pt(Me)$_2$I$_2$(phen)] complex:

$${}_{\text{MLCT}}^{*}[\text{Pt}^{\text{II}}(\text{Me})_2(\text{phen})] \xrightarrow{\text{i-PrI}} [\text{Pt}^{\text{III}}(\text{Me})_2\text{I}(\text{phen})] \xrightarrow{\text{i-PrI}} [\text{Pt}^{\text{IV}}(\text{Me})_2\text{I}_2(\text{phen})] \qquad (4.29)$$

In the absence of the free-radical inhibitor the complex $[Pt^{IV}(Me)_2(i\text{-}Pr)I(phen)]$ is formed.

Four complexes with the formula $[Pt^{IV}(L)Cl(CHClX)]$, where L- are C-deprotonated forms of 2-phenylpyridine and 2-(2-thionyl)pyridine and X is H or Cl, were prepared [186] via oxidative addition of CH_2Cl_2 or $CHCl_3$ to a $^*[PtL_2]$ complex. It is probable that also in this instance the MLCT triplet excited state will be photochemically active [emissive state of the starting Pt(II) complex]. Both the Pt(II) starting and Pt(IV) final complexes give strong luminescence in the visible region.

It can be assumed that other reactions, for example [187]

$$[Pt^{II}(bpy)_2Cl_2] \xrightarrow[CHCl_3]{h\nu} [Pt^{IV}(bpy)Cl_4] \tag{4.30}$$

also start with the abstraction of an atom by the excited complex in the primary photochemical step.

In some reactions, however, the coordination number of the central atom is increased, but only as a consequence of a secondary thermal reaction occurring after formation of a coordinatively unsaturated intermediate in the primary photochemical process. It can be exemplified by the following reaction [188]:

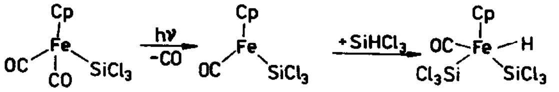

(4.31)

Of the various photoredox eliminations, the elimination of hydrogen from hydride complexes has been the most studied. Irradiation of the $[FeH_2(dp)_2]$ complex in the IL region localized on the diphos ligand results in the primary photochemical process of elimination of an H_2 molecule [189]:

$$[Fe^{II}H_2(diphos)_2] \xrightarrow{h\nu} [Fe^0(diphos)_2] + H_2 \tag{4.32}$$

From an analogous complex, $[FeD_2(diphos)_2]$, D_2 is released during irradiation. Application of EPR spectroscopy and the spin-trapping method has shown that in the irradiated systems neither atomic hydrogen nor deuterium is formed. Using mass spectrometry, the presence of H_2 and D_2, but no HD molecules, was proved in irradiated systems containing both $[FeH_2(diphos)_2]$ and $[FeD_2(diphos)_2]$. These results show that molecules of H_2 and D_2 leave the solvent cage of the complexes, and the photoelimination can be characterized as non-radical. A similar result [190] was achieved on irradiating systems of complexes of the *trans*-$[PtHX(PPh_3)_2]$ type, where X = CH_2CN, $CH_2(CH)_2CN$ or CF_3, when the HX compounds but not H_2 or X–X, were identified as reaction products.

A coordinatively unsaturated complex (product of the primary photochemical elimination reaction) is usually very reactive and increases its coordination number by an orthometallation reaction, formation of a polynuclear complex or an insertion reaction. These are the secondary thermal reactions.

During the coordination of an O_2 molecule, transfer of the electron density into π^*-antibonding orbitals localized on the dioxygen molecule takes place, depending on the properties of the central atom and the composition and symmetry of the coordination sphere, yielding the formation of superoxide or peroxide groups. Cases in which the negative charge is not increased during the coordination of the O_2 molecule rarely occur [191].

Irradiation of dioxygen adducts of complexes can result (particularly with the formation of the excited state of charge transfer from the dioxygen moiety to the central atom) in elimination of the dioxygen molecule and in a decrease in the coordination number. It was found [192] that the dioxygen adduct of Co(II) tetraphenylporphyrin [usually formulated as a superoxo complex of Co(III)] undergoes photoinduced elimination of dioxygen:

$$[\mathrm{Co^{III}(O_2^-)(TTP)}] \xrightarrow{h\nu} [\mathrm{Co^{II}(TPP)}] + \mathrm{O_2} \qquad (4.33)$$

owing to the homolytic cleavage of the dioxygen–cobalt bond.

In most instances, photolyses of peroxo and dioxygen complexes of transition metals lead to the formation of O_2 in its triplet ground state. In contrast, the photolysis of $[PtO_2(PPh_3)_2]$ produces electronically excited singlet dioxygen [193], which was evidenced using a singlet oxygen scavenger.

The photochemical properties of azido complexes strongly depend on the properties of the central atom. The photodecomposition of azido complexes can yield photosubstitution reactions, azide radical formation, coordinated nitrone (singlet or triplet) formation or, in addition, reductive elimination of azide. Such elimination and molecular nitrogen formation was found to occur [194] on irradiating *trans*-$[Pt(CN)_4(N_3)_2]^{2-}$ in water or ethanol:

$$trans\text{-}[\mathrm{Pt^{IV}(CN)_4(N_3)_2}]^{2-} \xrightarrow{h\nu} [\mathrm{Pt^{II}(CN)_4}]^{2-} + 3\mathrm{N_2} \qquad (4.34)$$

The decrease in the quantum yield of reaction 4.34 with increasing pressure was interpreted as evidence for the formation of a caged radical species via simultaneous scission of both Pt–N_3 bonds in the LMCT state.

The mechanism of nitrogen elimination from azido complexes of other central atoms [Ni(II), Rh(III), Ir(III), Cr(III)] is different and production of nitrene intermediate in the primary photochemical step is suggested. Nitrene formation is favoured for central atoms that do not have a stable lower oxidation number, and for central atoms that possess filled *d*-orbitals that can back-donate into the vacant nitrogen-atom orbitals and thus stabilize the metal nitrene. With the $[Cr^{III}(salen)N_3]$ complex, the nitrogen photoelimination is accompanied by oxidation of the central atom and formation of a Cr(V) nitrido complex, which was demonstrated [195] by EPR spectroscopy:

$$[Cr^{III}(salen)N_3] \xrightarrow{h\nu} [Cr^{V}(salen)N] + N_2 \tag{4.35}$$

With regard to the change in the oxidation number of the central atom, reaction 4.35 is an oxidative elimination that does not include a change in the coordination number or in the chromophore.

Available data on photochemical and photophysical deactivation pathways still do not enable conclusions to be drawn on the relationship between the type of the excited state (electronic and molecular structure of the complex in this state) and the ability of the complex to undergo photochemical addition and elimination reactions.

Studies focused on these topics are very promising, as the formation of not only the final stable products but also of intermediates can be of great importance for the practical application of the knowledge available from the photochemistry of complexes (see Chapter 5).

4.2.5 Inner-sphere photoredox reactions of complexes

In this section, redox reactions of monomolecular complexes are discussed in which, after the exchange of an electron between the central atom and one of the coordinated ligands in the primary photochemical step, the given redox-changed ligand leaves the first coordination sphere of the complex and the composition of the complex is changed. In most inner-sphere photoredox reactions, the central atom of a complex is reduced and a ligand is oxidized. Frequently, the products of the primary photoredox step (oxidized ligand, in particular) undergo secondary thermal redox reactions. The processes under consideration are a consequence of the radial redistribution of electron density and occur from the LMCT excited states in most instances.

The formation of the LMCT state and redox decomposition can be brought about in several ways, as follows.

The LMCT excited state from which the photoredox deactivation process originates can be populated directly by photoexcitation (it is identical with the spectroscopically populated LMCT state) as, e.g., in the irradiation of gaseous Fe_2Cl_6:

$$[Fe_2Cl_6]_{(g)} \xrightarrow[365\,nm]{h\nu} {}_{LMCT}^{*}[Fe_2Cl_6] \rightarrow 2FeCl_{2(s)} + 2Cl^{\bullet} \tag{4.36}$$

and solutions of Cu(II) carboxylate complexes:

$$[CuOOCCH_3]^{+}_{solv} \xrightarrow{h\nu} {}_{LMCT}^{*}[CuOOCCH_3]^{+}_{solv} \rightarrow Cu^{+}_{solv} + CH_3^{\bullet} + CO_2 \tag{4.37}$$

Achieving the LMCT state by internal conversion from another, energetically higher excited state and by energy transfer was exemplified [196] in the study of the photoredox decomposition of the $[Co(phen)_3]^{3+}$ complex. On irradiating the complex with light at 254 nm [the region of the MLCT transition $3d_\pi(Co) \rightarrow \pi^*(phen)$], Co^{2+} ions are generated with a quantum yield of 0.004 in the solution. Irradiation with light at 313 nm (region of the IL transition) does not result in a photoredox process. On irradiation of solutions containing both the $[Co(phen)_3]^{3+}$ complex and free 1,10-phenanthroline at 313 nm, the intensity of fluorescence of 1,10-phenanthroline decreases with increasing concentration of the complex, and Co^{2+} ions are formed in these systems. The monoprotonated form of 1,10-phenanthroline does not sensitize the reduction of Co(III) to Co(II) on irradiation, and its fluorescence is not quenched by the complex. The IL state energies for free and monoprotonated 1,10-phenanthroline are 3.66 and 3.27 eV, respectively. The limiting quantum yield of the photosensitized reduction of Co(III) to Co(II) is 0.1. It follows from the above experimental data that in a system in which light is absorbed especially by free 1,10-phenanthroline, the energy transfer from the singlet state of 1,10-phenanthroline to the $[Co(phen)_3]^{3+}$ complex leads to the formation of the redox reactive MLCT state:

$$[Co(phen)_3]^{3+} + {}^{*}_{IL}(phen) \rightarrow phen + {}^{*}_{LMCT}[Co(phen)_3]^{3+} \qquad (4.38)$$

which is deactivated by redox decomposition:

$${}^{*}_{LMCT}[Co(phen)_3]^{3+} \xrightarrow{H_2O} Co^{2+}_{aq} + 2phen + \text{products of phen oxidation} \qquad (4.39)$$

The energy of the LMCT state of the complex is lower than 3.66 and higher than 3.27 eV. As the properties of coordinated 1,10-phenanthroline are similar to those of the monoprotonated form $(Hphen)^+$, apparently the IL state of the coordinated ligand will also be energetically lower than the LMCT state, and therefore irradiation of the complex in the region of the IL transitions does not cause any photoredox processes. The electron distribution in the MLCT state of the complex obtained by irradiation at 254 nm is not suitable for Co(III) photoreduction and hence the redox reactive LMCT state is populated from this state by internal conversion. On comparing the quantum yields of Co(II) in direct and sensitized photoreduction of Co(III), it appears that the conversion of the spectroscopically populated MLCT state to the LMCT state is low.

If in the complex being generated the central atom possesses an electron configuration conditioning the kinetic inertness of the complex, only its partial decomposition takes place, e.g.,

$$[IrCl_6]^{2-} + H_2O \xrightarrow{h\nu} [IrCl_5(H_2O)]^{2-} + Cl^{\bullet} \qquad (4.40)$$

In other instances [e.g., the production of kinetically labile Co(II) complex], complete decomposition of the complex can be observed.

Proposals for the mechanisms of inner-sphere photoredox reactions of coordination compounds are based first on identification of the radical products of the primary photochemical reactions. Of the methods available for this purpose, especially the EPR technique at low tempertures, in the presence of spin-trapping agents, and flash photolysis with radical spectra measurements are being used. The presence of some radicals in the irradiated systems was proved with radical scavengers. Examples of the results obtained by the different methods are given below.

Irradiation of the $[\mathrm{Co(NH_3)_5N_3}]^{2+}$ or $[\mathrm{Co(CN)_5N_3}]^{3-}$ complex in the region of the LMCT transitions, apart from leading to photoaquation, also results in reduction of Co(III) to Co(II). Reduction of the central atom can be due to outer-sphere transfer of electrons from the solvent molecules to the complex as a consequence of the increase in the oxidation potential of the complex on excitation, or to inner-complex electron transfer from the coordinated azide ligand to the Co(III) central atom. Based on EPR spectra of the irradiated azide complex systems in the presence of spin-trapping agents (phenyl-*N*-*tert*-butylnitrone, PBN, or nitrosodurene, ND) it was found [197] that in these systems adducts of the above agents with the $\mathrm{N}_3^\bullet$ radical are formed; adducts of trace amounts of $\dot{\mathrm{C}}\mathrm{H_2OH}$ radical are also formed in methanol solutions. On the basis of these results, homolytic cleavage of the $\mathrm{Co^{III}}$–$\mathrm{N_3^-}$ bond in the LMCT state has been postulated as the primary photochemical process. The reaction rate constant of the $\mathrm{N}_3^\bullet$ radicals with the spin-trapping agents is much higher than that with the molecules of methanol, which explains the formation of only trace amounts of the $\dot{\mathrm{C}}\mathrm{H_2OH}$ radicals. In the absence of spin-trapping agents the $\mathrm{N}_3^\bullet$ radicals were not identified by the EPR method even on irradiating the systems at low temperatures.

When using the PBN and ND spin traps, the problem of the determination of the primary photochemical reactions in the course of CT irradiation of the $[\mathrm{Mo(CN)_8}]^{3-}$ complex in the presence of methanol from the region of CT bands was also solved [198]. On the basis of the characteristic features of the EPR spectra, the presence of $[\mathrm{Mo(CN)_7}]^{2-}$, $\mathrm{CH_3O}^\bullet$, $\mathrm{CN}^\bullet$ and $\dot{\mathrm{C}}\mathrm{H_2OH}$ radicals was proved, and the following mechanism of the primary processes was suggested:

$$[\mathrm{Mo(CN)_8}]^{3-} \xrightarrow[\mathrm{CH_3OH}]{h\nu} \begin{array}{lr} [\mathrm{Mo(CN)_8}]^{4-} + \mathrm{H}^+ + \mathrm{CH_3O}^\bullet & (4.41) \\ [\mathrm{Mo(CN)_7}]^{2-} + \mathrm{CN}^- & (4.42) \\ [\mathrm{Mo(CN)_7}]^{3-} + \mathrm{CN}^\bullet & (4.43) \end{array}$$

Hence the primary processes involve both outer-sphere electron transfer (eqn. 4.41) and inner-sphere redox (eqn. 4.43) and non-redox (eqn. 4.42) processes.

The intermediates $[Mo(CN)_7]^{2-}$ and $CH_3O^{\bullet}$ subsequently undergo thermal secondary reactions, leading to the production of $[(CN)_7Mo{-}CN{-}Mo(CN)_7]^{6-}$ and $\dot{C}H_2OH$ radicals.

In several instances, valuable information on the mechanism of photoredox reactions was provided by pulsed-laser flash photolysis. The absorption spectrum of a system of Cu(II) chloro complexes in acetonitrile measured within a few nanoseconds after the pulse [199] [light with a wavelength of 437 nm, corresponding to the LMCT transitions, which is the region of LMCT transitions in the case of Cu(II) chloro complexes] shows a band that is assigned to the Cl_2^- anion radical according to its characteristics ($\varepsilon \approx 10\,000$ l mol^{-1} cm^{-1}). From the rates of decrease in absorbance of the Cl_2^- radical in the presence of different concentrations of Cu^{2+} and Cu^+ ions, the rate constants for the reactions of this radical with the above-mentioned cations were calculated. On the basis of the evidence of Cl_2^- radicals in the irradiated system, a mechanism of the primary process (eqn. 4.44) and of subsequent secondary thermal reactions of the generated $Cl^{\bullet}$ radical (eqn. 4.45) has been suggested:

$$[CuCl_4]^{2-} \xrightarrow[\text{LMCT}]{h\nu} [CuCl_3]^{2-} + Cl^{\bullet} \tag{4.44}$$

$$Cl^{\bullet} + Cl^- \rightarrow Cl_2^- \tag{4.45}$$

The Cl_2^- and Br_2^- radicals in the irradiated systems of chloro and bromo complexes of Fe(III) were identified [200] analogously by the method of pulsed photolysis, and the primary process was postulated as the photoredox decomposition of the Fe(III) halide complex. It should be noted that the presence of the X_2^- radical in this system and others is not evidence of an inner-sphere electron-transfer mechanism between the ligand X^- and the central atom, nor evidence that the $X^{\bullet}$ radical generation is the primary photochemical process. Theoretical treatment of EPR studies of the systems of $[FeX_4]^-$ and $[CuX_4]^{2-}$ complexes has shown [201] that the primary electron transfer takes place between the complex in its excited state and the particle in the secondary coordination sphere of the complex.

When using benzoic acid as the radical scavenger, the presence of the $OH^{\bullet}$ (but not of chloro radicals) [202] has been demonstrated in irradiated aqueous solutions of Fe(III) chloro complexes, as the reaction product of the scavenger was salicylic and not chlorobenzoic acid. Because the quantum yield of Fe(II) obtained by Fe(III) photoreduction decreases with increasing concentration of NaCl and HCl in the system, and increases with increasing concentration of solvated $(Fe^{3+}\,.\,OH^-)_{\mathrm{solv}}$ ions, the hydroxo but not chloro complexes of Fe(III) are considered to be photosensitive, and the primary process was proposed to be homolytic cleavage of the $Fe(III){-}OH^-$ bond in the excited state.

It can be seen from the data available that the conclusions drawn from the study of a particular problem are not necessarily identical when using different experimental techniques, however, they do not rule each other out. One of the reasons is the fact that it is not always the products of the primary photochemical processes that are identified by the methods employed, but the species produced in the fast secondary reactions of these products. Another reason is that in the irradiated system several primary photochemical reactions may occur, and not all of the methods used are equally sensitive to all products of these processes.

The solvent properties can also have a marked influence on the kinetic parameters of photochemical reactions, even if the molecules of the solvent do not take part directly in these reactions. This can be demonstrated [203] by the effect of the viscosity of the medium (water, glycerol and their mixtures) on the quantum yields of the photoredox decomposition of the $[Co(NH_3)_5(NO_2)]^{2+}$ complex and nitro-nitrito isomerization of the above-mentioned complex during irradiation of the system into the LMCT band ($\lambda_{irr} = 366$ nm).

The generation of $NO_2^{\bullet}$ radicals and Co(II) is considered to be a primary photochemical process:

$$[Co(NH_3)_5(NO_2)]^{2+}_{(solv)} \xrightarrow{h\nu} [Co^{II}(NH_3)_5(NO_2^{\bullet})]^{2+}_{solv} \tag{4.46}$$

A decrease in viscosity increases the probability of diffusion of the $NO_2^{\bullet}$ radicals from the solvent cage of the radical pair, and thus the quantum yield of the photoredox process increases:

$$\{[Co(NH_3)_5]^{2+}, (NO_2^{\bullet})\}_{solv} \xrightarrow{H_2O} Co^{2+}_{aq} + 5NH_3 + (NO_2^{\bullet})_{solv} \tag{4.47}$$

With increasing viscosity of the medium, the strength of the solvent cage also increases. The probability of the radical separation decreases and the probability of back-coordination of the $NO_2^{\bullet}$ radical increases, not only by nitrogen, but also by the oxygen atom. Hence the quantum yield of isomerization increases with increasing viscosity of the medium.

Irradiation of the $[Co(NH_3)_5(NO_2)]^{2+}$ complex with monochromatic radiation at eleven different wavelengths in water–ethanol mixture with constant viscosity, and determination of both the quantum yields of photoreduction of Co(III) to Co(II) and of nitro-nitrito photoisomerization showed [204] that the ratio of the quantum yields does not depend on the wavelength of the excitation radiation. On irradiating in the region of the LMCT transitions, the quantum yield of the photoredox reaction decreases with decreasing energy of photons; on irradiating in the LF bands, it does not depend on the energy of photons. It was deduced from these results that the vibrational relaxation in the LF state is much faster than any other photophysical or photochemical deactivation mode and a thexi LF state is formed from which the LMCT state with a zero or very low vibrational level is achieved by internal conversion. In the LMCT state population, chemical deactivation is a much faster process than the achievement of the thexi state; by increasing the energy of the excitation light the kinetic energy of the primary photochemical reaction products increases and hence also the probability of these products escaping from the solvent cage.

The data obtained from the study of inner-complex photoredox reactions can be referred to various energetic characteristics of the irradiated complex and products of its decomposition. Relationships between the threshold energy of the reaction, E_{th}, the energy of the bond split in the primary process, ΔH_{b}, characteristics of the central atom and ligand undergoing a redox change (ionization energies, IE; electronegativity, χ; electron affinities, EA), solvation energies, ΔH_{s}, and ligand-field stabilization energies, LFSE, were applied in particular to pentaammine complexes of Co(III) and Rh(III) with acido ligands X^-. These complexes will be designated $[ML_5X]^{2+}$.

Generally, the relationship between ΔH_{b} and E_{th} for a process in which the spin remains unchanged is

$$\Delta H_{\mathrm{b}} = E_{\mathrm{th}} + \Delta H_{\mathrm{s}} + \Delta H_{\mathrm{spin}} \tag{4.48}$$

where ΔH_{s} represents a change in the solvation energy of the reactant and product for the process

$$[L_5M^{\mathrm{III}}\text{–}X^-]^{2+} \xrightarrow[E_{\mathrm{th}}]{h\nu} [L_5M^{\mathrm{II}}, X^{\bullet}] \tag{4.49}$$

and can be calculated from thermodynamic cycles and ΔH_{spin} is the energy related to the spin changes in the reaction (e.g., $[CoL_5X]^{2+}$ complexes are of a low-spin type, the $[CoL_5]^{2+}$ particle has a high-spin quartet ground state). The energy E_{th} thus represents the difference between the energies of the reactant and product in their ground states.

$$\begin{tikzcd}
M^{3+}_{(g)} + 5L + X^-_{(g)} \arrow[r, "\mathrm{IE} + \mathrm{EA}"] \arrow[d, "U_0 +"', "\mathrm{LFSE}[M^{\mathrm{III}}L_5X^-]"] & M^{2+}_{(g)} + 5L + X^{\bullet}_{(g)} \arrow[d, "U_0' +"', "\mathrm{LFSE}[M^{\mathrm{II}}L_5]"] \\
M^{\mathrm{III}}L_5X^- \arrow[r, "\Delta H_b"] \arrow[d, "\Delta H_s"] & M^{\mathrm{II}}L_5, X^{\bullet}_{(g)} \arrow[d, "\Delta H_s"] \\
[M^{\mathrm{III}}L_5X^-]_{\mathrm{solv}} \arrow[r, "\Delta H_b + \Delta H_s"] & [M^{\mathrm{II}}L_5, X^{\bullet}]_{\mathrm{solv}}
\end{tikzcd}$$

Fig. 13. Schematic diagram showing the relationship between thermodynamic parameters of inner-sphere electron-transfer reaction for $[M^{\mathrm{III}}L_5X]^{2+}$ complexes.

Relationships between the energy parameters are frequently illustrated in schemes of energy cycles. One of them is shown in Fig. 13 [205] (for the sake of simplicity the given particles are presented without charges). It follows from the scheme that

$$\Delta H_b = \mathrm{IE} + \mathrm{EA} + \Delta U_0 + \Delta\mathrm{LFSE} \qquad (4.50)$$

where IE is the second ionization energy of the atom M, EA the electron affinity of the particle $X^{\bullet}$, ΔU_0 the difference between the spherical components of the ligand field potential and ΔLFSE the difference between the stabilization energies for the species $[M^{III}L_5]$ and $[M^{II}L_5]$, provided the following equation is valid:

$$^{\mathrm{LFSE}}[M^{III}L_5] = {}^{\mathrm{LFSE}}[M^{III}L_5X] - 4\mathrm{Dq}(X^-) \qquad (4.51)$$

ΔH_b is related to the properties of the central atom and ligand X^- as follows:

$$\Delta H_b = [125(\chi_X - \chi_M)^2 + (E_{M_2}E_{X_2})]^{0.5} + 4\mathrm{Dq}(X^-) + \Delta\mathrm{LFSE} \qquad (4.52)$$

In eqn. 4.52, the Allred–Rochow electronegativity values are used (other parameters being in kJ). The term containing electronegativities (χ) expresses the ionic contribution to the bond energy; the term consisting of energies of the M–M and X–X bonds expresses the covalent contribution. For illustration, data on the calculation of ΔH_b, according to eqns. 4.48 and 4.52, for $[Co(NH_3]_5X]^{2+}$ complexes are presented [205] in Table 13 ($\Delta H_{\mathrm{spin}} = 47$ kJ mol^{-1}, $E_{\mathrm{Co}_2} = 51$ kJ mol^{-1}).

TABLE 13

Spectral and thermodynamic data for complexes of $[Co(NH_3)_5X]^{2+}$(for details, see text). Energy quantities are in kJ mol^{-1} [205]

X	E_{th}	ΔH_s	ΔH_b(obs)	χ_X	4Dq(X$^-$)	ΔLFSE	ΔH_b(calc)
Cl	310	83	273	2.87	74	83	278
Br	260	73	236	2.74	66	80	245
I	198	55	186	2.21	46	91	173
NO_2	248	60	273	2.6	149	77	290
N_3	259	60	247	2.77	75	79	220
NCS	285	60	273	2.61	99	86	232
SCN	236	60	225	2.53	88	90	213

Most photochemical studies deal with kinetically inert complexes. Calculation of the kinetic parameters of the deactivation processes of the individual kinetically labile complexes with the dynamic equilibrium

$$M \overset{L}{\rightleftharpoons} ML \ldots \overset{L}{\rightleftharpoons} ML_i \ldots \overset{L}{\rightleftharpoons} ML_n \tag{4.53}$$

where M and ML_i are solvated ions of the central atom and solvated complexes and n is the maximum number of ligands coordinated to the central atom (charges of the particles are not given), is more complicated than for systems containing only one photochemically active complex.

Conditions for the calculation are documented [206] using the determination of the quantum yields of a photoredox deactivation of the individual kinetically labile complexes, Φ_i^{red}, which was applied to the study of the inner-complex photoredox reactions of Cu(II) chloro complexes in acetonitrile during which photoreduction of Cu(II) to Cu(I) took place.

The distribution of the individual ML_i complexes depends on their stability constants, β_i, under the given conditions and can be expressed in terms of fractional concentrations, α_i:

$$\alpha_i = \frac{c_i}{c_M} = \frac{\beta_i c_M c_L^i}{\sum_i^n \beta_i c_M c_L^i} \tag{4.54}$$

where c_i and c_M (c_L) denote the equilibrium concentration of the ML_i complex and total concentrations of M and L, respectively. In a system with different $c_M : c_L$ ratios (for the calculation, the photochemical properties of a minimum of n systems must be studied), the α_i parameters assume different values, while it always holds that

$$\sum_i^n \alpha_i = 1 \tag{4.55}$$

From the spectral properties of all n systems for any wavelength it is possible from n equations:

$$A_\lambda = c_M d \sum_i^n \alpha_i \varepsilon_{i,\lambda} \tag{4.56}$$

to calculate the values of the molar absorption coefficients, $\varepsilon_{i,\lambda}$, for each complex (d is the optical cell thickness).

The number of photons absorbed per time unit by the ith complex during irradiation of systems with monochromatic light of wavelength λ, I_i, can be calculated from the following relationship:

$$I_i = I_0 \left(1 - 10^{-c_M d \sum_i^n \alpha_i \varepsilon_{i,\lambda}}\right) \frac{\alpha_i \varepsilon_{i,\lambda}}{\sum_i^n \alpha_i \varepsilon_{i,\lambda}} \tag{4.57}$$

or, when introducing I_{abs} (I_0 and I_{abs} are the number of photons entering or absorbed in the system, respectively, per unit time):

$$I_i = I_{abs} \frac{a_i \varepsilon_{i,\lambda}}{\sum_i^n a_i \varepsilon_{i,\lambda}} \tag{4.58}$$

From the definition of the experimentally determinable rate of photochemical reactions:

$$v_{exp} = -\frac{dc_M}{dt} = -\sum_i^n \frac{dc_i}{dt} = \Phi_{exp} I_{abs} \tag{4.59}$$

and an analogous relationship valid for each of the n complexes:

$$v_i = -\frac{dc_i}{dt} = \Phi_i I_i \tag{4.60}$$

n equations can be derived:

$$\Phi_{exp} = \frac{\sum_i^n \Phi_i a_i \varepsilon_{i,\lambda}}{\sum_i^n a_i \varepsilon_{i,\lambda}} \tag{4.61}$$

and calculated from the Φ_i values (Φ_{exp} are experimentally found quantum yields of the reaction or product in each of the n systems studied).

The results for systems of Cu(II) chloro complexes irradiated with 470-nm light are given in Table 14.

TABLE 14
Values of molar absorption coefficients, $\varepsilon_{470\,nm}$, and quantum yields of Cu(I), $\Phi_{Cu(I)}$, for photoreduction of chlorocopper(II) complexes in acetonitrile [206]

Complex [a]	$\varepsilon_{470\,nm}$ ($l\,mol^{-1}\,cm^{-1}$)	$\Phi_{Cu(I)}$
$[CuCl_2(ACN)_2]$	217	0.299
$[CuCl_3(ACN)]^-$	1574	0.093
$[CuCl_4]^{2-}$	1289	0.053

[a] Complexes $[Cu(ACN)_4]^{2+}$ and $[CuCl(ACN)_3]^+$ do not absorb at 470 nm.

The above method can also be applied to photophysical processes, e.g., emission of radiation, however, the equations:

$$\Phi_{\text{exp}}^{\text{em}} = \frac{\sum_{i}^{n} \Phi_i^{\text{em}} a_i \varepsilon_{i,\lambda}}{\sum_{i}^{n} a_i \varepsilon_{i,\lambda}} \tag{4.62}$$

must include the a_i values obtained under the conditions of the measurement of emission spectra (often at low temperatures).

It is known that efficiency of the conversion of light into chemical energy in green plants and algae is high, which has attracted the interest of photochemists. It was found that following the absorption of a photon by chlorophyll, the first electron transfer reaction is extremely fast ($k > 10^{11}\ \text{s}^{-1}$) and proceeds from a singlet excited state. The quantum yield of the subsequent electron transfer is nearly unity. To understand the processes of photosynthesis in detail, several types of model systems have been prepared and the course of their intramolecular electron-transfer reactions has been investigated. The results obtained should be mentioned in this section in spite of the fact that no net chemical change (redox decomposition of primary excited systems) was observed.

In Zn(II) porphyrin-linked-to quinone molecules, ZnP–R–′Q, where R is an organic linking group bridging the porphyrin complex with the quinone ′Q, the rate constant of electron transfer:

$$*[\text{ZnP–R–}'\text{Q}] \xrightarrow{k} [\text{ZnP}^{+}\text{–R–}'\text{Q}^{-}] \tag{4.63}$$

depends on the driving force of the reaction, the porphyrin–quinone distance and the solvent [207]. The relationship between the rate constant and the above factors is not unambiguous and, moreover, the rate constant will probably be influenced by the mutual orientation of the porphyrin and quinone moieties, the properties of the linking group R and external influences.

The sensitivity of light-driven intramolecular electron-transfer reactions to solvation and structural changes was demonstrated [208, 209] by the investigation of the photochemical behaviour of doubly linked diporphyrins consisting of magnesium(II) and free base protonated subunits, MgP–H$_2$P. It was shown that the course of deactivation processes was influenced particularly by the mutual orientation of the porphyrin rings and the properties of the solvent. In any of the systems studied, the primary process of electron transfer did not result from the excited singlet state

$$^{1}[\text{MgP–H}_2\text{P}]* \xrightarrow{\tau < 6\text{ps}} (\text{MgP}^{+}\text{–H}_2\text{P}^{-}] \tag{4.64}$$

into decomposition of the diporphyrin moiety.

It is evident from the results presented in this section that the study of the kinetics, thermodynamics and quantum-mechanical aspects of inner-sphere photoredox decomposition reactions can contribute markedly to a more detailed understanding of bond-making and bond-breaking processes and thus to the reactivity of chemical compounds in general.

The inner-sphere photoredox reactions are of great importance to polymer chemistry and other fields of practical application of photochemistry (see Chapter 5). Simultaneously with the development of the theory of such reactions, an increase of their practical applications can also be expected.

4.2.6 Photoredox reactions of polynuclear complexes

Together with the development of the knowledge of the electronic structure of polynuclear complexes (particularly with metal–metal bonds) obtained by photoelectron spectroscopy, quantum chemistry and electronic absorption and emission spectroscopy, the study of photochemical deactivation processes of these complexes has also been developed.

Polynuclear complexes provide redox reactions analogous to mononuclear complexes (see previous sections). In this section, redox reactions that are only typical for polynuclear complexes will be discussed, namely intramolecular electron-transfer reactions from one to another central atom, connected by a bridging ligand, redox decomposition of polynuclear complexes forming mononuclear compounds, redox synthesis of polynuclear complexes and redox rearrangements accompanied by changes in the composition of polynuclear complexes.

Much effort has been devoted to the study of both thermal and photochemical intramolecular electron-transfer reactions. Unlike outer-sphere reactions, where the precursor and successor complexes are ion pairs or outer-sphere complexes, for intramolecular redox reactions the precursor and successor are binuclear (or polynuclear, in general) complexes in which a bridging ligand(s) connect(s) two central atoms. Thus, the successor and precursor may be regarded as redox isomers.

In the context of theoretical approaches applied to studies of thermal and photochemical electron transfer, ligand-bridged mixed-valence compounds are of great interest. In these dimers, the redox sites are held at a well-defined distance and geometry relative to one another, electron transfer between sites is often a reversible process and, using transient photolysis techniques, much valuable information can be obtained experimentally.

Electron transfer between the central atoms can include both redox changes localized on ligands and intramolecular energy transfer depending on the redox potentials of redox sites, the energy content of individual excited states and the wavelength of the exciting light.

As during excitation the redox sites are in direct interaction, the rate constant of electron transfer, k_{et}, can be higher than the diffusion-limited rate constant, k_{dif}.

A relatively simple mechanism of electron transfer in a mixed valence complex can be exemplified [210] by a reaction involving reduction of the pyrazine bridging ligand and a change of the oxidation number of the central atoms:

$$\begin{tikzcd}[column sep=small]
{[(\mathrm{NH_3})_5\mathrm{Ru^{II}(pz)Ru^{III}(EDTA)}]^+} \arrow[rr, "h\nu"] & & {[(\mathrm{NH_3})_5\mathrm{Ru^{III}}(\mathrm{pz}\overset{-}{\bullet})\mathrm{)Ru^{III}(EDTA)}]^+} \arrow[dl, "k_1"] \\
& {[(\mathrm{NH_3})_5\mathrm{Ru^{III}(pz)Ru^{II}(EDTA)}]^+} \arrow[ul, "k_2"] &
\end{tikzcd} \tag{4.65}$$

for which rate constants of electron transfer of $k_1 > 10^{11}\ \mathrm{s^{-1}}$ and $k_2 = 8 \times 10^9\ \mathrm{s^{-1}}$ have been determined.

The electron-transfer rate constant for the reaction

$$_{\mathrm{IVCT}}^{*}[(\mathrm{S})_2\mathrm{ClRu^{III}(L)Ru^{II}Cl(bpy)_2}]^{3+} \xrightarrow{k_{et}} {}_{\mathrm{GS}}[(\mathrm{S})_2\mathrm{ClRu^{II}(L)Ru^{III}Cl(bpy)_2}]^{3+} \tag{4.66}$$

where bridging ligand L = 4,4′-bipyridine or 1,2-dipyridylethylene and S denotes the bidentate ligand 1,2-diphenylthioethane, is $k_{ek} = 6 \times 10^{10}\ \mathrm{s^{-1}}$ [211]. The intervalence charge-transfer excited state was formed by the following sequence:

$$\mathrm{GS} \xrightarrow{h\nu} \mathrm{Ru^{II}} \rightarrow \mathrm{L(CT)} \xrightarrow{\text{fast}} \mathrm{Ru^{II}} \rightarrow \mathrm{(bpy)(CT)} \xrightarrow{\text{slow}} \mathrm{IVCT} \tag{4.67}$$

which corresponds to the lowering of the energies of the given excited states.

If the binuclear redox isomer has at least one central atom forming kinetically labile complexes, decomposition of the complex from the IVCT excited state can take place. This assumption was verified by the study of thermally stable binuclear $\mathrm{Co^{III}{-}Ru^{II}}$, $\mathrm{Cr^{III}{-}Fe^{II}}$ and other complexes. For instance [44], irradiation of a thermally stable ($E^0([\mathrm{Co(NH_3)_6}])^{3+/2+} = 0{,}11$ V, $E^0([\mathrm{Ru(CN)_6}])^{3-/4-} = 0.86$ V), kinetically inert complex with a bridging cyanide ligand, $[(\mathrm{NH_3})_5\mathrm{Co^{III}{-}NC{-}Ru^{II}(CN)_5}]^-$, in the region of the IVCT transition ($\lambda_{max} = 375$ nm) leads to the following redox decomposition:

$$[(\mathrm{NH_3})_5\mathrm{Co^{III}NCRu^{II}(CN_5)}]^- \xrightarrow[\mathrm{IVCT}]{h\nu} {}^*[(\mathrm{NH_3})_5\mathrm{Co^{II}NCRu^{III}(CN)_5}]^- \rightarrow$$

$$\rightarrow \mathrm{Co^{2+}_{aq}} + 5\mathrm{NH_3} + [\mathrm{Ru^{III}(CN)_6}]^{3-} \tag{4.68}$$

owing to the lability of the Co(II) centre. The same mechanism was suggested [44] for the redox decomposition of the IVCT excited state of the $[(NH_3)_4(H_2O)Cr^{III}-NC-Fe^{II}(CN)_5]^-$ complex [owing to the formation of a kinetically labile Cr(II) centre].

Photoredox decomposition of polynuclear complexes can also be found with species other than mixed-valence compounds in their IVCT states.

Of the binuclear bridging complexes, particularly Co(III) complexes were studied with regard of their photochemical properties [7]. Irradiation of the systems of such complexes results in dissociation into monomolecular complexes, e.g.,

$$[(NH_3]_5Co^{III}-O_2^{-}-Co^{III}(NH_3)_5]^{5+} \xrightarrow[H_2O+H_3O_+]{h\nu} Co^{2+}_{aq} + O_2 + 5NH_4^+ + [Co^{III}(NH_3)_5(H_2O)]^{3+} \qquad (4.69)$$

It is probable that the complex dissociation takes place from the superoxo ligand to the central atom excited state.

Within the framework of the study of the roles of iron-containing enzymes (cytochrome P-450, horseradish peroxidase, etc.) in both oxygen-transfer and electron-transfer processes, the redox photodisproportionation of model complexes, such as μ-oxobisporphyriniron(III), has been investigated using continuous and flash photolysis and spin-trapping ESR [212–214]. The primary photochemical step is redox photodisproportionation of the dimer:

$$[(TPP)Fe^{III}-O-Fe^{III}(TPP)] \xrightarrow{h\nu} [Fe^{IV}O(TPP)] + [Fe^{II}(TPP)] \qquad (4.70)$$

In the absence of an oxidizable compound, primary (cage) and secondary recombination are very effective processes and the quantum yield of the mononuclear complexes is very low ($\Phi < 10^{-5}$).

A careful analysis of the experimental data (the dependence of the quantum yield on the excitation energy for oxygen-, nitrogen- and carbon-bridging dimers) led to the conclusion [212] that a highly distorted, vibrationally nonrelaxed CT state is responsible for the primary photochemical step. The reactive CT state can be obtained by photoexcitation or by internal conversion (triplet–triplet transition) from the porphyrin-localized IL excited state. The ferryl complex represents a strong oxygen-donor or electron-acceptor oxidant.

A different photochemical behaviour from that of the usual metalloporphyrins that have one central atom incorporated in a porphyrin ligand is exhibited by dinuclear complexes with a porphyrin acting as a bridging ligand and two central atoms located on each side of the porphyrin plane. A typical example of such compounds is (μ-tetraphenylporphinato)bis(dicarbonylrhodium(I)), $[(TPP)\{Rh^{I}(CO)_2\}_2]$. The dinuclear rhodium complex photodecomposes from the lowest vibrational level of each higher excited singlet state, S_n $(n > 2)$, as was deduced [154, 215] on the basis of an interpretation of experimental results(the wavelength dependence of the quantum yield, transient spectra measurements, steady-state and laser flash photolyses). The primary photochemical step following the excitation into a higher singlet state was proposed to be

$$[(TPP)\{Rh^{I}(CO)_2\}_2] \xrightarrow{h\nu} [(TPP)Rh^{II}(CO)_2] + Rh^0 + 2CO \qquad (4.71)$$

In benzene, an intermediate $[(TPP)Rh^{II}(CO)_2]$ is converted into a diamagnetic dinuclear Rh(II) complex:

$$2[(TPP)Rh(CO)_2] \rightarrow [(TPP)Rh]_2 + 4CO \qquad (4.72)$$

In the presence of carbon tetrachloride, mononuclear Rh(III) complex is formed according to the reaction

$$[(TPP)Rh^{II}(CO)_2] + CCl_4 \rightarrow [(TPP)Rh^{III}Cl(CO)] + CO + CCl_3^{\bullet} \qquad (4.73)$$

In connection with the exploitation of photochemistry for the preparation of organometallic and coordination compounds, and with the catalytic properties of compounds with metal–metal bonds, the photochemical and photophysical behaviour of polynuclear compounds with metal–metal bonds has been extensively investigated. It should be noted that the photochemistry of binuclear complexes (in particular those with a single metal–metal bond) differs from that of cluster compounds.

Irradiation of binuclear complexes with a single metal–metal bond in the region of transition localized on the central atoms frequently results in homopolar cleavage of this bond, forming coordinatively unsaturated fragments [9, 216] that are able to undergo a redox process, for example [9]

$$[(CO)_5Mn\text{–}Re(CO)_5] \xrightarrow[CCl_4]{h\nu} [Mn(CO)_5Cl] + [Re(CO)_5Cl] \qquad (4.74)$$

As neither energy transfer from the excited binuclear complex nor luminescence takes place, the rate constant of the Mn–Re bond cleavage must be higher than $10^{10}\ s^{-1}$. The bond cleavage is not connected only with σ^*-orbital population but also with depopulation of σ- or d_π(M)-orbitals localized on the metal–metal fragment. This is evident from the fact that an analogous bond breaking occurs also when the MLCT state is the energetically lowest excited state. This can be exemplified by homolytic splitting of the Re–Re bond during irradiation of the complex $[(CO)_5Re{-}Re(CO)_3(phen)]$ in the region of the $\sigma(Re{-}Re) \rightarrow \pi^*(phen)$ transition.

In polynuclear complexes with simple metal–metal bonds, the probability that monoelectron excitation results in decomposition of the complex is low. An example of a reaction during which declustering takes place is decomposition of the $[HCCo_3(CO)_9]$ complex with a tetragonal arrangement of the C and Co atoms [9]

$$2[HCCo_3(CO)_9] + 6CO + 3H_2 \xrightarrow{h\nu} 3[Co_2(CO)_8] + 2CH_4 \qquad (4.75)$$

Redox reactions of large clusters, such as $[Ta_6Br_{12}]^{2+}$, $[Mo_6Cl_{14}]^{2-}$ and $[W_6Br_{14}]^{2-}$, are not usually associated with their decomposition owing to delocalization of the redox orbitals over the whole particle [217]. Unlike binuclear complexes, however, clusters may undergo bimolecular electron-transfer reactions with participation of two or more electrons. The excited states of clusters can be distorted but, owing to delocalized molecular orbitals, distortions are not likely to be strong.

Photoexcitation of mononuclear complexes and deactivation connected with the formation of coordinatively unsaturated monomeric intermediates may result in the production of polynuclear complexes. The composition of a product and its structure depend on the properties of the central atom. This statement can be supported by results obtained by irradiation of solutions of $[IrH(PF_3)_4]$, $[CoH(PF_3)_4]$ or their mixture. In the former instance [218], a complex with a metal–metal single bond is formed:

$$2[Ir^IH(PF_3)_4] \xrightarrow{h\nu} H_2 + [(PF_3)_4Ir^0{-}Ir^0(PF_3)_4] \qquad (4.76)$$

In the latter two instances [219, 220], double-bridged compounds were prepared:

$$2[CoH(PF_3)_4] \xrightarrow{h\nu} [(PF_3)_3Co(\mu\text{-}H)(\mu\text{-}PF_2)Co(PF_3)_3] + HF + PF_3 \qquad (4.77)$$

$$[CoH(PF_3)_4] + [IrH(PF_3)_4] \xrightarrow{h\nu} [(PF_3)_3Co(\mu\text{-}H)(\mu\text{-}PF_2)Ir(PF_3)_3] + HF + PF_3 \qquad (4.78)$$

Complexes with multiple metal–metal bonds also undergo photoredox reactions. The primary process in irradiation of the systems of such complexes is not the formation of mononuclear fragments, but an attack of the excited complex by the solvent, electron or atom transfer. As an example, the photoredox properties of the $[Mo_2Cl_8]^{4-}$ complex with a quadruple bond between the molybdenum atoms can be considered. Irradiation of the complex in the region $p_\pi(\mathrm{Cl}^-) \rightarrow \sigma^*(\mathrm{Mo{-}Mo})$ leads to the following reaction [33]:

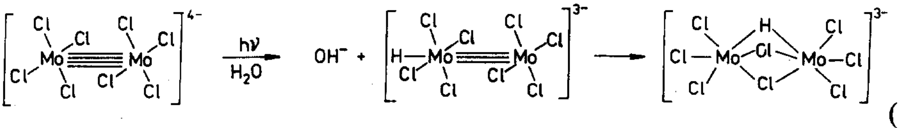

(4.79)

In acidic media, the last complex is converted into an aquated cation, $[\mathrm{Mo}(\mu\text{-}\mathrm{OH})\mathrm{Mo}]^{4+}$, and hydrogen escapes from the system. Studies of the photochemical properties of complexes with a quadruple metal–metal bond (molybdenum and rhenium compounds) indicate that this bond is split only from the energetically higher excited states and the reactions are influenced by axial interactions in the complexes.

A complicated redox rearrangement occurs [221] on irradiating the $[\mathrm{Re_2Cl_8}]^{2-}$ anion, which possesses a quadruple Re(III)–Re(III) bond. The complex in its $\delta\delta^*$ singlet state is a very powerful reductant and in dichloromethane solution in the presence of $[\mathrm{PtCl_6}]^{2-}$ yields a triple-bridged rhenium(IV) binuclear complex, $[\mathrm{Cl_3Re}(\mu\text{-}\mathrm{Cl})_3\mathrm{ReCl_3}]^-$:

$$[\mathrm{Re_2Cl_8}]^{2-} + [\mathrm{PtCl_6}]^{2-} \xrightarrow{h\nu} [\mathrm{Re_2Cl_9}]^- + [\mathrm{PtCl_4}]^{2-} + \mathrm{Cl}^- \qquad (4.80)$$

During the above-specified photochemical reactions of $[\mathrm{Mo_2Cl_8}]^{4-}$ and $[\mathrm{Re_2Cl_8}]^{2-}$ complexes, the metal–metal bond is cleaved, and an oxidative addition process and rearrangement of the complex take place. Opposite processes appear during the irradiation [222] of several hydride-bridged binuclear complexes of platinum(II) when a reductive elimination process gives rise to a binuclear platinum(I) complex containing a single Pt–Pt bond. Reactions can be expressed in the form shown in eqn. 4.81, where $X = \mathrm{H}$ or $\mathrm{CH_3}$, $Y = \mathrm{H}$ or $\mathrm{CH_3}$, L is a solvent molecule (pyridine, acetonitrile, acetone) and P–P denotes a $\mathrm{Ph_2P{-}CH_2{-}PPh_2}$ bridging ligand:

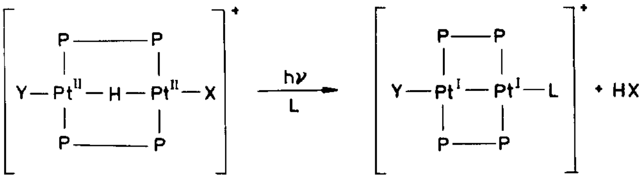

(4.81)

Using deuterated compounds and determining the products by mass spectrometry, it was proved that the reductive elimination of HX was an intramolecular process. The primary photochemical step was probably cleavage of the $\mathrm{Pt}(\mu\text{-}\mathrm{H})\mathrm{Pt}$ linkage by excitation of an electron to a σ^*-antibonding orbital localized on the Pt–Pt moiety.

In contradistinction to the hitherto presented elimination and addition redox reactions of binuclear complexes accompanied by metal–metal bond-making or bond-breaking processes, redox additions and eliminations can also occur without such processes. In this way [223], oxidative additions of ArX (Ar = aryl, X = Br, I) to the excited $^*[Pt_2(\mu\text{-}P_2O_5H_2)_4]^{4-}$ species take place, giving the axially disubstituted complexes $[Pt_2(\mu\text{-}P_2O_5H_2)_4(Ar)X]^{4-}$. It was proved that aryl halide addition occurred by a double activation induced by a single electron-transfer pathway. The transfer of an electron from the long-lived excited triplet state represented by $(d_{z^2})^2(d^*_{z^2})^1(p_z)^1$ owing to its strong reducing properties $\{E([Pt_2(\mu\text{-}P_2O_5H_2)_4^{3-/4-})^* = -1\ \mathrm{V}\}$ to an aryl halide molecule yields the $ArX^{\bullet}$ radical ion, which rapidly dissociates to $Ar^{\bullet}$ and X^-. Both the $Ar^{\bullet}$ and X^- particles coordinate to the platinum atoms of the oxidized binuclear complex forming the final product. From the viewpoint of stoichiometry, the photoredox addition can be described as follows:

$$[Pt^{II}(\mu\text{-}P_2O_5H_2)_4Pt^{II}]^{4-} + ArX \overset{h\nu}{\rightarrow} [ArPt^{III}(\mu\text{-}P_2O_5H_2)_4Pt^{III}X]^{4-} \qquad (4.82)$$

A description of the electronic structure of polynuclear complexes in the language of localized molecular orbitals [for the given Pt(II) complexes, for example, $GS(d_{z^2})^2(d^*_{z^2})^2 \rightarrow ES(d_{z^2})^2(d^*_{z^2})^1(p_z)^1)$] is a very rough approximation of reality. Substantial delocalization of valence orbitals, spin–orbit coupling and relativistic effects complicate significantly the description of the real electronic structure of the excited polynuclear complexes. Quantum chemical studies at the ab initio level for polynuclear excited particles are still very rare. These and other factors have made it impossible so far to formulate the relationships between the type of the excited state and the reactivity of polynuclear complexes.

4.2.7 Photoredox reactions of coordinated ligands

Inorganic photochemists have focused their attention on the reactions involving changes localized on the central atom of a complex. In addition to central atom-localized redox processes, there are also photoredox reactions in which the central atom seems to be untouched and the redox process is localized on a coordinated ligand(s) only. Ligand-localized photoredox reactions may occur when the central atom itself is redox stable towards the given redox change [for example, Co(III) towards the oxidation, Zn(II) towards the reduction and oxidation] and a macrocyclic unsaturated polydentate ligand is coordinated on the central atom. It should be noted, however, that ligand-localized photoredox processes are not limited to porphyrin, corrin or phthalocyanine complexes. In a few instances it was observed that also complexes with monodentate ligands can undergo the discussed photoredox changes.

It is well known that free (protonated) porphyrins and metalloporphyrins can be oxidized (to the π-radical cation or π- dication) or reduced (to chlorines and hydrogenated compounds) [224]. As an example [224], the photooxidation of tin(IV) tetrakis(*N*-methyl-4-pyridyl)porphine can be considered. On excitation in the visible region [Sn^{IV}(TMPyP)]$^{4+}$ forms the triplet excited state possessing a long lifetime, which is quenched by an oxidant producing a π-radical cation. The secondary thermal reactions lead to the final product, ketoporphyrin. The mechanism of reaction 4.83 is not simple and consists of several steps which, for the sake of simplicity, have been omitted.

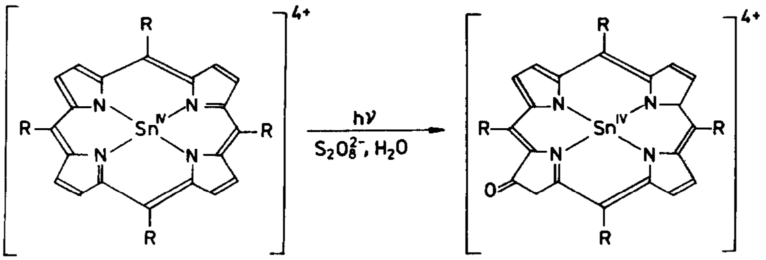

(4.83)

The importance of vitamin B_{12} for living organisms led to a systematic study of its preparation and physicochemical and biological properties, and also of its model systems within the context of which attention was also paid to its photochemical behaviour. A well-known chemical effect of the interaction of light with Co(III) corrinoid complexes is the homolytic cleavage of a Co(III)-axially coordinated ligand bond (usually a Co–C bond), yielding a Co(II) complex. Such a reaction occurs from an axial ligand-to-central atom CT excited state. From the viewpoint of the contents of this section, other types of photoredox reactions, not involving the central atom, are of interest.

A systematic investigation [225–227] of Co(III) cobyrinate compounds and of vitamin B_{12} has shown that under certain conditions (irradiation in methanol or CCl_4 solution in the presence of molecular oxygen and a sensitizer) the axial coordinate remained unchanged and the photoredox reaction was localized on the macrocyclic ligand. In all instances, irradiation resulted in the cleavage of the corrinoid macrocycle producing a dioxo ligand. For the hexamethyl Coα,Coβ-dicyano-7-de(carboxymethyl)-7,8-didehydrocobyrinate ($R = -CH_2CH_2CO_2CH_3$), the process of opening of the ring and formation of the dioxo compound can be expressed as follows:

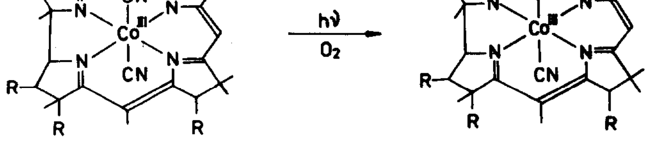

(4.84)

The reaction mechanism seems to involve attack of electrophilic singlet oxygen on the corrinoid π-system. The singlet state of molecular oxygen is photogenerated via excitation of the Co(III) complex. Some of the photooxygenation products were photochemically prepared in a substantial yield, which means that photochemical synthesis should be a convenient tool for preparing such "cleavage" compounds.

The ability of a ligand to undergo the redox change does not depend only on the ligand itself, but also on the properties of the central atom, the medium, other ligands in the coordination sphere and the radiation wavelength. The effect of these factors (especially of the central atom) was elucidated [222–232] by means of photoredox properties of complexes with phthalocyanine (Pc) derivatives. Three types of the primary photoredox step have been observed with these complexes.

A photoinduced dissociation of dimeric complexes into ligand-radical products has been observed on ultraviolet irradiation of Cu(II), Fe(II) and diaquacobalt(III)tetrasulphophthalocyanines:

$$[\mathrm{M}^{n+}(\mathrm{Pc})]_2^{(12-2n)-} \xrightarrow{h\nu} [\mathrm{M}^{n+}(\mathrm{Pc}\overset{-}{\cdot})]^{(7-n)-} + [\mathrm{M}^{n+}(\mathrm{Pc}\overset{+}{\cdot})]^{(5-n)-} \tag{4.85}$$

The central atom does not undergo an observable photochemical redox change.

With the Co(II) dimeric complex, a photoredox dissociation into metal-oxidized and metal-reduced species has been observed:

$$[\mathrm{Co^{II}(Pc)}]_2^{8-} \xrightarrow{h\nu} [\mathrm{Co^{III}(Pc)}]^{3-} + [\mathrm{Co^{I}(Pc)}]^{5-} \tag{4.86}$$

and the macrocyclic ligand does not participate in the primary photoredox step.

The complexes $[\mathrm{Co^{III}(Pc)X}]^{4-}$, where X^- is an axially coordinated Cl^-, Br^- or SCN^- ligand, under the action of ultraviolet light decompose, yielding $[\mathrm{Co^{II}(Pc)}]^{4-}$ and radical $\mathrm{X}^{\bullet}$ in the primary step.

Ligand-oxidized or ligand-reduced intermediates undergo secondary thermal (usually redox) reactions, or they can be photolysed if they are stable enough. Cation radicals $[\mathrm{Rh^{III}(Pc\overset{+}{\cdot})(CH_3OH)X}]^+$ may serve as a good example, as they are stable for more than 3 days in solution protected from oxygen, water and light. The photoredox behaviour of these compounds, with an unpaired electron localized in a π-HOMO of phthalocyanine ligand, depends strongly on the excitation wavelength. Irradiation in the UV region ($\lambda \leqslant 320\,\mathrm{nm}$) leads to photoproduction of the ligand radical (back to the parent Pc^{2-}), accompanied by the photooxidation of a solvent molecule. Irradiation in the visible region ($\lambda = 525\,\mathrm{nm}$) gives rise to photodecomposition of the macrocycle. Different products are due to the different distributions of electron density in the excited states involved, and are also evidence of low communication between these two excited states (low efficiency of interconversion).

As mentioned before, monodentate ligands are capable, although only in rare cases, of being photoreduced (oxidized). In the context of the study of iron(II) diphosphine complexes [189, 233], the photochemical behaviour of [Fe(diphos)$_2$(CH$_3$CN)$_2$] and [Fe(diphos)$_2$(CD$_3$CN)$_2$] was investigated in detail. In addition to other results, it was found that abstraction of a hydrogen (deuterium) atom by an excited Fe(0) complex in CH$_3$CN or CD$_3$CN solution:

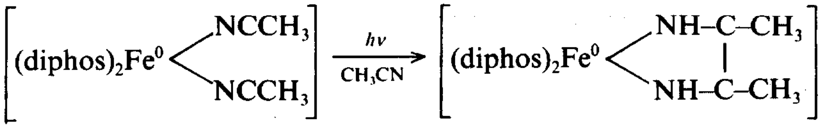

$$\left[(\text{diphos})_2\text{Fe}^0 \begin{matrix}\text{NCCH}_3\\ \text{NCCH}_3\end{matrix}\right] \xrightarrow[\text{CH}_3\text{CN}]{h\nu} \left[(\text{diphos})_2\text{Fe}^0 \begin{matrix}\text{NH–C–CH}_3\\ |\\ \text{NH–C–CH}_3\end{matrix}\right] \qquad (4.87)$$

takes place from solvent molecules and not the dp ligand. A consequence of the coordinated acetonitrile reduction is carbon–carbon bond formation.

It seems that photoredox reactions of coordinated ligands deserve more attention, especially because of the possibilities offered by photochemistry in the synthesis of new ligands.

4.3 Photoisomerization reactions of coordination compounds

4.3.1 Classification of photoisomerization reactions

Photoisomerization reactions are light-induced processes in which the composition of compounds is preserved, and their structure and properties are changed. Photoisomerizations may be divided into redox and non-redox reactions. The former were discussed in Section 4.2.3 and the latter are presented in this section.

For the sake of convenience, photoisomerizations are classified according to the changes in the structure, ligand composition and spin state into the following classes:

— photoisomerization of optical isomers (4.3.2),
— phototautomerization reactions of complexes (4.3.3),
— photoisomerization reactions of spin isomers (4.3.4),
— reactions of photoisomerization of coordinated ligands (4.3.5),
— photoisomerization of geometrical isomers (4.3.6),
— linkage photoisomerization reactions (4.3.7).

In the first four groups (Sections 4.3.2–4.3.5), neither the chromophore composition nor its structure is changed. In the reactions included in the group of mutual conversions of geometrical isomers, their structure but not the chromophore composition is changed. A change in both the composition and symmetry of the chromophore takes place during linkage photoisomerization. Other types of possible photoisomerization reactions (mutual conversion of distortion isomers [234, 235], coligand isomers [181], etc.) have not been investigated so far, although when, for example, the spin isomers have different internuclear distances between the central atom and donor atoms of ligands, the reactions in Section 4.3.5 can also be considered to be photochemical mutual transformation of distortion isomers.

The data available indicated that whereas the changes took place in the chromophore in the primary photochemical step, the reactions took place from the LF excited states, in the case of ligand-localized changes the corresponding photoreactive state was an IL state. Linkage photoisomerizations often take place from the LMCT excited state. However, inclusion of another type of excited state in mechanisms of photoisomerizations cannot be eliminated.

4.3.2 Photoisomerization interconversion reactions of optical isomers

Of the possible mutual conversions of optical isomers, conversions of one enantiomer into another have been studied in the photochemistry of coordination compounds [236, 237]. In the studies of such photoenantiomerizations, which are not numerous, some complexes [particularly Cr(III), Co(III), Rh(III) and Ru(II) with symmetric ligands such as acac$^-$, ox^{2-}, phen, bpy, denoted AA and BB, and also with asymmetric ligands such as tfacac$^-$, atc$^-$, denoted AB] were used. These bifunctional ligands were bonded in complexes of the type $[M(AA)_3]^{n+}$, $[M(AA)_2(BB)]^{n+}$ and *cis*- and *trans*-$[M(AB)_3]^{n+}$(n depends on the central atom and ligand charges). The coordination sphere of the investigated complexes may also contain monodentate ligands.

The quantum yields of the conversion of enantiomers D → L and L → D are identical owing to the analogous symmetry properties of enantiomers. Irradiation of one of enantiomers with non-polarized or plane-polarized light may even result in the production of a racemic mixture. Such a process, L $\xrightarrow{h\nu}$ rac or D $\xrightarrow{h\nu}$ rac, was observed when irradiating $[Cr(ox)_3]^{3-}$, $[Cr(phen)_3]^{3+}$, $[Cr(acac)_3]$ and others. In contrast, on irradiating a racemic mixture with circularly polarized light in a region with different molar absorption coefficients of enantiomers, $\varepsilon_{L,\lambda}$, $\varepsilon_{D,\lambda}$, a system rotating the plane of polarized light, containing different amounts of the two enantiomers, is formed. As the value of the dissymmetry factor, g, is low ($\varepsilon_{N,\lambda}$ is the value of molar absorption coefficient when using non-polarized light):

$$g = \frac{(\varepsilon_{L,\lambda} - \varepsilon_{D,\lambda})}{\varepsilon_{N,\lambda}} \tag{4.88}$$

no distinct photoresolution takes place (see the data in Table 15).

The quantum yields of photoenantiomerizations are calculated from the time dependence of the CD spectra of irradiated systems.

TABLE 15
Optical photoracemization and photoresolutions of complexes

Complex	Photoreaction[a]	Data, conditions	Ref.
$[Cr(en)_3]^{3+}$	Rac, 400 nm	$\Phi = 0.015$, $t = 30°C$, H_2O	[260]
$[Cr(ox)_3]^{3-}$	Rac, 420 nm	$\Phi = 0.11$, H_2O, 25°C	[261]
		$\Phi = 0{,}036$, $DMSO/H_2O = 1:10$ (molar)	
		$\Phi = 0.0005$, DMSO	
	Res, CP 546 nm	1.4°C	[262]
$[Cr(ox)_2(phen)]^-$	Res, CP 514 nm	% res = 2.0, 15°C, H_2O	[263]
$[Cr(ox)(phen)_2]^+$	Res, CP 496 nm or 514 nm	% res = 1.6, 15 °C, H_2O	[263]
$[Cr(phen)_3]^{3+}$	Res, CP 546 nm	% res = 1.7, 25 °C, H_2O	[264]
	Rac, 350 nm	$\Phi = 0.016$, H_2O	
$[Cr(acac)_3]$	Rac, 546 nm	$\Phi = 0.0098$, 31.4°C, acetone	[265]
		$\Phi = 0.0068$, 31.4°C, acetylacetone	
		$\Phi = 0.0055$, 25°C, C_6H_5Cl	
		$\Phi = 0.0059$, 41.3°C, C_6H_5Cl	
		$\Phi = 0.0073$, 52.3°C, C_6H_5Cl	
		$\Phi = 0.0382$, 61.8°C, C_6H_5Cl	
		$\Phi = 0.0091$, 69.7°C, C_6H_5Cl	
$[Ru(bpy)_3]^{2+}$	Rac, 458 nm	$\Phi = 5.2 \times 10^{-5}$, 3°C, H_2O	[237]
		$\Phi = 2.9 \times 10^{-4}$, 23°C, H_2O	
		$\Phi = 9.3 \times 10^{-4}$, 40°C, H_2O	

[a] Rac = photoracemization, unpolarized light; Res = photoresolution, circularly polarized light.

For photoenantiomerizations, four types of mechanism have been suggested. The first group covers reactions during which none of the bonds in a complex is cleaved in the primary photochemical step, and the transition of one enantiomer into another takes place by a twisting mechanism. It should be noted that the probability of such a reaction mechanism is low, particularly for complexes containing rigid ligands having a large volume.

The study of the photoisomerization of Cr(III) complexes with ligands such as 1,10-phenanthroline, 2,2′-bipyridine or acetylacetone has shown that the twisting mechanism seems to be plausible for these complexes (denoted CrN_6 in reaction 4.89):

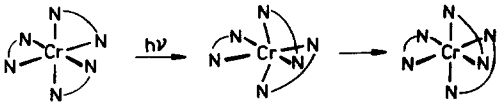

(4.89)

The second and third groups cover reactions in which heterolytic cleavage of one of the central atom–bidentate ligand bonds, as a consequence of the population of a $d\sigma^*$-antibonding orbital in the LF or LMCT excited states, is the primary process. Such a cleavage is expected in the $[Cr(ox)_3]^{3-}$ complex. Depending on the solvent properties, the reaction may proceed through a pentacoordinated trigonal-bipyramidal intermediate which can be partly distorted, as it is in aqueous solution:

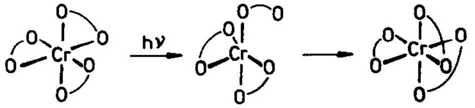

(4.90)

or through a hexacoordinated intermediate in which one site is occupied with a solvent molecule, S, as it is assumed for DMSO solutions:

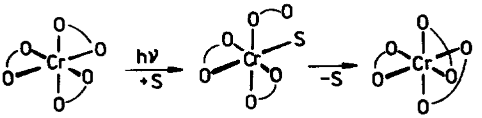

(4.91)

It is obvious that in reaction 4.91 not only coordination and displacement of the solvent molecule from the coordination sphere of the $[Cr(ox)_3]^{3-}$ complex takes place, but in the course of direct reaction distortion of the coordination polyhedra must occur in such a way that an optical isomer can be formed.

The fourth group of photoenantiomerizations covers processes in which a homolytic metal–ligand bond cleavage with the production of pentacoordinated intermediates with D_{3h} chromophore symmetry is the primary photochemical step, followed by intramolecular recombination yielding the optical isomer of a reactant. Such a mechanism is expected in the photoracemization of a Δ- or Λ-complex of $[Ru(bpy)_3]^{2+}$ [where bond breaking takes place from the MLCT triplet forming Ru(III) and reduced ligand], and also with the $[Rh(tfacac)_3]$ complex [with reduction of Rh(III) and oxidation of a tfa ligand in the LMCT state]:

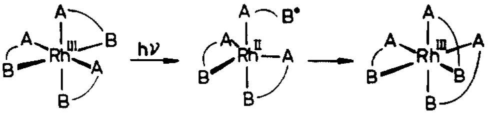

(4.92)

Hence the mechanisms of photoenantiomerizations are analogous to those of thermal isomerizations of optical isomers.

The appearance of induced optical activity was observed [237] on irradiating a system containing a mixture of Δ-$(Ru(bpy)_3]^{2+}$ and racemic $[Co(acac)_3]$. This occurs because of a higher rate of bimolecular deactivation of excited $^*[Ru(bpy)_3]^{2+}$ by the Λ-isomer of the $[Co(acac)_3]$ complex in comparison with that caused by the Δ-isomer. Although the mechanism of quenching consists in the electron-transfer process in which the triplet MLCT excited Ru(II) complex acts as an electron donor, no permanent decrease in the $[Ru(bpy)_3]^{2+}$ concentration was observed.

4.3.3 Phototautomerization reactions

These reactions are rare in the photochemistry of coordination compounds, and no systematic attention has been paid to them so far.

Phototautomerizations taking place together with *cis-trans* isomerization of azomethine group helped to explain the photochromism of several metal dithizonates, such as [238]

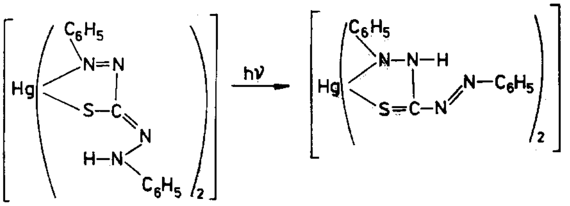

(4.93)

Thus, with dithizonates the reaction is an inner-ligand proton transfer connected with a change in the ligand structure and localization of π-bonds.

The proton transfer between two coordinated ligands was observed [240] during irradiation of the $[Ir(bpy)_3(H_2O)]^{3+}$ complex, in which one of the 2,2′-bipyridine ligands was bonded monofunctionally:

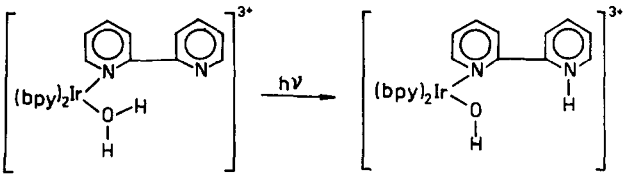

(4.94)

The increased proton affinity of a non-coordinated nitrogen atom of a monofunctionally bonded ligand is due to the increase in the negative charge on this ligand in the MLCT excited state.

It can be assumed that also in other instances the phototautomerization reactions will be connected with the change in the electron density distribution on the ligand, and unless they result in the decomposition of the complex, these will be reverse processes. It is known [241, 242] that in organic systems excited-state proton-transfer reactions occur very rapidly (in several instances the rate constant of the intramolecular excited-state proton-transfer reaction is $k_{PT} > 10^{11}$ s^{-1}, even at 4 K) and the reaction has no potential barrier. The k_{PT} values and hence the values of phototautomerizations have not yet been measured for inorganic compounds, but they also are expected to be high.

4.3.4 Photoisomerization reactions of spin isomers

In living organisms, compounds exist whose biological function is connected with changes in their spin state. A classical example is haemoglobin, providing a diamagnetic dioxygen molecule-containing complex with the coordination number 6, and a high-spin pentacoordinated complex not containing oxygen. There are many iron(II) compounds that, depending on the conditions (temperature, pressure), exist in both a low-spin diamagnetic singlet state and a high-spin paramagnetic quintet state. These compounds are known to exhibit thermally (or pressure) [72] induced high-spin⇄low-spin transitions [243] ($^5T_{2g} \rightleftharpoons {}^1A_{1g}$ in the ligand field of octahedral symmetry).

It was observed that low-spin→high-spin isomer conversion can also be light-induced and the high-spin isomer trapped at a sufficiently low temperature. Such a phenomenon has been called "light-induced excited-spin-state trapping" [244, 245].

Conversions of spin isomers can be light-induced in one or both directions:

$$^1[Fe(ptz)_6](BF_4)_2 \underset{h\nu\,(\lambda > 700\,nm)}{\overset{h\nu\,(\lambda < 14\,nm)}{\rightleftharpoons}} {}^5[Fe(ptz)_6](BF_4)_2 \qquad (4.95)$$

and these complexes, such as $[Fe(ptz)_6](BF_4)_2$, $[Fe(phen)_2(NCS)_2]$ and $[Fe(2\text{-pic})_3]Cl_2 . C_2H_5OH$, exhibit photochromic behaviour.

The energy content of the low-spin ground-state $^1A_{1g}$, high-spin ground-state $^5T_{2g}$ and excited states taking part in the photoexcitation and deactivation processes increase in the following order: $^1A_{1g} < {}^5T_{2g} < {}^3T_{1g} < {}^3T_{2g} < {}^5E_g < {}^1T_{1g} < {}^1T_{2g}$. Photochromism of the given spin-crossover compounds lies in these processes, the photoexcitation of a low-spin complex leads to a population of the excited singlet states $^1T_{1g}$ or $^1T_{2g}$. The excited singlet states are very short-lived and decay to both the ground-state $^1A_{1g}$ by internal conversion, and to the triplet state $^3T_{1g}$ via intersystem crossing. The triplet state will decay either to the ground-state $^1A_{1g}$ or the high-spin $^5T_{2g}$ state, both through intersystem crossing. Provided that the temperature is sufficiently low, the energy barrier between the $^1A_{1g}$ and $^5T_{2g}$ states is not thermally overcome, the high-spin isomer of a complex remains trapped. Given that the M–L bonds in the high-spin isomer are longer than in the low-spin isomer, the partial molar volumes of the isomers differ (a consequence of the presence of electrons in iron-localized e_g-orbitals), the phase transitions $^1A_{1g} \rightarrow {}^5T_{2g}$ may be accompanied by the destruction of a crystal.

Photoisomerization reactions of spin isomers can also occur in solution [72]. An investigation of the pressure effect on the spin relaxation dynamics for spin-crossover Fe(II) coordination compounds shows that the changes in geometry associated with the intersystem crossing at high-spin → low-spin conversion involve a radial compression of the M–L bonds, i.e., the volume of each activated complex is smaller than that of the respective high-spin isomer.

Based on the experimental data obtained from the study of several spin-crossover coordination compounds, it seems to be well established that light-induced excited-spin-state trapping is a general phenomenon in such compounds.

4.3.5 Photoisomerization reactions of coordinated ligands

Photoisomerizations of coordinated ligands are non-redox processes in which the change in ligand structure takes place and both the composition and symmetry of the chromophore are preserved. Of the hitherto known reactions, photochemical *cis-trans* isomerizations of coordinated substituted olefins, atropisomerization of a porphyrin ligand and "envelope" isomerization of coordinated dideuterobutadiene will be discussed in this section.

Of photoisomerizations of coordinated olefins, *cis-trans* isomerization of 4-styrylpyridine has been studied in detail. The reactions taking place during irradiation of the complex system with this ligand, $[Ru(bpy)_2(stpy)_2]^{2+}$, can be illustrated [246, 247] as follows:

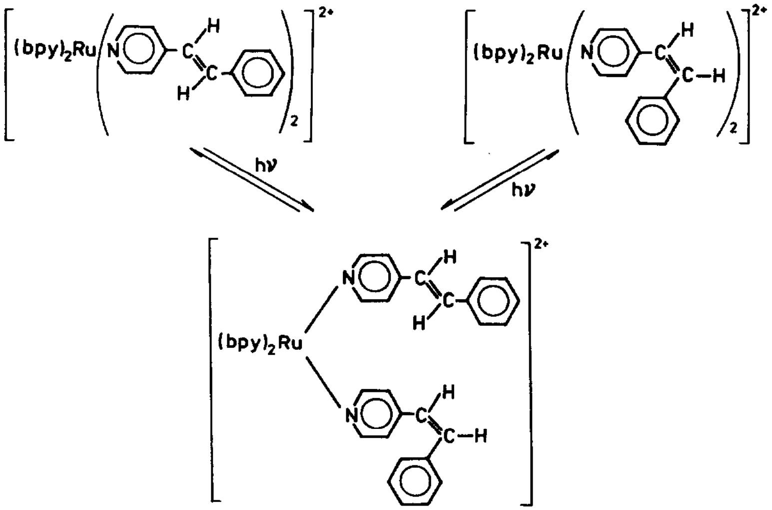

(4.96)

Cis-trans isomerization of coordinated 4-styrylpyridine in the Ru(II), W(0) and Re(I) complexes and the ratio of isomers in the photostationary state depend to a great extent on the radiation wavelength. The dependence of the *cis* → *trans* and *trans* → *cis* quantum yields on the excitation wavelength has been elucidated by two different independent methods. When interpreting the properties of the W(0) and Re(I) compounds, it is assumed that photochemically active states are the singlet $^1\mathrm{IL}(\pi \rightarrow \pi^*)$(stpy), achieved by photoexcitation at 313 nm, and the triplet ^{3}IL, reached by internal conversion (intersystem crossing) from the energetically higher LF or MLCT states. The assumption of the photochemically active ^{3}IL state was confirmed [248] by a study of the reaction

$$[\mathrm{ReX(CO)_3}(\mathit{trans}\text{-stpy})_2] \xrightarrow{*\mathrm{T}} [\mathrm{ReX(CO)_3}(\mathit{trans}\text{-stpy})(\mathit{cis}\text{-stpy})] \qquad (4.97)$$

(X = Cl, Br), sensitized by the excited molecules in their triplet state *T and analogous reaction of free *trans*-stpy.

Interpretation of the results for the Ru(II) compounds is based on the presumption that photoisomerization takes place from both the ^{1}IL state and the MLCT state, whereas the ^{1}IL state does not undergo internal conversion into the MLCT state because of its very short lifetime ($\tau^0(^1\mathrm{IL}) \leqslant 2 \times 10^{-13}$ s). This result is in agreement with the knowledge that the lifetimes of IL states are strongly influenced by coordination of the given ligand. It also can be assumed that *cis-trans* isomerizations of olefins, catalysed by metal carbonyls, also occur in the coordination sphere of a catalyst.

Irradiation of atropisomers of some porphyrin Zn(II) and Pd(II) complexes results in processes [249] that can be illustrated schematically as follows:

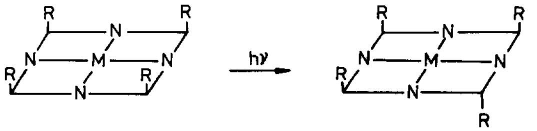
(4.98)

where R are sterically hindered organic groups bonded to the porphyrin ring. Quenching of reactions with dioxygen indicates that photoatropisomerizations take place from the triplet state of complexes. After a sufficiently long period of irradiation a photostationary state is stabilized in a system that contains all four isomers. The Cu(II) complexes do not undergo photoatropisomerizations owing to the very short lifetime of their excited states.

By means of stereochemical labelling experiments, a photochemical envelope isomerization of 1,3-butadiene derivatives coordinated on the cobalt(I) central atom in the π-complex [Co(Cp)(diene)] was studied [250]. The results clearly show that the given photodiastereoisomerization reaction occurs by the envelope inversion mechanism synchronous with isotopomerization without ligand crossover (R = $C_6H_5CH_2CH_2CH_3$):

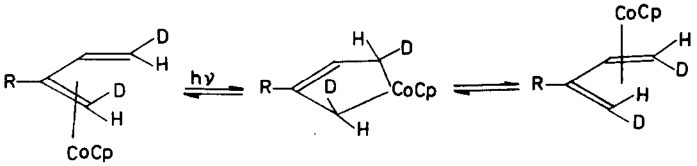
(4.99)

The reverse process is also light-induced, and irradiation leads to equilibrium of the reactant with the product.

4.3.6 *Photoisomerization reactions of geometrical isomers*

During the mutual conversions of geometrical isomers to be discussed in this section, a change in the symmetry of the chromophore takes place while the chromophore composition and the primary coordination sphere of the complex are preserved.

So far, studies have been oriented particularly at the photochemical *cis-trans* isomerizations of square-planar complexes of the [MA_2B_2] type and of octahedral complexes of the [MA_4B_2] type, and *mer-fac* isomerizations of the octahedral complexes of the [MA_3B_3] type, where A and B are the donor atoms of ligands [7, 236] (see the data in Table 16).

The suggested mechanisms of the reactions discussed are analogous to those for photoracemizations (Section 4.3.2), and for *trans* → *cis* (*mer* → *fac*) photoisomerizations they can be expressed using 4.100 (for the reverse course the picture is analogous).

TABLE 16
Photoisomerization of geometrical isomers

Complex	Isomerization	Data, conditions	Ref.
trans-$[PdI_2(PPr^n)_2]$	*trans* → *cis*	$\Phi = 0.02$, $\lambda = 313$ nm, CH_3OH	[266]
trans-$[PdBr_2(PPr^n_3)_2]$	*trans* → *cis*	$\Phi = 0.11$, $\lambda = 313$ nm, CH_3OH	[266]
trans-$[PdCl_2(PPr^n_3)_2]$	*trans* → *cis*	$\Phi = 0.19$, $\lambda = 313$ nm, CH_3OH	[266]
		72% *cis*, $\lambda = 313$ nm, nitromethane	
		64% *cis*, $\lambda = 313$ nm, DMF	
		56% *cis*, $\lambda = 313$ nm, acetone	
		40% *cis*, $\lambda = 313$ nm, methanol	
		18% *cis*, $\lambda = 313$ nm, $CHCl_3$	
cis-$[PtCl_2(PPh_3)_2]$	*cis* → *trans*	60% *trans*, $\lambda = 366$ nm, $CHCl_3$	[252]
cis-$[PtCl_2(PEt_3)_2]$	*cis* → *trans*	$\Phi = 0.13$, $\lambda = 313$ nm, CH_3OH	[267]
trans-$[PtCl_2(PEt_3)_2]$	*trans* → *cis*	$\Phi = 1.00$, $\lambda = 313$ nm, CH_3OH	[267]
cis-$[Ru(bpy)_2(H_2O)_2]$	*cis* → *trans*	$\Phi = 0.045$, $\lambda = 450$ nm, H_2O	[268]
trans-$[Ru(bpy)_2(H_2O)_2]$	*trans* → *cis*	$\Phi = 0.023$, $\lambda = 450$ nm, H_2O	[268]
Λ-*cis*-$[Co(en)_2Cl_2]^+$	*cis* → *trans*	solid state, $\lambda = 520–580$ nm, simultaneous Cl^- substitution by CO_3^{2-}	[269]
cis-$[Rh(NH_3)_4(H_2O)Cl]^{2+}$	*cis* → *trans*	$\Phi = 0.54$, $\lambda = 366$ nm, H_2O	[270]
trans-$[Rh(NH_3)_4(H_2O)Cl]^{2+}$	*trans* → *cis*	$\Phi = 0.064$, $\lambda = 366$ nm, H_2O	[270]
cis-$[Rh(NH_3)_4(H_2O)_2]^{2+}$	*cis* → *trans*	$\Phi = 0.10$, $\lambda = 366$ nm, H_2O	[270]
trans-$[Rh(NH_3)_4(H_2O)_2]^{2+}$	*trans* → *cis*	$\Phi = 0.011$, $\lambda = 366$ nm, H_2O	[270]
trans-$[Cr(NH_3)_4(H_2O)_2]^{3+}$	*trans* → *cis*	$\Phi = 0.35$, $\lambda > 400$ nm, H_2O	[74]
$[Ni(dpp)Cl_2]$ (planar)	planar → tetrahedral	$\lambda = 530$ nm, $k = 4.5 \times 10^5\ s^{-1}$, CH_3CN	[257]
$[Ni(dpp)Cl_2]$ (tetrahedral)	tetrahedral → planar	$\lambda = 1060$ nm, $k = 6 \times 10^5\ s^{-1}$, CH_3CN	[257]

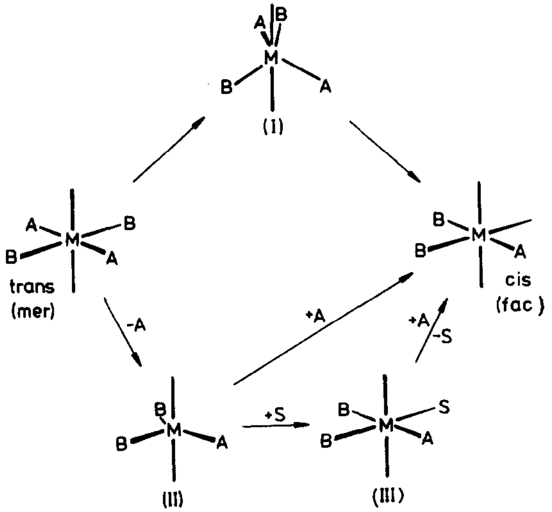

(4.100)

It should be noted that the structures of intermediates represent equilibrated structures of thexi states obtained during vibrational relaxation. An excitation itself is not accompanied by changes in molecular structures.

The marked axial positions are not occupied in square-planar complexes. In *cis-trans* isomerization reactions of octahedral complexes they are occupied by identical ligands A, A; in *mer-fac* isomerizations there are different ligands A, B. The symbol S denotes solvent molecules, or a molecule of another of the ligands present in the solution in excess (accordingly, the processes are called "solvent-assisted path" and "ligand-assisted path").

The intermediates I and II in process 4.100 have a tetrahedral and trigonal-bipyramidal structure, respectively, and their formation is a consequence of the formation of a complex in an excited state. The studies carried out hitherto with square-planar complexes [Pt(II) and Pd(II) compounds] and with octahedral complexes [particularly of Cr(III, Co(III) and Ir(III)] show [236] that the photochemically active states are mostly spin-forbidden LF states. The fact that, for example, in Pt(II) complexes the quantum yield of photoisomerizations does not depend on the excitation wavelength, is taken as evidence that the primary photochemical process takes place from the energetically lowest triplet thexi state. The photochemical reactivity of Cr(III) and Co(III) complexes in their LF states will be analysed in more detail in Section 4.4.

The course of the photoisomerization reaction by the intramolecular "twisting" mechanism (formation of the intermediate I) has been studied with a number of Pt(II) complexes, e.g. [251, 252]

$$cis\text{-}[PtCl_2(PEt_3)_2] \underset{h\nu}{\overset{h\nu}{\rightleftharpoons}} trans\text{-}[PtCl_2(PEt_3)_2] \qquad (4.101)$$

The amount of *cis*-isomer in the photostationary state increases with increasing polarity of the solvent in which the reaction takes place. Under suitable experimental conditions (e.g., use of a solvent in which the two isomers have different solubilities), photochemistry can be employed as a method for the synthesis of one of the isomers. A discussion of the Pt(II) and Pd(II) complexes prepared by photochemical synthesis will be presented in Section 5.3.

Experiments (use of the triplet-state quenchers, determination of quantum yields of *cis* → *trans* isomerizations, etc.) have demonstrated that photoisomerizations include the triplet thexi state and the *cis*-isomers of the Pt(II) complexes are mostly thermodynamically more stable than the Pd(II) compounds. The potential energy surfaces of the energetically lowest triplet state of the Pt(II) complexes show two minima corresponding to the pseudo-tetrahedral "transoidal" and "cisoidal" geometries. It is probable that the existence of two minima (on the potential energy curve of the ground state is one local minimum in the tetrahedral configuration) is due to the analogous vibronic interactions as applied in the case of Jahn–Teller deformations.

Unlike the photoisomerizations of Pt(II) complexes, where the course of the reactions by the twisting mechanism was proved by means of the labelled ligand method (for example, labelled free chloride ions in process 4.100 did not enter the coordination sphere), with octahedral complexes the course of photoisomerizations through the above-specified mechanism is only a matter of deduction.

An example of a solvent-assisted path mechanism [253] involving intermediate III is *cis* → *trans* photoisomerization of the *cis*-$[PtCl_2(py)_2]$ complex in chloroform, during which pyridine was identified in the solution. However, the study of the kinetics of reactions taking place in this system (slow re-coordination of the released pyridine, not corresponding to the value $\Phi_{isom} = 0.038$) indicated that photoisomerization by the twisting mechanism also takes place. A further complication might arise from the low coordination ability of chloroform molecules.

Photoisomerization involving the intermediate II with a coordination number one unit lower than that in the reactant can be observed particularly in the octahedral complex. However, such a mechanism cannot be ruled out with square-planar complexes either.

As in photosubstitution reactions, in the primary photochemical step of the photoisomerizations of octahedral complexes with intermediate II, a release of one of the ligands from the primary coordination sphere of the complex, and subsequently a heterolytic cleavage of one of the bonds between the central atom and polydentate ligand, take place. The identity of this ligand can be determined [so far for the Cr(III) and Co(III) compounds] by means of the Adamson rules, or other models of the photosubstitutional reactivity of complexes (see Section 4.4.4). The primarily formed intermediate with a square-pyramidal structure (not shown in process 4.100) is converted into intermediate II. By the interaction of intermediate II with the original ligand in a medium that does not contain competing ligands a new isomer is formed, for example [254]

$$mer\text{-}[IrCl_3(PEt_3)_3] \xrightarrow{h\nu} fac\text{-}[IrCl_3(PEt_3)_3] \tag{4.102}$$

If the system contains other possible ligands, a photosubstitution reaction can occur, e.g. [255]

$$mer\text{-}[IrCl_3(PEt_3)_3] + 3NCO^- \xrightarrow{h\nu} fac\text{-}[Ir(NCO)_3(PEt_3)_3] + 3Cl^- \tag{4.103}$$

The *mer-fac* change indicates that reaction 4.103 involves the intermediate with the structure II.

A frequent competing process of photoisomerization is a photoaquation reaction during which the labilized ligand (Section 4.4) is substituted in the coordination sphere by a water molecule (for example, aquation of the "en" ligand in $[Cr(en)_2(H_2O)(OH)]^{2+}$).

It can be deduced from the symmetry properties and thermodynamic stability of isomers that in several instances photoisomerization takes place in one direction only [256], e.g. *cis* → *trans* in the case of the complexes $[Cr(en)_2X_2]^+$ running by the solvent-assisted path mechanism. A reverse process observed in such instances (photochemical *trans* → *cis* isomerization) occurs by the twisting mechanism.

The group of photochemical reactions discussed can also include photoinduced conversions of configuration isomers, e.g., diamagnetic square-planar to paramagnetic tetrahedral Ni(II) complexes. As opposed to the Pt(II) and Pd(II) complexes, several Ni(II) compounds with tetrahedral configuration of the donor atoms are stable and cannot be considered to be intermediates. One of the few Ni(II) complexes whose isomerization was studied is $[Ni(dpp)Cl_2]$ which is present in acetonitrile in both isomeric forms. It was found [257] that depending on the excitation wavelength a change in the equilibrium in the directions

$$sq\text{-}[Ni(dpp)Cl_2] \underset{\lambda = 1060\ nm}{\overset{\lambda = 530\ nm}{\rightleftharpoons}} td\text{-}[Ni(dpp)Cl_2] \tag{4.104}$$

takes place (sq denotes a square-planar and td a tetrahedral structure).

The conversions of isomers can be explained in such a way that the absorption of a photon at 530 nm by the square-planar isomer populates the electron-density transfer from the d_{xz} or d_{yz} orbitals into the $d_{x^2-y^2}$ orbital, and the triplet state formed is stabilized by tetrahedral symmetry. A light quantum of $\lambda = 1060$ nm absorbed by the tetrahedral isomer induces the electron-density transfer in opposite direction, thus stabilizing the square-planar complex. Owing to the kinetic lability [Ni(II) complexes are thermally equilibrated within ca 10^{-6} s], the individual isomeric forms were not isolated or separated. For the same reason, evaluation of the kinetic data on the equilibria discussed calls for the use of fast relaxation techniques.

It should be noted that understanding the mechanisms of photoisomerization reactions requires many detailed studies, as there are some areas in this field with missing information. For example, the mechanisms proposed do not involve the associative type, although the change in the molecular structure conditioning isomerization can be due to both dissociation and association. In no case with octahedral complexes has a ligand-exchange study been performed, so that proof for or against a bond-breaking mechanism is missing. In addition to redox-stable platinum(II) and chromium(III) complexes, some cobalt(III) compounds undergo photoisomerization, but it is not clear whether the reactions are associated with the reduction of Co(III) or not. No data are known concerning photoinduced trigonal bipyramid ↔ tetragonal pyramid conversions for pentacoordinated complexes, although such a step is assumed in the mechanism of photoisomerization reactions.

Answers to these and other questions should contribute not only to the elucidation of the course of photoisomerization but also of photosubstitution and other photochemical reactions of complexes.

4.3.7 *Linkage photoisomerization reactions of complexes*

Electron excitation of complexes with polyatomic ligands involving non-equivalent donor atoms X, Y (which need not necessarily be different) can result in a change in ligand coordination, i.e., in mutual conversion of linkage isomers. The reaction can be simply expressed as follows:

$$[L_nM\text{-}XY]^{m+} \xrightarrow{h\nu} [L_nM\text{-}YX]^{m+} \qquad (4.105)$$

During these photoisomerizations, the structure of the chromophore is usually changed. In some instances the symmetry of the chromophore and the structure of a ligand, are changed, too.

In contradistinction to the spontaneous mutual changes of the linkage isomers, conversion of a thermodynamically more stable to a less stable isomer can also be performed photochemically, and photochemistry can be employed as a tool in the synthesis of such isomers (examples are shown in Section 5.3).

Another difference between the thermal and photochemical isomerization reactions of the linkage isomers is the fact that the primary step in the thermal reactions consists in heterolytic cleavage of the M–XY bond, whereas the photochemical process usually involves homolytic splitting of the M–XY bond, resulting in the reduction of the central atom and oxidation of the XY ligand. As the most convenient distribution of the electron density for this redox intramolecular process is that in the LMCT state, it is assumed that the primary photochemical process takes place from such a state. Experiments, particularly those with Co(III) complexes, confirm this. Simultaneously with linkage photoisomerization a photoredox process often also takes place.

In studies of linkage photoisomerization, Co(III), Pt(IV), Fe(II) and Mo(II) compounds with NO_2^-, SCN^-, $HCOO^-$ and $O_2S–C_2H_4–NH_2$ have so far been used (see Table 17).

Detailed experimental information is available [236] for a small number of coordination compounds undergoing linkage photoisomerization in solution or in the solid state, e.g., $[Co(NH_3)_5(NO_2)]^{2+}$ and $[Co(NH_3)_5(SCN)]^{2+}$. The photochemical behaviour of these complexes in solution consists of simultaneously occurring redox decomposition yielding solvated Co^{2+} ions, and nitro → nitrito or thiocyanato → isothiocyanato linkage isomerization. The quantum yields of the photoreactions increase with increasing energy of the exciting light, but the $\Phi_{redox}:\Phi_{isom}$ ratio is constant and independent of the wavelength of the light. In the solid state only linkage photoisomerization was observed.

The mechanism of the reactions is demonstrated by the following scheme ($L = NH_3$):

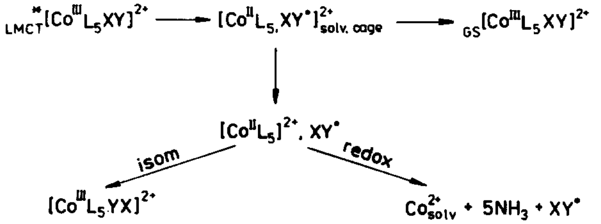

(4.106)

The higher the kinetic energy of primary radicals (i.e., the higher the proportion of photon energy that can be converted to kinetic energy of the radicals in the relaxation of the dissociative LMCT excited state), the greater the probability of the formation of a solvent-separated radical pair, and the greater the probability of the occurrence of both photochemical processes. Their ratio in the given medium is constant. The more rigid the environment, the lower is the probability of a photoredox decomposition of a complex (the $XY^{\bullet}$ radical is not able to escape), and hence the higher is the $\Phi_{isom}:\Phi_{redox}$ ratio. The experimental data also indicate that whereas the primary caged radicals can produce only the reactant by back reaction, the solvent-separated radical pair provides only the

TABLE 17

Linkage photoisomerization of complexes

Complex	Photoprocess	Data, conditions	Ref.
$[Co(NH_3)_5(NO_2)]^{2+}$	$NO_2 \rightarrow ONO$	$\Phi = 0.13$, $\lambda = 254$ nm, H_2O	[236]
		$\Phi = 0.11$, $\lambda = 313$ nm, H_2O	[236]
		$\Phi = 0.055$, $\lambda = 365$ nm, H_2O	[236]
		$\Phi = 0.035$, $\lambda = 442$ nm, H_2O	[236]
		$\Phi = 0.18$, $\lambda = 365$ nm, 10% glycerol	[203]
		$\Phi = 0.09$, $\lambda = 365$ nm, 20% glycerol	[203]
		$\Phi = 0.10$, $\lambda = 365$ nm, 30% glycerol	[203]
		$\Phi = 0.15$, $\lambda = 365$ nm, 50% glycerol	[203]
		$\Phi = 0.21$, $\lambda = 365$ nm, 70% glycerol	[203]
$[Co(NH_3)_5(SCN)]^{2+}$	$SCN \rightarrow NCS$	$\Phi = 0.15$, $\lambda = 333$ nm, H_2O	[236]
		$\Phi = 0.012$, $\lambda = 470$ nm, H_2O	[236]
$[Mo(Cp)(CO)_3(SCN)]$	$SCN \leftrightarrow NCS$	$\lambda = 366$ nm, THF	[259]
$[Fe(Cp)(CO)_2(SCN)]$	$SCN \leftrightarrow NCS$	$\lambda = 366$ nm, THF, photostationary 1/1 mixture	[259]
$[Co(NH_3)_5(HCOO)]^{2+}$	$O_2CH \rightarrow CO_2H$	$\lambda = 254$ nm, H_2O,–CO_2H isomer as transient	[258]
$[Co(en)_2(SO_2–C_2H_4–NH_2)_2]^{2+}$	$SO_2C_2H_4NH_2 \rightarrow OSOC_2H_4NH_2$	$\lambda = 400$ nm, H_2O	[271]
$[Pt(NH_3)_4(NH_2)(NO)]^{2+}$	$NO_2 \rightarrow ONO$	$\lambda = 254$ nm, $\Phi = 0.11$, H_2O	[272]
$[Co(NH_3)_5(NO_2)]X_2$	$NO_2 \rightarrow ONO$	$\lambda = 486$ nm, solid state	[272]
($X = Cl, Br, NO_3$)	disintegration of crystals	$\lambda = 313$ nm, $\Phi = 0.29$, H_2O	[273]

linkage isomer of the reactant. This was indicated by experimental finding that on LMCT excitation of the nitrito complex $[Co(NH_3)_5(ONO)]^{2+}$ or the isothiocyanato complex $[Co(NH_3)_5(NCS)]^{2+}$, no linkage photoisomerization was observed, although the solvent-separated radical pairs should be indistinguishable from those originating from nitro or thiocyanato complexes.

The question of multiplicity of the LMCT state from which the primary radical pairs originate has not yet been satisfactorily answered. A theoretical treatment of the discussed photoreaction has shown that the photoreactive LMCT state is a dissociative one (energies of spectroscopically available Franck–Condon levels of the LMCT state pass into the region of non-quantum energies of the radical pair without achieving a minimum). The region of "dissociation continuum" is energetically lower than the energy of the LF state, which confirms the photoredox decomposition of complexes also during their irradiation into LF bands.

As opposed to the relatively stable nitrito, isothiocyanato and S-sulphinato complexes of Co(III), the complex containing an $HCOO^-$ ligand coordinated by a carbon atom is short-lived intermediate (lifetime ca 0.1 s). The reaction mechanism [236, 258] involves two different excited states, the triplet LMCT state and the IL state. The former state is responsible for the photoredox decomposition of the complex producing Co^{2+}, NH_3 and $HCO_2^{\bullet}$ radicals. The latter state probably corresponds to the n–π^* transition localized on the formate ligand. Such an IL state results in the production of an intermediate (linkage isomer) that undergoes decomposition in the subsequent thermal reaction with formation of solvated Co^{2+} ions and $HCO_2^{\bullet}$ radicals. The multiplicity of the IL state and the overall mechanism are not sufficiently explained and the question of the relationship between the properties of the $[Co(NH_3)_5(HCOO)]^{2+}$ complex in different excited states and its deactivation modes from these states requires further study.

A mechanism that does not involve the formation of redox intermediates was suggested for the linkage photoisomerization of the complexes $[M(Cp)(CO)_n(SCN)]$, where M = Fe and $n = 2$ or M = Mo and $n = 3$. Thiocyanato and isothiocyanato complexes are interconverted in tetrahydrofuran solution by 366-nm light [259]:

$$[M(Cp)(CO)_n(SCN)] \overset{h\nu}{\underset{h\nu}{\rightleftharpoons}} (M(Cp)(CO)_n(NCS)] \tag{4.107}$$

Both iron(II) isomers are thermally stable; the photostationary state is a 1:1 mixture of them. The molybdenum thiocynato complex is not thermally stable and is converted spontaneously into the isothiocyanato complex.

The photochemical interconversion of the dihydrido-bridged complex $[(PEt_3)_2HPt(\mu\text{-}H)_2Pt(PEt_3)_2]^+$ to its monohydrido-bridged structural isomer $[(PEt_3)_2HPt(\mu\text{-}H)PtH(PEt_3)_2]^+$ [239] can also be mentioned in this section as it is connected with a different coordination mode of a ligand (a hydrido ligand in this case).

4.4 Photosubstitution reactions of coordination compounds

The term photosubstitution reactions denotes such photochemical non-redox transformations during which an exchange of ligand(s) between the primary and secondary coordination spheres takes place, the composition of the complex changes and the coordination number of the central atom is retained. Reactions of photosubstitution of the central atom have not been studied. The results of the study of photosubstitution reactions markedly influenced progress in the understanding of the photochemistry of complexes, particularly connected with the deactivation of LF excited states.

This section is focused particularly on the typical features of photosubstitutions that have been described so far, and the examples presented also demonstrate the relationship between the character of the deactivation process and the properties of the reactive excited state. The reactions are discussed together with a presentation of the type of the excited state primarily populated by photon absorption (LF, MLCT, LMCT, CTTS, IL). The above facts should, together with the results of other experimental and theoretical procedures, enable the nature of the excited state from which a complex is deactivated by the substitution process to be identified. More results of studies of photosubstitution reactions carried out for other purposes (e.g., photochemical preparation of complexes) are presented in the appropriate sections.

The studies of photosubstitution reactions carried out so far were focused mostly on kinetically substituted inert complexes; this was determined by practical advantages in the analysis of the composition of the systems investigated and interpretations of the experimental data. Particular attention was paid to hexacoordinated Cr(III) complexes [274, 275] of $3d^3$ configuration, Co(III) [276] ($3d^6$) and its $4d^6$ and $5d^6$ homologues [277–280], Ru(II), Rh(III), Ir(III) and Pt(IV) and d^5 complexes of Ru(III) and Ir(IV). There are no data on photosubstitution reactions of $4d^3$ and $5d^3$ complexes, except the $4d^3$ Tc(IV) complex anion $[TcCl_6]^{2-}$ [282].

Of the square planar complexes with the d^8 configuration, particularly the behaviour of Pt(II) has been studied [236, 281, 283], but many results have also been obtained by investigation of the Ni(II) complexes [284]. The study of eight-coordinated complexes was focused on cyano complexes [281] of Mo(V), W(V) and Mo(IV). Within the context of the study of catalytic and preparation aspects of the photochemistry of organometallic compounds, photosubstitutions of CO in $Fe(CO)_5$ (d^8, symmetry D_{3h}) have been investigated [9]; photosubstitution reactions of some other metal carbonyls [3, 285] such as Cr, Mo, W, Mn and Rh have also been reported. The study of the photosubstitution reactions of coordination compounds with other central atoms and different stereochemistry has been carried out only sporadically.

Most photosubstitution reactions differ distinctly from the thermal substitution reactions of the given complex in their kinetics and the composition and stereochemistry of the products (which is of great importance particularly from the viewpoint of synthesis).

Several examples exist of a drastic increase in the substitution reactivity of a complex in its excited state in comparison with ground state. For example [286], substitution of the ligand $X = Cl^-$ in the energetically lowest excited state in $[Rh(NH_3)_5X]^{2+}$ is characterized by a rate constant ($k_p = 1.3 \times 10^7\ s^{-1}$) that is as much as 14 orders of magnitude higher than that for an analogous thermal reaction; similar increases in rate constants have also been determined for the complexes of other central atoms. In general, photosubstitutions in the excited complexes last for a few picoseconds.

The differences in the compositions of the products of thermal and photochemical substitution reactions can be illustrated by aquation reactions of the $[Cr(NH_3)_5X]^{2+}$ complex in aqueous media ($X = Cl$, Br, NCS, ...) [275]. In contrast to thermal substitution of the ligand X

$$[Cr(NH_3)_5X]^{2+} + H_2O \xrightarrow{\Delta} [Cr(NH_3)_5(H_2O)]^{3+} + X^- \tag{4.108}$$

the photochemical reaction leads to products of different composition formed by photosubstitution of the NH_3 molecule:

$$[Cr(NH_3)_5X]^{2+} + H_3O^+ \xrightarrow{h\nu} cis\text{-}[Cr(NH_3)_4(H_2O)X]^{2+} + NH_4^+ \tag{4.109}$$

The difference in the factors that influence the course of thermal and photochemical reactions has been manifested in their stereospecificity [275, 279, 287]. For example [275], the complex ion *trans*-$[Cr(NH_3)_4Cl_2]^+$ undergoes thermal aquation of the Cl^- ligand without a stereochemical change:

$$trans\text{-}[Cr(NH_3)_4Cl_2]^+ + H_2O \xrightarrow{\Delta} trans\text{-}[Cr(NH_3)_4(H_2O)Cl]^{2+} + Cl^- \tag{4.110}$$

However, its irradiation results in the formation of a *cis*-isomer:

$$trans\text{-}[Cr(NH_3)_4Cl_2]^+ + H_2O \xrightarrow{h\nu} cis\text{-}[Cr(NH_3)_4(H_2O)Cl]^{2+} + Cl^- \tag{4.111}$$

4.4.1 *Types of complex systems involving photosubstitutions*

Photoexcitation of a complex by irradiation from the region corresponding to the LF transitions usually leads to non-redox deactivation reactions (photosubstitution, photoisomerization, etc.), and only in complexes with a few central atoms [e.g., Co(III)] also to photoredox deactivations. In this section, examples of photosubstitutions with one and more products will be presented as examples in which photosubstitution is accompanied by simultaneous photoisomerization and by a photoredox reaction.

Analogously with other deactivation processes of electronically excited coordination compounds, photosubstitutions will also be determined by many factors, e.g., by the character of the central atom and ligands, the structure of the complex and excited state conditions.

The most common consequence of the LF excitation of complex with d^3 and d^6 configuration is labilization of ligands and substitution of one of them [8]. For example, for the $[M(NH_3)_6]^{3+}$ complexes where M = Cr, Rh or Ir, NH_3 photosubstitution in aqueous medium was observed:

$$[M(NH_3)_6]^{3+} + H_2O \overset{h\nu}{\rightarrow} [M(NH_3)_5(H_2O)]^{3+} + NH_3 \tag{4.112}$$

The photosubstitution quantum yields for the Rh(III) and Ir(III) complexes ($\Phi_s = 0.07$–0.09) did not depend on the irradiation wavelength [288, 289]. The energetically lowest triplet LF state $^3T_{1g}$ was photochemically active. Analogous conclusions have also been drawn [290] with $[Co(CN)_6]^{3-}$; however, this is in sharp contrast with much lower values of Φ_s (ca 5×10^{-4}–5×10^{-3}) for the $[Co(NH_3)_6]^{3+}$ complex [291], which significantly increase with decreasing excitation radiation wavelength. These facts indicate that NH_3 photosubstitution in $[Co(NH_3)_6]^{3+}$ frequently takes place from energetically higher, probably vibrationally excited, states than the energetically lowest electronic excited (thexi) state. Such a situation is typical of the Co(III) complexes, and photosubstitution probably takes place only in the case of the complexes with higher vibrationally excited states the energy content of which, E_{vibr}, satisfies the relationship

$$E_{\mathrm{vibr}} \geqslant E^{\neq} \approx E_{\mathrm{th}} > E_{\mathrm{thexi}} \tag{4.113}$$

where E_{thexi} is the energy content of the thexi state.

The experimental data indicate that the threshold energy of photochemical substitution (E_{th}) and the activation energy of analogous thermal substitution ($E^{\neq}$) are identical within the limit of experimental errors (e.g., for replacement of Cl^- by a molecule of H_2O in the $[Co(NH_3)_5Cl]^{2+}$ complex the values $E^{\neq} = 100.8 \pm 4.2$ kJ mol^{-1} and $E_{\mathrm{th}} = 109.2 + 12.6$ kJ mol^{-1} were measured [13, 292, 293]). If the thexi state is achieved by vibrational relaxation, only non-radiative deactivation to the ground electron state of the complex takes place.

Rh(III) and Ir (III) excited complexes are deactivated from their thexi states, which is in agreement with the conclusions obtained from the ESA spectra and the luminescence measurements.

Also in other instances a conclusion was drawn that photoaquation takes place from the lowest excited state of the given multiplicity [for a Cr(III) complex, the ^2E_g and $^4T_{2g}$ states in O_h symmetry]. The Cr(III) complexes with the chromophore of O_h symmetry [138] (with a homogeneous coordination sphere involving NCS^-, NH_3, CN^-, ox^{2-}, en and urea ligands) are deactivated by photoaquation; the Φ_s values do not depend on the irradiation wavelength, but they are well correlated with the position of ligands in the spectrochemical series: the higher the Dq(L) value, the higher is the value of Φ_s.

The effect of the medium or the secondary coordination sphere on photoaquation can be properly demonstrated using the supercomplex [295] $Co(CN)_6[32\text{-}N_8H_8]^{5+}$. Surrounding $[Co(CN)_6]^{3-}$ by the entirely protonated form of the macrocyclic ligand (Fig. 14) partially restrains the photoaquation reaction of CN^-:

$$Co(CN)_6(32\text{-}N_8H_8]^{5+} \xrightarrow[H_2O]{h\nu} Co(CN)_5(H_2O)[32\text{-}N_8H_8]^{6+} + CN^- \qquad (4.114)$$

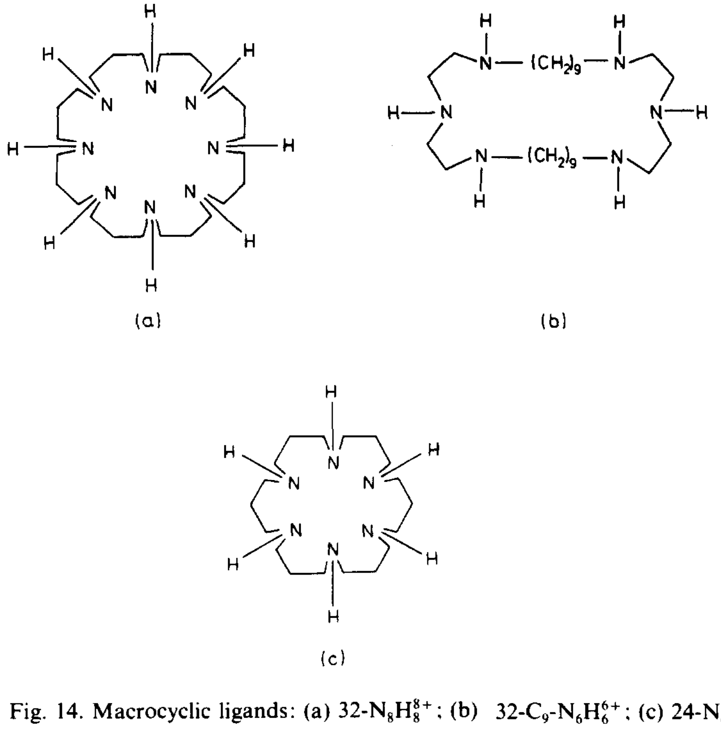
(a) (b) (c)

Fig. 14. Macrocyclic ligands: (a) $32\text{-}N_8H_8^{8+}$; (b) $32\text{-}C_9\text{-}N_6H_6^{6+}$; (c) $24\text{-}N_6H_6^{6+}$.

with a decrease in the quantum yield to 0.10, 0.11 and 0.16 [296, 297] for the supercomplexes of $[Co(CN)_6]^{3-}$ with polyammonium macrocyclic ligands $32\text{-}N_8H_8^{8+}$, $32\text{-}C_9\text{-}N_6H_6^{6+}$ and $24\text{-}N_6H_6^{6+}$, respectively, in comparison with 0.31 for the complex anion [298] $[Co(CN)_6]^{3-}$.

It is assumed [295] that a macrocyclic ligand does not influence the character of the reactive LF excited state, but it enables the ligand photosubstitution to be controlled and altered by using a suitable molecule of macrocycle. This possibility was verified by the study of several supercomplexes [299] consisting of, for example, $[Fe(CN)_6]^{4-}$, $[Ru(CN)_6]^{4-}$ and protonated forms of some macrocycles (Fig. 14a, b and c).

Another example of photosubstitution with one product is photoanation reactions, e.g. [300]

$$[Cr(H_2O)_6]^{3+} + X^- \rightleftharpoons \{[Cr(H_2O)_6]^{3+}, X^-\}^{2+} \xrightarrow{h\nu} [Cr(H_2O)_5X]^{2+} + H_2O \quad (4.115)$$

where X = Cl or NCS. It is assumed that this reaction, with a relatively low quantum yield ($\Phi_s \approx 10^{-2}$–10^{-4}), is based on the photolysis of an pair, $\{[Cr(H_2O)_6]^{3+}, X^-\}^{2+}$.

The range of reactions studied that are due to LF excitation was considerably extended for complexes with a heterogeneous coordination sphere. In general, two or more simultaneous chemical deactivation processes are observed, where the prevailing photochemical reaction often differs from the dominating thermal reaction.

A typical example of deactivation of the LF excited state by two different photosubstitution reactions is photosolvation of NH_3 with halide X^- ligand in the complex ion [301] of $[Rh(NH_3)_5X]^{2+}$:

$$[Rh(NH_3)_5X]^{2+} + S \xrightarrow{h\nu} \begin{cases} trans\text{-}[Rh(NH_3)_4SX]^{2+} + NH_3 & (4.116) \\ [Rh(NH_3)_5S]^{3+} + X^- & (4.117) \end{cases}$$

Which of the processes dominates depend on the X^- ligand and the solvent S [286]. If X = Cl and S = H_2O, the ratio of the quantum yields of photoactivation of Cl^- and NH_3 is 9:1; for X = Br in water reaction 4.116 is dominant. In organic solvents, NH_3 is preferentially substituted.

As the spectral properties of the $[Rh(NH_3)_5Cl]^{2+}$ complex are almost independent of the solvent, the basis of the different photoreactivity will not lie in perturbation of the electronic system of the complex by the solvent, but in the change in the kinetic parameters determining the deactivation of the complex.

A change in the rate constant of Cl^- substitution (in the equation $\Phi_s = k\tau$) from $10^5\ s^{-1}$ in DMF to $10^7\ s^{-1}$ in H_2O is explained [286] by the ability of the H_2O molecules to stabilize charge separation of the $[(NH_3)_5Rh]^{3+}–Cl^-$ bonds in the transition state; with NH_3 no similar separation takes place. The results obtained by a detailed study by pulsed-laser flash photolysis, quenching and luminescent measurements and the determined quantum yields have led to the conclusion that a photoreactive state is the energetically lowest excited LF thexi state produced by non-radiative deactivation ($\Phi_{ic} = 1$) of the primarily populated singlet excited state.

Another type of system in which two deactivation reactions take place simultaneously is that involving photoaquation and photoisomerization of, e.g. [256], the *cis*-$[Cr(en)_2(OH)_2]^+$ complex:

$$\begin{tikzcd} & \textit{trans}\text{-}[Cr(en)_2(OH)_2]^+ & (4.118) \\ \textit{cis}\text{-}[Cr(en)_2(OH)_2]^+ \arrow[ur, "h\nu"] \arrow[dr] & & \\ & [Cr(en)(H_2O)_2(OH)_2]^+ + en & (4.119) \end{tikzcd}$$

In both instances, the photosubstitution of different ligands can be accompanied by isomerization. For example [302],

$$\begin{tikzcd} & \textit{cis}\text{-}[Cr(NH_3)_4(H_2O)(NCS)]^{2+} + Cl^- \quad (4.120) \\ \textit{trans}\text{-}[Cr(NH_3)_4(NCS)Cl]^+ + H_2O \arrow[ur, "h\nu"] \arrow[dr] & \\ & \textit{cis}\text{-}[Cr(NH_3)_4(H_2O)Cl]^{2+} + NCS^- \quad (4.121) \end{tikzcd}$$

Photostereochemical changes in the above examples are in agreement with the Kirk rule (Section 4.4.4).

The complex ion *trans*-$[Cr(NH_3)_4(DMF)Cl]^{2+}$ offers three photoaquation reactions [303] (see Section 4.7); two of the products have a *cis*-configuration, viz., *cis*-$[Cr(NH_3)_4(H_2O)Cl]^{2+}$ and *cis*-$[Cr(NH_3)_4(DMF)(H_2O)]^{3+}$.

Experimentally, *cis-trans* isomerization was also observed accompanying the photosubstitution [304]:

$$\textit{cis}\text{-}[Rh(NH_3)_4Cl_2]^+ + H_2O \xrightarrow{h\nu} \textit{trans}\text{-}[Rh(NH_3)_4(H_2O)Cl]^{2+} + H_2O \qquad (4.122)$$

Similar cases of the photoaquation of two different ligands with a simultaneous change in stereochemistry of at least one of the photoproducts have also been reported for some binuclear complexes, e.g. [305], the complex ion of *trans*-$[(NH_3)_5Cr–(OH)–Cr(NH_3)_4Cl]^{4+}$.

In the course of photochemical studies with $[Ru(bpy)_3]^{2+}$, a novel photosubstitution reaction (cation-assisted ligand photosubstitution) has been observed [306]. Irradiation of $[Ru(bpy)_3]^{2+}$ in the presence of Ag^+ in acetonitrile leads to the formation of $[Ru(bpy)_2(CH_3CN)_2]^{2+}$. The photosubstitution does not occur in the absence of Ag^+ or acetonitrile. The suggested mechanism [306] involves decay of the MLCT state via a *d–d* excited state to a ligand-labilized intermediate which is intercepted by Ag^+ in a process that assists the substitution by removal of a bpy ligand.

The frequently observed stereospecificity of the products of photosubstitution reactions has led some authors to the already accepted opinion that the stereochemical change [mainly with Cr(III) complexes] will be a generally valid phenomenon conditioning the course of a photochemical reaction.

The effect of the medium on photochemical reactions was illustrated [269] using the properties of the Λ-*cis*-$[Co(en)_2Cl_2]^+$ complex, which after being anchored on silica gel, undergoes the following reaction in the presence of K_2CO_3 during LF excitation:

$$\begin{aligned}(x + y)\Lambda\text{-}cis\text{-}[Co(en)_2Cl_2]^+ + yK_2CO_3 \xrightarrow{h\nu} y\text{-}rac\text{-}[Co(en)_2CO_3] + {} \\ + x\text{-}trans\text{-}[Co(en)_2Cl_2]^+ + 2y\,KCl\end{aligned} \tag{4.123}$$

This reaction is markedly influenced by the active centres of the carrier; *cis-trans* isomerization takes place only in the presence of CO_3^{2-} ions.

Another elegant demonstration of the effect of the medium on the photochemical behaviour of complexes is the efficient ligand photosubstitution obtained [307] in a layered solid of approximate composition $H_{0.7}[Cr(NH_3)_6]_{0.1}\,UO_2PO_4.6H_2O$. The high efficiency of this reaction, in addition to energy transfer from the excited host UO_2^{2+} chromophore to the Cr(III) complex, illustrates the ability of lamellar solids to serve as novel media for studying excited-state processes. Thus, layered solids consisting of alternating inorganic and organic layers [308–312] are promising not only because of their sorptive and catalytic properties, but also as an interesting system for host-to-guest excited-state photochemistry and photophysics.

All the above photosubstitutions and similar reactions occurred as a result of LF excitation; the LF excited state was usually also a photoreactive excited state. The sequence of LF excitation–redox deactivation could only take place if the CT and LF bands overlap. Similarly, in some complexes of cobalt a photosubstitution reaction has been recorded in the case of the LMCT excitation, where the quantum yields achieved a maximum on irradiation in the near-UV region, in which considerable overlapping of the bands of LF and LMCT transitions could be observed; at higher energies of irradiation the quantum yields of photosubstitution decreased.

More frequent are simultaneous photosubstitution and photoredox reactions on irradiating the complex from the region of CT transitions; thus, CT excitation need not necessarily result in a redox reaction only. From this viewpoint, the example of the photochemical behaviour of the azide complex $[Co(NH_3)_5N_3]^{2+}$ is interesting as it mainly provides a photoaquation reaction (4.124) [66, 313] within the whole LMCT region of irradiation:

$$[Co(NH_3)_5N_3]^{2+} + H_2O \xrightarrow[\text{LMCT}]{h\nu} (Co(NH_3)_4(H_2O)N_3]^{2+} + NH_3 \qquad (4.124)$$

It is worth noting that the quantum yield of photoaquation [dominating with respect to the photoreduction Co(III) → Co(II)] increases when higher energy irradiation ($\lambda_{irr} = 254$ nm; CT region) is used, with a decrease in $\Phi_{Co(II)}$. Although no unambiguous interpretation of the experimental results has been presented, it is assumed that NH_3 photoaquation (and the nature of the excited state "responsible" for this photochemical deactivation) has nothing to do with the process of photoreduction of Co(III) (see Section 4.2.5).

A different situation has been recorded in the case of several Rh(III) ammine complexes, where the LMCT excitation seems to lead to a simple photosubstitution reaction [314, 315]:

$$[Rh(NH_3)_5I)^{2+} + H_2O \xrightarrow[\text{LMCT}]{h\nu} trans\text{-}[Rh(NH_3)_4(H_2O)I]^{2+} + NH_3 \qquad (4.125)$$

In contradistinction to eqn. 4.124, a detailed study by flash photolysis has shown that the precondition for NH_3 photoaquation (eqn. 4.125) is a redox process, i.e., photoreduction of Rh(III) → Rh(II) with simultaneous oxidation of the ligand I^- to the radical $I^\bullet$. In agreement with the experimental data, the conclusion was drawn that internal conversion from the LMCT state to the LF states of the complex $[Rh(NH_3)_5I]^{2+}$ takes place with an efficiency not higher than 0.5. At the same time, direct non-radiative deactivation from the MLCT to the ground state proceeds simultaneously with the internal conversion to the LF excited state(s).

The fact that also irradiation in the region of the MLCT transitions causes photosubstitution reactions can be demonstrated, for example, on the series of pentaammine complexes of Ru(II) with the ligands of the substituted pyridine type (py-X) [316, 317]

$$\begin{tikzcd}[column sep=small]
 & {[Ru(NH_3)_5(H_2O)^{2+} + (py\text{-}X)} & \\
{[Ru(NH_3)_5(py\text{-}X)]^{2+} + H_2O} \arrow[ur, "h\nu"] \arrow[dr, "\text{MLCT}"'] & & (4.126) \\
 & {[Ru(NH_3)_4(H_2O)(py\text{-}X)]^{2+} + NH_3} &
\end{tikzcd}$$

(4.127)

The known dependence of the energy of MLCT transitions on the solvent properties (Section 2.2) and the possibility [318] of influencing this energy by the nature of the X substituent enabled both the photochemical and photophysical properties of complexes to be modified ("tuning" experiments [89, 316, 317, 319]). This results in the fact that if X has distinct electron-withdrawing properties (e.g., X = *p*-CHO or *p*-$CONH_2$), the energetically lowest excited state is the MLCT state from which photosubstitution takes place with only a low probability ($\Phi_s = 10^{-4}$). If X = H or a substituent with electron-donor properties, the energetically lowest excited state is the LF state and $\Phi_s > 10^{-1}$. Moreover, when the energy levels of the lowest MLCT and LF states are sufficiently close [317], it is possible to "tune" the photoreactivity by variations of the solvent.

Owing to the considerable energy dependence of the MLCT states on extramolecular factors (character of the solvent), a change of the sequence of energy levels of the lowest lying excited states can occur which, in accordance with the "tuning model" [89, 280, 316–318], determines the observed photochemical reactivity of the complexes. An example is the decrease in the quantum yields of photosubstitution in complexes of the $[Ru(NH_3)_5(py\text{-}X)]^{2+}$ type in different solvents in the order $CH_3CN > H_2O > DMSO \approx DMF$. An interpretation of the observed change in photoreactivity is illustrated in Fig. 15, expressing schematically two extreme cases (Fig. 15a and b) of the "tuning model": a decrease in the energy of the photoreactive MLCT state (solvent DMSO or DMF or substituent X with marked electron-withdrawing properties in the py-X ligand; Fig. 15a), or an increase (solvent CH_3CN or substituent X with electron-donor properties in the py-X ligand; Fig. 15b). The effect of the solvent on energy position of the LF states is hardly manifested in comparison with the MLCT states. The tuning model was also successfully applied to some

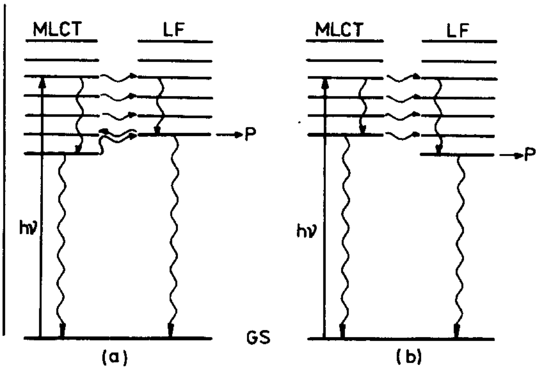

Fig. 15. Scheme of two extreme examples (a, b) of the "tuning model" for the photochemistry of $[Ru(NH_3)_5(py\text{-}X)]^{2+}$ complexes and analogous systems: (a) energetically lowest is the MLCT state (considerably reduced tendency for photosubstitution reaction), (b) energetically lowest is the LF state (increased tendency for photosubstitution reaction). P = products.

other substituted pyridine complexes, e.g., Re(π-C_5H_5)$(CO)_2$(py-X) [320], $[Fe(CN)_5(py\text{-}X)]^{3-}$ [188] and $W(CO)_5$(py-X) [322].

The observed low photosubstitution reactivity on IL excitation of some complexes [89, 94] (e.g., $[Ir(dmphen)_2Cl_2]^+$, $[Ru(bpy)_3]^{3+}$, is interpreted as a consequence of the reactivity of the LF states being energetically very close to the lowest lying excited state, attributed to a state of IL character on the basis of luminescent measurements for the above complexes. Complex with energetically higher IL states often provide photosubstitution reactions as a consequence of irradiation in the region of IL transitions (e.g., photoactivation of benzonitrile in the $[Rh(NH_3)_5(bzn)]^{3+}$ complex was demonstrated experimentally). Some authors are of the opinion that the origin of these reactions is due to the nature of LF [323] or LMCT [324] states populated from intraligand IL excited states. However, the results of some thoroughly studied systems of d^6 complexes have shown that the originally populated IL state leads to a chemical (stereochemical) change on the appropriate ligand (see Section 4.3.3) accompanied by intramolecular energy transfer to other states.

Few quantitative data on photosubstitution reactions of complexes irradiated in the region of the CTTS transitions have been published. If such reactions are observed (e.g., substitution of the CN^- ligand by a molecule of H_2O in $[Fe(CN)_6]^{4-}$ [325], or NH_3 by a molecule of H_2O in $[Ru(NH_3)_6]^{2+}$ [290]), owing to overlapping of the CTTS and LF transition bands, either the LF excited states are formed directly during photoexcitation or formation of the LF state by intersystem crossing from the primarily populated CTTS state is assumed [326]. Together with the photosubstitution reactions, also photoredox reactions take place in such cases.

4.4.2 Nature of the photoreactive excited state

Although a number of studies on the nature of the excited state of complexes of different central atoms have been reported, it would be useful to discuss briefly the problems of the so-called doublet-quartet hypothesis concerning Cr(III) complexes [274, 275]. Discussions over the last two decades have provided an illustrative demonstration of the development of ideas about possible interpretations of the experimental results, the importance of the selection of a suitable method for investigating the problem and the considerable complexity of the question being studied, viz., which and when is one of the possible excited states a reactive doublet or quartet?

At first, attention was paid particularly to a comparison of the quantum yields of photochemical reactions as a consequence of photolysis of the complex by radiation corresponding to the quartet or doublet state. Providing that the doublet is photoreactive and the intersystem crossing from the quartet (Q) to the doublet (D) has a value lower than unity, an increase in the quantum yield was expected with doublet excitation. However, this assumption was not confirmed experimentally, and the Φ values found were equal, regardless of the type of excitation. This observation can be interpreted in at least three ways: (a) the efficiency of the intersystem Q → D crossing is $\eta_{isc} = 1$ and therefore the reaction is observable from the D state only; (b) reaction takes place from the Q state, but Q and D are in equilibrium; or (c) reaction is observed from both states with coincidentally equal quantum yields.

The first results which moved the solution to the problem forward include particularly those of comparative studies of the simultaneous quenching of a photochemical reaction and luminescence of the D state. This was based on the fact [275] that the D states of the Cr(III) complexes have a relatively long lifetime, in the range 5 ns–0.1 ms (transition from the D state to the ground state is spin forbidden); absolute quantum yields of emission ranged from 10^{-8} to 10^{-3} in solution at room temperature. These measurements have shown unambiguously [327–329] that the photosubstitution reactive state for $[Cr(CN)_6]^{3-}$ is the Q state reacting within a few nanoseconds, representing the upper limit of time needed for D state to occur.

Whereas the solvent distinctly affects [327] the photoluminescent properties of this complex, the photochemical deactivation shows only slight changes. The emission quenching of the D state in DMF–water mixture was not observed on evaluating the quantum yield of the photochemical reaction (0.11) [327] and no reaction from the vibrationally relaxed D^0 state was observed [328].

These conclusions are not definitive, however, as the same kinetic behaviour could be obtained if the reaction occurred via some other very fast-reacting intermediate state. The essential criterion is that any such hypothetical state must be incapable of crossing over to the doublet state prior to the reaction.

It has also been found that if the Q and D states are energetically sufficiently close, thermal repopulation of the Q and D states can take place simultaneously with other deactivation processes of the doublet. In addition, the rate of intersystem crossing to D is comparable to the vibrational relaxation on the Q state and, in the extreme case, both vibrationally relaxed Q^0 and D^0 states can be in equilibrium. Subsequent experiments have shown that the relaxed Q^0 state can only be achieved through the doublet, which is in direct contradistinction with the conclusions of earlier work dealing with population of the doublet exclusively through the relaxed Q^0 state. The above facts have necessarily led to some caution when evaluating hitherto published results on the kinetic analysis of the deactivation processes of Cr(III) complexes, and in many instances they had to be revised.

In spite of some discrepancies in the literature, an unambiguous conclusion was drawn, namely that a certain proportion of a photochemical reaction (unquenchable photochemistry) has its origin in the excited state preceding the doublet population. However, it has not yet been sufficiently proved [275] whether it is a vibrationally relaxed electronically excited quartet, a vibrationally excited quartet or some other state; frequently one encounters the opinion [329] that the most probable state is that of a mixed D–Q character. Because of the very short lifetime of these states (ranging probably from 20 ps to 1 ns), it was impossible to characterize them more clearly; for example, the energy of a thermally relaxed (thexi) quartet state is not reliably known for any complex in solution at room temperature. However, on the other hand, the nature of the doublet states has been characterized in more detail.

The currently accepted idea on the kinetic scheme for the photochemistry of d^3 complexes is illustrated in Fig. 16, which also includes the potential energy levels of the individual states.

Figure 16 indicates that the Franck–Condon principle is obeyed in the case of radiation absorption ($h\nu$), i.e., a vertical transition, resulting in the spectroscopic Q^{FC} state without an observable distortion towards GS from which it was populated, takes place. Similarly, no (or only a slight) change in configuration is observed during the relaxation of the Q^{FC} to the D^0 state (t_{2g}^3 non-bonding electrons as in the GS state). On the other hand, the relaxation to the Q^0 state is accompanied by considerable distortion due to its $t_{2g}^2 e_g^{*1}$ configuration (Jahn–Teller effect in the excited state). This results, for example [275], with the Cr(III)

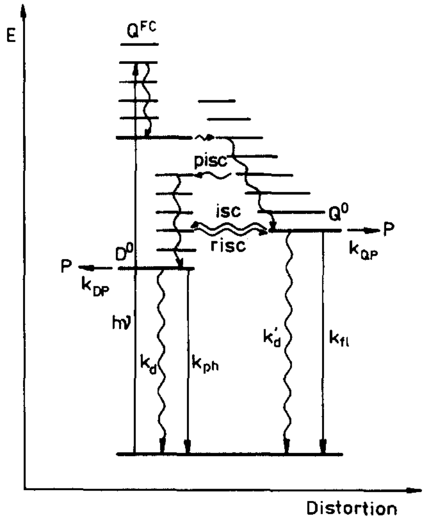

Fig. 16. Modified Jablonski diagram for photochemical and photophysical processes of d^3 complexes. Q^{FC} = spectroscopic Franck–Condon states, Q^0 = vibrationally relaxed lowest electronically excited quartet state, D^0 = vibrationally relaxed lowest electronically excited doublet state, k_{QP} = rate constant of photochemical reaction from Q^0 state, k_{DP} = rate constant of photochemical reaction from D^0 state, k_d, k'_d = rate constants for radiationless deactivation, k_{fl}, k_{ph} = rate constants for fluorescence and phosphorescence, respectively, isc = intersystem crossing: prompt (pisc) and reverse (risc), P = product(s) of photochemical reaction.

acidoammine complexes, in a tetragonally distorted excited state (elongation in the direction of the z-axis). The presence of the vacant t_{2g} orbital will be reflected in an increased probability of the occurrence of penta- and heptacoordinated intermediates (see the discussion on mechanisms in Section 4.4.3).

The distorted Q^0 state that occurs in the Q^{FC} relaxation process (vibrational relaxation and changes in solvation) can undergo a photochemical reaction (k_{QP}), it can be deactivated non-radiatively (k_d') or by fluorescence (k_{fl}) (although rather seldom), or it can provide the D^0 state through intersystem crossing (isc). Analogously, the doublet D^0 can react photochemically with a rate constant k_{DP}, undergo a non-radiative deactivation (k_d) or phosphorescence (k_{ph}) to the ground state, and eventually by the thermal activation process (risc, sometimes called bisc–back intersystem crossing) the quartet Q^0 is repopulated. Recent results have also shown [156, 330] the importance of the fast (pisc) intersystem crossing from Q^{FC} to D^0, the efficiency of which can even equal unity.

In connection with Fig. 16, particularly the possibilities of the deactivation modes which are applied in a different way and with a different efficiency in the given system should be pointed out; thus, for example, some complexes react only through a quartet, others only through a doublet and some through a quartet or a state of mixed doublet–quartet character. Also in these apparently solved systems of complexes the participation of the quartet is not ruled out (owing to the efficient risc); similar problems also seem to arise through the quartet-reacting complexes.

All of these possibilities are shown schematically in Fig. 17a, b and c in terms of three possible kinetic schemes [274] for fast (unquenchable photochemistry) and "slow" (quenchable reaction) product formation (here slow corresponds,

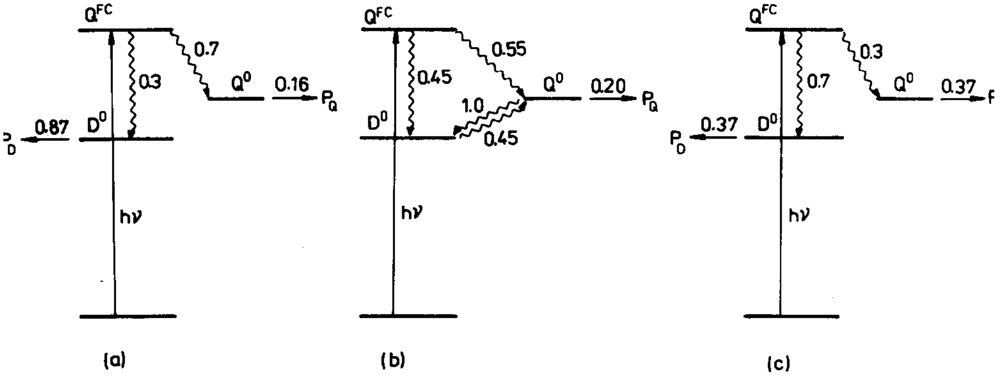

Fig. 17. Possible kinetic schemes of slow and fast photochemistry. P_D = product(s) formed from doublet; P_Q = product(s) formed from quartet (for other symbols see text and Fig. 16). (a) D^0 and Q^0 isolated, initial 0.3:0.7 population (without further isc); both react with different efficiencies. (b) D^0 and Q^0 in equilibrium, initial 0.45:0.55 population; forward and risc fast; only Q^0 reacts. (c) D^0 and Q^0 isolated, initial 0.7:0.3 population (no subsequent forward and risc); both react with the same efficiency.

with $[Cr(en)_3]^{3+}$, to a doublet lifetime of 1.8 µs or more). It should be noted that the three situations presented are not exclusive of all the others and many intermediate possibilities fit the observed time dependence of the yields and quenching results.

In Fig. 17a, the D^0 and Q^0 states are isolated and after their initial 0.3:0.7 population both react. The D^0 state reacts with an efficiency of 0.87 to give the "slow" quantum yield $\Phi_{PD} = 0.87 \times 0.3 = 0.26$ and Q^0 (or Q^* or some other state preceding D^0) gives the fast yield $\Phi_{PQ} = 0.7 \times 0.16 = 0.11$ (fractional efficiency 0.16). The observed overall quantum yield is then $\Phi_P = \Phi_{PD} + \Phi_{PQ} = 0.37$.

In Fig. 17 b, the D^0 and Q^0 states are populated with efficiencies of 0.45 and 0.55, respectively (arbitrarily chosen $\eta_{isc} = \eta_{pisc}$ and equivalent-to-0.7 population of D^0), and both forward and risc are fast enough to allow the equilibrium $D^0 \rightleftharpoons Q^0$. The D^0 state acts as a reservoir that feeds Q^0 by risc and gives a slow yield, $\Phi_D = (0.45 + 0.55 \times 0.45) \times 0.20/1 - 0.45 \times 1.0 = 0.25$. The fast population of Q^0 of 0.55 gives finally (reaction efficiency of 0.20) a fast yield of $\Phi_Q = 0.55 \times 0.20 = 0.11$ (and $\Phi_{PQ} = 0.25 + 0.11 = 0.36$).

The D^0 and Q^0 states initially populated (Fig. 17c) with efficiencies of 0.7 and 0.3 are isolated (no subsequent forward and risc) and react with the same efficiency of 0.37 to give a "slow" yield of $\Phi_{PD} = 0.7 \times 0.37 = 0.26$ and a fast yield of $\Phi_{PQ} = 0.3 \times 0.37 = 0.11$, respectively.

Based on the general scheme in Fig. 16, the following equations have been derived [274] for fast and slow photochemistry:

$$\Phi_{chem}(\text{fast, via } Q^0) = (1 - \eta_{pisc})\eta_{QP} \tag{4.128}$$

$$\Phi_{chem}(\text{slow, via } D^0 \text{ and } Q^0) = \frac{[\eta_{pisc} + (1 - \eta_{pisc})\eta_{isc}](\eta_{DP} + \eta_{risc}\eta_{QP})}{1 - \eta_{isc}\ \eta_{risc}} \tag{4.129}$$

where η_{isc} is the efficiency of intersystem crossing, η_{pisc} the efficiency of prompt intersystem crossing, η_{risc} the efficiency of reverse intersystem crossing and η_{QP} the efficiency of the quartet state Q^0 reaction. Essentially equivalent results have also been obtained in a more complex treatment assuming steady-state conditions [330].

Thus, for example, 50% of the photochemical reaction of the complex *trans*-$[Cr(NH_3)_2(NCS)_4]^-$ in $H_2O/CH_3OH/C_2H_4(OH)_2$ at −65°C is realized directly from the quartet state and the remainder through risc and quartet reaction; as this very short doublet lifetime at room temperature (the quantum yield increased to 0.31) does not allow quenching experiments to be carried out, the proportion of the fast quartet reaction is not known [331]. The data on the emission lifetimes [332, 333] indicate that it is more probably a reaction through a doublet and not a risc.

Moreover, the Jablonski diagram (Fig. 16) includes the participation of other possible states (of intermediate character) already mentioned. Hence, the scheme for an actual situation (analogous to the above-mentioned system) will therefore be different and will depend on the overall system (type of complex, its composition and symmetry, medium, solvent, etc.). Even more complicated is the situation with complexes of metals of the second and the third transition row in which, owing to the strong spin–orbit interaction, analogous labelling of the multiplicity of discrete excited states (see the coordination compounds of the central atoms of the first transition series) frequently loses much of its meaning, although it is used extensively in the literature.

As shown in the above brief outline of the basic characteristics of the deactivation processes for d^3 complexes, the interpretation of the experimental results cannot be considered completely adequate, although it does reflect reality. The great complexity of the problem (many fast and mutually competing processes, extremely short lifetimes of the excited states, their intercommunication, insufficient characterization of their nature and energy levels, non-adequate influence of the medium, e.g., solvent and state conditions, and the absence of an adequate theoretical approach) requires the advanced development of experimental (particularly in the nano-, pico- and femtosecond regions) and theoretical approaches in the future which will permit a more intensive and more comprehensive elucidation at the quantitative level.

4.4.3 Mechanisms of photosubstitution reactions

As already mentioned, the analysis of experimental results on the ligand photosubstitution in complexes (particularly d^3 and d^6) resulted in the conclusion that stereochemical changes, being in many instances part of these reaction mechanisms, should be taken into consideration.

Interest in the possible stereochemical aspects of photosubstitution deactivations has catalysed to a certain extent the formulation of the Adamson empirical rules [6] (see Section 4.4.4). The following photochemical studies revealed the extreme stereospecificity [334, 335] of the photosubstitution reactions of the Cr(III) complexes and resulted in the conclusion that the ligand photosubstitutions are usually accompanied by stereochemical changes. Attempts to take into consideration also the stereochemistry of photosubstitutions stimulated the appearance of several models of the photochemical reactivity. Therefore, it is natural that this section, emphasizing the stereochemical aspects of photosubstitutions, will overlap to a certain extent the discussion on the photoreactivity models described in more detail in Section 4.4.4, mostly because of other non-stereochemical aspects (e.g., prediction of labilized ligand).

The questions of stereochemical changes connected with photosubstitution of the Cr(III) complexes have been discussed many times. Of the two limiting mechanisms of the substitution of ligand, a dissociative one [155, 304, 305]:

$$[ML_5X]^* \rightarrow [ML_5] + X^- \tag{4.130}$$

$$[ML_5] + S \rightarrow [ML_5S] \tag{4.131}$$

and an associative:

$$[ML_5X]^* + S \rightarrow [ML_5XS] \rightarrow [ML_5S] + X^- \tag{4.132}$$

all theoretical models stimulating the Adamson rules explicitly assume (more or less) the dissociative mechanisms. On the other hand, the study of the effect of a solvent on photosubstitution processes of the Cr(III) complexes and the activation volumes of these reactions resulted in more data supporting the associative mechanism. The strongest arguments [276] in favour of this mechanism have been provided by the experimentally found extreme stereospecificity; if the substitution took place through the pentacoordinated intermediate, a mixture of isomers would be produced (according to the statistics, two thirds *cis* and one third *trans* isomer). However, with *trans*-$[CrL_4XY]$, for example, 100% of *cis*-$[CrL_4X(H_2O)]$ is produced by photosubstitution. This led Kirk to formulate the stereochemical rule [334] (Kirk's rule; edge displacement model): "the entering ligand will stereospecifically occupy that position which corresponds to its entry into the coordination sphere in the *trans* position with respect to the leaving ligand".

The edge displacement mechanism [334] explains simply the stereochemical change during the photochemical reaction for anionic ammine complexes of Cr(III), provided that the ligand to be substituted has been determined on the basis of the strong field/weak axis rule. For example, for the complex cation *trans*-$[CrL_4XY]^{2+}$ a solvent molecule will enter the coordination sphere of the complex in the *trans* position with respect to the substituted Y ligand; regardless of which of the edges is attacked, the Y ligand is substituted by the L_1 ligand (by circular motion according to Fig. 18) and *cis*-$[CrL_4XS]^{2+}$ is produced with 100% stereomobility, which was considered to be evidence for an associative mechanism.

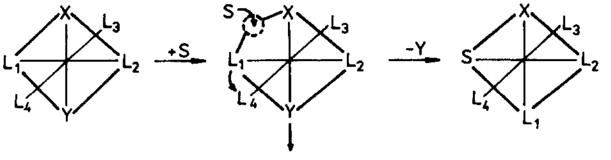

Fig. 18.

The mechanism of the occurrence of a heptacoordinated transition state of Cr(III) complexes is also supported by a higher possibility of attack by the entering ligand S due to the presence of a vacant t_{2g} orbital.

Although the Kirk model does not explain clearly the important question of why the ligand S enters just in the *trans* position, this fact is not of major significance (see the following text).

The quantum yields and stereochemistry of the product of photosubstitution reactions depend on the rigidity of the coordination sphere of Cr(III) complexes. For example, with the *trans* isomers $[Cr(NH_3)_4Cl_2]^+$, $[Cr(en)_2Cl_2]^+$ and $[Cr(tet)Cl_2]^+$ the quantum yields [302, 335, 336] of photoaquation decrease with increasing rigidity of the equatorial plane (0.44, 0.32 and 0.06, respectively), producing *cis* isomers. However, the presence of a markedly rigid cyclic ligand in the $[Cr(cyclam)Cl_2]^+$ complex leads to the production [336, 337] of *trans*-$[Cr(cyclam)(H_2O)Cl]^{2+}$ with a relatively low quantum yield ($\Phi = 3.3 \times 10^{-4}$) in a system with a lower possibility of distortion unavoidable for the occurrence of a heptacoordinated intermediate, provided that the associative mechanism is applied.

There are a number of complexes whose stereochemical changes during substitution can be interpreted according to both the Kirk and VC models (applying the Woodward–Hoffman rules in inorganic photochemistry) with the same result (e.g., identical prediction of stereotransformation of the *trans*-

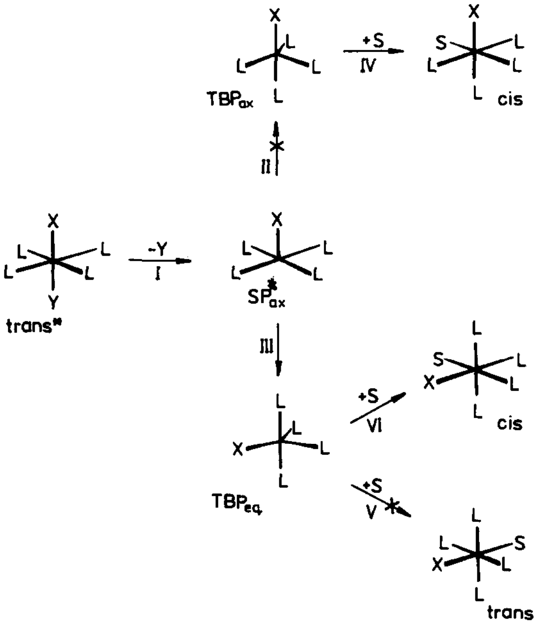

Fig. 19. Dissociative mechanism for ligand photosubstitution (S ≠ Y) (VC model) and *trans-cis* photoisomerization (S = Y) in excited tetragonal d^3 ML_4XY complexes. SP^*_{ax} = excited square pyramidal ML_4X fragment, TBP = ground-state trigonal-bipyramidal intermediate with an axial X ligand (TBP_{ax}) or an equatorial X ligand (TBP_{eq}), S = solvent molecule, X = symmetry-forbidden paths.

$[CrL_4XY]^+$ complex to *cis*-$[CrL_4(H_2O)X]^{2+}$. However, there are cases with markedly different predictions of both approaches; for example, with *cis*-$[Cr(NH_3)_4F_2]^+$ it was found [339] that the Kirk model does not express the distribution of the products properly (experiment contradicts the prediction of a statistically predominating *fac* isomer), and it must be replaced by more convenient VC model (see also Section 4.4.4) based on the dissociative type of mechanism (Fig. 19).

The approach [338, 340, 341] illustrated schematically in Fig. 19 represents photosubstitution of the tetragonal *trans*-$[CrL_4XY]^+$ complexes as a series of characteristic elementary steps, I–VI, during simultaneous *trans-cis* isomerization. In agreement with other photoreactivity models (Section 4.4.4), heterolytic cleavage of the weakest bond in the lowest quartet excited state takes place in the first step (step I) of the reaction sequence. Such an excited square pyramidal fragment, SP^*_{ax}, relaxes, providing a trigonal bipyramidal TBP intermediate (in the ground state) in two ways: with ligand X in an axial position (TBP_{ax}), step II (a forbidden process according to the symmetry rules), or with X in the equatorial plane (TBP_{eq}), step III (a symmetrically allowed process). Of the two possible routes of attack of a solvent molecule on TBP_{eq}, step V, providing the *trans* product, is forbidden, and step VI is allowed (formation of a *cis* product). The equatorial coordination of solvent to TBP_{ax} can result in the occurrence of a *cis* product only (step IV). Application of selection symmetry rules to this dissociative type of mechanism thus explains very well the experimentally observed distinct stereospecificity of the discussed photosubstitution of d^3 complexes with respect to these rules of an allowed sequence of the partial steps $I \rightarrow III \rightarrow VI$.

It should be noted that despite the indisputable success of the above model, experimental data have been obtained that cast doubt on correctness of the assumption about the dissociative mechanism. As shown by the results of a study of the effect of pressure [342] on Φ_s in Cr(III) complexes, the cationic complexes $[Cr(NH_3)_5X]^{2+}$ and $[Cr(NH_3)_6]^{3+}$ (X = Cl, Br, NCS) undergo photoactivation through an associative mechanism (activation volumes $\Delta V^{\neq} < 0$), whereas in the anionic complexes [343] $[Cr(CN)_6]^{3-}$, $[Cr(NCS)_6]^{3-}$ and $[Co(CN)_6]^{3-}$ a dissociative mechanism applies ($\Delta V^{\neq} > 0$).

The observed simultaneous photoactivation and photoisomerization of the *cis*-$[Rh(NH_3)_4Cl_2]^+$ complex ion [304] and the general stereolability in the process of a photosubstitution reaction of some other complexes [156, 214] of Co(III), Ir(III) and Ru(II) stimulated the development of a theoretical model [345, 346] for d^6 complexes; this model was formulated by modification of the VC model [347]. The model based on the dissociative mechanism is illustrated schematically in Fig. 20 (Ford model).

The interpretation of stereochemical changes of complexes of the ML_4XY type, connected with their photosubstitution, takes into consideration the elec-

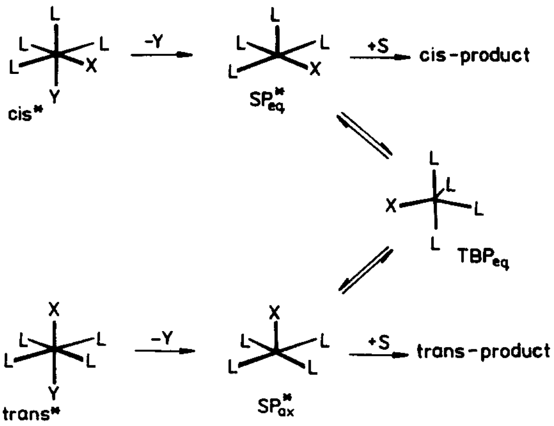

Fig. 20. Dissociative mechanism for ligand photosubstitution and photoisomerizations (*cis-trans* and *trans-cis*) in excited tetragonal d^6 ML_4XY complexes. SP* = excited square-pyramidal ML_4X fragment with an axial X ligand (SP^*_{ax}) or an equatorial X ligand (SP^*_{eq}), respectively, TBP_{eq} = ground-state trigonal-bipyramidal intermediate, S = solvent molecule.

tronically excited pentacoordinated intermediate produced by dissociation of the most labile Y ligand from the originally hexacoordinated complex in the triplet LF state:

$$ML_4XY \xrightarrow{h\nu} ML_4XY^* \rightarrow ML_4X^* + Y \qquad (4.133)$$

Such an excited square-pyramidal (SP*) intermediate has two isomers, SP^*_{ax} (ligand X in an axial position) and SP^*_{eq} (ligand X in the equatorial plane), which are in equilibrium:

(4.134)

However, they can undergo simultaneously deactivation and reaction with a solvent molecule S, forming the *trans*- or *cis*-ML_4XS product.

Whereas the mutual conversion of these two intermediates results in the occurrence of a *cis* and *trans* isomer via another trigonal-bipyramidal (TBP_{eq}) intermediate, simultaneous non-radiative deactivation (isc) to the ground state of SP with subsequent reaction with a solvent molecule S again provides a hexacoordinated product. In agreement with the suggested model, relative energies SP_{ax} and SP_{eq} and the rate of their mutual conversion (eqn. 4.134) distinctly depend on the character of L and X. If the ligand X is a weaker

σ-donor than L (e.g., X = Cl^-, Br^- and L = NH_3), the SP_{ax} isomer is energetically lower (in the axial position the σ-donor of X is weaker) and therefore *cis-trans* isomerization is preferred [for Rh(III) complexes]. Such a *trans-cis* photoisomerization has actually been proved for ammine complexes [344, 345, 348] with M = Rh(III), Ir(III), X = OH^-or M = Co(III), X = CN^-, as the σ-donor properties of the ligand X were always greater in these instances than those of NH_3.

Although this model is known in the literature as a generalized one (theoretical model for d^6 complexes), the extent of generalization does not correspond completely to the meaning of this word; it is also not generally valid for the above-mentioned central atoms, e.g., if the most labilized bond is M–L and not M–X. The possibilities of the application of this model also to d^5 systems (for example [349], *cis*- and *trans*-$[Ru(en)_2Cl_2]^+$), are the subject of discussion [350]. Therefore, it should be noted that for the complexes of other configurations (e.g., d^5 and d^8), no models of comparable quality to those for d^3 and d^6 systems exist, although the predictions on the identity of the substituted ligand and hence the stereochemistry in the ground state have proved fairly satisfactory [e.g., *trans* effect with Pt(II) complexes].

4.4.4 *Models of photochemical reactivity*

Similarly to other scientific branches, the accumulation of a certain amount of experimental data provided the prerequisites for a new quality of understanding also in the photochemistry of coordination compounds. The main feature of this new quality is the formulation of principles that not only enable the photochemical properties of complexes to be elucidated, but also to be predicted. Because of the complex problems and the relatively recent introduction of the photochemistry of coordination compounds as an individual interdisciplinary field, it is natural that the process of the development of concepts in the formulation of the principles of the photochemical reactivity of complexes cannot yet be considered complete. As will be shown below, this development is reflected in the change in quality and the degree of generalization of the hitherto formulated "rules" or "models" of photoreactivity, which are limited even in their present form; the boundaries of their applicability are restricted, for example, by the central atom, symmetry of the complex and type of photochemical reaction (the models existing so far cover only photosubstitution reactions).

The essential problem in the interpretation of the results of photochemical studies and the criteria for the selection of a subsequent experiment, is to obtain information on which of the excited states are photochemically active and what their structures and properties are. As the experimental possibilities for obtaining such knowledge have already been presented (Section 2.3), this section will focus on a discussion of the contribution of the results of theoretical study to the solution of the problems concerning the chemical reactivity of the photoexcited states of coordination compounds and their prediction. These approaches, aimed at revealing the relationships between the composition, structure and photochemical reactivity of complexes, have been steadily developing, and in the literature they are known as photochemical models, or models of predicting photochemical reactivity.

It should be mentioned that the development of theoretical ideas about photochemical reactivity and its prediction has been closely connected with experimental studies. In many instances, the theoretical conclusions had a considerable influence on the orientation of experimental studies and, vice versa, the results obtained by new experimental approaches either disproved or confirmed current theoretical ideas and stimulated further and more intensive theoretical studies.

In contrast with an older idea [2] that light causes only an increase in the reactivity of the ground state and does not change the state, at present the idea of the excited state as a new chemical species differing from the ground state not only in having a higher energy content, but also in its molecular and electronic structure, and thus having different properties, is generally accepted (see Section 2.2).

It should be noted in this connection that in most instances observed photochemical reactions can be classified from the mechanistic point of view in the same way as thermal (spontaneous, dark) reactions; qualitative differences are not observed. Thus, for example, substitution processes take place in both instances by dissociative, associative (limiting cases) and exchange-dissociative or exchange-associative mechanisms. Isomerization reactions and acid–base equilibria are analogous. The Marcus theory is used for both outer-sphere electron exchange thermal and photochemical reactions.

Based on the observed different thermal and photochemical reactivities of Cr(III) complexes, Adamson introduced the term "antithermal behaviour" [351] of excited states, and in 1967 he published empirical rules [6] known as Adamson rules (strong field/weak axis rule). These rules enabled the type of photochemical non-redox reaction of excited Cr(III) complexes with a heterogeneous coordination sphere to be predicted. The rules are as follows.

Rule 1

Consider the six ligands to lie in pairs at the ends of three mutually perpendicular axes. That axis having the weakest average ligand field (determined from the position of ligands correspoding to this axis in the spectrochemical scale) will be the one that is labilized, and the total quantum yield will be about that for an O_h complex of the same average field.

Rule 2

If the labilized axis contains two different ligands, then the ligand of greater ligand field strength preferentially aquates. It might be considered as a certain type of *trans* effect.*

Based on these rules, it can be assumed, for example [351–353], for a complex ion of tetragonal symmetry $[Cr(NH_3)_5Cl]^{2+}$ that the NH_3 ligand will undergo aquation preferentially as it is characterized by a higher ligand field parameter (Dq), and is situated on the axis along which the value of the average ligand field is the lowest (NH_3–Cr–Cl) with respect to other axes (NH_3–Cr–NH_3). Therefore, it will be labilized.

Testing of the Adamson rules on more than 70 hexacoordinated complexes confirmed the validity [278] of Rule 1 not only for d^3, but also of the low-spin d^6 complexes; for d^3 complex compounds, the lowest excited LF quartet is considered to be photochemically active, and in the low-spin d^6 complexes it is the lowest triplet excited LF state. An exception for which the photochemical reactivity cannot be explained on the basis of the above rules is fluoro complexes, e.g., *trans*- $[Cr(en)_2F_2]^+$ and *trans*-$[Cr(NH_3)_4F_2]^+$ ions [339, 354]; aquation of NH_3 ions takes place preferentially although it is not situated on the axis with the lowest value of the average ligand field.

In 1971–1974, several models were proposed [354–359]. Ligand field theory was used to explain the photosubstitutional reactivity of the Cr(III) complexes, which confirmed the Adamson rules theoretically.

Although the Adamson rules were considered to be empirical, the later published models of photochemical reactivity have shown that the rules can be explained by means of the localization of the electron density of an electron in the antibonding σ-orbital in the quartet state along the axis with a low value of the ligand field strength. Moreover, the models presented (also called MO–LF σ/π bonding models [354–358]) explain the importance of the π-bonding effects in the stabilization of the π-donor and destabilization of the π-acceptor properties of ligands. Generally, each of the suggested models estimates particularly the electron density redistribution and (generated) bond labilization which occurred after the absorption of light by the complex.

Zink theoretically proved [355–357], on the basis of the nature of metal–ligand bond changes in different excited states, that the orbital of the preferably

---

* In the original paper [6], a Rule 3 was presented (later not cited by the author himself), which in fact predicts that the quantum yields for disfavoured reactions should increase with decreasing wavelength of irradiation.

Rule 3

The discrimination implied by rules 1 and 2 will occur to a greater extent if it is the L_1 rather than the L_2 band which is irradiated (the L_1 band corresponds to a ${}^4A_{2g} \rightarrow {}^4T_{2g}$ transition; L_2 is ascribed to a ${}^4A_{2g} \rightarrow {}^4T_{1g}$ transition).

substituted ligand should have the highest value of the overlap integral of the antibonding σ-orbital of the central atom, and focused attention [356] (as did Kirk) [334] on the role of the vacant t_{2g} orbital when evaluating the photochemical reactivity of the lowest quartet excited LF state.

Possibilities for the hitherto discussed models and their role in the explanation of the experimentally observed photochemical reactivity can be demonstrated using, for example [303], the complex cation of *trans*-$[Cr(NH_3)_4(DMF)Cl]^{2+}$ (4.135); this ion offers three different simultaneous photochemical primary processes (as one of a few of experimentally well elaborated systems) whose interpretation is based on the very different bonding properties of one anionic and two neutral ligands in the Cr(III) coordination sphere. Moreover, the spectrochemical and bonding properties of DMF are fairly similar to those of water and allow comparisons between analogous DMF and H_2O systems [361].

It is assumed that all approaches to the evaluation of photochemical reactivity published so far contribute to the explanation of experimentally obtained data (eqn. 4.135):

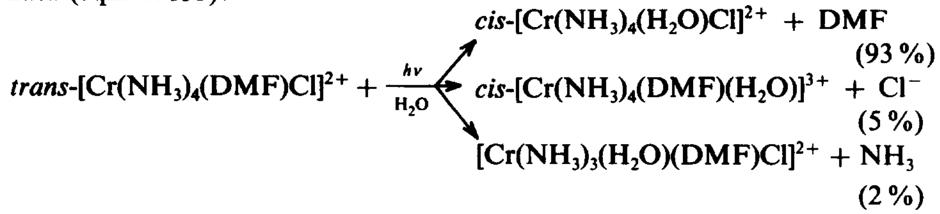

$$\textit{trans}\text{-}[Cr(NH_3)_4(DMF)Cl]^{2+} + \xrightarrow[H_2O]{h\nu} \left\{ \begin{array}{ll} \textit{cis}\text{-}[Cr(NH_3)_4(H_2O)Cl]^{2+} + DMF & (93\,\%) \\ \textit{cis}\text{-}[Cr(NH_3)_4(DMF)(H_2O)]^{3+} + Cl^- & (5\,\%) \\ [Cr(NH_3)_3(H_2O)(DMF)Cl]^{2+} + NH_3 & (2\,\%) \end{array} \right.$$

(4.135)

In the sense of the Adamson semiempirical rules, the ligand that is preferentially labilized along the weaker DMF–Cr–Cl axis (when considering the average ligand field) is DMF, as it has the largest LF parameter. According to MO–LF σ/π bonding models, the excitation $^4B_1 \rightarrow {}^4E$, $(d_{xz}, d_{yz}) \rightarrow \sigma^*$ (mostly d_{z^2}) weakens the σ-bond in the direction of the DMF–Cr–Cl axis (z-axis); however, simultaneously the π-dative bond becomes stronger along this axis. As the π-dative ability of Cl^- is higher than that of DMF, substitution of the DMF ligand will be dominant. On the other hand, by the $^4B_1 \rightarrow {}^4B_2$ transition, $\pi(d_{xy}) \rightarrow \sigma(d_{x^2-y^2})$, the σ-bond in the equatorial $(NH_3)_4$ plane is destabilized (the π-dative NH_3 bond need not be considered, as NH_3 is only the σ-donor).

In concluding the above discussion, it should be emphasized that the Adamson rules and MO–LF. σ/π models in many instances permitted good assessment of the photochemical behaviour of Cr(III) complexes from the viewpoint of the first approach. They also provided a firm basis for the development of ideas to solve the problem of the prediction of photochemical reactivity and catalysed the formulation of current, more exact models.

In spite of indisputable advantages, these models have a number of drawbacks that limit the possibilities of their more extensive application. For example, the most purposefully elaborated and detailed Zink model is particularly inadequate in explaining experimentally observed stereochemical changes and the question of the doublet versus quartet photoreactivity. The models are required to perform MO calculations, which may be difficult for experimentalists. One of the most serious disadvantages is that they do not emphasize satisfactorily the aspect of bond labilization in place of the total strength of the bond in an excited state.

As these models preferably consider electronic factors, their predictive ability is weakened when the photochemical deactivation is markedly influenced by, e.g., steric interactions or effects of the medium (effect of solvent).

Currently, the most acceptable model for almost all complexes of the first-row transition metals is the semiempirical theory of ligand labilization based on the angular overlap model proposed in 1977–1979 by Vanquickenborne and Ceulemans (VC model, I* model) [287, 338, 340, 341]. It seems that this approach, based on the dissociative mechanism, is able not only to predict satisfactorily the labilized ligand and to offer an adequate interpretation of the stereochemistry of photochemical processes, but also to evaluate the effect of equatorial rigidity on the quantum yield of photosubstitution.

The model predicts the possibilities of photochemical reactivity (ligand labilization) based on the determination of the absolute energies I*(M–L) of the particular bonds in the excited state. It is assumed that a photosubstitution takes place from the lowest quartet (d^3) or triplet (d^6) excited state, and the strength of the I*(M–L) bond is calculated using the semiempirical LF model from σ-donor– and π-donor–π-acceptor parameters of ligands obtained from spectral data.

Although the conclusions based on the VC model were identical in many instances with those resulting from the Adamson rules, exceptions that exist showed that these two approaches were not identical. Whereas the Adamson rules (strong field/weak axis rule) consider only weakening of the bond in the excited state towards the ground state [I*(M–L) – I(M–L)], the VC model predicts the dependence on I*(M–L).

Another essential difference with the VC model is that that it refers labilization to the plane (and not to the axis) of the weakest average ligand field (either xz or yz) in a general case where Dq(z-axis) < Dq(x- and y-axes). The VC model enables, with a certain degree of approximation, the Adamson rules to be reduced to a single rule: "the leaving ligand is the ligand characterized by the largest labilization energy I–I*". However, it is obvious in the sense of the VC model that the labilized ligand will be determined primarily by the lowest I*(M–L) value and not to such a great extent by the highest I–I* difference.

The I* model also predicts with great success the photochemical reactivity for Cr(III) complexes where the Adamson rules and other models fail and for some other Co(III) complexes. Thus, for example [362, 363], for the $[Cr(NH_3)_5F]^{2+}$ complex cation the VC model predicts substitution of an ammonia molecule as a ligand (in agreement with experiment), but according to the Adamson rules aquation of the fluoride anion should take place.

The comparison of predictions given by the various photolytic models discussed above (including the VC model) can be effectively demonstrated by recent results [364] on the ligand-field photolysis of three *trans*-$[Cr(NH_3)_4(CN)X]^{n+}$ ions with X = H_2O, NCS^- and F^- ($n = 1, 2$). These systems under discussion differ from most of the complexes investigated to date (with axial ligands of lower spectrochemical strength than the equatorial amines) in having spectrochemically higher lying axial groups.

These complexes are electronically unusual in that the CN^- and X axial groups act in opposition in the splittings of the octahedral LF states on descending from O_h to C_{4v} symmetry and, moreover, are π-acceptors and π-donors, respectively. It seemed worthwhile exploring this new situation arising from the presence on the tetragonal axis of both a strong- and a weak-field ligand.

In each instance photoaquation (eqn. 4.136) of all three types of ligand is observed, taking *trans-cis* photoisomerization (for X = H_2O) as a measure of water photoexchange. The common precursor $^4E/^4B_2$ is suggested for all photoreactions, and hence doublet deactivation mainly via back intersystem crossing to the lowest excited quartet state(s).

$$\textit{trans}\text{-}[Cr(NH_3)_4(CN)X]^{2+} \xrightarrow[H_2O]{h\nu} \begin{array}{l} \nearrow \textit{cis}\text{-}[Cr(NH_3)_4(H_2O)X]^{(z+1)+} + CN^- \\ \rightarrow \textit{cis}\text{-}[Cr(NH_3)_4(CN)(H_2O)]^{2+} + X \\ \searrow [Cr(NH_3)_3(H_2O)(CN)X]^{z+} + NH_3 \end{array} \qquad (4.136)$$

According to the early rules by Adamson [6], the first rule is obeyed by the aquo and thiocyanato complexes, but not by the fluoro complex owing to the lack of consideration of bonding aspects by the rules (the formally weaker field axis of the latter complex contains two strongly bound ligands). The second rule holds for X = NCS^- and F^- but not for X = H_2O; this inadequacy is explained again by the different bonding properties of water and cyanide. It is of interest that with *trans*-$[Cr(NH_3)_4(CN)F]^+$ the second rule is obeyed, as the ligand-field discrimination can emerge owing to the similar bond strengths of cyanide and fluoride.

Application of MO–LF σ/π qualitative models [355–358] leads to the prediction of a larger degree of labilization for CN^- than for X in all three instances. The wrong prediction for X = H_2O is essentially connected with the fact that these models do not take into account the differences in the ground-state energies (which are large when the Cr–CN^- and Cr–H_2O bonds are compared) because they are based on general excited state weakening, combined with π-donor stabilization and π-acceptor destabilization.

The comparison in terms of the additive angular overlap (VC) model [287, 338, 340, 341] results in accord between predictions and experiment for two complexes: *trans*-$[Cr(NH_3)_4(H_2O)(CN)]^{2+}$ and *trans*-$[Cr(NH_3)_4(CN)F]^+$. The I* values within the $^4T_{2g}$ approximation are given by eqn. 4.137, assuming complete state degeneracy [341]:

$$I^*(^4T_{2g}) = \frac{1}{3} I^*(^4B_2) + \frac{2}{3} I^*(^4E) \qquad (4.137)$$

This equation predicts the preferential displacement of an H_2O molecule for the former complex and NH_3 for the latter. Even for *trans*-$[Cr(NH_3)_4(CN)(NCS)]^+$, which loses mainly NH_3, such an approximation is not far from being completely correct. Because the *trans*-$[Cr(NH_3)_4(CN)(NCS)]^+$ complex ion represents the first Cr(III) system with a relatively slow doublet decay under photolysis [364], the discrepancy between the Φ_{NCS} results and the predictions of the VC theory may lie in possibility [364] that some specific doublet chemistry was superimposed on the quartet reactivity on which the VC model is solely based.

The VC theoretical approach has been applied to complexes with D_{2h} microsymmetry [365] and higher lying quartet excited states (e.g., $^4B_{2g}$) and satisfactorily explained the observed dependence of the quantum yields on wavelength and temperature. By application of the angular overlap model [340] to the calculation of energy parameters of different reactions, the first theory of the photostereochemistry of d^3 (and d^6) complexes was developed that employs the symmetry-based selection rules in the solution of a complex photochemical problem.

Petersen et al. [345, 346] theoretically extended the VC model to d^6 systems in spite of certain doubts [349] in the applicability of this model, e.g., for d^5 systems *cis*- and *trans*-$[Ru(en)_2Cl_2]^+$ and some d^6 systems of the $[M(en)_2XY]^{2+}$ type, where [366] M = Rh(III) or Ir(III) [344]. Later, the validity of the model was not only proved but good prospects [350] of extending it to other d^n systems were demonstrated, covering the photosubstitution processes as a consequence of the LF excitation.

However, the necessity to take into consideration the existing fine equilibrium in the dynamics of the processes leading to geometrical rearrangement and photophysical deactivation of excited states (excited-state rearrangement model) was pointed out. Thus, the formation of products of specific geometries is expected and is observed experimentally if the stereochemical rearrangement takes place earlier (faster) than the triplet–singlet deactivation of the MA_4X fragment (five coordinated intermediate) formed by release of the Y ligand from the MA_4XY complex in the lowest triplet excited state (see Section 4.4.3).

The effort to master also the problems of the prediction of photophysical processes led Walters and Adamson to formulate the following "emission rules" [367], which were based on the analysis of the ever growing amount of information on the photophysics of Cr(III) complexes.

Rule 1

For complexes with six equivalent Cr–L bonds, the emission lifetime in a fluid solution at room temperature decreases with decreasing ligand field strength.

Rule 2

If two different kinds of ligand are coordinated, the emission lifetime will be relatively short ($< 1\ \mu s$) if that ligand which is preferentially substituted in the thermal reaction lies on the weak ligand field axis.

It is noteworthy that interpretation of the rules again takes into consideration the hypothesis on the doublet and not the quartet photoreactive state of the Cr(III) complexes. The main reason for the return to the doublet hypothesis in the problem discussed for over two decades was the assumption that the vacant t_{2g} orbital in the doublet state probably facilitates the bimolecular substitution process. There have been further discussions about whether this is true or not, as the existence of a vacant orbital is in disagreement with the electronic configuration (half-occupied levels) connected with it.

Although for certain complexes an agreement between prediction and experiment was found, there are a large number of coordination compounds for which this agreement was not found; this results in certain doubts about the general validity of these rules.

Increasing evidence has been obtained experimentally that the rate of a photochemical deactivation is comparable to rates of such fast processes as vibrational relaxation and internal conversion. Langford and Hollebone [368, 369] pointed to the necessity for another theoretical approach for a description of "prompt" reactions and that it is impossible to continue with the application of transition-state theory. A new idea [370] that the processes occur in conjunction with extremely prompt reaction of the excited states of complexes has been called DOSENCO (Decay on a Specific Nuclear Coordinate).

For the class of slow reactions, a certain mechanism is determined by a random distribution at the Boltzmann temperature; the processes following the population of the thexi state have been called DERCOS (Decay on Random Coordinate Selection) processes [370].

The Zink model did not distinguish between DOSENCO (rapid limit) and DERCOS (slow limit) processes, as in the MO approach LF parameters from absorption spectroscopy (corresponding to "vertical" transitions) are used. However, it partially takes into consideration the competition between the rate of chemical reaction, non-radiative deactivation to the ground state and luminescence, thus suggesting the possibility of rapid DOSENCO process behaviour in the sense of the "relaxability theory" proposed by Devaquet [371].

Based on the parameters resulting from vertical transitions and ground-state geometry, this theory suggests the most probable "initial" directions and trends in the distortions during the excited-state relaxation which is applicable to both DERCOS and DOSENCO processes. Bearing in mind the category of "slow" reaction limit, the direction of relaxation (in the sense of motion of nuclei) in the discussed theory tends towards the DERCOS state. As the DERCOS state is similar to the transition state, conclusions about reactivity for a photochemical reaction can also be drawn from the information on DERCOS.

So far, the extent to which the coordination compounds will have DOSENCO behaviour is not known; more definite conclusions can be drawn after analysing a sufficient number of experimental and theoretical data. This analysis could lead to a new theory of vibronic selectivity.

Finally, some typical characteristics common for all of the above rules and models of photochemical reactivity should be mentioned; all discussions have concerned the photosubstitution reactivity of kinetically inter, mostly octahedral complexes.

From the current state of knowledge of the possibilities of predicting photochemical reactivity and their development, it can be expected that further theoretical and experimental development will also enable adequate models of redox photoreactivity to be formulated. Several papers have been published on photoredox reactions (e.g., Endicott [66, 155, 372]) carried out with the aim of generalizing the information achieved and applying it to the prediction of redox photoreactivity. In fact, such rules appeared approximately in the 1970s (Vogler and Adamson [373]), or earlier (Adamson's simple model of radical pairs) [374, 375]; however, a model for the prediction of photoredox reactivity elaborated to the same level as the models for photosubstitution has not so far been published.

Of the theoretical approaches contributing to the establishment of models for the prediction of photochemical reactivity, successful progress has been made in gradually coping with the photochemically induced geometrical changes that do not involve octahedral complexes (four and five coordinations, mutual equilibria between 4–5 and 4–6 coordination, and equilibrium of complexes of $T_d \rightleftharpoons D_{4h}$ symmetry, recently studied by Vanquickenborne et al. for Ni(II) complexes [284]).

4.5 Photochemical insertion, elimination and addition reactions

In this section, non-redox reactions involving the central atom are considered, in which:

— a molecule enters the bond between the central atom and one of the ligands, and the other central atom–ligand bonds remain unchanged;

— the coordination number of the central atom is reduced by elimination;

— a stable product with a higher coordination number than that of the reactant is formed by addition.

Photoinsertion reactions have been observed in organometallic compounds of several transition metals and, to a lesser extent, in coordination compounds. Their mechanism either consists of a series of elimination and addition reactions, or is based on the production of radicals in the primary photoredox deactivation process of an excited complex.

On the basis of the observed methyl-exchange process:

$$[(PPh_3)Au{-}CD_3] + CH_3^{\bullet} \rightarrow [(PPh_3)Au{-}CH_3] + CD_3^{\bullet} \qquad (4.138)$$

a free-radical mechanism rather than an addition–elimination sequence was favoured [378] for the insertion reactions:

$$[(PE_3)Au{-}CH_3] + C_2F_4 \xrightarrow{h\nu} [(PE_3)Au{-}C_2F_4{-}CH_3] \qquad (4.139)$$

where $E_3 = Ph_3$ or Ph_2Me. Similarly, via the photoinduced homolysis of the $Au{-}CH_3$ bond, hexafluoro-2-butene reacted to give an insertion product.

Irradiation of a solution containing $[Ti(Cp)_2(CH_3)_2]$ and $C_6F_5C \equiv CC_6F_5$ yielded exclusively [377] the insertion product:

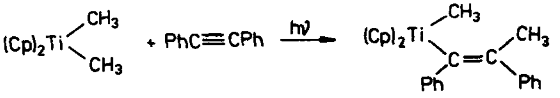

(4.140)

Despite the fact that mechanism of photoredox reactions of cyclopentadienyltitanium(IV) compounds was studied by spin-trapping ESR and using deuterium-labelled compounds, it has not been unambiguously proved whether or not free radicals are formed in the course of the reactions.

In studies of the photochemical properties of Co(III) corrinoids, the occurrence of insertions of these complexes was also found. Irradiation of a deoxygenated aqueous solution of methylcobalamin in a CO atmosphere (at a pressure of 3.1 MPa) at room temperature led to the formation of acetylcobalamin in 70% yield. The primary photochemical step is the homolytic splitting of the $Co(III){-}CH_3$ bond to produce a $CH_3^{\bullet}$ radical and Co(II) cobalamin. The $CH_3^{\bullet}$ radical either combines with Co(II) cobalamin or it is trapped by CO molecule. Of course, the higher the CO pressure, the greater the probability of a reaction of $CH_3^{\bullet}$ and CO and thus also the production of the $CH_3CO^{\bullet}$ radical. The trapping of the $CH_3CO^{\bullet}$ radical by Co(II) cobalamin yields the final product, acetylcobalamin. The reaction is interesting from the viewpoint of carbon–carbon bond formation. The reaction mechanism is as follows ([Co] denotes cobalamin) [378]:

$$[\mathrm{Co^{III}}]\text{–}\mathrm{CH_3} \overset{h\nu}{\rightleftharpoons} [\mathrm{Co^{II}}],\ \mathrm{CH_3^{\bullet}} \xrightarrow{\mathrm{CO}} [\mathrm{Co^{II}}],\ \mathrm{CH_3CO^{\bullet}} \rightarrow [\mathrm{Co^{III}}]\text{–}\mathrm{COCH_3} \tag{4.141}$$

The photochemistry of cobaloximes is similar to that of cobalamines except that the quantum yields are lower. Homolytic cleavage of the Co(III)–CH_3 bond was proposed [379] in the mechanism of the dioxygen insertion reaction of methylcobaloxime, denoted in reaction (4.142) as [Co]–CH_3:

$$[\mathrm{Co^{III}}]\text{–}\mathrm{CH_3} + \mathrm{O_2} \xrightarrow{h\nu} [\mathrm{Co^{III}}]\text{–}\mathrm{OOCH_3} \tag{4.142}$$

The first step of the reaction is photoaquation of the axial ligand. In the following step, the Co(III)–CH_3 bond is cleaved and the resultant $CH_3^{\bullet}$ radical can scavenge O_2 to give the peroxo radical $CH_3COO^{\bullet}$, which can then recombine with Co(II) to form the peroxo complex. It has been generally accepted that the homolytic splitting of the Co(III)–CH_3 bond is a consequence of population of the d_{z^2} orbital, which is antibonding towards the Co(III)–CH_3 bond. The electron occupying a d_{z^2} orbital may come from the cobalt–carbon bonding orbital (via LMCT transition) or from the Co(d_π)-orbital (via LF transition).

Typical photoelimination reactions have been described [380] in a series of $[NiX_2(PMe_3)_3]$ complexes (X = Br, I, CN):

$$[\mathrm{NiX_2(PMe_3)_3}] \xrightarrow{h\nu} [\mathrm{NiX_2(PMe_3)_2}] + \mathrm{PMe_3} \tag{4.143}$$

Under experimental conditions where the thermal reaction hardly takes place, a photoinduced elimination of one PMe_3 ligand yielding the square-planar *trans*-$[NiX_2(PMe_3)_2]$ complex occurs. It seems that the second singlet LF state is the photochemically active state.

The quantum yield of PMe_3 photoelimination during the photolysis of the *trans*-$[Ni(CN)_2(PMe_3)_3]$ complex of D_{3h} symmetry was lower than those for bromide and iodide complex (trigonal-bipyramidal complexes of C_{2v} symmetry) and increased with decreasing wavelength of the incident light.

Octahedral complexes can also undergo photoinduced eliminations. Irradiation ($\lambda_{\mathrm{irr}} = 1060$ or 530 nm) of the high-spin complex $[Ni(tet)(H_2O)_2]^{2+}$ leads [381] to the photoelimination of two water molecules with the simultaneous production of a square-planar low-spin ion, $[Ni(tet)]^{2+}$, of D_{4h} symmetry.

Nickel porphyrins are attractive compounds for the investigation of non-redox eliminations and additions as they can be four-coordinate low-spin (in non-coordinating or weakly coordinating solvents), five-coordinate high-spin (the coordination number determined by the ligand structure and the environment of the complex) or six-coordinate high-spin (in strongly coordinating solvents). As Raman modes are very sensitive to the metalloporphyrin spin state, the structure of metalloporphyrins and ligation changes can be readily studied, in addition to transient absorption measurements, by time-resolved resonance Raman scattering.

The results obtained can be summarized [382, 383] as follows. As a consequence of excitation of a six-coordinate ($^3B_{1g}$) complex, the excited $^1A_{1g}$ state is achieved. Owing to the filling of the Ni($3d_{z^2}$) orbital, axial ligands temporarily dissociate and a four-coordinate complex is formed. The axial ligands are released in less than 35 ps. An example is the shift of the equilibrium between a four- and six-coordinate Ni(II) complex in pyridine on laser irradiation at 406.7 nm:

$$\textit{trans}\text{-[Ni(TPP)(py)}_2] \overset{h\nu}{\rightleftharpoons} \text{[Ni(TPP)]} + 2\text{py} \tag{4.144}$$

Excitation of a four-coordinate complex ($^1A_{1g}$ ground state) results in the formation of the unligated $^3B_{1g}$ state in less than 15 ps. In the presence of strong coordination ligands, the unligated $^3B_{1g}$ state traps two molecules, forming a six-coordinate complex:

$$\text{[Ni(OEP)]} + 2\text{py} \underset{h\nu}{\overset{h\nu}{\rightleftharpoons}} \textit{trans}\text{-[Ni(OEP)(py)}_2] \tag{4.145}$$

Nickel(II) forms analogues of the native iron(II) haemoglobin (NiHb) and myoglobin (NiMb), in which owing to the unique influence of the five-coordinate protein is stabilized. No photoinduced ligation changes are observed for these NiHb and NiMb compounds, regardless of the excitation wavelength. On the other hand, four-coordinate NiHb and NiMb are photoreactive and their excitation leads to the photoaddition of a ligand into an axial position and the formation of a five-coordinate complex. It is worth repeating that the complexes produced by photoexcitation do not persist for a long time in the system and should be regarded as transient species.

Photochemical non-redox additions or eliminations involving the central atom include reactions in which both the chromophore of the complex and the composition of ligands are changed, but the coordination number is preserved. A typical reaction of this type is the following reaction [384]:

$$\textit{trans}\text{-[Cr(en)}_2\text{F}_2]^+ + \text{H}_3\text{O}^+ \xrightarrow{h\nu} \text{[Cr(en)(enH)(H}_2\text{O)F}_2]^{2+} \tag{4.146}$$

In this reaction, protonation of one ethylenediamine molecule in the excited state takes place. This molecule thus becomes monodentate, and a water molecule is bonded to the released coordination site.

A hydrolysis reaction associated with the addition of a water molecule to the coordinated α-amino acid derivative in excited Zn(II) complexes leads to the photochromic behaviour of the complex [385]. Photochromism can be described as follows:

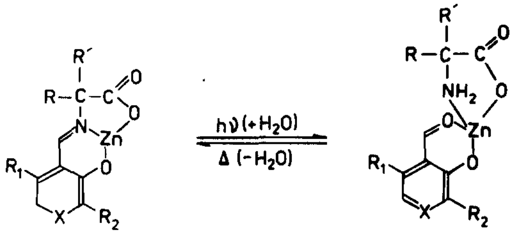

(4.147)

where for pyridoxal 5'-phosphate-α-amino acid complexes $X = N$, $R_1 = [CH_2OPO_3]^{2-}$, and $R_2 = CH_3$, and for salicylaldehyde-α-amino acid complexes $X = CH$ and $R_1 = R_2 = H$. Alanine and α-aminoisobutyric acid were used.

Metal-free pyridoxal 5'-phosphate-α-amino acid Schiff bases undergo photochemical decarboxylation, and the coordination of the carboxylato group to Zn(II) depresses the photoinduced release of CO_2. The mechanism of the photodeactivation processes cannot be discussed as the complexes were irradiated by polychromatic light.

Unlike the above-mentioned Zn(II) compounds where the amino acid was stabilized towards photodecarboxylation through its coordination, glycinato complexes are photosensitive and from the excited states can be deactivated by decarboxylation, as in Co(III) complexes [386, 387]:

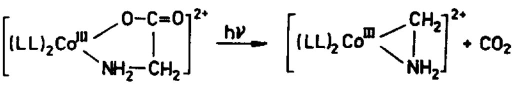

(4.148)

The reaction mechanism consists of several redox steps. The primary photochemical process is probably the homolytic splitting of the Co(III)–O bond. Subsequently, a CO_2 molecule is released from an amino acid radical, and the $NH_2CH_2^{\bullet}$ radical recoordinates with Co(II), thus producing the three-membered Co(III) metallocycle. The bidentate LL ligands (1,10-phenanthroline or 2,2'-bipyridine) apparently do not take part in the reaction.

4.6 Photochemical changes in composition of coordinated ligands

Photoredox reactions of coordinated ligands and non-redox processes involving the central atom of a complex were discussed in previous sections. In this section, light-induced non-redox ligand-localized changes not involving the

central atom of a complex are introduced. Of this type of photochemical reactions, the following have been studied so far:
- non-redox rearrangement reactions;
- acid–base equilibria;
- ligand-localized photosubstitutions;
- ligand decomposition reactions.

The first group covers, for example, the formation of π-complexes, for which, in general, the term "oxidation number" loses its meaning. Such a complex is produced by the reaction [388]:

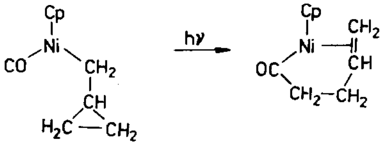

(4.149)

From the viewpoint of their relationship, the reactant and the product are coligand isomers.

The change in the energy of a complex during transitions from the ground state to an excited state may result in a change in its acid-base properties (see Section 2.5). The extent of this change depends on the direction and localization of the redistribution of electron density within the transition. In general, if the electron density on the ligand increases during excitation (MLCT transition), the ligand affinity to proton is increased and thus also the pK value increases (pK^* > pK). If the excitation is not associated with the change in the radial distribution of the negative charge in a complex (LF or IL excited states), also the ability of the complex to bind a proton is not changed, and therefore pK^* ≈ pK. In the LMCT excited state, pK^* should be lower than pK.

TABLE 18
Acid–base equilibrium constants of complexes in their ground state (pK_i) and the lowest excited state (pK_i^*)

Complex (base)	Excited state	pK_i	pK_i^*	Ref.
$[Ru(bpy)_2(4\text{-}COO\text{-}4'\text{-}CH_3\text{-}bpy)]$	MLCT	$pK_1 = 3.0$	$pK_1^* = 4.85$	[390]
$[Ru(bpy)_2(4,4'\text{-}(COO)_2bpy)]$	MLCT	$pK_1 = 1.8$ $pK_2 = 2.65$	$pK_1^* = 3.7$ $pK_2^* = 4.5$	[389] [390]
$[Ru(bpy)_2(CN)_2]$	MLCT	$pK_1 = 1.2$ $pK_2 = 2.0$	$pK_1^* = 4.3$ $pK_2^* = 6.7$	[391] [64] [240]
$[Ir(bpy)_3(OH)]^{2+}$	IL + MLCT	$pK_1 = 3.0$	$pK_1^* = 3.5$	[240]
$[Cr(4,4'\text{-}(COO)_2bpy)_3]^{3-}$	LF	$pK_i \doteq pK_i^*$		[176]

Experimental data for pK_i and pK_i^* values for some complexes in the ground and energetically lowest excited states are given in Table 18. It is obvious that in Ru(II) complexes, for which in their non-protonated (basic) form the lowest excited state is ^{3}MLCT in nature (in protonated forms it is the ^{3}IL state), $pK_i^* > pK_i$. For the Ir(III) complex the pK^* value is only slightly higher than pK as the emitting (lowest) excited state is predominantly an intraligand state mixed only to a slight extent with the MLCT state.

The electron densities at the protonation sites in both the ^4E_g ground state and the metal-centred, intraconfigurational ^2E_g excited state are expected to be virtually identical. Therefore, the pK^* and pK values for the Cr(III) complex are approximately the same.

Acid–base equilibria of the LMCT excited complexes have not yet been investigated.

Photosubstitution reactions localized on a ligand are not very common in the photochemistry of coordination compounds. Such reactions can be exemplified [392] using a process whose stoichiometry is expressed by the following reaction:

$$[Fe(Cp)_2] + CH_2Cl_2 + C_2H_5OH \xrightarrow{h\nu} [Fe(Cp)(C_5H_4{-}CH_2{-}OC_2H_5)] + 2HCl \tag{4.150}$$

The reaction occurs during irradiation of ferrocene in a mixture of CH_2Cl_2 and C_2H_5OH; its mechanism is complex and involves several redox steps. In addition to the substituted ferrocene, also redox iron(III) compounds are produced.

A very intensively studied group of complexes that deactivate from their excited states by ligand decomposition (together with other deactivation pathways) are azido complexes of transition metals. The modes of chemical deactivation are strongly influenced by the properties of the central atom, which determine the nature of the lowest lying, photochemically active excited state.

It has been shown that irradiation of the systems of Co(III) azido complexes results, in addition to substitution in an innersphere electron-transfer reaction followed by decomposition of the complex yielding Co(II) and an $N_3^{\bullet}$ radical.

The Cr(III) azido complexes are photochemically decomposed, producing nitrido complexes of chromium(V). It is assumed that in the systems of Ir(III) and Rh(III) complexes the primary photochemical step is the formation of nitrene intermediates [393–395]:

$$[M(NH_3)_5N_3]^{2+} \xrightarrow{h\nu} [M(NH_3)_5N]^{2+} + N_2 \tag{4.151}$$

which are highly reactive species and react with the particles of the medium, e.g.,

$$[M(NH_3)_5N]^{2+} + 2H^+ + Cl^- \rightarrow [M(NH_3)_5NH_2Cl]^{3+} \tag{4.152}$$

The production of the nitrene intermediate was not characterized by the authors [393–395] as a redox process. In the systems of Rh(III) complexes the photoreduction of Rh(III) to Rh(II) also takes place.

The differences in the photochemical properties of the Cr(III), Co(III), Rh(III) and Ir(III) azido complexes are probably due to the different energies of the LMCT and azide-localized IL states. In Co(III) complexes, the LMCT state is energetically lower than the IL state and reduction of the central atom takes place. In Rh(III) complexes both states have similar energy; for the Ir(III) complex the IL state is energetically lower than the LMCT state and the complex is deactivated by releasing N_2 only.

A more complicated mechanism involving photosubstitution processes in addition to the azido ligand decomposition is that of photochemical reactions of molybdenum(II) organometallic compounds, $[Mo(Cp)(CO)_x(PPh_3)_{3-x}N_3]$, where $x = 1$ or 2. The compounds provide $[Mo(Cp)(CO)_x(PPh_3)_{3-x}(NCO)]$, isocyanato complexes, under unfiltered UV radiation in the presence of CO and PPh_3 [396]. The reactions are consistent with the formation of organometallic nitrenes, which capture a CO molecule to produce the isocyanate ligand. The photodeactivation pathways were not evaluated.

5 APPLICATIONS OF PHOTOCHEMISTRY OF COORDINATION COMPOUNDS

Together with theoretical research into the photophysical and photochemical properties of coordination compounds, there is an ever increasing need to utilize the available knowledge for practical purposes. Practical applications not only depend on the results of basic research but, together with the development of experimental techniques, they also have a considerable influence on the direction and depth of the photochemical studies. The qualitative stage of the linkage between theory and practice is not the same for all fields. Whereas in the chemistry of polymers only the knowledge of the kinetics and mechanisms of photochemical processes is applied, there are other fields (e.g., the transformation and storage of solar energy) that contribute to the development of solutions to basic scientific problems. A knowledge on the kinetics and thermodynamics of photoprocesses, although unbalanced, has been achieved. New tasks for research have appeared, such as photoelectrosynthesis and the photochemistry of colloid systems.

The level of the hithertho achieved knowledge and the efforts to apply it in practice are reflected in the organization of regular symposia devoted to certain fields (e.g., International Conference on Photochemical Conversion and Storage of Solar Energy). Books have been published that covered some applications of the results of the photochemistry of coordination compounds. However, there has been no paper or book so far dealing with the application of complex photochemistry in a wider scope.

This chapter represents an attempt to remedy this lack, at least partially. Of various possibilities for covering actual and potential applications of the photochemistry of coordination compounds, mainly those which are most frequently at present are stressed.

Section 5.1 presents the terminology and the results relating to photocatalysis. The defined terms are used in Section 5.2, including information on the conversion and storage of solar energy. The photochemical preparation of complexes is discussed in Section 5.3. Section 5.4 deals with the application of the knowledge of the photochemistry of coordination compounds in the chemistry of polymers, and the final part (Section 5.5) is devoted to other applications.

5.1 Photocatalysis

The intense development of the photochemistry of coordination compounds with emphasis on the photocatalytic aspects in the last decade has been reflected in several published review papers [397–409]. Research on systems designated photocatalytic in fact proceeds in two directions: one is focused on the study of mechanisms of catalytic reactions taking place with the assistance of light radiation, resulting in the development of theory and terminology, and the second stresses practical applications of photocatalytic processes. One can assume that by a symbiosis of both directions it will be possible to achieve the preparation of substances with predetermined properties applicable in photocatalytic processes.

As the terminology (still being discussed [402–404, 406, 410, 411]) referred to in this section is also used in other sections, it is necessary to define the fundamental terms in accordance with the present state of knowledge and conventions used in the literature.

The term *photogenerated catalysis* (and also true photocatalysis or photoinduced catalytic reactions) designates sequence of processes that start by the formation of a catalyst K in a photochemical reaction from a thermally stable, catalytically inactive precursor A:

$$\mathrm{A} \xrightarrow{h\nu} \mathrm{A}^* \rightarrow \mathrm{K} \qquad (5.1)$$

and continuing in subsequent, exclusively thermal chemical transformations of the reactant R to the product P catalysed by the catalyst K formed photochemically, which is not consumed in the course of a reaction:

$$\mathrm{K} + \mathrm{R} \rightarrow \mathrm{K{-}R} \qquad (5.2)$$

$$\begin{tikzcd}[row sep=small] & & \mathrm{K} + \mathrm{P} & (5.3) \\ \mathrm{K{-}R} \arrow[r] & (\mathrm{K{-}P}) \arrow[ur] \arrow[dr] & & \\ & & \mathrm{K{-}R} + \mathrm{P} & (5.4) \end{tikzcd}$$

Thus, to carry out a catalytic cycle, an interaction between K and R is unavoidable, producing either an intermediate product or a transient K–R state which undergoes a chemical transformation to K–P. Then, the formation of P from K–P (eqns. 5.3 and 5.4) is accompanied by the regeneration of K (Scheme 2), or directly by K–R as a consequence of the replacement of P with the reactant R in K–P (Scheme 3).

It follows that a catalysed process starts after a certain time period (induction period) required for the formation of K in the system and also continues after irradiation has ceased.

An induction period and "post-photochemical" reaction are unique characteristics of photogenerated catalytic processes.

As the catalyst generated by the action of a single photon might promote the transformation of many substrate molecules into the product, photogenerated catalysis may be catalytic in photons.

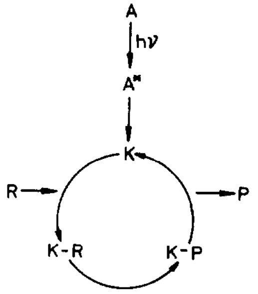

Scheme 2

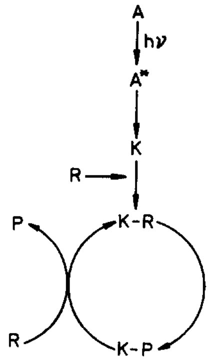

Scheme 3

The overall quantum yield of the generation of product P, Φ_P, can be higher than unity in the course of a photogenerated catalysis.

The observation of an induction period, a "post-photochemical" reaction, with $\Phi_P > 1$, is presumptive evidence for the operation of a purely thermal catalytic cycle. It is important to recognize that a photogenerated catalysis is not necessarily catalytic in photons. However, often the catalyst K undergoes side-reactions that lead to consumption of the catalyst ("poisoning"). Therefore, depending on the initial quantum yield for the formation of the catalyst and the turnover number, i.e., the number of cycles initiated by the catalyst, the overall quantum yield may not necessarily be $\Phi_P > 1$.

An example of photogenerated catalysis is the reaction [412] of the $[Co(en)_3]^{3+}$ ion with the bis(2-hydroxymethyl)dithiocarbamate anion (htc^-) to form the $[Co(htc)_3]$ complex; this reaction takes place in the course of photolysis by radiation of wavelength $\lambda_{irr} = 451$ nm. The photogenerated catalyst is the $[Co(en)_3]^{2+}$ ion:

$$\{[Co(en)_3]^{3+}, htc^-\} \xrightarrow{h\nu} [Co(en)_3]^{2+} + htc^\bullet \qquad (5.5)$$

which permits the formation of $[Co(htc)_3]^-$ in a thermal catalytic cycle, and subsequently even the formation of the $[Co(htc)_3]$ complex:

$$[Co(en)_3]^{2+} + 3htc^- \rightarrow [Co(htc)_3]^- + 3en \qquad (5.6)$$

$$[Co(htc)_3]^- + [Co(en)_3]^{3+} \rightarrow [Co(htc)_3] + [Co(en)_3]^{2+} \qquad (5.7)$$

restoring simultaneously the catalytically active $[Co(en)_3]^{2+}$.

The catalyst K can be represented by a complex (mostly coordinationally unsaturated, formed in situ in the system), reactive ions or radicals.

The term *catalysed photolysis* (frequently called photoassisted reaction) is a sequence of processes in which the catalyst K permits photoexcitation of the reactant R followed by its chemical transformation into the product P:

$$\mathrm{K} + \mathrm{R} \rightarrow \mathrm{KR} \tag{5.8}$$

$$\mathrm{KR} \xrightarrow{h\nu} \begin{array}{ll} \nearrow \mathrm{KR}^* & (5.9)\\ \searrow \mathrm{KR}^* \longrightarrow \mathrm{R}^* + \mathrm{K} & (5.10)\end{array}$$

$$\mathrm{KR}^* \rightarrow \mathrm{P} + \mathrm{K} \tag{5.11}$$

$$\mathrm{R}^* \rightarrow \mathrm{P} \tag{5.12}$$

The catalyst K in this instance is sometimes also called a photoassistor [406] or pseudo-catalyst [411].

In contrast to photogenerated catalysis, the catalyst K is not formed in the photochemical step, but in the course of each cycle its interaction (or, depending on the behaviour of K, its coordination) with R must necessarily take place, resulting with simultaneous irradiation in the formation of the excited state R* (eqn. 5.10, Scheme 4) or KR* (eqn. 5.9, Scheme 5). The product P is formed in the process of chemical deactivation of the excited R* and KR* states; the catalyst K is regenerated either simultaneously with this process (eqn. 5.11) or in the process of the production of R* (eqn. 5.10).

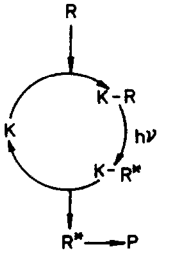

Scheme 4

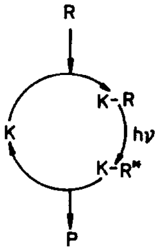

Scheme 5

It follows from the mechanism that the quantum yield of the product formation must be $\Phi_P \geqslant 1$; interruption of irradiation also stops the catalysed photolysis. The already mentioned characteristics (post-photochemical effect, value of Φ_P) can be used to distinguish between photogenerated catalysis and catalysed photolysis.

A typical example of catalysed photolysis is the valence photoisomerization [413] of norbornadiene (NBD) to quadricyclene (Q′) catalysed by Cu(I) halides.

The first step of the reaction mechanism is the production of the π-complex of ClCu–NBD, characterized by an intense band with absorption in the UV region up to 350 nm (NBD itself absorbs radiation at $\lambda \leqslant 270$ nm). Photoexcitation of the π-complex ($\lambda_{irr} = 313$ nm, solvent $CHCl_3$ or EtOH) results in the formation of Q′ with a conversion of 90%. It has been found that using 1 mole of CuCl it is possible to produce more than 200 moles of Q′. The possibilities of the practical utilization of Q′ formation from NBD are discussed in Section 5.2.

The preconditions for catalysed photolysis are sufficient stability of the K–R adduct in the ground state (and the lowest stability in the excited state) and different spectral properties of the K–R adduct and R and K themselves (K–R should absorb in the region where K and R do not absorb). Catalysts used are mainly compounds of transition element with low oxidation states Cr(O), Cu(I), Rh(I), etc., and the reactants include various olefins. The systematically studied reactions are particularly isomerizations and hydrogenations.

In addition to these reactions, many other examples of photoassisted reactions (redox in nature) are known. The importance of some of them (e.g., photooxidations or photooxygenations of organic substrates in the presence of coordination compounds) was recognized and therefore considerable attention has been paid to this class of phototransformations [414–416], and their classification. The formation of the chloro radical (evidenced by pulsed-laser flash photolysis [42, 199, 417] and the spin-trapping technique [418, 419]) and Cu(I) during photolysis of an acetonitrile solution of chlorocopper(II) complexes [41, 420] in the region of their lowest spin-allowed charge-transfer excited state led to the suggestion of a photoassisted catalytic reaction of the Cu(II)–Cu(I) redox cycle [199]. Such a cycle would render possible the oxidation of an organic substrate, e.g., aliphatic alcohols [421] or phenols [422–424]. The photoassisted oxidation of alcohols was also observed in the presence of V(III) complexes [425] (with simultaneous production of hydrogen), of the Wilkinson complex $[Rh(PPh_3)_3Cl]$ [426], of the macrocyclic [Co(III)TPPS] complex [427] and of chromic acid esters [428], etc. The photoassistor present in the above systems is usually restored by O_2 oxidation (aerobic conditions) [422, 423, 427, 428].

The only recently defined term of a *catalysed photoreaction* [403, 406] (differing in its meaning from the discussed catalysed photolysis or photoassisted reaction) involves the reaction of a catalyst with a molecule of substrate in the excited state to form a product; light is absorbed by the substrate R, and activation of the catalyst K is not necessary.

$$R \xrightarrow{h\nu} R^* \tag{5.13}$$

$$R^* \xrightarrow{[K]} P \tag{5.14}$$

Catalysed photoreactions have been discussed in detail [403, 429] recently.

The first step of *sensitized photochemical reactions* (also called photosensitized reactions) is photoexcitation of the catalyst K:

$$K \xrightarrow{h\nu} K^* \tag{5.15}$$

The next step is either the formation of an exciplex:

$$K^* + R \rightarrow (K\text{–}R)^* \tag{5.16}$$

or energy transfer from K* to a particle of reactant R:

$$K^* + R \rightarrow K + R^* \tag{5.17}$$

Sometimes K* may transfer its energy to R by an electron transfer:

$$K^* + R \rightarrow K^+ + R^- \tag{5.18}$$

$$K^* + R \rightarrow K^- + R^+ \tag{5.19}$$

The reaction product is formed by decay of the exciplex (eqn. 5.20, Scheme 6), or by deactivation of $R^*(R^+, R^-)$ (eqn. 5.21, Scheme 7)

$$(K\text{–}R)^* \rightarrow P + K \tag{5.20}$$

$$R^*(R^+, R^-) \rightarrow P \tag{5.21}$$

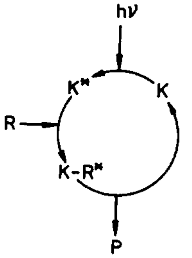

Scheme 6

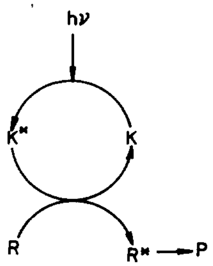

Scheme 7

It results from the mechanism of sensitized photochemical reactions that the quantum yield of the product must be $\Phi_P \leqslant 1$. When K functions in this way, it is usually called a sensitizer.

During the study of the isomerization NBD → Q′, if the $[Cu(BH_4)(PPh_3)_2]$ complex is used as a catalyst with light of wavelength 313 nm, it has been found [430] that the photoexcited $[Cu(BH_4)(PPh_3)_2]^*$ also reacts both by the formation of an exciplex with NBD:

$$[Cu(BH_4)(PPh_3)_2]^* + NBD \rightarrow [Cu(BH_4)(PPh_3)_2(NBD)]^* \tag{5.22}$$

and by energy transfer with formation of the triplet IL state of NBD*:

$$[Cu(BH_4)(PPh_3)_2]^* + NBD \rightarrow [Cu(BH_4)(PPh_3)_2] + NBD^* \qquad (5.23)$$

The exciplex and NBD* are deactivated, producing quadricyclene, Q′.

The conditions for exciplex formation and energy transfer were discussed in Sections 2.4 and 3.4. The sensitized photochemical reactions take place when the catalyst K and reactant R do not form an adduct in the ground state and the excitation radiation is not absorbed by the reactant but mostly by the catalyst. A priori it is assumed that the excited catalyst does not undergo decomposition reactions.

Some authors [431] also differentiate the term "sensitizer" and others [403] exclude it entirely from the category of catalysts. For example, in conjunction with a study of the chemiluminescence of systems including coordination compounds, the term photosensitizer has been suggested [431, 432] for a substance that photosensitizes the light absorption (*light absorption sensitizer*; LAS); substances that function as mediators of the conversion of chemical energy into light energy (*chemiluminescence inducer*; CLI) are called *light emission sensitizers* (LES).

All of the hitherto mentioned mechanisms involved absorption of one photon in the catalytic cycle, and were tested using homogeneous systems. It should be mentioned that the range of possibilities of reactions catalysed in the presence of light radiation is more extensive, and examples are known that include absorption of two photons in the catalytic cycle (e.g., some [9] photoisomerization and photohydrogenation reactions of alkenes taking place in the presence of $M(CO)_6$, where $M = Cr$, Mo and W) and processes in heterogeneous systems [433] (photolysis of water in the presence of substances of a semiconductor type, or systems containing colloidal platinum and $[Ru(bpy)_3]^{2+}$ ions).

One of the essential differences between thermally catalysed processes (where the conversion of $R \rightarrow P$ requires $\Delta G < 0$) and photocatalysed reactions is the possibility of the formation of products with a higher energy content than that of the reactants. Thus, the energy of an absorbed photon is used not only to overcome the energy barrier of the catalysed reaction, but also to satisfy the thermodynamic conditions of the reaction.

Of the practical advantages of photocatalysed reactions, one could also mention their lower (compared with thermal reactions) energy demands, which is particularly due to the fact that the energy need not be supplied to the whole system but only to a certain part, the frequently high selectivity of reactions and the possibility (e.g., by directing the light energy input) of optimizing the conversion of the reactants to products.

Based on the above and on some recent knowledge (e.g., [434] relationships between the symmetry of coordination of a metal ion and the photocatalytic activity that can be obtained by photoluminescence measurements), one can expect that interest in the study of photocatalytic systems will be intensified in the future.

5.2 Solar energy conversion and storage

The gradual exhaustion of world reserves of fossile fuels and the increase in their prices in the early 1970s prompted worldwide research to develop alternative sources of energy, including processes of guided nuclear synthesis and nuclear fission and also solar energy. The exploitation of solar energy is an especially attractive trend as this resource is infinitely abundant, environmentally clean and embargo-proof. This research has been directed towards obtaining storable, pollution-free chemical and electrical energy from sunshine at an economically acceptable cost. However, because of the diffuseness (low power per unit area) and intermittent availability of solar radiation, some methods of storage must be provided so that energy can be stored when there is a plentiful supply until the time when demand exceeds supply.

The focus on the study of the possibilities of solar energy utilization [435–440] resulted from several facts. It is energy with a continuous supply, the quantity of which (approximately 2×10^{24} J of solar energy fall on the Earth annually) markedly exceeds the energy demands of mankind (3×10^{20} J per year). From the ecological viewpoint it is the "purest" energy. A stimulating factor is also the utilization and conversion of solar energy into chemical energy with a relatively high conversion (ca 6%) in biosystems.

Energy storage by means of photosynthesis in green plants has been carried out for millions of years; carbon dioxide and water are converted photochemically to oxygen and combustible carbohydrates. Based on this fact, scientists focused their attention on photochemical, photoelectrochemical, photovoltaic and photobiological solar energy conversion. The aim of photochemists was to propose and implement an artificial (e.g., non-biological) cycle that would enable a storable fuel to be produced from readily available and inexpensive raw materials. This required really multidisciplinary approach involving photochemistry, photophysics, theoretical chemistry, photobiology, solid-state physics, synthetic chemistry, polymer chemistry, colloid chemistry, electrochemistry, biophysics and cell biology. The great interest in obtaining solutions in research into artificial photosynthesis problems is illustrated by a number of review papers [441–453].

Owing to the considerable attention paid to the study of the possibilities of solar energy utilization [454] some solar technologies have been successfully developed. According to the opinion of specialists in the United Nations Economics Commission for Europe [455], the proportion of new and renewable sources in the total energy consumption within the sphere of the Commission should increase to 15–17% in 2000 (in 1978 it was 8.9%). Here (in 2000) water energy participates to the greatest extent (5.2%) whereas solar energy participates with 1.5% (360–720 milliard kWh).

However, there also are various disadvantages of solar energy utilization (too high dilution, changes in the intensivity of radiation during night and day and during the seasons). Wider possibilities of the solar energy utilization have been discussed in several books [436, 438, 456, 457]. Of the wide range of potential means of solar energy utilization, this chapter will deal with those in which the active components are coordination compounds. This involves systems in which solar energy is converted into chemical or electrical energy [436–438, 458–460].

In fact, the conversion of solar energy to chemical energy takes place during each endoergonic photochemical reaction. If the products of such a reaction are kinetically stable, storable, transportable and then convertible into new or original compounds with a simultaneous release of energy, they can be considered to be potential fuels.

In the process of a hypothetical "photochemical energy storage cycle" (Fig. 21) product P is formed within the primary photochemical process from the photoreactive excited state R* of the reactant, coupled with a total change in

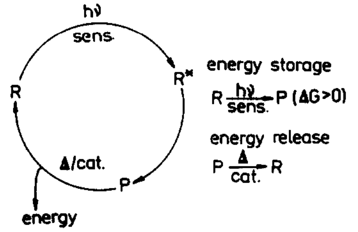

Fig. 21. Scheme of photochemical solar energy conversion and storage cycle (sens. = sensitizer, Δ = heat, cat. = catalyst).

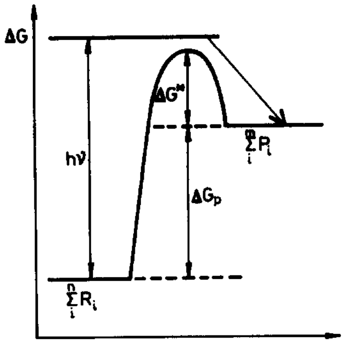

Fig. 22. Conversion of solar energy to chemical energy during photochemical conversion of reactants R_i to the products P_i; ΔG_P is accumulated energy in the products of the photochemical reaction; ΔG^* is activation Gibbs energy of the reverse reaction P → R.

free energy ΔG. Provided that a photosensitizer is present in the system, the light need not be absorbed directly by the reactant(s).

If the energy E_{exc} represents the absorbed photon energy then $\Delta G/E_{exc}$ represents the proportion of it that was converted and stored in the form of chemical energy (Fig. 22) in product P (higher compared with the ground state of the reactant R). In the reverse reaction of P to R, it is necessary to overcome the kinetic barrier $\Delta G^{\neq}$ (by increasing the temperature or adding a suitable catalyst), this energy being released in the form of heat or electricity. Hence it is possible to implement almost infinite solar energy storage within a cyclic process as schematically shown in Fig. 23.

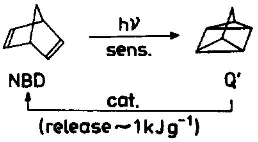

Fig. 23. System for solar energy storage employing reversible valence photoisomerization of NBD to Q′ (sens. = sensitizer, cat. = catalyst).

The practical realization of photochemical energy-storage cycles (Fig. 21) is conditioned by the spectral, thermodynamic and kinetic properties of the components of the systems being studied, and also by economic factors, and in general, it must satisfy the following criteria [461]:

(a) A photochemical reaction must be endoergonic ($\Delta G > 0$) with a high quantum yield.

(b) To have a cyclic process, no side-reactions resulting in the destruction of a reactant(s), product(s), sensitizer or catalyst are to occur in the system (or only to a minimum extent).

(c) A photochemical reaction should take place within the broadest region of the solar radiation spectrum; the reactants should absorb the greatest possible amount of impinging solar radiation and the absorption by photoproducts should be minimal.

(d) The amount of stored energy relative to unit weight or volume of the photoproduct formed should be as high as possible.

(e) The initial reactants and other components of the system should be readily available, cheap and non-toxic.

(f) Overall handling with the system must be simple and the products of photochemical reaction should be easy to store and transport.

(g) The reverse exothermic reaction R ← P accompanied by release of stored energy at room temperature should be extremely slow, however, under certain conditions (e.g., addition of a suitable catalyst or heating) it should be fast, specific, controllable and with a high efficiency.

As shown by Bolton [462] for an ideal system in which all photons with energy $\geqslant E_{exc}$ are absorbed and the product P is formed with unit quantum yield, the maximum achievable efficiency of the conversion of solar energy to chemical energy can be approximately 32%. Considering thermodynamic and kinetic limitations of a real system, it has been found that it is not likely that the maximum conversion efficiency would exceed 12–13%. In this connection, it is interesting that the efficiency of the conversion of photosynthesis (so far the only known really working process that satisfies almost all of the above requirements) is only about 5–6% under controllable laboratory conditions.

The systems that include coordination compounds and that were studied in connection with the storage and conversion of solar energy to chemical energy can be classified into photoisomerization and photoredox according to the type of photochemical reactions utilized.

The first type is based on a photochemical change of R to high-energy product P in the process of an endoergonic photoisomerization reaction. The photoredox reaction that has attracted the greatest attention in recent years, is the photosensitized decomposition of water into H_2 and O_2, which is interesting from chemical (artificial photosynthesis), biological (biomimetic systems) and economic points of view (potential fuel source).

It has been shown that most photochemical reactions of coordination compounds of transition elements are not suitable for the purposes of solar energy conversion (very low ΔG, low quantum yields, side-reactions, etc.).

The most promising are photoisomerization reactions of coordinated ligands involving also the valence photoisomerization of norbornadiene (NBD) to a quadricyclene (Q′), which has been the most often studied [413, 436, 461, 463, 464].

Most of the criteria for an efficiently working system of solar energy storage are satisfied by the isomerization of NBD to Q′. In 1 mole of quadricyclene as a high-energy NBD isomer, 92 kJ of energy are accumulated [465], which is less than that for the products of redox photoreactions. On the other hand, the practical advantage of this system is that the energy barrier of the reversible thermal reaction Q′ → NBD is relatively high, and under normal conditions quadricyclene is stable.

The disadvantage of the zero absorption of NBD in the visible region of the spectrum was partially solved using organic sensitizers or complexes, particularly based on Cu(I), which shift the absorption of the system above 300 nm.

Although the quantum yield of sensitization is high, the total efficiency of the system is markedly reduced because under these circumstances only a small proportion of impinging solar energy is absorbed. Of the Cu(I) compounds, simple CuX salts provided positive results ($X = Cl, Br, I, C_2H_3O_2$).

The most important step in the reaction mechanism is the formation of a photoreactive XCu–NBD complex; an analogous mechanism is that of the reaction of the $[CuHB(pz)_3]CO$ complex.

Another type of reaction mechanism is observed during the sensitized photoisomerization of NBD to Q′, in which copper(I) complexes with ligands of the triphenylphosphane type, e.g., $[Cu(BH_4)(PPh_3)_2]$, $[Cu(BH_4)(PPh_2Me)_3]$ and $[Cu(BH_4)(diphos)]$, are used as sensitizers (for details of both mechanisms see Section 5.1), or Ir(III) complexes, e.g., $[Ir(bpy)_2(bpy')OH]^{2+}$ and $[Ir(bpy)_2(bpy')OH_2]^{3+}$, where bpy′ denotes a monodentate coordinated molecule of the bpy ligand. Ir(III) complexes [466] in comparison with Cu(I) compounds are considered to be markedly more attractive because, in addition to the comparably high sensitizing efficiency they absorb a larger amount of visible radiation and can easily be anchored on the surface of a heterogeneous, transparent and chemically inert surface, which is of great importance particularly from the practical viewpoint.

The observed novel behaviour during the valence isomerization of Q′ to NBD in the presence of $PdCl_2(\eta^4\text{-NBD})$ [467, 468] was attributed to the operation of a redox-chain mechanism involving the formation of the quadricyclene radical Q^+ and its rapid rearrangement to NBD^+; such a reaction (generation of a thermally active catalyst as a result of the photoinduced electron transfer) can be classified as photogenerated catalysis (true photocatalysis).

Solving the problem of the reversible reaction of Q′ to NBD with the release of stored energy in the form of heat, catalysts were sought that would permit a prompt and specific conversion of Q′ to NBD.

Of a number of complexes studied [469], the most suitable seemed to be, e.g., dithiolene complexes of the type $[(CF_3)_2C_2S_2]_3M$ where M = Mo, W, Ni, square-planar complexes of Rh(I) $[Rh(CO)_2Cl]_2$, $[Rh(dien)Cl]_2$ and other Rh(I) complexes with ligands of the PPh_3, $acac^-$, Cp^- type and their derivatives or NiL_2, where $L = 1{,}5\text{-}C_8H_{12}$ or $CH_2 = CHCN$ and triphenylcyclopropenylnickel complexes $(Ph)_3C_3Ni(CO)X$, where X = Cl, Br. However, because of their undesirable solubility, side-reactions, low efficiency or too high air sensitivity, these complexes were not used in real systems. The square-planar cobalt(II) complexes with ligands of the porphyrine type and its derivatives seem to be more promising; their palladium(II) analogues show significantly poorer properties.

However, it has been found [470] that Cu(I) complexes can catalyse isomerization reactions even on irradiation with visible light ($\lambda > 390$ nm). The first example of Cu(I) photocatalysis efficient under visible-light irradiation is the system $[Cu(CH_3CN)_4]^+$–biL (where biL = bpy, phen, 2,9- or 4,7-dimethyl-1,10-phenanthroline or dpphen), utilized in *trans-cis* photoizomerization of stilbene [470]. In the course of the reaction a high conversion of *trans-* to *cis*-stylbene takes place, and solar energy is stored (approximately 45 kJ mol^{-1}).

Other examples of *cis-trans* photoisomerizations have been published, e.g., with coordinated stilbene [471] or azo compounds [472] as ligands. However, no viable energy-storage cycles based on such isomerizations have been proposed so far.

In spite of the fact that several of the requirements for solar energy-storage systems were satisfied by the NBD–Q′ system [465, 473] (availability, non-toxicity, acceptable cost, easy storability and transportability of the products, etc.), there are still some problems that are to be solved. These include particularly the low absorption of the system in the region above 450 nm, which enables only few percent of the solar energy reaching the Earth to be utilized. A solution may lie in the use of substituted NBD compounds which absorb irradiation even above 500 nm, or triplet sensitizers (complexes or organic sensitizers [474]). However, no practical realization of solar energy storage in a cyclic process based on the chemical transformation NBD → Q′ → NBD has yet been reported.

The above systems can be characterized as models whose most important contribution is to the theory necessary for the realization of systems for the practical utilization of the conversion and accumulation of solar energy in the future.

Another possibility of solar energy storage and conversion, in addition to the above photoisomerization reaction, is provided by photoredox reactions.

The processes of photoinduced electron transfer [453, 475–478] belong to the most efficient means of converting solar energy into chemical energy. It has been found that by electron transfer to a long-lived reduced molecule, almost all of the energy of the excited state can be utilized. A concrete system, the thermodynamics of which are illustrated in Fig. 24, must consist of a donor and an acceptor (D, A), between which photoinduced electron transfer involving an excite state *D (or *A) takes place, providing energetically rich substances D^+ and A^- (or D^- and A^+).

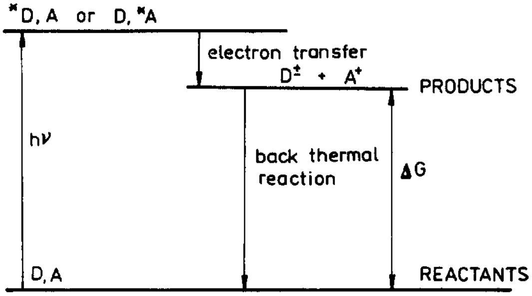

Fig. 24. Conversion of solar energy to chemical energy by excited-state electron transfer.

The most serious problem for the realization of the conversion of solar energy into chemical energy is to prevent the thermal reaction of back electron transfer, which should be slow enough so that the high energy content of D^+, A^- or D^-, A^+ can be utilized. It has been shown experimentally that a back electron transfer between the products of the primary photochemical process frequently takes place with a rate constant equal or close to the diffusion-controlled limit.

There are several ways of preventing the back reaction, but their application to concrete system usually leads to a loss of energy, thus lowering the efficiency of the overall energy conversion. One of the possibilities is the separation of photoproducts by removing one of them from the reaction medium (gas, precipitant) using membranes or adsorption. The back reaction can be suppressed by adding to the reaction system a scavenger that reacts with one of the photoproducts in a very fast thermal reaction to form the reactant again.

Using organized microenvironments [479–481], such as micelles [482–487], charged colloids [488–491], microemulsions [492, 493] (Fig. 25) and vesicles [448, 494–496] the rate of the reversible reactions was successfully reduced by even more than 10^3-fold. Relative progress has been achieved by application of multiphase systems, such as monolayers, lipid bilayers and polyelectrolytes.

From a practical viewpoint the conversion (and storage) of solar energy that would enable cheap and readily available raw material to be transformed into

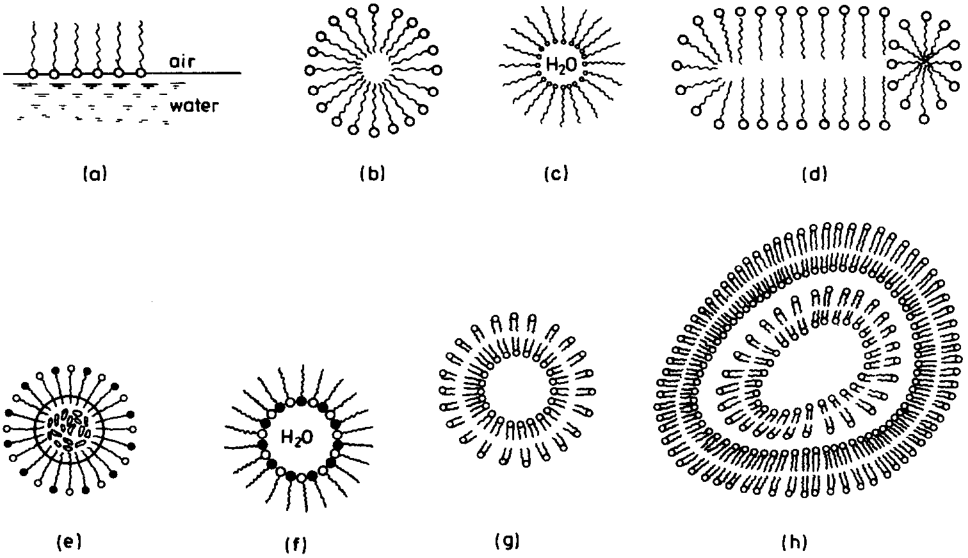

Fig. 25. Structural features of some of the organized assemblies employed in the photochemistry of coordination compounds. (a) monolayer, (b) spherical micelle, (c) reversed micelle, (d) rod-like micelle, (e) microemulsion (oil-in-water), (f) microemulsion (water-in-oil), (g) single compartment vesicle, (h) multicompartment vesicle:

0	surfactant,	○∿∿∿∿○	cosurfactant,
●∿∿∿	simple functional,	○∿∿∿	hydrocarbon.

fuel is of particular interest. Taking into consideration the economic, ecological and energetic criteria, the most attractive raw materials are water, carbon dioxide and nitrogen. Using endoergonic processes requiring an energy of ca 1.2 eV, it is possible to obtain from them excellent fuels, such as hydrogen, methanol and ammonia. Although the visible-light energy of solar radiation (3.1 eV > $Nh\nu$ > 1.6 eV) in fact suppresses such a conversion, the transformation of water, CO_2 and N_2 by direct photochemical means is impossible as these substances do not absorb visible radiation. For example, for the reaction of the formation of H_2 and O_2 from water (eqn. 5.24), an energy corresponding to radiation with a wavelength of $\lambda \leqslant 1000$ nm ($Nh\nu \geqslant 1.23$ eV) should be sufficient, but absorption by water is only possible above 6.5 eV (190 nm).

$$1/2H_2O(l) \xrightarrow{h\nu} 1/2H_2(g) + 1/2O_2(g), \quad \Delta G = +1.23\,\text{eV} \tag{5.24}$$

However, the photochemical redox decomposition of water into H_2 and O_2 can be performed by using, e.g., coordination compounds of transition elements as sensitizers whose redox properties in the excited state permit the reduction (eqn. 5.25) and oxidation (eqn. 5.26) of water from consideration of thermodynamics:

$$2e^- + 2H_2O \rightleftharpoons 2OH^- + H_2, \quad E^0 = -0.41\,\text{V} \tag{5.25}$$

$$2H_2O \rightleftharpoons 4H^+ + O_2 + 4e^-, \quad E^0 = +0.82\,\text{V} \tag{5.26}$$

The values of the reduction potentials (E^0) of the half-reactions 5.25 and 5.26 refer to pH 7 and a pressure of 101.325 kPa as a standard state for gases.

It is complicated to carry out a multielectron transfer ($2e^-$ for H_2 and $4e^-$ for O_2) by means of single-electron redox changes (considered with respect to one absorbed photon) of the complexes of transition elements so as to avoid the production of undesirable high-energy radical intermediates. This obstacle can be eliminated by using a catalyst (charge-storage catalyst) that mediates the required multielectron transfer also in the case of splitting of water by photons of relatively low energy.

As the result of initial research on the possibilities of the photoredox decomposition of water, several systems including complexes of ions (with Ce^{3+}, Fe^{2+} or Mo_2^{4+} as the central atoms) whose photooxidized form permitted the generation of O_2 or H_2 have been published [461]. These systems, although of interest as model systems, were of little importance from the practical viewpoint, as they required high-energy radiation (UV region) and they showed low quantum yields in the production of H_2 and O_2 and simultaneous absorption of radiation by the products of photochemical reactions. The number of analogously functioning complex compounds has been extended in recent years, overcoming some of the above shortcomings [e.g., increase in Φ_{H_2} almost to a value of unity for Cu(I) complexes]. However, they did not find practical application possibilities as it was necessary to overcome the problem of their incorporation into the cyclic photosensitized splitting of water.

The photosensitized decomposition of water in a cyclic process that consists in a bimolecular photoinduced electron transfer between the sensitizer S* (in its excited state) and the reactant R (in its ground state) is the basis of another approach that has been intensively studied in recent years. As illustrated in Fig. 26, the light-induced electron transfer between S* and R (relay) resulted in the production of energetically rich substances S^+ and R^-; the reduction properties of R^- are employed in the reduction of H_2O to H_2 (catalysed by catalyst K_2), and S^+ oxidizes H_2O to O_2 (the oxidation being catalysed by K_1).

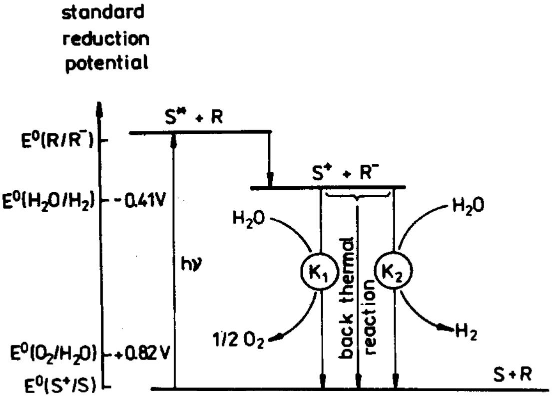

Fig. 26. Photosensitized splitting of water in a cyclic process based on photoinduced electron transfer. K_2 and K_1 denote the catalysts of reduction and oxidation of H_2O to H_2 and O_2, respectively.

Although from the viewpoint of the concepts involved, this is the simplest photochemical water-splitting system, its realization encounters various difficulties. In addition to the above requirements for the photoelectron-transfer reaction (efficient forward and hindered back reaction) for the photosensitizer (S) and relay (R), a number of other kinetic, thermodynamic, spectroscopic and excited-state requirements should be satisfied.

The photon-absorbing substance (the photosensitizer S) is a chemical species that induces the electron-transfer reaction between two substrate species; S must be involved in excitation and redox processes without being consumed. As the relay, R, is involved only in the ground-state redox process, there must be many more requirements for an ideal photosensitizer, S, than for the relay, R.

An ideal photosensitizer should be [497]:

— a complex of a transition metal (in order to ensure the presence of a redox site at a suitable potential) of the second or third transition row which should not have the MC lowest excited state (with an extremely short lifetime);

- a complex with easily reducible ligands in order to have the lowest MLCT excited state; this ensures a long lifetime, small S–T energy gap, high efficiency (η_{isc}), intense absorption bands at low energy and a favourable electronic factor for oxidative quenching (see below);
- photochemically and thermally stable (influenced by the selection of ligands).

There are many known examples of coordination compounds [461] as sensitizers which show these spectral and redox properties (although not always completely satisfactory properties, especially for application to solar energy conversion); in addition to the most thoroughly investigated and employed complex [543, 544] of $[Ru(bpy)_3]^{2+}$ (for its redox properties in the ground and excited states, see Section 2.5), there are $[Ru(bpz)_3]^{2+}$ [545], polypyridine complexes [546–553] of Ru(II), Rh(III), Os(II) and Cr(III), porphyrinate [554] phthalocyaninate and quinolinate complexes of some transition metals [497] and polynuclear complexes [555, 556] of Mo, Re and Rh. It should be noted [497] that of the hundreds of polypyridine Ru(II) complexes prepared in the last few years, none is a substantially better photosensitizer than the "classical" $[Ru(bpy)_3]^{2+}$.

However, photoreduction of water, as shown in Fig. 26, requires the presence of an electron donor, D, in addition to the sensitizer (sacrificial electron donor) for reoxidation of S^+ (and hence its recovery), a renewable electron acceptor, R, capable of reduction (electron relay) and a redox catalyst, K_2 (eqn. 5.27); examples are shown in Fig. 27.

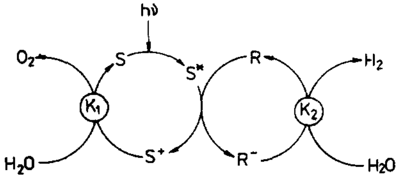

Fig. 27. System for photochemical reduction of H_2O to H_2. $S = [Ru(bpy)_3]^{2+}$, $[Zn(TMPy)]^{4+}$; D = TEOA, EDTA; R = MV^{2+}, Eu^{3+}, V^{3+} and their salicylate complexes; $[Ru(bpy)_3]^{3+}$, macrocyclic complexes of cobalt; K_2 = colloidal Pt, TEOA = triethanolamine; EDTA = ethylenediaminetetraacetic acid; MV^{2+} = methylviologen; 4,4′-dimethylpyridine.

$$2R^- + 2H_2O \xrightarrow[(2e^-\ \text{reduction})]{K_2} 2R + 2OH^- + H_2\uparrow \qquad (5.27)$$

Efforts to employ substances that absorb solar radiation within the widest possible spectral (visible) region resulted in an intensive study of the photochemical and photophysical properties of complexes with ligands of aromatic character (2,2′-bipyridine, 1,10-phenanthroline and their derivates, porphyrins, phthalocyanines), the greatest attention being paid to $[Ru(bpy)_3]^{2+}$. This complex ion [447, 453, 478] absorbs radiation in the UV and visible regions of the spectrum up to 520 nm; the energy content of its MLCT thexi state is 205 kJ mol^{-1}.

Comparison of the redox potentials of the pairs $E^0(Ru)/(Ru(I)) = +0.84$ V, $E^0(Ru(III)/(Ru(II)) = -0.86$ V (the composition of the coordination sphere is not presented for the sake of clarity) and $E^0(H_3O^+/H_2) = -0.41$ V, $E^0(O_2/H_2O) = +0.84$ V (at pH 7) indicates that the excited complex is able to decompose water [449, 478] into H_2 and O_2:

$$4{*}Ru(II) + 4H_3O^+ \rightarrow 4Ru(III) + 2H_2\uparrow, \quad \Delta G = -173 \text{ kJ} \tag{5.28}$$

$$4{*}Ru(II) + 6H_2O \rightarrow 4Ru(I) + O_2\uparrow + H_2O, \quad \Delta G = -77 \text{ kJ} \tag{5.29}$$

with a maximum achievable energy accumulation of 31.25 kJ/$Nh\nu$.

The amount of accumulated energy in the products of a photoredox process can be even higher, depending on the reaction partners. Thus, for example [498], in the reaction

$$2{*}Ru(II) + PQ^{2+} + DMA \rightarrow Ru(III) + Ru(I) + PQ^+ + DMA^+ \tag{5.30}$$

where PQ^{2+} is a paraquate dication, it is theoretically possible to accumulate energy up to 185 kJ/$Nh\nu$ in the reaction products. If a cyclic function of the system is required, the amount of accumulated energy will be lower owing to the recovery of the catalyst by the reaction

$$Ru(III) + Ru(I) \rightarrow 2Ru(II) \tag{5.31}$$

In homogeneous systems almost no accumulation of energy takes place as the excited particles are deactivated by other routes than the electron transfer resulting in a product, or reaction product are transformed to the reactants of photochemical processes in ground state through very fast reversible processes.

These disadvantages of a kinetic character (relatively low energy barrier of the spontaneous reaction of high-energy product to low-energy reactants) (Fig. 22) can be eliminated in two ways [461]. The first consists in adding a compound to the system that reacts with one of the products of the photoredox process [e.g., EDTA or TEOA, which reacts with Ru(III), thus preventing its recombination with Ru(I)]. In the second method the rate of the reversible reaction is suppressed using multiphase systems such as lipidic bilayers [499–501] and polyelectrolytes or other organized molecular assemblies [502].

The surface potentials on micelles form a barrier against recombination reactions (ca 150 mV). It should be noted that the redox reactions taking place in the process of photosynthesis are also determined by potentials on membranes of photosynthetic organelles.

Similarly, an ideal relay must [497]:

- be a thermally stable (using a single multidentate cage-type ligand the photochemical ligand dissociation reactions should also be avoided) complex of a transition metal of the second or third transition row with reversible redox and good kinetic properties whose lowest excited state should not be a metal-centred state in nature;
- involve ligands in the molecule that are difficult to oxidize or to reduce in order to avoid interferences in the redox process, light absorption by low-lying CT excited states and quenching via energy transfer.

Some transition metal complexes, e.g., $[Rh(bpy)_3]^{3+}$ [503], $[Co(bpy)_3]^{2+}$ [504] or viologens (Fig. 28) [453, 505], have been used as relays with some success. It should be noted that the most popular relay, MV^{2+}, is an expensive and very toxic substance that can hardly be used for large-scale applications. More promising seems to be a use of cage-type complexes, e.g., sepulchrates, $[M(sep)]^{3+}$ (M = Co, Cr) [506], catenands of macrocyclic phenanthroline derivates [507], cryptands (Fig. 29) containing bpy and phen [508] or carcerands [514]. One can expect in the future great developments in the field of such cage complexes (and their photochemistry and photophysics), or more generally, in the class of supermolecular structures (complexes of complexes, i.e., supercomplexes [509–512]) within the so-called concave or host-guest chemistry [513].

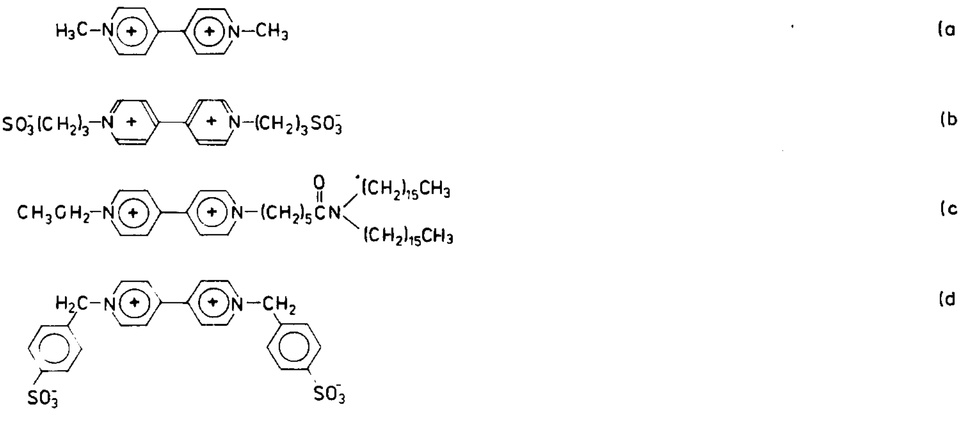

Fig. 28. Viologen electron relays. (a) methylviologen (MV^{2+} = *N,N'*-dimethyl-4,4'-bipyridinium), (b) zwitterionic propylviologen sulphonate, (c) amphiphilic viologen containing two hexadecyl groups, (d) dibenzylmethylviologen sulphonate.

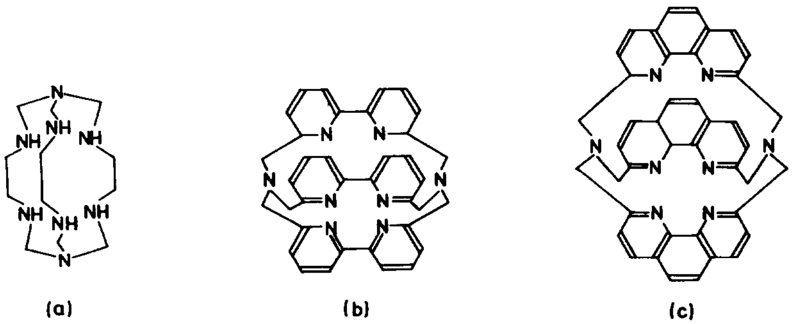

Fig. 29. Macrocyclic ligands: (a) sepulchrate; (b) containing 2,2′-bipyridine; (c) containing 1,10-phenanthroline.

Similarly, for the photooxidation of water (eqn. 5.32) S^* must interact with an electron acceptor R, which is decomposed in the process of photoreduction, and a redox catalyst K_1, which in the presence of a sacrificial electron acceptor A permits the oxidation of water to O_2 by a sufficiently strong oxidant S^+; concrete examples are given in Fig. 30.

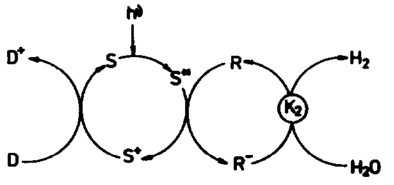

Fig. 30. System of photochemical oxidation of H_2O to O_2. $S = [Ru(bpy)_3]^{2+}$, $[Fe(bpy)_3]^{2+}$; $R = [Co(NH_3)_5Cl]^{2+}$, Tl^{3+}, Ag^+; $K_2 = RuO_2$ suspension.

$$4S^+ + 2H_2O \xrightarrow[(4e^-\ \text{oxidation})]{K_1} 4S + 4H^+ + O_2\uparrow \qquad (5.32)$$

A more than 12-fold increase in the total O_2 yield in micellar solutions of sodium dodecylsulphate has been observed [515] in comparison with the same but homogeneous solution containing $[Ru(bpy)_3]^{2+}$, the catalyst $CoCl_2$ and an irreversible electron acceptor $[Co(NH_3)_5Cl]^{2+}$ or $S_2O_8^{2-}$.

From the knowledge and experience acquired by research on the systems shown in Figs. 27 and 30, Grätzel [449] succeeded in performing a complete closed cyclic splitting of water with visible light using a double-functional redox catalyst (Fig. 31).

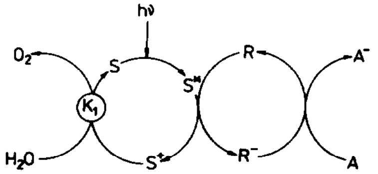

Fig. 31. System of cyclic photochemical splitting of H_2O to H_2 and O_2. S = $[Ru(bpy)_3]^{2+}$; R = MV^{2+} [449]. K_1 = K_2 used as a double functional catalyst in the form of TiO_2 doped with RuO_2 and colloidal Pt.

Another interesting complete water splitting system has been reported to work [516] using $[Ru(bpy)_3]^{2+}$ in combination with Prussian Blue colloids functioning as a coupling element (electron pool) of the oxidative and reductive half-reactions of photochemical water splitting. Other more promising examples of electron pools constructed with aligned viologen units on molecular assemblies have also been suggested [517].

The visible light irradiation of a mixed colloidal system prepared from sepiolite-$[Ru(bpy)_3]^{2+}$–RuO_2 composite particles and $Al_xEu_{1-x}(OH)_3$ gels leads to the oscillatory evolution of hydrogen and oxygen in the presence [518] or absence [519] of a platinum catalyst.

The highly efficient photochemical reduction of water was observed fairly recently [520] also in system based on energy transfer (and not electron transfer) from excited $*[Ru(bpy)_3]^{2+}$ to Ac^- (anthracene acceptor). As effective electron transfer from $*[Cu(dpp)_2]^+$ is less efficient than energy transfer, besides a classical electron acceptor such as C_3-$bipy^{2+}$ (*N*,*N*′-propylene-2,2′-bipyridinium), an additional realy Ac^- (anthracene 9-carboxylate) was used in another system for

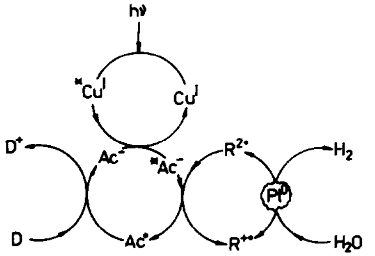

Fig. 32. Photochemical reduction of water via energy-transfer sensitizer Cu^I = $[Cu(dpp)_2]^+$, where dpp = 2,9-diphenyl-1,10-phenanthroline; energy-electron relay Ac^- (anthracene-9-carboxylate); electron acceptor R (C_3-bpy = *N*, *N*′-propylene-2,2′-bipyridinium)

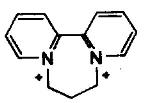

C_3-bpy^{2+}

Sacrificial electron donor D (TEOA = 2,2′,2,2″-triethanolamine). Pt^0 = catalyst for hydrogen formation (TiO_2-supported platinum).

the production of hydrogen from water [521] based on energy transfer (Fig. 32).

The triplet excited state of anthracene-9-carboxylate $*(A^{\bullet}C^{-} = {}^{T}AC^{-})$ populated by energy transfer from $[Cu(dpp)_2]^+$ is further able to transfer an electron to the acceptor R ($R = C_3\text{-bipy}^{2+}$). Titanium dioxide-supported platinum is used as a catalyst for the formation of hydrogen [522] from water and $C_3\text{-bipy}^+$.

Thus, the condition for obtaining an efficient system for the photoreduction of water based on energy transfer (still fairly rare) is the presence of both AC^- (energy-electron relay) and a sensitizer $[Cu(dpp)_2]^+$ (highly rigid and encaging complex). The Cu(I) sensitizer plays the role of an antenna able to collect low-energy photons prior to the formation of an active, long-lived triplet excited state of AC^-. The photoactive substance is therefore not involved in any redox process as in the natural photosynthetic apparatus.

The expense of complexes that sensitize water photolysis and other processes of high-energy product formation and other required components of the systems (colloidal Pt, colloidal RuO_2, complexes of Ru, Os, Pt, etc.), the insufficiently efficient conversion of solar to chemical energy and its accumulation in the form of the products of redox reactions are the main reasons why the above types of systems have not been used to a wider extent.

The conversion of solar to electrical energy [523, 524] takes place in photogalvanic or photovoltaic cells. In the former instance, radiation is absorbed by some of the particles in the solution, which is itself in an excited state, or products of its reactions induce a change in the potentials of electrodes, which results in a flow of electric current between electrodes.

As an example of a photogalvanic cell in which not only current is induced, but also solar energy is converted into chemical energy, a system is presented [525] in which the cathodic area comprises a Pt electrode and the anodic area a Pt electrode ("sponge platinum"), $[Ru(bpy)_3]^{2+}$, PQ^{2+} and TEAO. Both parts are connected through a salt bridge and the electrodes by a conductor. The photoexcitation of $[Ru(bpy)_3]^{2+}$ with a subsequent reaction with PQ^{2+}:

$$*[Ru(bpy)_3]^{2+} + PQ^{2+} \rightarrow [Ru(bpy)_3]^{3+} + PQ^{+} \tag{5.33}$$

and irreversible redox decomposition of TEAO:

$$[Ru(bpy)_3]^{3+} + \text{TEAO} \rightarrow [Ru(bpy)_3]^{2+} + \text{products of TEAO oxidation} \tag{5.34}$$

results in the oxidation of PQ^+ in the anodic area:

$$PQ^{+} - e^{-} \xrightarrow[\text{anode}]{} PQ^{2+} \tag{5.35}$$

The electron deficiency on the anode is compensated by the current flow to the anode from the cathode where hydrogen is released:

$$2H_3O^+ + 2e^- \xrightarrow[\text{cathode}]{} H_2\uparrow + 2H_2O \tag{5.36}$$

Irradiation of this cell with light at 436 nm resulted in a current flow of intensity of 2×10^{-4} A. Identical conditions of irradiation [526] ($\lambda = 436$ nm) resulted in the system $[Ru(bpy)_3]^{2+}$, $[Co(C_2O_4)_3]^{3-}$–platinum electrode, generating O_2 on the anode and a current of 9×10^{-5} A.

Another means of solar energy conversion published in [527] consists in photodissociation of the CO ligand from an iron complex; an irradiated electrode of a photogalvanic cell coated with a porphyrinate complex of iron in the presence of an excess of imidazole and CO was used, the photogenerated voltage being ca 200 mV.

According to current opinion, photovoltaic cells are more promising for the conversion of solar energy into electrical energy; in these cells radiation is absorbed by a solid material with semiconductor properties [524, 528], serving as one of the electrodes. In an ideal case, the semiconductor should not undergo corrosion and the width of the forbidden band should be approximately 1.3 eV (most of the semiconductors used have a greater width of the forbidden band, and therefore they absorb radiation mostly in the UV region).

As a simple illustrative example [529] of a photovoltaic cell one can use a cell with a semiconductor anode of n-$GaAs_{0.7}P_{0.3}$, and Pt cathode, acetonitrile as a solvent and ferrocene ($FeCp_2$). By photoexcitation of the material of the anode a "hole" is formed and the electron enters the conductive band. The positive "hole", h_+, is occupied by an electron in the reaction with $FeCp_2$, forming the $FeCp_2^+$ cation; in the reaction between the cation and the electron of the cathode ferrocene is again produced. The consequence of photoexcitation and the cycle

$$FeCp_2 \overset{-e^-}{\rightleftarrows} FeCp_2^+ \tag{5.37}$$

is a current flow through the conductor connecting anode and cathode between which a voltage of $E = 0.75$ V is generated. Similarly to the photogalvanic cell, also in the photovoltaic cell conversion of solar to chemical energy can take place.

In spite of the fact that under the model conditions conversion of solar to electrical energy [530] occurs (or electrical + chemical) with an efficiency of about 12%, the study of the possibilities of such a conversion has been of a basic research character so far, as the characteristics of the cells studied (spectral properties of semiconductors, their price and stability, or other factors) allow them to be considered as promising but currently non-profitable.

It is probable that intensive study [531–533] of the conversion of solar to electrical and chemical energy will also continue in the future, and emphasis on the synthesis of suitable materials (semiconductors, catalysts) is expected, in addition to the technological management of the processes. Although most work from the viewpoint of the photochemical preparation of fuels [530] has been devoted to the photosensitized decomposition of water into hydrogen and oxygen, other processes for the formation of high-energy products are also promising [534].

Currently, the most attractive process is the preparation of high-energy fuels that can be obtained from water and atmospheric gases, which are readily available, cheep and in almost inexhaustible supply. The amounts of energy accumulated in 1 mole of reduced material are listed in Table 19 for some processes with readily available reactants.

TABLE 19

Photochemical synthesis of fuel	ΔG (kJ mol^{-1})
$H_2O(l) + 1/2O_2(g) \xrightarrow{h\nu} H_2O_2(l)$	120.0
$CO_2(g) \xrightarrow{h\nu} CO(g) + 1/2O_2(g)$	256.0
$H_2O(l) \xrightarrow{h\nu} H_2(g) + 1/2O_2(g)$	237.4
$N_2(g) + 3H_2O(l) \xrightarrow{h\nu} 2NH_3(g) + 3/2O_2(g)$	339.5
$CO_2(g) + 2H_2O \xrightarrow{h\nu} CH_3OH(l) + 3/2O_2(g)$	700.0
$N_2(g) + 2H_2O(l) \xrightarrow{h\nu} N_2H_4(l) + O_2(g)$	759.2
$CO_2(g) + 2H_2O(l) \xrightarrow{h\nu} CH_4(g) + 2O_2(g)$	818.7
$2CO_2(g) + 3H_2O(l) \xrightarrow{h\nu} C_2H_5OH(l) + 3O_2(g)$	1332.8

Reactions that give products with a high energy content (hydrogen, hydrogen peroxide, ammonia, carbon oxide, methanol, ethanol, methane and hydrazine) also satisfy the thermodynamic criteria for high efficiency under the action of solar light [462, 500, 535]. It should be noted that many such processes are known to occur in vivo via photosynthesis (with subsequent fermentation of the resulting products to H_2, CH_4 or alcohols), or via atmospheric-nitrogen fixation. However, outside living organisms, these processes do not occur under the action of solar radiation.

Reduction of CO_2 to carbon monoxide [536, 542], formate [537, 538] and organic acids [539] has been reported, using homogeneous catalysts [536, 537], semiconductor particles [538] or artificially enzyme-catalysed coupled systems [539]. The cyclic photocatalysed visible light reduction of CO_2 to methane using $[Ru(bpz)_3]^{2+}$ as a sensitizer, a Ru metal colloid as catalyst and TEOA as electron donor has been reported recently [540]. The photoinduced reduction of CO_2 to CO has also been observed during photolysis at 436 nm in the system TEOA–DMF–$ReBr(CO)_3(bpy)$ with a CO quantum yield formation of 0.15 [541].

5.3 Photochemical synthesis of coordination compounds

In recent decades, the photochemistry of coordination compounds has been studied very extensively, and the amount of new experimental data is growing unceasingly. Much work has been directed to the investigation of the thermodynamics, kinetics and mechanisms of the photoreactions of complexes.

In addition to theoretical studies, many investigations were stimulated by increasing interest in the practical exploitation of the knowledge obtained in the field of photochemistry of coordination compounds. Papers dealing with photocatalytic processes [400, 401, 405, 406], biochemical aspects [541–556] of the photochemistry of complexes [557, 558], analytical use of photochemical processes [559, 560], separation of isotopes using lasers [561, 562], application of coordination compounds as photostabilizers [563], etc., can serve as examples.

Although photochemistry has been used for a long time in the preparation of organic compounds [564–566], only in the last few years greater attention has been paid to the use of photochemistry for the synthesis of transition metal complexes. Processes by which complexes (photoreaction products) were separated from irradiated systems and characterized by physicochemical and analytical methods frequently followed from studies of key problems in chemistry, e.g., fixation and reactivity of coordinated molecular nitrogen, conversion of solar energy to chemical and electrical energy and the preparation of compounds with catalytic properties.

No comprehensive paper summarizing all data published on the photochemical preparation of coordination compounds has been published. The only attempt to demonstrate the possibilities of photochemistry as a means for the synthesis of coordination compounds was a conference contribution [567]. Since a new chemical species is the product of each photochemical reaction, this chapter includes, for practical reasons, the photochemical synthesis of only those complexes that have been isolated as pure substances from the reaction mixture, and were satisfactorily characterized. Hence this section gathers all available data from the relevant field with the aim to show both the present status and the prospects for the utilization of photochemistry in the preparation of coordination compounds. The photochemical synthesis of organometallic compounds is beyond the scope of this section; aspects of organometallic photochemistry (including photochemical synthesis) were published in another book [9].

This section summarizes all available data published in the area of the photochemical synthesis of coordination compounds. In agreement with the commonly used classification in inorganic or coordination chemistry, the data are arranged according to the position of the central atoms of the complexes in the Periodic Table.

All data obtainable from the original publications that are useful for the photochemical preparation of complexes (source of radiation, time of irradiation, solvent used, yield of product, etc.) are gathered in Table 20. The composition and the stereochemistry of the complex prepared were, in almost all instances, determined after their isolation from irradiated systems using elemental analysis, various spectral methods (IR, NMR, UV and visible spectra) and in some instances also by means of single-crystal X-ray analysis. In some cases, when the photochemically prepared complexes are also obtainable by thermal reactions, a comparison of the properties of photochemically and thermally prepared compounds was used to identify the former products. There are but few examples where the photosynthesis was not carried out in the solution of a reactant; these are noted in the table.

The possibilities of photochemistry serving as a synthetic method are illustrated by the preparation of more than 250 complexes separated from irradiated systems and then characterized. It can be assumed that in the future photochemical preparations will be performed on a much more wider scale than up to date.

Most synthetic studies (and those in the field of the photochemistry of coordination compounds generally) were performed in solutions; only exceptionally was the solid phase or surface properties employed. The original preparative method, utilized by Benda and Hájek [269], suggests that there are also other possibilities of an experimental arrangement to that usually used.

Mainly Hg lamps were employed as radiation sources, but the use of visible light (sunlight) should also have wide potential. The use of unfiltered light or sunlight increases the energetic efficiency of syntheses, but it hinders the identification of the relationships between the type of excited states and the photochemical reactivity of complexes.

With respect to the amounts of prepared complexes, the yields obtained are rarely given in the literature; mostly they do not exceed a few grams. This was mainly due to improperly performed experiments (from the viewpoint of preparation), irradiation of millimole amounts of the starting complex, use of cells without exploitation of all the light emitted by a source of light, etc.

Systematic studies of the photochemical preparation of coordination compounds has so far been focused only on complexes of a few central atoms (Pd, Pt, U), or with a few ligands (N_2, H^-, phosphanes), and the possibilities of photochemical syntheses of coordination compounds have not been applied at all to complexes of the elements of Groups II, III, IV and V of the Periodic Table, though several organometallics of these elements have been prepared in this way.

In the near future there is likely to be a wider application of photochemistry as a method of preparation of coordination compounds, particularly based on a more effective use of the theoretical knowledge of photochemistry and on selectivity determined by attaining certain excited states. No doubt, the develop-

TABLE 20

Starting system	Product, yield	Conditions	Ref.
Λ-$[Cr(en)_3]Cl_3$	Δ-$[Cr(en)_3]Cl_3$ $\Phi = 0.015$	Solvent H_2O; sunlight, $\lambda_{irr} > 400$ nm; temp. 30°C; $t_{irr} < 1$ h	[260]
$Cr(CO)_6$ + Hacac	$[Cr(acac)_3]$, 80%	Solvent CCl_4; 250-W sunlamp; atmosphere of Ar; t_{irr} = few hours	[568]
$[Cr(acac)_3]$ + HL L = (*S*)-alanine; (*S*)-valine; (*S*)-phenylalanine	$[Cr(acac)_2L]$, 2 stereoisomers for each L isolated $\Phi \approx 10^{-2}$;	Solvent H_2O–CH_3OH–NaOH; RPR-3500 lamp; $t_{irr} = 12$ h	[569]
$[Cr(salen)N_3] . H_2O$	$[Cr^V(salen)N] . H_2O$	Solvent butanol; high-pressure Hg lamp, [Cr^V identified by EPR]	[195]
$Mo(CO)_6$ + Hacac $W(CO)_6$ + Hacac	$[Mo(acac)_3]$, 95% $[WO_2(OH)(acac)_2]$, 84%	Solvent diisopropyl ketone, or C_6H_6 250-W sunlamp; atmosphere of Ar; t_{irr} = few hours	[568]
$M_4[M'(CN)_8]$ M = K for M′ = Mo and W M = Na for M′ = Mo	$M_4[M'O_2(CN)_4] . nH_2O$ $n = 6$ or 8 70–90%; a few grams	Solvent H_2O; 450-W Hg lamp, $\lambda_{irr} >$ 300 nm; t_{irr} = few hours	[570]
$K_4[Mo(CN)_8] . 2H_2O$	$K_3[MoO(OH)(CN)_4] . H_2O$ $K_4[Mo(O)_2(CN)_4] . 8H_2O$ tens of grams	Solvent H_2O–NH_3 for hydroxo complex, H_2O–NH_3–KOH for dioxo complex; 100-W Hg lamp; $t_{irr} = 12$–24 h	[571]
$K_4[Mo(CN)_8]$	$K_6[Mo^{IV}_2Mo^{VI}(CN)_8O_6] . 2H_2O$ (diamagnetic)	Solvent H_2O; atmosphere of O_2; medium-pressure Hg lamp, $\lambda_{irr} = 340$–430 nm; temp. 10°C	[572]
$H_4[Mo(CN)_8]$ + $AgNO_3$	$Ag_3[Mo(CN)_7H_2O]$	Solvent H_2O; Hg lamp, $\lambda_{irr} = 340$–430 nm; temp. 0°C; atmosphere of Ar	(573]
$H_4[Mo(CN)_8]$ $K_4[Mo(CN)_7(OH)]$ $H_3[Mo(CN)_7(H_2O)]$ $K_4[Mo(CN)_8]$	$H_3[Mo(CN)_7H_2O]$ $K_3[MoO(OH)(CN)_4] . 2H_2O$ $H_2[MoO(CN)_6H_2O]$ $K_3[MoO(OH)(CN)_4] . 2H_2O$	Solvent H_2O with various pH; medium-pressure Hg lamp, $\lambda_{irr} = 340$–430 nm; temp. 0°C; atmosphere of N_2	[574]

TABLE 20 (continued)

Starting system	Product, yield	Conditions	Ref.
$K_4[Mo(CN)_8] + NH_3$ or $N_2H_4 + Cd^{2+}$ or Mn^{2+}	$Cd_2[Mo(CN)_8].2NH_3.4H_2O$ $Cd_2[Mo(CN)_8].2N_2H_4.4H_2O$ $Cd_2[Mo(CO)_8(H_2O)_2].nH_2O$ $Mn_2[Mo(CN)_8].2NH_3$	Solvent H_2O–$NH_3(N_2H_4)$; sunlight; deaerated solutions; low temperature	[575, 576]
$K_4[M(CN)_8] + KOH$ M = Mo or W	$K_4[M(CN)_4(OH)_4]$	Solvent H_2O; Hg lamp, or sunlight	[577]
$K_2[Mo(CN)_4(OH)_2(phen)]$ $K_2[W(CN)_4(OH)_2(phen)]$ $K_2[Mo(CN)_4(OH)_2(bpy)]$ $K_2[W(CN)_4(OH)_2(bpy)]$	$[Mo(OH)_3(CN)(phen)_2].2H_2O$ $[W(OH)_3(CN)(phen)_2].2H_2O$ $[Mo(OH)_3(CN)(bpy)_2].3H_2O$ $[W(OH)_3(CN)(bpy)_2].H_2O$ $\Phi \approx 0.80$–8.00×10^{-2} for Mo complexes $\Phi \approx 0.30$–1.10×10^{-2} for W complexes	Aqueous solution, presence of 1,10-phenanthroline and 2,2′-bipyridyl, tungsten filament lamp (Wotan Ultra Vitalux, 300-W), $\lambda_{irr} \approx 370$ nm, $t_{irr} = 4$ h	[578]
$[MH_4L_4] + N_2$ M = Mo or W; L = PPh_3, $PMePh_2$, $PEtPh_2$, PEt_2Ph, $PPrPh_2$ or $PBuPh_2$, 1/2 diphos	*trans*-$[M(N_2)_2L_4]$ 18–91%; $\Phi \approx 10^{-3}$–10^{-1}	Solvent cyclohexane, $\lambda_{irr} = 254$ nm; $t_{irr} = 1$h; $p(N_2) = 1$ atm for Mo compounds, 16 atm for W complexes; temp. 25°C	[579, 580]
$[MoH_4L_4] + N_2$ L = 1/2 diphos, $PMePh_2$	*trans*-$[Mo(N_2)_2L_4]$ 93%	Solvent benzene; 450- or 100-W lamp, $\lambda_{irr} = 350$ or 365 nm; $t_{irr} = 12$ h; temp. 25°C	[581]
$[Mo(N_2)_2(diphos)_2] + CH_3Br$ or + $Bu^nBr + CH_3OH$	$[MoBr(N_2CH_3)(diphos)_2]$ $[MoBr(N_2Bu)(diphos)_2].CH_3OH$ 50–95%	Solvent benzene; 100- or 3 × 150-W lamps; t_{irr} = few hours	[582]
$[M(N_2)_2(diphos)_2] + RBr$ M = Mo or W; R = Me, Et, Pr^n, Pr^i, Bu^t	$[MBr(N_2R)(diphos)_2]$ $[MBr(N_2R_2)(diphos)_2]Br$ $(MBr(N_2HR)(diphos)_2]Br$ 9 complexes prepared in several gram amounts	Solvent benzene; 150-W lamp; $t_{irr} = 4$–12 h	[583, 584]

TABLE 20 (continued)

Starting system	Product, yield	Conditions	Ref.
$[M(N_2)_2(diphos)_2] + C_4H_8O$ M = Mo or W	$[MBr(N_2{=}CH(CH_2)_3)OH(diphos)_2]Br$ structure obtained by single-crystal analysis	Solvent tetrahydrofuran; W lamp	[585]
$[W(N_2)_2(diphos)_2] + CH_2Br_2$	$[WBr(N_2CH_2)(diphos)_2]Br$ 30%, diamagnetic compound	Solvent benzene	[586]
$[Mo(N_2)_2(diphos)_2] + RX$	$[MoX(N_2)(diphos)_2]$ for R = Me and X = Cl, Br; and for R = xylene and X = Br $[MoX(N_2R)(diphos)_2]$ for R = Me and X = Br, I; and for R = cyclohexane and X = I tens of grams	Solvent benzene; $\lambda_{irr} = 366$ nm; $t_{irr} = 18$–40 h; 100-W lamp	[587]
$K_3[W_2Cl_9] + KCN$	$K_5[W(CN)_7].H_2O$ 80%, 0.1 g	Solvent H_2O, deaerated; UV light; $t_{irr} = 8$ h	[588]
$[H_5Re(PMe_2Ph)_2]$	$[H_8Re_2(PMe_2Ph)_4]$	Solvent hexane or isooctane; 550-W medium-pressure Hg lamp or 100-W B100A lamp, $\lambda_{irr} = 366$ nm, or filtered through Pyrex glass; t_{irr} = few hours	[589, 590]
$[ReH_3(diphos)_2] + CO_2$ or $+ N_2$	$[Re(HCOO)(diphos)_2]$ $[ReD(N_2)(diphos)_2]$ 50%	Solvent C_6H_6(C_6D_6 for the deuterido complex); 450-W medium-pressure Hg lamp, $\lambda_{irr} = 366$ nm; atmosphere of CO_2 or N_2; t_{irr} = few hours	[9, 591]
$[ReH_3(diphos)_2]$ $[ReH(N_2)(diphos)_2] + CO_2$	$[Re(C_6H_4PhPC_2H_4PPh_2)(diphos)]$ $[Re(HCOO)(diphos)_2]$		[9]
$Fe(CO)_5 + HL$ HL = acetylacetone; hexafluoroacetylacetone; dibenzoylmethane; 8-hydroxyquinolinate	$[FeL_3]$ 50–95%	Solvent CCl_4 or benzene; 250-W sunlamp; atmosphere of Ar; t_{irr} = few hours	[568]
$[Fe(PF_3)_5] + H_2$ $[FeH_2(PF_3)_4] + C_2H_5SH$ or $+ I_2$	$[FeH_2(PF_3)_4]$ $[(PF_3)_3Fe(\mu\text{-}SC_2H_5)(\mu\text{-}PF_2)Fe(PF_3)_3]$	Solvent ethanol; temp. −20 °C; TQ-150 UV lamp	[218]

TABLE 20 (continued)

Starting system	Product, yield	Conditions	Ref.
$[FeX_2(diphos)_2]$ $X_2 = H_2$, D_2 or HCl	$[(PF_3)_3Fe(\mu\text{-}I)(\mu\text{-}PF_2)Fe(PF_3)_3]$ $[FeH(C_6H_4PhPC_2H_4PPh_2)(diphos)]$	Solvent benzene, toluene or CX_3CN; RPR-3500 lamp or low-pressure Hg lamp; atmosphere of Ar, temp. 5°C	[189, 233]
$[FeH_2(diphos)_2] + CH_3CN$ or $+ CD_3CN$	$[Fe(diphos)_2(CH_3CN)]$ $[Fe(diphos)_2(CD_3CN)]$		
$[Fe(diphos)_2CX_3CN] + CX_3CN$ X = H or D	$[Fe(diphos)_2(C_4X_8N_2)]$		
$[Fe(Et_2dtc)_3] + C_6H_5Cl$	$[FeCl(Et_2dtc)_2]$ 70%	Solvent C_6H_5Cl; 450-W Hg lamp; temp. 30°C	[592]
$[Fe(dbacac)_3]$	$Fe(OH)[(OCOC)(OH)(C_6H_5)]_2$	Solvent benzene; atmosphere of O_2; 250-W Hg lamp; $t_{irr} = 7$ days	[593]
$[Fe_3O(L)_6(H_2O)_3](ClO_4)_7$ L = *L*-proline	$[Fe(L)(OCH_3)(H_2O)_2]_2(ClO_4)_2 \cdot 2CH_3OH$ 20–47%, a few grams	Solvent CH_3OH; $\lambda_{irr} = 300$ or 254 nm; $t_{irr} = 7$ days	[594]
heptamethyl Coα,Coβ-dicyano-cobyrinate	heptamethyl Coα,Coβ-dicyano-5,6-dioxo-5,6-secocobyrinate, 47%; heptamethyl Coα,Coβ-dicyano-14,15-dioxo-14,15-seco-cobyrinate, 25%	Solvent CH_3OH, CH_3OD, CD_3OD; A15 150-W halogen lamp; sensitizer methylene blue, molecular oxygen; $\lambda_{irr} < 550$ nm; $t_{irr} = 90$ min	[225]
hexamethyl Coα,Coβ-dicyano-7-de(carboxymethyl)-7,8-di(dehydro-cobyrinate)	hexamethyl Coα,Coβ-dicyano-5,6-dioxo-7-de(carboxymethyl)-7,8-didehydro-5,6-secocobyrinate 96%	Solvent CCl_4; visible light; presence of molecular oxygen	[226]
vitamin B_{12}	potassium dicyano-5′,6′-dimethyl-benzimidazolyl-5,6-dioxo-5,6-seco-cobamid (10%) and its regioisomer (24%)	Solvent CD_3OD, ACN;sensitizer methylene blue; molecular oxygen; $t = -70$°C; $t_{irr} = 45$ min; 150-W tungsten lamp	[227]
$[Co(EDTA)]^-$	$[Co(HEDTrA)(en)]ClO_4 \cdot 2H_2O$ 40%, 1.5 g $[Co(HEDTrA)(en)]Cl \cdot 3H_2O$ a few grams	Solvent H_2O; DRK-120 Hg lamp; $\lambda_{irr} < 300$ nm; room temperature; acidified by $HClO_4$ or HCl; $t_{irr} = 4$ h	[595]

TABLE 20 (continued)

Starting system	Product, yield	Conditions	Ref.
$[Co(NH_3)_5NO_2]Cl_2$	$[Co(NH_3)_5ONO]Cl_2$ quantitatively	Solid state, starting isomer between 2 glasses; 100-W lamp; $t_{irr} = 6$ h	[596]
$[Co(en)_2(SO_2C_2H_4NH_2)](ClO_4)_2$	$[Co(en)_2(OSOC_2H_4NH_2)](ClO_4)_2$ quantitatively	Solvent H_2O; λ_{irr} 400 nm	[271]
Λ-*cis*-$[Co(en)_2Cl_2]Cl + K_2CO_3$ or + RCONHOK (R = Me, Et, Ph)	*rac*-$[CoCO_3(en)_2]Cl$ + *trans*-$[Co(en)_2Cl_2]Cl$ *rac*-$[Co(en)_2(RCONHO)]Cl_2$	Starting products deposited on silica gel; 400-W Hg lamp, $\lambda_{irr} = 520$–580 nm; $t_{irr} = 3$–10 s	[269]
$[CoL_2(NH_2CH_2COO)](ClO_4)_2$ L = bpy, phen or en	$[CoL_2(CH_2NH_2)](ClO_4)_2$	Solvent H_2O; UV light; temp. 20°C or -77°C; $t_{irr} = 1$ h	[386, 387]
$[CoH(PF_3)_4]$	$[(PF_3)_3Co(\mu\text{-}H)(\mu\text{-}PF_2)Co(PF_3)_3]$	Solvent diethyl ether	[220]
$[CoH(PF_3)_4] + [IrH(PF_3)_4]$	$[(PF_3)_3Co(\mu\text{-}H)(\mu\text{-}PF_2)Ir(PF_3)_3]$		
$[Co(en)_3]Cl_3 + K_4[Fe(CN)_6]$	$Na_2[ClCo(en)_2\text{–}NC\text{–}Fe(CN)_5]\cdot 5H_2O$ 50%	Solvent aq. NaCl; 1000-W Hg-Xe lamp, $\lambda_{irr} = 436$ nm; or laser with $\lambda_{irr} = 457.9$, 514.5, 647.1 nm; temp. 25°C	[597]
$[CoL](ClO_4) + [Ru(CN)_6]^{4-}$ L = imidazolylbis(histidinato) anion	$Zn_3[LCo\text{–}NC\text{–}Ru(CN)_5]_2$	Solvent aq. of Zn^{2+} salt; 15-W lamp or Ar-laser, $\lambda_{irr} = 514.5$ nm; temp. 25°C	[598]
trans-$[CoL(H_2O)_2](ClO_4)_3$ L = Me_4[14]tetraeneN$_4$	*trans*-$[CoLCl_2](ClO_4)$ 58%	Solvent H_2O; Xe lamp, $\lambda_{irr} = 254$, 265, 313 or 365 nm; deaerated solutions; pH < 7	[599]
$[Co(NH_3)_5(CH_3COO)](ClO_4)_2$ $[CoL](ClO_4)_2$ L = [14]aneN$_4$ or 4,11-[14]dieneN$_4$	$[CoL(H_2O)(CH_3)](ClO_4)_2$ 50%	Solvent 0.1 M $HClO_4$; low-pressure Hg lamp; atmosphere of N_2	[600]
$[Co(sep)](BPh_4)_3$	$[Co(sep)](BPh_4)_2$	Solvent tetrahydrofuran; deaerated solutions; laser 448.0 or 514.5 nm; room temperature	[601]

TABLE 20 (continued)

Starting system	Product, yield	Conditions	Ref.
$[Co(CN)_2(ceb)] + O_2$	$[Co(CN)_2(5,6\text{-dioxocob})]$ $[Co(CN)_2(14,15\text{-dioxocob})]$ 47% and 25%	Solvent CH_3OH; sensitizer methylene blue; 150-W halogen lamp, $\lambda_{irr} = 550$ nm; atmosphere of O_2	[225]
$[Co(EDTeP)]^-$	$[Co(H_2O)(EDTrP)]$	Solvent H_2O; $\lambda_{irr} = 260$ nm	[602]
$[Ni[14]aneN_4](ClO_4)_2$	$[Ni_2(dehydrobis)[14]aneN_4]\ (ClO_4)_4$ 3%	Solvent CH_3CN; sensitizer benzophenone; $\lambda_{irr} = 360$ nm	[603]
$[Ru(bpy)_3]X_2$, X = NCS, Br, Cl, I, NO_2, N_3^-, CN^-, 1/2 malonate	$[Ru(bpy)_2X_2]$ 15–35%	Solvent C_2H_5OH; 100- or 500-W Hg lamp, or 150-W Xe lamp; atmosphere of N_2; t_{irr} = few hours	[604–606]
$[Ru(bpy)_3](IO_3)_2$	$[Ru(bpy)_2I_2]$	Solvent C_2H_5OH; 500-W Hg lamp; $t_{irr} = 4$ h; atmosphere of N_2	[606]
$[Ru(bpy)_3](NCSe)_2$	$[Ru(bpy)_2(N_3)_2]$		
$[Ru(bpy)_2(NO)Cl](PF_6)_2$	$[Ru(bpy)_2(CH_3CN)Cl](PF_6)_2$ 82%, 0.1 g	Solvent CH_3CN; RPR-3000 lamp; atmosphere of O_2; $t_{irr} = 1$ h	[607]
cis-$[Ru(bpy)_2(H_2O)_2](ClO_4)_2$	*trans*-$[Ru(bpy)_2(H_2O)_2](ClO_4)_2$	Solvent H_2O; 250-W sunlamp; $t_{irr} = 90$ min	[268]
$[Ru(bpy)_2(py)_2](PF_6)_2 + L^-$ L = NO_3, NO_2, NCS, Cl and $p\text{-}CH_3C_6H_4SO_3$ for X = PF_6^-; L = ClO_4 for X = ClO_4^-;	$[Ru(bpy)_2(py)L]X$	Solvent CH_2Cl_2; 275-W GE lamp, light filtered through Pyrex; $t_{irr} = 10$–200 min	[608]
$[Ru(bpy)_2(py)_2](PF_6)_2 + H_2O$	$[Ru(bpy)_2(py)(H_2O)](PF_6)_2.H_2O$		
$[Ru(bpy)_2(py)_2](PF_6)_2 + Br^-$	$[Ru(bpy)_2Br_2].2H_2O$		
$[Ru(bpy)_2(CH_3CN)_2](PF_6)_2 + NCS^-$	$[Ru(bpy)_2(NCS)_2].H_2O$		
$[Ru(bpy)_2(Bupy)_2](PF_6)_2 + CF_3COO^-$	$[Ru(bpy)_2(Bupy)(CF_3COO)](PF_6)_2$ 70–80%		
$K_4[Ru(CN)_6].3H_2O$ + 2,2′-bipyridine	$K_2[Ru(bpy)(CN)_4]$ yellow precipitate, 30%	Solvent methanol/water (1:3); 254-nm immersion lamp; $t_{irr} = 16$ h	[609]

TABLE 20 (continued)

Starting system	Product, yield	Conditions	Ref.
$[Ru(N_3)Cl(das)_2] + O_2$	$[Ru(NO_2)Cl(das)_2]$ 50%	Solvent CH_2Cl_2; fluorescent tube; $t_{irr} = 10\,h$	[610]
$[Ru(R_2dtc)_3] + R'Cl$ R = Me, Et; $R' = CH_2Cl, CHCl_2$	$[Ru(R_2dtc)_3Cl]$ α-$Ru_2(R_2dtc)_5Cl$	Solvent CH_2Cl_2; $CHCl_3$; Hanovia Hg lamp, $\lambda_{irr} = 265\,nm$	[611]
$[Rh(en)_2(NO_2)_2]X + O_2$ $X = Cl, NO_3$	$[Rh(en)_2(NO_2)O_2]X$		[612]
cis- and *trans*- $[Rh(en)_2(NO_2)X]^+$ $X = NO_2^-, Cl^-$ or ONO^-	$[Rh(en)_2(H_2O)(O_2)]^{2+}$ $[X(en)_2Rh(O_2)Rh(en)_2X]^{n+}$	Aqueous solution, sunlight or ME/D 250-W medium-pressure mercury lamp, presence of O_2; room temperature	[613]
$[Rh(NH_3)_5N_3](ClO_4)_2 + Cl^-$ $[Ir(NH_3)_5N_3](ClO_4)_2 + Cl^- + Na_2SO_3$	$[Rh(NH_3)_5NH_2OH]Cl_2$ $[Ir(NH_3)_5NH_2SO_3]Cl_2$	Solvent H_2O with pH < 7; 100-W medium-pressure Hg lamp, $\lambda_{irr} > 270\,nm$; $t_{irr} < 1\,h$	[614, 394, 395]
$[M(NH_3)_5N_3](ClO_4)_2 + HCl$ M = Ir or Rh	$[M(NH_3)_5NH_2Cl](ClO_4)_2$ 45–62%		
$[IrH(PF_3)_4]$	$[(PF_3)_4Ir–Ir(PF_3)_4]$ 20%	Solvent diethyl ether; $t_{irr} = 17\,h$	[220]
mer-$[IrX_3(PY)_3]$ X = Cl, Br, I; $Y = Me_3, Et_3, Bu^n_3, Me_2Ph, Et_2Ph, Pr^n_2Ph, Bu^n_2Ph$;	*fac*-$[IrX_3(PY)_3]$	Solvent: C_6H_6, CH_3OH, acetone, H_2O or their mixtures; daylight fluorescent tube; t_{irr} = few hours	[254, 255]
trans-mer-$[IrHX_2L_3]$ $L = PPr^n_2Ph, PBu^n_2Ph$;	*cis-mer*-$[IrHX_2L_3]$		
mer-$[IrCl_3(PEt_3)_3] + KX$ $X = NCO, NCS, N_3$	*fac*-$[IrX_3(PEt_3)_3]$		[254, 255]
mer-$[IrCl_3L_3] + PMe_2Ph$ $L = AsMe_2Ph, PBu^n_3, PEt_3$;	$[IrCl_3L_2(PMe_2Ph)]$ 46–96%		
mer-$[IrCl_3(SEt_2)_3]$	$[IrCl_2(SEt_2)(\mu\text{-}Cl)_2IrCl_2(SEt_2)_2]$ $[IrCl_2(SEt_2)(\mu\text{-}Cl)(\mu\text{-}SEt_2)$ $[IrCl_2(SEt_2)_2]$	Solvent benzene or toulene; 75-W lamp or sunlight	[615]

TABLE 20 (continued)

Starting system	Product, yield	Conditions	Ref.
$[IrH_2Cl(PPh_3)_3]$	$[IrCl(PPh_3)_3]$ $[IrHCl(C_6H_4PPh_2)(PPh_3)_2]$	Solvent C_6H_6 or CH_2Cl_2; 450-W Hg lamp or low-pressure Hg lamp; t_{irr} = few hours	[616]
$[IrH_3(PPh_3)_3]$	$[Ir(C_6H_4PPh_2)(PPh_3)_2]$		
$[IrH_3(PPh_3)_3] + H_2$	$[IrH_5(PPh_3)_2]$		
trans-$[PdCl_2(PPr^n_3)_2]$	*cis*-$[PdCl_2(PPr^n_3)_2]$ $[Pd_2Cl_4(PPr^n_3)_2]$	Solvent CH_3OH; Hanau Q400 Hg lamp, $\lambda_{irr} = 280\,nm$; $t_{irr} = 10\,h$ for dinuclear complex, 2 h for *cis*-isomer	[617, 618]
trans-$[PdCl_2L_2]$ $L = PEt_3, PPr^n_3, PBu^n_3$;	*cis*-$[PdCl_2L_2]$ 70%	Solvent CH_3NO_2; 200 Hg-Xe lamp; temp. 10°C	[619, 620]
$Pd_2(dppm)_2(\mu\text{-}CNPh)Cl_2$ $Pd_2(dppm)_2Cl_2$	mixture of products including $Pd(dppm)Cl_2$	Solvent CH_2Cl_2, 100-W tungsten lamp, $t_{irr} = 0.5–1\,h$	[621]
cis-$[PtX_2(PPh_3)_2]$ X = Cl, Br	*trans*-$[PtX_2(PPh_3)_2]$	Solvent $CHCl_3$; 200-W Hg lamp, $\lambda_{irr} = 366\,nm$; $t_{irr} = 4\,h$	[252]
$[Pt_2(\mu\text{-}P_2O_5H_2)_4]^{4-}$	$[Pt_2\text{-}(\mu\text{-}P_2O_5H_2)_4ArX]^{4-}$ ArX = aryl bromide or iodide	Solvent H_2O, 200-W mercury lamp, fan-cooled Ealing Corp. housing equipped with a Schott (WG 335) sharp cut-off filter	[253]
$[PtMe_2(phen)]$ + isopropyl iodide	$[PtIMe_2\text{-i-}Pr(phen)]$ 100%	Solvent acetone; medium-pressure Hg lamp, $\lambda_{irr} > 420\,nm$; $t_{irr} = 5\,min$	[185]
	a 1:1 mixture of $[PtIMe_2\text{-i-}Pr(phen)]$ and $[PtI_2Me_2(phen)]$	Solvent acetone, 4-methoxyphenol added as radical inhibitor; 150-W high-pressure Xe lamp; $t_{irr} = 5\,min$	
$[Pt_2Me_3(\mu\text{-}dppm)_2]^+$	$[Pt_2Me_2(\mu\text{-}Cl)(\mu\text{-}dppm)_2]^+$ quantitatively	Solvent CH_2Cl_2, irradiated with a Jasco CRM-FA spectroirradiator; $\lambda_{irr} = 362 \pm 7\,nm$	[222]
cis-$[PtCl_2L_2]$ L-py, isoquinoline	*trans*-$[PtCl_2L_2]$ 60–80%		[252]
$[PtL_2CO_3] + L'$	$[PtL_2L'_n]$	Solvent C_2H_5OH; temp. 40 °C	[622]

TABLE 20 (continued)

Starting system	Product, yield	Conditions	Ref.
L = PPh_3, $AsPh_3$, $PMePh_2$ L′ = PPh_3, CO, C_2H_4, PhCCPh $[Pt(PPh_3)_2(C_2O_4)] + PPh_3 + CHCl_3$	$[Pt_2(PPh_3)_4]$ $[Pt(PPh_3)_4]$ *cis*-$[PtCl_2(PPh_3)_2]$ 60%	Solvent C_2H_5OH; 200-W Hg lamp; atmosphere of O_2; $t_{irr} = 25$ h	[623]
cis-$[Pt(NH_3)_2(H_2O)_2]SO_4$ or $[Pt_2(NH_3)_4(OH)_2](ClO_4)_2 + SO_4^{2-}$	$[Pt_2^{II}Pt^{IV}(OH)_6(NH_3)_4]SO_4$	Solvent H_2O; pH 2.5; low-pressure Hg lamp; $t_{irr} = 70$ min	[624, 625]
cis-$[PtCl_2(NH_3)_2]$ *trans*-$[PtCl_2(NH_3)_2]$ $K[PtCl_3(NH_3)]$	$H_2[Pt_4Cl_3(OH)_9(NH_3)_3].H_2O$ complex of Pt^{II}–Pt^{IV} (3:1) in two isomeric forms	Solvent H_2O; Hg UV lamp, $\lambda_{irr} = 250$–300 nm; $t_{irr} = 30$ min (first isomer), 2 months (second isomer)	[626]
$[Pt_2H_3(dppm)_2](PF_6) + CH_3CN$ $[Pt_2H_3(dppm)_2](PF_6) + THF$ $[Pt_2H_2Cl(dppm)_2](PF_6) + THF$	$[Pt_2H(CH_3CN)(dppm)](PF_6)$ $[Pt_2H(THF)(dppm)](PF_6)$ $[Pt_2Cl(THF)(dppm)](PF_6)$ $\Phi = 0.06$–0.62	Solvent CH_3CN (tetrahydrofuran); $\lambda_{irr} = 300$ nm; deaerated solutions	[627]
$[Pt_2H_2(\mu\text{-}H)(\mu\text{-}dppm)_2](PF_6)$ L = py or CH_3CN	$[Pt_2HL(\mu\text{-}dppm)_2](PF_6)$ 100%	Solvent py or CH_3CN; high-pressure Xe lamp; temp. 0°C	[628]
$[Pt(C_5H_9SO_2)_2]$	$[Pt(OH)_2(C_5H_{10}SO_2)_2]$	Solvent H_2O; Hg lamp, filtered through glass	[629, 630]
$[Pt(Thpy)_2]$ $[Pt(Phpy)_2]$ ($Thpy^-$ and $Phpy^-$ are the C-deprotonated forms of 2-(2-thienyl)pyridine and 2-phenylpyridine)	$[Pt(Thpy)_2(CH_2Cl)Cl]$ $[Pt(Thpy)_2(CHCl_2)Cl]$ $[Pt(Phpy)_2(CH_2Cl)Cl]$ $[Pt(Phpy)_2(CHCl_2)Cl]$ quantitatively	Solvent deaerated CH_2Cl_2; medium-pressure Hg lamp, $\lambda_{irr} > 400$ nm; a completely analogous photochemical reaction takes place with $Pt(Thpy)_2$ and $Pt(Phpy)_2$ in $CHCl_3$	[186]
$[UO_2(py)_2(NO_3)_2] + C_2H_5OH$	$[UO_2(py)(C_2H_5OH)(NO_3)_2]$ $[UO_2(NO_3)_2 . NH_2(CH)_4CHO]$	Solvent C_2H_5OH; low-pressure Hg lamp; temp. 25°C; t_{irr}, if short the first complex is the product, if long enough the second complex is produced	[631]

TABLE 20 (continued)

Starting system	Product, yield	Conditions	Ref.
$[(UO_2(py)_2Cl_2] + C_2H_5OH$	$[UOCl_5(py)_2]$ $[U(OC_2H_5)_5]$ a few grams	Solvent C_2H_5OH; Hanau 400-W or Philips 150-W lamp, $\lambda_{irr} = 405$ or 436 nm; $t_{irr} = 10$ h (first product), 50 h (second product)	[632]
$[UO_2Cl_2(py)_2] + C_2H_5OH$ $[UOCl_3 . (py\text{–}HCl)_2] + C_2H_5OH$	$[UOCl_3]$ $[U(OC_2H_5)_5]$	Solvent C_2H_5OH; Hanau Q400 Hg lamp, $\lambda_{irr} = 405$ nm	[633]
$[UO_2(NO_3)_2] + nH_xL$ $L^- = CH_2OHCOO^-$, $CH_3OCH_2COO^-$, $HOOCCOCHCOO^-$, $^-OOCCH_2CNHCH_2COO^-$	$[UL_{4/x}].yH_2O$ $y = 0$ or 2	Solvent H_2O; Hg lamp, $\lambda_{irr} = 436$ nm; t_{irr} = few hours; ligand in excess	[634] [635]
$[UO_2(hfacac)_2].THF$	$[U(hfacac)_4]$	Solvent heptane, isopentane; Hg lamp, $\lambda_{irr} = 360\text{–}450$ nm	[636]
$[Cu(acac)_2] + PPh_3$	$[Cu(acac)(PPh_3)_2]$ 94%	Solvent H_2O, sensitizer benzophenone; 150-W Hanovia lamp; atmosphere of N_2; t_{irr} = few hours	[637]

ment of synthetic photochemical studies will also be stimulated by the possibilities given by photochemistry in solving theoretical problems, especially those relating to the mechanisms of photoreactions. These possibilities were manifested in several cases, as can be seen from the data in Table 20. Thus, the isolation of Cr(salen)N [195], $Rh(NH_3)_5NH_2X$ and $Ir(NH_3)_5NH_2X$ [394, 395, 614] showed the effect of the central atom on the course of the photoreactivity of the coordinated N_3^- ion. The formation of $ReD(N_2)(diphos)_2$ [9, 591] during irradiation of $ReH_3(diphos)_2$ in C_6D_6 contributed to the knowledge of mechanisms of hydrogen abstraction reactions. Mass spectrometric identification of H_2 and D_2 (with no HD) [189, 233] evolved on irradiation of a solution containing $FeH_2(diphos)_2$ and $FeD_2(diphos)_2$, proved the mechanism of non-radical reductive eliminations, based on the results obtained by the investigation of the photochemical properties of some platinum complexes.

The applicability of photochemistry in the synthesis of thermodynamically unstable compounds has been shown by the preparation of Co(III) nitrito [596] and *O*-sulfinato [271] complexes and some *cis* isomers of Pd(II) complexes [619, 620]. Photochemistry provides valuable information concerning the preparation of complexes with coordinated N_2 molecules, and the reactivity of such nitrogen. Many of the cited complexes were only prepared by the photochemical route.

The knowledge obtained on the photochemical preparation of coordination compounds may also be applied to the in situ photochemical generation of complexes with required catalytic properties.

5.4 Application of photochemistry of coordination compounds in the chemistry of polymers

The chemical, physical and mechanical properties of synthetic polymers and their technological processing and utilization depend on the presence in the systems of additives consisting of a monomer or a polymer. One of the groups of compounds that influence not only the production and utilization but also the ecological consequences of the application of polymers are coordination compounds. The knowledge of the photochemical and photophysical properties of coordination compounds is applied in the chemistry of polymers in the three basic directions:

— photoinitiation of the polymerization reactions;
— photostabilization of polymers to oxidation, destruction and the loss of the required properties;
— photodestruction of polymers.

These trends are closely connected with the thermal properties of polymers and their ability to undergo thermochemical changes. Therefore, corresponding thermal processes occurring in polymers containing a coordination compound will also be presented together with the light-driven processes.

Initiation of the radical polymerization of an unsaturated monomer depends on the presence of substances whose reactions result in reactive radicals, usually owing to the addition of thermal or light energy [638]. Such substances are organic compounds (organic peroxides or azo compounds) and coordination compounds.

The initiation of a radical polymerization consists, in general, of two steps. The first is the production of primary radicals as a consequence of decomposition of the initiator and the second is addition of the primary radical to a monomer molecule, thus generating a monomer radical. Radiation can increase the efficiency of the initiator in initiating thermally occurring polymerization, or it can induce polymerization which would not take place thermally under the given conditions. From the viewpoint of photochemical processes, the complex-initiator is applied in the first step of initiation. Usually, the primary radical product is an oxidized ligand $X^{\bullet}$ (for the sake of simplicity the charges of the particles are omitted):

$$[L_mM^{n+}\text{–}X^-] \xrightarrow{h\nu} [L_mM^{(n-1)}] + X^{\bullet} \tag{5.38}$$

One may assume that homolytic splitting of the M–X bond takes place from the LMCT excited state of the complex. The radical $X^{\bullet}$ reacts with the molecule of $R_2C{=}CR_2$ (where R = H, or various functional groups) in the thermal step:

$$X^{\bullet} + R_2C{=}CR_2 \rightarrow XR + R_2C{=}CR^{\bullet} \tag{5.39}$$

Other reactions of the $R_2C{=}CR^{\bullet}$ radical result in polymerization. Depending on the composition of the system, cross-linked polymers, copolymers, etc., can be formed.

Of inorganic compounds, the following were used for the photoinitiation of the polymerization of different monomers (methyl methacrylate, styrene, vinyl acetate, acrylonitrile, acrylamide, etc.): $[Mn(acac)_3]$, $[VO(chin)_2(OCH_3)]$, $[Fe(SCN)_3(py)_3]$, $[Co(NH_3)_5X]Y_2$ (where X = Cl, N_3, NCS; Y = N_3, NO_3), polyamine complexes of Fe(III), complexes of Cu(II) with amino acids (see Table 21) [639–643].

Conversions of a monomer to polymer have reached levels of several tens percent. If a kinetically inert complex or a chelate complex is used as an initiator, the monomer molecules do not enter the coordination sphere of the complex. The rate of polymerization then depends primarily on the intensity of the radiation, I, absorbed by the complex and on the concentration of the complex. An example [641] is the polymerization of methyl methacrylate and styrene in the presence of $[Mn(acac)_3]$, where the rate of polymerization, v, was evaluated as

$$v = k\ [Mn^{III}]^{0.5}\, I^{0.5} \qquad (5.40)$$

The primary photochemical process is an intramolecular redox decomposition:

$${}_{LMCT}^{\ *}[MN^{III}(acac)_3] \xrightarrow{h\nu} [Mn^{II}(acac)_2] + acac^{\bullet} \qquad (5.41)$$

TABLE 21
Radical polymerization initiated by complexes

Monomer	Complex	Radical	Ref.
methyl methacrylate	$[Mn(acac)_3]$	$acac^{\bullet}$	[639]
	$[VO(chin)_2(OCH)_3]$	$CH_3O^{\bullet}$, $\dot{C}H_2OH$	[641]
	$[Fe(SCN)_3(py)_3]$	$SCN^{\bullet}$	[642]
	$[Fe^{III}–NH_2R]^a$	NH_2R, $CCl^{\bullet}_3$	[644]
	$NiCl_2$	$S^{\bullet}$, $MMA^{\bullet a}$	[646]
styrene	$[Mn(acac)_3]$	$acac^{\bullet}$	[639]
	$[Fe(SCN)_3(py)_3]$	$SCN^{\bullet}$	[642]
acrylamide	$[Co(NH_3)_5X]^{2+b}$	$X^{\bullet}$	[643]
	$[CuL_2]^c$	$L^{\bullet}$	[640]
	$[Fe^{III}–HGl]^d$	$Gl^{\bullet}$	[645]
acrylonitrile	$[Fe(SCN)_3(py)_3]$	$SCN^{\bullet}$	[642]
	$[Fe^{III}–HGl]^d$	$Gl^{\bullet}$	[645]

a — NH_2R = triethylenetetraamine; b — X = NCS, N_3, NO_2; c — HL = serine; d — HGl = glucose; e — $S^{\bullet}$, $MMA^{\bullet}$ = radicals of solvent HS and methyl methacrylate.

It has been found that in the initiation step, species other than the primarily originated radicals can also participate. A detailed study [641] of the polymerization of methyl methacrylate photoinitiated by the $[VO(chin)_2(OCH_3)]$ complex has shown that in addition to the radicals $CH_3O^{\bullet}$ produced by the reaction

$$[VO(chin)_2(OCH_3)] \xrightarrow{h\nu} [VO(chin)_2] + CH_3O^{\bullet} \qquad (5.42)$$

$\dot{C}H_2OH$ radicals also occur, as was demonstrated by spin-trapping ESR.

The initiation of polymerization by radicals other than those generated in the first step was observed in the polymerization of methyl methacrylate in the presence of Fe(III) complexes with a non-cyclic saturated tetraamine ligand and CCl_4. Under the effect of UV radiation, a photoredox decay of the excited Fe(III) complex takes place [644]:

$$[Fe^{III}–NH_2R] \xrightarrow{h\nu} Fe^{II} + \overset{+}{N}H_2R \qquad (5.43)$$

The cation-radical $\overset{+}{N}H_2R$ reacts with CCl_4, providing $CCl_3^{\bullet}$ radicals:

$$\overset{+}{N}H_2R + CCl_4 \rightarrow NHCl–R + H^+ + CCl_3^{\bullet} \qquad (5.44)$$

The reaction mechanism involves several substitution and redox steps; the process of polymerization continued after switching off the light.

In the case of an initiator (a kinetically labile complex with monodentate ligands), the monomer can enter the coordination sphere and the rate of polymerization also depends on the monomer concentration. The polymerization of vinyl monomers in the presence of the photoinitiator $[Fe(SCN)_3(py)_3]$ represents [642] such a case. Provided that the intensity of absorbed radiation is constant, the polymerization rate obeys the following kinetic equation:

$$v = k[\mathrm{Fe^{III}}]^{0.5}[\mathrm{monomer}]^{1.5} \qquad (5.45)$$

Polymerization is initiated by the $SCN^{\bullet}$ radical formed by photolysis of the Fe(III) complex containing a molecule of monomer in its coordination sphere.

Participation of a molecule of a monomer in the process of electron transfer was suggested [646] when elucidating the polymerization of methyl methacrylate in the presence of $NiCl_2$. The photochemically reactive state is the triplet excited state of the Ni(II) complex with methyl methacrylate molecules in the coordination sphere. The triplet state was generated from the singlet excited state via intersystem crossing. By interaction of the excited triplet (i.e., biradical species) with a molecule of the hydrogen-atom donor RH (solvent, molecule of methyl methacrylate), the radical $R^{\bullet}$ and also the radical $CH_2=C(CH_3)C^{\bullet}(OH)OCH_3$ are formed. Polymerization is initiated by the radical $R^{\bullet}$.

The objective of the theoretical studies of photoinitiated polymerization is to elucidate the mechanism of the investigated processes, to find the relationships between the composition of the complex and kinetic parameters of polymerization and to optimize the composition of systems and the conditions of polymerization.

The photostabilization of light-sensitive polymers involves retardation or elimination of various photoprocesses that occur during polymer decomposition. Depending on the type of stabilizer and the mechanism that is operative with the given polymer, photostabilization may be achieved in different ways.

A coordination compound as a photostabilizer can be effective in a polymer by the following modes [647]:

(a) The coordination compound itself absorbs or reflects radiation (especially in the UV region), thus lowering the probability of the absorption of radiation by the polymer, its additives (residues of the catalyst, dyestuffs, materials modifying the mechanical properties of the polymer) or the products of the reactions of the polymer and monomer (carbonyls, peroxides). The efficiency of this group of photostabilizers (UV absorbers) depends on high values of the molar absorption coefficients of the complex in the UV region ($\varepsilon > 10^4$ l mol^{-1} cm^{-1}), redox stability of the photoexcited complex and fast internal photophysical deactivation processes of the complex. The UV absorbers are, e.g., bis(2-hydroxyacetophenoneoximato) complexes of Ni(II) and Cu(II), designated $[M(HAOX)_2]$, bis(*N*-n-butylsalicylaldiminato) nickel(II) complex, $[Ni(NBS)_2]$ and bis(3,5-diisopropylsalicylato)nickel(II) complex, $[Ni(DIPS)_2]$.

(b) A coordination compound can act as the acceptor of energy from the excited polymer (its carbonyl groups), or from molecules (singlet dioxygen, $^1O_2$), causing destruction of the polymer or its additives.

From the viewpoint of thermodynamics, energy transfer can take place to the majority of transition metal complexes with low-lying LF excited states. Practical application is conditioned by the highest possible values of the quenching constant, k_q, which for the reaction [647]

$$[Ni(SDT)_2] + {}^1O_2 \xrightarrow{k_q} {}^*[Ni(SDT)_2] + {}^3O_2 \tag{5.46}$$

is $k_q = 2.2 \times 10^{10}\,l\,mol^{-1}\,cm^{-1}$; for an analogous process with the $[Ni(DTP)_2]$ complex, $k_q = 1.7 \times 10^{10}\,l\,mol^{-1}\,cm^{-1}$. With respect to practical utilization, it is of great importance that the complex is deactivated from the excited state via non-redox processes, which is usually fulfilled for the complexes in their LF states (see Section 4.4).

(c) There are more complexes showing photostabilizing properties due to the reaction with radical products of the polymer destruction, thus avoiding the continuation of the destruction process. In such reactions, either non-radical products, e.g. [647] when using $[Co(acac)_3]$,

$$RO_2^{\bullet} + [Co(acac)_3] \rightarrow [Co(acac)_2] + RO_2acac \tag{5.47}$$

or only slightly reactive radicals of the complex ligand are formed [647]:

$$2RO_2^{\bullet} + [Ni(NBS)_2] \rightarrow 2RO_2^- + Ni^{2+} + 2NBS^{\bullet} \tag{5.48}$$

The phenoxy radicals (and also $HAOX^{\bullet}$, $DIPS^{\bullet}$ and similar radicals) are fairly well stabilized by the resonance mechanism and hence they are non-reactive; the RO_2^- anion generated by the transfer of an electron to the reactive $RO_2^{\bullet}$ radical is also non-reactive. Very efficient antioxidants also include dialkyldithiocarbamate complexes of several transition [Ni(II), Fe(III)] and non-transition [Bi(III), Sb(III), Pb(II), Cd(II), Zn(II)] elements [647].

The use of a photostabilizer depends on its properties and also on the properties of the polymer. For the isoprene–styrene copolymer with an average molar weight of $M \approx 100\,000\,g\,mol^{-1}$, compounds of the type $[M^{n+}(S_2C{-}N(R){-}CH_2{-}R)_n]$, where M = Ni(II), Cu(II), Zn(II) and Co(III) and R = 2-thienyl, 2-methoxy-5-ethyl-3-thienyl and 2-benzothienyl, seem to be suitable photostabilizers [648]. On the other hand, the respective Fe(III) complex showed a low photostabilizing effect. Based on experimental results, it was deduced that the efficiency of the photostabilizers depends on the electron density on the central atom, determined by the electron-donor properties of the groups R and R′. The copolymer stabilization is based on the decomposition of hydroperoxides.

There are some polymers that undergo photodestruction although they themselves do not absorb any solar energy. A typical polymer of this type is PVC, which is photodegraded as a result of the light absorption by its additives (residues of polymerization catalysts, carbonyl groups and other impurities), and undergoes photooxidation and photodechlorination. Of the thermo- and photostabilizers of PVC containing a metal atom, Sn(IV) compounds of the type R_2SnX_2 have been used, where R is methyl, n-butyl or n-octyl and X^- are anions of maleic acid or mercaptides [649].

The light-induced degradation of PVC is determined by the processes of photolysis, sensitization phenomena and energy-transfer processes. An important role may be played by singlet oxygen reactions.

The study of the photostabilizing effect has shown that a good photostabilizer must also be a good thermal stabilizer. There are several methods for the enhancement of the photostability of PVC. One method is pigmentation of PVC [649], but it has been found that only those pigments which do not possess sensitizing properties may be used (a good pigment is, for example, rutile TiO_2). Another method is to combine a photostabilizer with an UV absorber. For example, organotin maleate photostabilizers exhibit light stability per se, but the stability can be improved by adding a hydroxyphenylbenzotriazole derivative (UV absorber).

Very efficient stabilizers of PVC also include complexes of Cu(II), Zn(II) Co(II) and Ni(II) with benzol P [2-(2-hydroxy-5-methylphenyl)benzotriazole] [650].

Polyolefins (polyethylene and polypropylene) represent the most widely used family of plastics. Additional applications will undoubtedly arise as further technology is developed in order to obtain a higher resistance to oxidation.

The knowledge of the photochemical and photophysical properties of polyolefins and their additives and impurities can lead to improvements in composition and processing in order to increase their durability and service life. There is a growing consensus that hydroperoxides dominate the photodestruction of polyolefins (polypropylene in particular) during outdoor use. However, some researchers still believe that carbonyl impurities are at least as important as hydroperoxides. As no hydroperoxide groups were detected in photooxidized polyethylene, the conclusion was drawn that for this polymer ketone-group photolysis was responsible for photodestruction. Studies of the photodestruction of polyolefins indicated that the most efficient stabilizers are those which are able to react effectively with hydroperoxides, carbonyl compounds and their reaction products. Photostabilizers that operate solely as excited-state quenchers or UV absorbers do not provide commercially adequate photostability.

Complexes whose photostabilizing effect is based mainly on the quenching of potentially active excited singlet and triplet states of both aliphatic and aromatic carbonyl compounds and polynuclear aromatic hydrocarbons include tris(dibenzoylmethanato) chelates of Fe(III) and Cr(III), nickel oxime chelates and the Ni(II) complex Cyasorb UV 1084 (Fig. 33) [651].

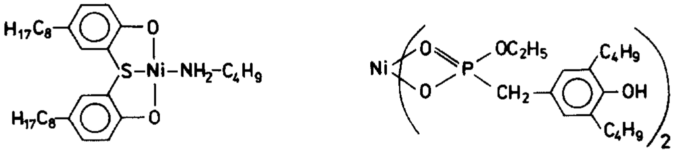
CYASORB UV 1084 IRGASTAB 2002

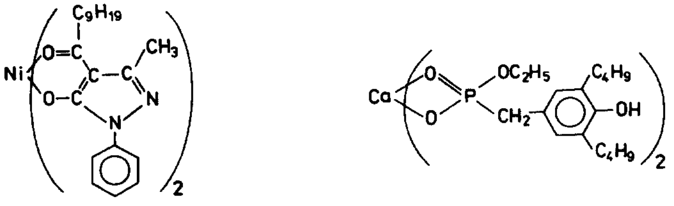
SANDUVOR NPU IRGANOX 1425

Fig. 33. Complexes used as photostabilizers in polymer chemistry.

It was found that variation of the substituent R in Ni(II) oxime chelates produced stabilizers whose quenching efficiency for triplet organic molecules correlated with their photostabilizing effects in polyolefins. Complexes containing sulphur donor ligands, such as Cyasorb UV 1084, have been found to be effective quenchers of singlet dioxygen. The interrelationship between the composition and structure of the complex and its quenching efficiency is not yet understood, however.

The mode of action of complexes is associated almost wholly with their ability to prevent the formation of, or to destroy, hydroperoxides. Peroxide decomposers fall into two categories. The first includes stoichiometric reducing agents, e.g. [652], Ni(II) oxime chelates, and the second type are catalytic hydroperoxide decomposers, which apparently destroy peroxides via the formation of an acidic product in a radical-generating reaction involving the hydroperoxides. A wide variety of sulphur-containing photostabilizers [651–654] [Ni(II) and Zn(II) dithiocarbamates, dithiophosphates, xanthates, mercaptobenzothiazoles, dithiolates] decompose hydroperoxides by a catalytic peroxidolytic mechanism.

As in the photostabilization of PVC, polyethylene and polypropylene photostabilizers are also effective thermal antioxidants. The antioxidant efficiency based on the prevention of hydroperoxide formation with commercially produced Cyasorb UV 1084, Irgastab 2809 and Irganox 1425 (Fig. 33) follows the same order as their light-stabilizing effect in polyolefins [651].

In real systems it is convenient to use stabilizers that function in several of the above modes simultaneously. For example, $[Ni(SDT)_2]$ reacts by energy transfer with $^1O_2$, it functions as a scavenger of reactive radicals, degrades peroxides and absorbs intensively in the UV region. Its application as a polypropylene stabilizer is also advantageous because it is thermally stable up to 280°C. Cyasorb UV 1084 is able [655] to absorb UV radiation, quench carbonyl triplet states and quench singlet oxygen. It can also decompose hydroperoxides and scavenge free radicals.

In conjunction with the solution of ecological problems, the conditions for the catalysis of the thermal and photochemical degradation of polymers have also been studied. It has been found that chelate complexes of several metals at a low concentration in a polymer act as catalysts of the oxidation of polymers and hence of their destruction, whereas at higher concentrations they function as inhibitors of the destruction reactions. Such behaviour has been observed [647] with the bis(phenylsalicyldiaminato)cobalt(II) complex in propylene, $[Fe(HAOX)_3]$ in polyethylene and other systems. Elucidation of this phenomenon is based on the assumption that the reaction of degradation initiation is a first-order and the reaction of degradation termination is a second-order process with respect to the concentration of the complex. Hence its catalytic effect dominates at low concentrations of the complex and its inhibitory effect on destruction at higher concentrations.

Efficient initiators of polymer oxidation are also some $DTC^\bullet$ radicals (dialkyldithiocarbamates) produced by, e.g., the following photochemical redox process [647]:

$$[Fe(DTC)_3] \xrightarrow{h\nu} [Fe(DTC)_2] + DTC^\bullet \tag{5.49}$$

The polymer Vistanex L-140 (polyisobutylene) undergoes a photochemical degradation sensitized by the complex $[Mn(tpican)_3]$ with the $[MnN_3S_3]$ chromophore [656].

Generally valid principles explaining the relationships between the composition and the structure of complexes and their properties applicable to the chemistry of polymers have not yet been found. Further progress in this field can be achieved by the study of the kinetic parameters and reaction mechanisms of the complexes themselves, and their systems with model substances (oxidants, radicals) and polymers.

5.5 Other applications

The results obtained by studies of photochemical reaction mechanisms contributed to a better understanding of the catalytic processes and enabled this knowledge to be used for practical catalyst preparation. They are great prospects but also there is a need to solve many problems in those fields of photochemistry connected with the simulation or the industrial application of some natural bioprocesses (dinitrogen fixation and reduction catalysed by Mo and Fe complexes; photosynthesis [657], systems of photosensitive metalloproteins, etc.). Much research is being directed towards the creation and protection of the environment (e.g., photosmog problems, photodestruction of polymer wastes [658–667]). Many possibilities are offered by photochemistry in the synthesis of very difficult to prepare or even thermally non-preparable organic [401, 402, 404–406, 413, 668, 669] and coordination compounds [567] or substances with a high energy content (higher than that of the reactants), which may serve as fuels [462, 534]. Materials with some special (e.g., photochromic) properties have also been prepared; for example, photochromic plastic lenses [670, 671] possessing considerable hardness and reversibility contain Hg(II) complexes of the type $(R^3N{:}N)\,(R^4NHN{:})\,CSHgSC\,(N{:}NR^5)\,({:}NNHR^6)$ or $(R^7N{:}N)(R^8NHN{:})CSHgR^9$, where R^3–R^9 = phenyl or naphthyl which may be totally or partially substituted by a halo, C_1–C_6 hydrocarbon, C_1–C_6 haloalkyl, C_1–C_6 alkoxyalkyl, C_1–C_6 carboxylalkyl, sulphonyl, CN or C_1–C_6 acyl group.

Within the context of studying luminescence as probes of catalysts, luminescence as a probe of rare earth ions and their complexes in zeolites has been examined [674]. Useful information on the coordination environments, changes due to thermal and chemical treatments and catalytic properties, in general, of rare earth complexes and oxides in zeolites has been obtained. Chiral catalysts were investigated by circularly polarized luminescence spectroscopy [675] in order to ascertain the absolute configurations and complexation of ligands with rare earth ions.

The luminescence properties of many different inorganic compounds (including complexes) are of interest in searching for materials used as displays [676]; for example, by irradiating of a thin layer (about 25 μm) of europium chelate dissolved in an organic fluid, strong visible fluorescence is produced [677]. The characteristics of such arrangements would seem to satisfy the requirements of a multiplexed display with a large number of rows.

The data obtained by the photochemistry of complexes have been applied in practice also in the field of unconventional photographic processes (image recording) [399, 406, 672, 673]; some of the systems described, e.g., Co(III) complexes [678, 679] in the presence of a sulphide source, Fe(III) oxalate mixed-ligand complexes [680] and octacyanomolybdate(IV)/heterocyclic carb-2-aldehyde [681, 682], are photocatalytic in nature.

Transition metal complexes immobilized on insoluble supports, called "third-generation" catalysts [683, 684], have received much attention in the past decade [685–688]. Such immobilized species have been used to combine the selectivity of homogeneous catalysts with the ease of separation of heterogeneous species. The thermal and photochemical reactivity of complexes anchored to surfaces are usually profoundly influenced by the properties of the inorganic support. This may lead not only to a new photochemistry of complexes but also to the generation, e.g., using photochemistry as a method of preparation of coordinatively unsaturated complexes acting as catalysts stabilized by the rigidity of inorganic supports. In this way, for example, a hydrosilation catalyst has been prepared [689] by linking a photoactive $[Pt(C_2O_4)L_2]$ complex to silica by using the functionalized ligand L (where $L = (OMe)_3Si(CH_2)_2PEt_2$).

The utilization of the photochemistry of coordination compounds in analytical chemistry is also of interest [690, 691]. The method of "photonometric titration" [559, 692, 693], later called "photochemical titration", has been used in systems containing, e.g., complexes of copper [559, 694, 695] and iron [696–699] for the quantitative determinations of various species in solution. The field of research that utilizes the application of photochemical kinetics in analytical chemistry has been termed "photochemical kinetic analysis" [560, 700].

Progress is also expected in bioapplications, e.g., in the field of photoinduced electron- or charge-transfer phenomena in solution (including metal complexes in biologically important systems) investigated by means of picosecond [701, 702] and nanosecond laser photolysis, transient absorption, fluorescence measurements and laser-induced photocurrent [308, 309] measurements.

6 CONCLUSION

In the previous chapters, the state achieved in the photochemistry of coordination compounds has been demonstrated. The conclusions formulated result from the variety of data for each of the topics discussed. Because of the extent and uneven scope of knowledge, only certain purposefully selected examples have been chosen to illustrate these topics.

The trends in the quantity, quality and orientation of published works indicate that photochemistry — not only of the coordination compounds — is a very promising field of chemistry with contributions to the development of science, practical needs and stimulating progress in experimental methods.

Analysis of the published data shows that the development of the photochemistry of coordination compounds has been uneven. The differences are manifested particularly in the topics of research (e.g., the number of studies on the photochemistry of transition element complexes of Groups VI and VIII exceeds those for Groups IV, V and VII). There is also unevenness in the types of photochemical reactions studied (e.g., the number of published papers dealing with photosubstitution and outer-sphere photoredox processes is markedly higher than that of the papers focused on the study of phototautomerizations, acid–base reactions and inner-sphere photoredox reactions). The stage of the theoretical elaboration also differs (e.g., compare the differences in the approaches towards the interpretation of the thermodynamics and kinetics of the outer- and inner-sphere photoredox reactions).

It seems increasingly necessary to communicate between photochemistry and other chemical disciplines and natural sciences, not only in order to improve the practical application of the knowledge of photochemistry but also to benefit the theoretical interpretation of the results of other fields of science. The prospects for photochemistry in the field of coordination compounds, which will be considered later, are not motivated by efforts to present unambiguous and unchangeable predictions for further development, as this is impossible in view of the rapid developments in this field. Hence, the ideas on the possibilities shown later represent the personal viewpoint of the present authors, resulting from the analysis of the current state and trends presented in the previous chapters.

In recent years, the theory of molecular orbitals has been increasingly used in the interpretation of results on the photophysical and photochemical properties of complexes. Provided that present trends continue (including computational possibilities), one can expect marked progress in the knowledge of electronic and molecular structure and of the reactivity of excited complexes.

The application of MO theory should not only consist in quantum chemical calculations (optimization of the structures of the excited complexes, study of reaction pathways based on the knowledge of the shape of the energy hypersurfaces, study of the efficiency and localization of the electron transfer during photoexcitation, etc.), but also on experimental work, particularly in the application of photoelectron spectroscopy to the study of the electronic systems of excited complexes.

The use and further development of currently applied experimental techniques in photochemistry (e.g., matrix isolation and time-resolved infrared spectroscopy, photoselection spectra, time-dependent emissions, holographic photochemistry, flash photolysis ESR, diffuse reflectance flash photolysis applied to solid-state transients, triboluminescence phenomena, pressure effects, X-ray diffraction in solutions, photoelectrochemistry, etc.) should catalyse not only the acquisition of original and interesting data, but also of new applications.

The application of other techniques (e.g., fast magnetic susceptibility, photochemistry in a magnetic field of high intensity, resonance Raman spectroscopy of excited states) can make considerable contributions to the solution of the problems associated with the determination of the number, multiplicity and actual structure of the reactive electronically excited states of coordination compounds. "Double excitations" (electronic and vibrational) have been already utilized for the separation of isotopes, and they are a suitable model for concomitant excitation and ionization (far-UV and X-ray regions).

The questions concerning the quartet–doublet hypothesis for the complexes of Cr(III) (Section 4.4.2) illustrate not only the complexity of the problems and the possibilities existing in understanding and interpreting the photochemistry of such complexes, but also the possibilities for the study of the properties of complexes with other central atoms. The effect of spin–orbit coupling on the deactivated processes of the complexes of the second and third transition rows is reflected in the attention devoted to these aspects by both quantum chemists (mastering the problems of "forbiddenness" and "allowance") and photochemists.

As in any other scientific discipline, also in the photochemistry of coordination compounds the change from quantity to quality has been demonstrated by the generalization of the results and the formulation of rules for the photochemical behaviour of complexes.

The attempt to understand the course of photochemical reactions to the extent enabling a more perfect rules of photoreactivity to be formulated requires an extension and intensification of research in this field, where only a relatively small amount of data has been available up to now (stereochemical changes of other than octahedral complexes, intramolecular redox processes, tautomerization processes, etc.), and also the generalization of the current knowledge. This can be exemplified by the study of the Bronsted alkalinity of complexes with MLCT excitation (Section 4.5), whereas the acidity of the complex during LMCT excitation and corresponding acid–base processes were not studied.

The experimentally verified effects of the environment of the complex on the properties of its electronic system (e.g., in the CTTS and MLCT states) and reactivity (see, e.g., Section 4.4.1) indicate that when discussing mechanisms and interpreting the results it will be necessary more than before to consider also the effect of the secondary coordination sphere of the complex. These facts are also of great importance with respect to methodology, as in fact all photosubstitution reactivity models (Section 4.7) truly determine which of the ligands will be substituted (a priori assuming dissociation of the labilized ligand); however, the experiments prove that an exchange associative mechanism of substitution is operative in many instances. On the other hand, the results of testing the various photolysis models have demonstrated that photochemistry may be helpful in assessing, e.g., more correct values of σ and π parameters.

The course of photochemical reactions from vibrationally (rotationally) non-relaxed complexes calls for the elaboration and application of a non-equilibrium thermodynamic approach to the description of the complexes in the excited states.

It is probable that analogously to the study of the conversion of solar energy to chemical energy which stimulated the elaboration of an equilibrium thermodynamic theory (and applying the theory of an activated complex of equilibrium kinetics) for excited particles, the understanding and mimicking of the function of complexes in biological systems can stimulate the introduction of non-equilibrium thermodynamics (and a new approach to kinetics).

In the application of the knowledge of the photochemistry of coordination compounds, a very promising area seems to be practical catalysis under the effect of light. This not only concerns the direct industrial utilization of photocatalysed reactions, but also the elucidation (and optimization of the processes) of the mechanism of the function of catalysts. Answers to questions such as why can important industrial processes (e.g., hydrogenation of CO, activation of C–H bonds, H_2 reduction) be catalysed by polynuclear complexes (clusters) only, can be obtained after explaining the processes of labilization of the metal–metal bonds and corresponding changes in the distribution of electron density, through photochemistry.

The second half of the 1970s and the early 1980s were noted for very intensive studies of the properties of model systems for the conversion of solar energy to chemical and electrical energy.

The results of the study of complex-containing colloid and supramolecular systems show that the potential possibilities of photochemistry in this field have not been properly utilized so far. The interest towards supramolecular systems (i.e. assemblies of two or more molecular components) can be regarded as the most noticeable trend in current years [556]. It is expected that within supramolecular photochemistry [13] a great deal of effort will be concentrated upon design, synthesis and characterization of photonic molecular devices (PMDs), i.e. assemblies of molecular components capable of performing valuable light-induced functions such as charge separation, energy migration and conformational changes [705]. Such development of PMDs might be very promising in their utilization in various fields, e.g. in producing molecular layers of controlled composition and thickness [706], self-organization of special types of chain molecules around metal ions [707], electrode derivatization [708], fabrication of microelectrochemical devices [709] or in microelectronics in general [710]. An analogous situation can be observed when following the trends in the application of photochemistry to the synthesis of coordination compounds. The published data indicate that the prospects, also depending on the optimization of the experimental conditions of the syntheses, lie in compounds with new ligands, thermodynamically unstable substances (e.g., compounds with photochromic properties) and the preparation of the substances with catalytic properties.

Increasing interest in systems based on light-sensitive coordination compounds that will have important photographic applications is also expected.

The recent results show that the qualitatively new knowledge that contributes markedly to the understanding of photophysical and photochemical properties not only of coordination compounds has been achieved by the application of newly developed or improved older techniques (e.g., the study of the electronic and molecular structures of excited particles and the study of the symmetry and properties of coordinatively unsaturated intermediates). The trends in the developments in this field indicate that there are possibilities for the further development of methods and instrumentation in photochemical research that are conditioned by both the tasks formulated and their objective necessity.

REFERENCES

1. J. Szychliński, Wiad. Chem. **16**, 607 (1962).
2. E. L. Wehry, Quart. Rev. **21**, 213 (1967).
3. A. W. Adamson, W. L. Waltz, E. Zinato, D. W. Watts, P. D. Fleischauer, R.D. Lindholm, Chem. Rev. **68**, 541 (1968).
4. A. W. Adamson, Coord. Chem. Rev. **3**, 169 (1968).
5. V. Balzani, L. Moggi, F. Scandola, V. Carassiti, Inorg. Chim. Acta Rev. **1**, 7 (1967).
6. A. W. Adamson, J. Phys. Chem. **71**, 798 (1967).
7. V. Balzani, V. Carassiti, Photochemistry of Coordination Compounds, Academic Press, London, 1970.
8. A.W. Adamson, P. D. Fleischauer (eds.), Concepts of Inorganic Photochemistry, Wiley, New York, 1975.
9. G. L. Geoffroy, M. S. Wrighton, Organometallic Photochemistry, Academic Press, New York, 1979.
10. J. Sýkora, J. Šima, Photochemistry of Coordination Compounds, Veda, Bratislava, 1986 (in Slovak).
11. H. Hennig, D. Rehorek, Photochemische und photokatalytische Reaktionen von Koordinationsverbindungen, Teubner, Stuttgart, 1988.
12. G. J. Ferraudi, Elements of Inorganic Photochemistry, Wiley, New York, 1988.
13. V. Balzani (ed.), Supramolecular Photochemistry, Reidel, Dordrecht, 1987.
14. C. H. Langford, H. B. Gray, Ligand Substitution Mechanisms, Benjamin, New York, 1966.
15. F. Basolo, R. G. Pearson, Mechanisms of Inorganic Reactions, Wiley, New York, 1966.
16. P. Pelikán, R. Boča, Quantum Chemistry of Coordination Compounds, Veda, Bratislava, 1987 (in Slovak).
17. A. B. P. Lever, Inorganic Electronic Spectroscopy, Elsevier, Amsterdam, 1984.
18. C. K. Jörgensen, Adv. Chem. Phys. **5**, 33 (1963).
19. F. Scandola, V. Balzani, J. Chem. Educ. **60**, 814 (1983).
20. J. N. Demas, J. W. Addington, S. H. Peterson, E. W. Harris, J. Phys. Chem. **81**, 1039 (1977).
21. J. F. Endicott, Coord. Chem. Rev. **64**, 293 (1985).
22. J. N. Demas, J. Chem. Educ. **60**, 803 (1983).
23. V. Balzani, F. Bolletta, J. Photochem. **17**, 479 (1981).
24. D. K. Liu, B. S. Brunschwig, C. Creutz, N. Sutin, J. Am. Chem. Soc. **108**, 1749 (1986).
25. E. Leyner, F. Zimmermann, J. I. Zink, G. Gliemann, Inorg. Chem. **24**, 102 (1985).
26. J. I. Zink, Acc. Chem. Res. **11**, 289 (1978).
27. J. V. Casper, T. D. Westmoreland, G. H. Allen, P. G. Bradley, T. J. Meyer, W. H. Woodruff, J. Am. Chem. Soc. **106**, 3492 (1984).
28. J. Ferguson, Prog. Inorg. Chem. **12**, 159 (1970).
29. K. B. Yatsimirskii, N. K. Davidenko, Coord. Chem. Rev. **27**, 223 (1978).

30. J. L. Ryan, C. K. Jörgensen, J. Phys. Chem. **70**, 2845 (1966).
31. M. Albin, W. N. Horocks, Inorg. Chem. **24**, 895 (1985).
32. V. H. Horelding, A. J. Frank, Inorg. Chem. **24**, 3664 (1985).
33. W. C. Trogler, H. B. Gray, Acc. Chem. Res. **11**, 232 (1978).
34. C. M. Che, W. P. Schaefer, H. B. Gray, K. K. Dickon, P. B. Stein, D. M. Roundhill, J. Am. Chem. Soc. **104**, 4253 (1982).
35. A. F. Cotton, R. A. Walton, Multiple Bonds Between Metal Atoms, Wiley, New York, 1982.
36. J. R. Perumareddi, Coord. Chem. Rev. **4**, 73 (1964).
37. J. R. Darwent, P. Douglas, A. Harriman, G. Porter, M. C. Richoux, Coord. Chem. Rev. **44**, 83 (1982).
38. J. V. Koester, Chem. Phys. Lett. **32**, 575 (1975).
39. A. Vogler, H. Kunkely, J. Am. Chem. Soc. **103**, 1559 (1981).
40. G. A. Crosboy, R. G. Highland, K. A. Truesdell, Coord. Chem. Rev. **64**, 41 (1985).
41. J. Sýkora, E. Horváth, J. Gažo, Z. Anorg. Allg. Chem. **442**, 245 (1978).
42. J. Sýkora, I. Giannini, F. Diomedi-Camassei, J. Chem. Soc, Chem. Commun. 207 (1978).
43. J. C. Curtis, B. P. Sullivan, T. J. Mayer, Inorg. Chem. **22**, 224 (1983).
44. A. Vogler, A. H. Osman, H. Kunkely, Coord. Chem. Rev. **64**, 159 (1985).
45. H. Hennig, D. Walther, P. Thomas, Z. Chem. **23**, 446 (1983).
46. N. Sabatini, V. Balzani, J. Less-Common Met. **112**, 381 (1985).
47. J. E. Curtis, T. J. Meyer, Inorg. Chem. **21**, 1562 (1982).
48. V. Balzani, F. Bolletta, M. T. Gandolfi, M. Maestri, Top. Curr. Chem. **75**, 1 (1978).
49. C. R. Bock, M. S. Wrighton, Inorg. Chem. **16**, 1309 (1977).
50. J. C. D. Brand, W. Snedden, Trans. Faraday Soc. **53**, 894 (1957).
51. A. W. Adamson, Pure Appl. Chem. **24**, 451 (1970).
52. L. Viane, A. Ceulemans, L. G. Vanquickenborne, Inorg. Chem. **24**, 1713 (1985).
53. P. J. Hay, J. Am. Chem. Soc. **104**, 7007 (1982).
54. W. Evans, J. I. Zink, J. Am. Chem. Soc. **103**, 2635 (1981).
55. R. Bensasson, C. Salet, V. Balzani, J. Am. Chem. Soc. **98**, 3722 (1976).
56. A. D. Kirk, P. E. Hoggard, G. B. Porter, M. G. Rockley, M. W. Windoor, Chem. Phys. Lett. **37**, 199 (1976).
57. C. M. Che, L. G. Butler, H. B. Gray, R. M. Crooks, W. H. Woodruff, J. Am. Chem. Soc. **105**, 5492 (1983).
58. J. I. Zink, Coord. Chem. Rev. **64**, 93 (1985).
59. S. F. Rice, V. M. Miskowski, H. B. Gray, Inorg. Chem. **27**, 4704 (1988).
60. D. E. Morris, W. H. Woodruff, J. Phys. Chem. **89**, 5795 (1985).
61. Z. R. Grabowski, A. Grabowska, Z. Phys. Chem., NF **101**, 197 (1976).
62. Z. R. Grabowski, W. Rubaszewska, J. Chem. Soc., Faraday Trans. 1 **73**, 11 (1977).
63. P. D. Fleischauer, A. W. Adamson, G. Sartori, Prog. Inorg. Chem. **17**, 1 (1972).
64. S. H. Peterson, J. N. Demas, J. Am. Chem. Soc. **98**, 7880 (1976).
65. W. D. K. Clark, N. Sutin, J. Am. Chem. Soc. **99**, 4676 (1977).
66. J. F. Endicott, G. J. Ferraudi, J. R. Barber, J. Phys. Chem. **79**, 630 (1978).
67. G. Ferraudi, Inorg. Chem. **19**, 438 (1980).
68. N. Serpone, in Photoelectrochemistry, Photocatalysis and Photoreactors, M. Schiavello (ed.), Reidel, Dordrecht, 1985, p. 351.
69. P. D. Fleischauer, A. W. Adamson, G. Sartori, in Inorganic Reaction Mechanisms, J. O. Edwards (ed.), Wiley, New York, 1972.
70. S. J. Milder, D. S. Kliger, J. Phys. Chem. **89**, 4170 (1985).
71. S. Tobida, M. Arakawa, I. Tanaka, J. Phys. Chem. **89**, 5649 (1985).
72. J. di Benedeto, P. C. Ford, Coord. Chem. Rev. **64**, 361 (1985).
73. K. K. Chatterjee, L. S. Forster, Spectrochim. Acta **23**, 1603 (1964).
74. D. W. H. Carsters, G. A. Crosby, J. Mol. Spectrosc. **34**, 113 (1970).

75. J. N. Demas, G. A. Crosby, J. Am. Chem. Soc. **92**, 7262 (1970).
76. T. R. Thomas, R. J. Watts, G. A. Crosby, J. Chem. Phys. **59**, 3123 (1973).
77. J. N. Demas, G. A. Crosby, J. Am. Chem. Soc. **93**, 2841 (1972).
78. S. J. Milder, Inorg. Chem. **24**, 3376 (1985).
79. C. A. Parker, Photoluminiscence of Solutions, Elsevier, Amsterdam, 1968.
80. J. N. Demas, Excited State Lifetime Measurements, Academic Press, New York, 1983.
81. S. H. Lee, W. L. Waltz, D. R. Demmer, R. T. Walter, Inorg. Chem. **24**, 1531 (1985).
82. P. A. Tanner, J. Chem. Soc., Faraday Trans. 2 **81**, 1285 (1985).
83. P. A. Tanner, Mol. Phys. **54**, 883 (1985).
84. C. D. Flint, P. A. Tanner, Mol. Phys. **53**, 437 (1984).
85. G. Visvanath, M. Kasha, J. Chem. Phys. **24**, 574 (1956).
86. L. A. Martano, Ch. P. Wang, W. W. Horocks, A. M. P. Goncalves, J. Phys. Chem. **80**, 2389 (1976).
87. Y. Kurabayashi, K. Kikuchi, H. Kokubun, Y. Kaizu, H. Kobayashi, J. Phys. Chem. **88**, 1308 (1984).
88. H. Kobayashi, Y. Kaizu, Coord. Chem. Rev. **64**, 53 (1985).
89. G. A. Crosby, R. J. Watts, D. W. Carstens, Science **170**, 1195 (1970).
90. G. B. Porter, H. L. Schläfer, Z. Phys. Chem. (Frankfurt) **37**, 109 (1963).
91. K. W. Hipps, G. A. Mewell, G. A. Crosby, J. Phys. Chem. **80**, 2232 (1976).
92. A. E. Stiegman, V. M. Miskowski, H. B. Gray, J. Am. Chem. Soc. **108**, D781 (1986).
93. D. G. Nocera, A. W. Maverick, J. R. Winkler, C. M. Che, H. B. Gray, ACS Symp. Ser. **211**, 21 (1983).
94. M. K. de Armond, J. E. Hillis, J. Chem. Phys. **54**, 2247 (1971).
95. M. K. de Armond, C. M. Carlin, Coord. Chem. Rev. **36**, 325 (1981).
96. M. L. Fetterolly, H. W. Offen, J. Phys. Chem. **89**, 3320 (1985).
97. W. J. Wining, J. W. Caspar, T. J. Meyer, J. Phys. Chem. **89**, 1095 (1985).
98. H. Yersin, E. Gallhuber, Inorg. Chem. **23**, 3745 (1984).
99. W. Weber, J. di Benedetto, H. Offen, R. van Eldik, P. C. Ford, Inorg. Chem. **23**. 2033 (1984).
100. S. W. Snyder, D. E. Raines, R. T. Rieger, J. N. Demas, Langmuir **1**, 548 (1985).
101. N. A. P. Kane-Maguire, M. M. Allen, J. M. Vaught, J. S. Hallok, A. L. Haetherington, Inorg. Chem. **22**, 3851 (1983).
102. D. Rehm, A. Weller, Isr. J. Chem. **8**, 259 (1970).
103. F. Wilkinson, C. Tsiamis, J. Phys. Chem. **85**, 4153 (1981).
104. H. D. Bist, T. Nishiya, M. Baba, I. Hanazaki, J. Am. Chem. Soc. **110**, 3043 (1988).
105. J. Šima, E. Horváth, J. Gažo, Inorg. Chim. Acta **31**, L460 (1978).
106. J. Šima, E. Horváth, H. Zliechovcová, J. Gažo, Z.Anorg. Allg. Chem. **451**, 151 (1979).
107. D. Valigura, J. Šima, Z. Anorg. Allg. Chem. **461**, 217 (1980).
108. J. Šima, H. Zliechovcová, J. Gažo, Chem. Zvesti **34**, 172 (1980).
109. H. Zliechovcová, J. Šima, D. Valigura, J. Sýkora, Chem. Zvesti **36**, 59 (1982).
110. P. D. Fleischauer, P. Fleischauer, Chem. Rev. **70**, 199 (1970).
111. A. van Die, G. Blasse, W. F. van der Weg, Mater. Chem. Phys. **14**, 513 (1986).
112. G. F. Stelmakh, M. P. Tsvirtko, Opt. Spektrosk. **55**, 858 (1983).
113. D. R. McMillin, J. R. Kirchhoff, K. V. Goodwin, Coord. Chem. Rev. **64**, 83 (1980).
114. D. F. Eaton, J. Am. Chem. Soc. **102**, 3280 (1980); **103**, 7235 (1981).
115. J. K. Nagle, B. A. Brennan, J. Am. Chem. Soc. **110**, 5931 (1988).
116. N. P. Ayala, J. N. Demas, B. A. DeGraff, J. Am. Chem. Soc. **110**, 1523 (1988).
117. A. Vogler, H. Kunkely, Inorg. Chim. Acta **45**, L265 (1980).
118. E. I. Kapinus, M. M. Aleksankina, I. I. Dilung, Dopov. Akad. Nauk RSR, Ser. B **9**, 35 (1984).
119. I. G. Lopp, R. W. Hendren, P. D. Wilder, D. G. Whitten, J. Am. Chem. Soc. **92**, 6440 (1970).
120. S. L. Bondarev, G. P. Guranovich, B. M. Dzhagarov, K. M. Salokhiddikov, Tezisy Dokl.

— Vses. Soveshch. Lyumin. 103 (1975).

121. J. A. Mercer-Smith, C. R. Sutcliffe, R. M. Schmell, D. G. Whitten, J. Am. Chem. Soc. **101**, 3995 (1979).
122. H. G. O. Becker, T. Lehmann, R. Schütz, J. Prakt. Chem. **327**, 21 (1985).
123. B. L. Gore, A. Harriman, M. C. Richoux, J. Photochem. **19**, 209 (1982).
124. M. Hoshino, H. Seki, H. Shizuka, J. Phys. Chem. **89**, 470 (1985).
125. J. K. Roy, D. G. Whitten, J. Am. Chem. Soc. **93**, 7093 (1971).
126. J. K. Roy, F. A. Carroll, D. G. Whitten, J. Am. Chem. Soc. **96**, 6349 (1974).
127. J. B. Callis, J. M. Knowles, M. Gouterman, J. Phys. Chem. **77**, 154 (1973).
128. M. A. Jamieson, N. Serpone, M. Z. Hoffman, F. Bolletta, Inorg. Chim. Acta **72**, 247 (1983).
129. M. E. Frink, D. K. Griger, G. Ferraudi, J. Phys. Chem. **90**, 1924 (1986).
130. M. E. Frink, G. Ferraudi, Chem. Phys. Lett. **124**, 576 (1986).
131. A. Slama-Schwok, S. Gerohumi, J. Rabani, H. Cohen, D. Meyerstein, J. Phys. Chem. **89**, 2460 (1985).
132. J. S. Winterle, D. S. Klinger, G. S. Hammond, J. Am. Chem. Soc. **98**, 3719 (1976).
133. P. A. Grutsch, Ch. Kutal, J. Am. Chem. Soc. **99**, 6460 (1977).
134. M. D. Marcantonatos, J. Chem. Soc.,Faraday Trans. 1 **75**, 2252 (1979); **76**, 1093 (1980).
135. M. D. Marcantonatos, Inorg. Chim. Acta **24**, L37 (1977); **25**, L101 (1977); **26**, 41 (1978).
136. M. D. Marcantonatos, M. Deschaux, Chem. Phys. Lett. **80**, 327 (1981).
137. K. Kasuga, H. Marimoto, M. Ando, Inorg. Chem. **25**, 2478 (1986).
138. D. R. Prasad, G. Ferraudi, Inorg. Chem. **22**, 1672 (1983).
139. E. I. Kapinus, V. P. Starii, I. I. Dilung. Teor. Eksp. Khim. **17**, 100 (1981); **18**, 450 (1982).
140. E. I. Kapinus, M. M. Aleksankina, V. P. Starii, V. I. Boghillo, I. I. Dilung, J. Chem. Soc., Faraday Trans. 2 **81**, 631 (1985).
141. N. E. Andreeva, A. K. Chibisov, Teor. Eksp. Khim. **15**, 668 (1979).
142. E. I. Kapinus, V. P. Starii, I. I. Dilung, Dokl. Akad. Nauk SSSR **261**, 907 (1981).
143. E. I. Kapinus, M. M. Aleksankina, I. I. Dilung, J. Photochem. **21**, 125 (1983).
144. P. A. Shakhvertov, Opt. Spektrosk. **30**, 81 (1971).
145. A. Harriman, G. Porter, N. Searle, J. Chem. Soc., Faraday Trans. 2 **75**, 1515 (1979).
146. D. R. McMillin, J. R. Kirchhoff, K. V. Goodwin, Coord. Chem. Rev. **64**, 83 (1985).
147. V. V. Sapunov, M. P. Tsvirko, Opt. Spektrosk. **49**, 283 (1980).
148. V. V. Sapurov, M. P. Tsvirko, Dokl. Akad. Nauk Bieloruss. SSR **20**, 208 (1976).
149. L. S. Degtyarev, E. I. Kapinus, E. Ya. Skuridin, Khim. Vys. Energ. **18**, 56 (1984).
150. A. B. P. Lever, P. Seymour, P. R. Auburn, Inorg. Chim. Acta **145**, 43 (1988).
151. V. Balzani, F. Scandola, in Photochemical Conversion and Storage of Solar Energy, J. S. Connolly (ed.), Academic Press, New York, 1981, p. 97.
152. N. J. Turro, Modern Molecular Photochemistry, Benjamin, Menlo Park, 1978.
153. A. A. Lamola, N. J. Turro (eds.), Energy Transfer and Organic Photochemistry, Interscience, New York, 1969.
154. S. Yamamoto, M. Hoshino, K. Yusufuku, M. Imamura, Inorg. Chem. **23**, 195 (1984).
155. J. F. Endicott, J. Chem. Educ. **60**, 824 (1983).
156. A. W. Adamson, J. Chem. Educ. **60**, 797 (1983).
157. A. Horváth, S. Papp, Acta Chim. Hung. **122**, 235 (1986).
158. O. Kalisky, H. Shirom, J. Photochem. **7**, 215 (1977).
159. M. Shirom, M. Tomkiewicz, J. Chem. Phys. **56**, 2731 (1972).
160. M. Basco, K. S. Vidyarthi, D. C. Walker, Can. J. Chem. **52**, 343 (1974).
161. M. Z. Hoffman, K. D. Whitburn, J. Chem. Educ. **58**, 119 (1981).
162. C. D. Jonah, M. S. Matheson, D. Meisel, J. Am. Chem. Soc. **100**, 1449 (1978).
163. N. Sutin, C. Creutz, J. Chem. Educ. **60**, 809 (1983).
164. V. Balzani, F. Scandola, F. Bolletta, R. Ballardini, Pure Appl. Chem. **51**, 299 (1979).
165. R. A. Marcus, Discuss. Faraday Soc. **29**, 21 (1960).

166. M. A. Fox, M. Chanon (eds.), Photoinduced Electron Transfer, Elsevier, Amsterdam, 1988.
167. G. McLendon, T. Guarr, M. McGuire, K. Simolo, S. Strauch, K. Taylor, Coord. Chem. Rev. **64**, 113 (1985).
168. E. Tsuchida, M. Kaneko, H. Nishide, M. Hoshino, J. Phys. Chem. **90**, 2283 (1986).
169. T. Guarr, M. McGuire, S. Strauch, G. McLendon, J. Am. Chem. Soc. **105**, 616 (1983).
170. J. S. Lindsey, D. C. Mauzerall, J. Am. Chem. Soc. **105**, 6528 (1983).
171. N. S. Hush, Coord. Chem. Rev. **64**, 135 (1985).
172. S. E. Peterson-Kennedy, J. L. McGourty, P. S. Ho, C. J. Sutoris, N. Liang, H. Zelemel, N. V. Blough, E. Margoliash, B. M. Hoffman, Coord. Chem. Rev. **64**, 125 (1985).
173. S. Sostero, O. Traverso, P. di Bernardo, T. J. Kemp, J. Chem. Soc., Dalton Trans. 658 (1979).
174. H. D. Burrows, S. J. Formosinho, J. Chem. Educ. **55**, 125 (1978).
175. R. G. Gamache, R. A. Rader, D. R. McMillin, J. Am. Chem. Soc. **107**, 1141 (1985).
176. V. Balzani, N. Sabbatini, F. Scandola, Chem. Rev. **86**, 319 (1986).
177. N. Sabbatini, A. Bonnazzi, M. Ciano, V. Balzani, J. Less-Common Met. **112**, 381 (1985).
178. H. Hennig, A. Rehorek, D. Rehorek, Ph. Thomas, Inorg. Chim. Acta **86**, 41 (1984).
179. T. Nyokong, Z. Gasyna, M. J. Stillman, Inorg. Chim. Acta **112**, 11 (1986).
180. Y. Kaizu, T. Mori, H. Kobayashi, J. Phys. Chem. **89**, 332 (1985).
181. M. Hvastijová, J. Kohout, J. Gažo, J. Coord. Chem. **12**, 27 (1982).
182. F. W. Grevels, E. Koerner von Gustorf, Justus Liebigs Ann. Chem. 547 (1975).
183. O. Traverso, V. Carassiti, M. Graziani, V. Belluco, J. Organomet. Chem. **57**, C22 (1973).
184. S. Sostero, O. Traverso, M. Lenarda, M. Graziani, J. Organomet. Chem. **134**, 259 (1977).
185. R. H. Hill, R. J. Puddephatt, J. Am. Chem. Soc. **107**, 1218 (1985).
186. L. Chassot, A. von Zelewsky, D. Sandrini, M. Maestri, V. Balzani, J. Am. Chem. Soc. **108**, 6084 (1986).
187. A. Vogler, H. Kunkely, Angew. Chem. **94**, 217 (1982).
188. W. Jetz, W. A. G. Graham, Inorg. Chem. **10**, 4 (1971).
189. A. Maldotti, S. Sostero, O. Traverso, J. Šima, Inorg. Chim. Acta **54**, L271 (1981).
190. S. Sostero, O. Traverso, V. Carassiti, Proc. 3rd Symp. Photochem. Thermal React. Coord. Comp., Krakow, Poland, 1980, p. 96.
191. R. Boča, Coord. Chem. Rev. **50**, 1 (1980).
192. M. Hoshino, Chem. Phys. Lett. **120**, 50 (1985).
193. A. Vogler, H. Kunkely, J. Am. Chem. Soc. **103**, 6222 (1981).
194. W. Weber, R. van Eldik, Inorg. Chim. Acta **111**, 129 (1986).
195. S. I. Arzhanov, A. L. Poznyak, Z. Anorg. Allg. Chem. **481**, 201 (1981).
196. L. Moggi, N. Sabbatini, O. Traverso, Mol. Photochem. **5**, 11 (1973).
197. D. Rehorek, Ph. Thomas, H. Hennig, Inorg. Chim. Acta **32**, L1 (1979).
198. D. Rehorek, J. Salvetter, A. Hantschmann, H. Hennig, A. Stasicka, A. Chodowska, Inorg. Chim. Acta **37**, L471 (1979).
199. E. Cervone, F. Diomedi-Camassei, I. Giannini, J. Sýkora, J. Photochem. **11**, 321 (1979).
200. A. T. Thorton, G. S. Laurence, J. Chem. Soc., Dalton Trans. 804 (1973).
201. N. M. Bazhin, V. V. Korolev, V. F. Pliusnin, Khim. Vys. Energ. **14**, 255 (1980).
202. P. G. David, J. Chem. Soc., Chem. Commun. 1924 (1972).
203. F. Scandola, C. Bartocci, M. A. Scandola, J. Am. Chem. Soc. **95**, 7898 (1973).
204. F. Scandola, C. Bartocci, M. A. Scandola, J. Phys. Chem. **78**, 572 (1974).
205. J. F. Endicott, Inorg. Chem. **16**, 494 (1977).
206. J. Sýkora, J. Šima, D. Valigura, Chem. Zvesti **35**, 345 (1981).
207. B. A. Leland, A. D. Joran, P. M. Felker, J. J. Hopfield, A. H. Zewail, P. B. Dervan, J. Phys. Chem. **89**, 5571 (1985).
208. I. Fujita, J. Fajer, C. K. Chang, C. B. Wang, M. A. Bergkamp, T. L. Netzel, J. Phys. Chem. **86**, 3754 (1982).
209. T. L. Netzel, M. A. Bergkamp, C. K. Chang, J. Am. Chem. Soc. **104**. 1952 (1982).

210. C. Creutz, P. Kroger, T. Matsubara, T. L. Netzel, N. Sutin, J. Am. Chem. Soc. **101**, 5442 (1979).
211. C. J. Curtis, J. S. Bernstein, R. H. Schmell, T. J. Meyer, Chem. Phys. Lett. **81**, 48 (1981).
212. M. W. Peterson, D. S. Rivers, R. M. Richman, J. Am. Chem. Soc. **107**, 2907 (1985).
213. M. W. Peterson, R. M. Richman, Inorg. Chem. **24**, 722 (1985).
214. T. Berthold, D. Rehorek, H. Hennig, Z. Chem. **26**, 183 (1986).
215. M. Hoshino, K. Yasufuku, Inorg. Chem. **24**, 4408 (1985)
216. T. J. Meyer, J. V. Caspar, Chem. Rev. **85**, 187 (1985).
217. A. Vogler, H. Kunkely, Inorg. Chem. **23**, 1360 (1984).
218. T. Kruck, G. Sylvester, I. P. Kunau, Angew. Chem. **10**, 275 (1971).
219. T. Kruck, R. Kobelt, Chem. Ber. **105**, 3765 (1972).
220. T. Kruck, G. Sylvester, I. P. Kunau, Z. Naturforsch. B **28**, 38 (1973).
221. D. G. Nocera, A. W. Maverick, J. R. Winkler, C. M. Che, H. B. Gray, ACS Symp. Ser. **221**, 21 (1983).
222. K. A. Azam, R. H. Hill, R. J. Puddephatt, Can. J. Chem. **62**, 2029 (1984).
223. D. M. Roundhill, J. Am. Chem. Soc. **107**, 4354 (1985).
224. A. Harriman, P. Walters, Inorg. Chim. Acta **83**, 151 (1984).
225. B. Kräutler, Helv. Chim. Acta **65**, 1941 (1982).
226. B. Kräutler, R. Stepanek, Helv. Chim. Acta **66**, 44 (1983).
227. B. Kräutler, R. Stepanek, Angew. Chem. **97**, 71 (1985).
228. G. Ferraudi, E. V. Srisankar, Inorg. Chem. **17**, 3164 (1978).
229. G. Ferraudi, Inorg. Chem. **18**, 1005 (1979).
230. S. Muralidharan, G. Ferraudi, K. Schamtz, Inorg. Chem. **21**, 2961 (1982).
231. G. Ferraudi, S. Oishi, S. Muralidharan, J. Phys. Chem. **88**, 5261 (1984).
232. D. K. Geiger, G. Ferraudi, K. Madden, J. Granifo, P. D. Rillema, J. Phys. Chem. **89**, 3890 (1985).
233. J. Šima, S. Sostero, A. Maldotti, O. Traverso, V. Carassiti, XIII Congresso Naz. Chim. Inorg., Camerino, Italy, 1980, p. 202.
234. J. Gažo, Pure Appl. Chem. **38**, 279 (1974).
235. J. Gažo, R. Boča, E. Jóna, M. Kabešová, Ľ. Macášková, J. Šima, P. Pelikán, F. Valach, Coord. Chem. Rev. **43**, 87 (1982).
236. F. Scandola, Rearrangements in Ground and Excited States, Vol. 3, Academic Press, New York, 1980, p. 549.
237. G. B. Porter, R. H. Sparks, J. Photochem. **13**, 123 (1980).
238. L. S. Meriwether, E. C. Breitner, C. L. Sloan, J. Am. Chem. Soc. **87**, 4441 (1965).
239. P.Bergamini, S. di Martino, S. Sostero, O. Traverso, L. M. Venanzi, Int. Symp. Photochem. Synth. Catal., Abstracts, Ferrara, 1989, p. 119.
240. R. J. Watts, S. F. Bergeron, J. Phys. Chem. **83**, 424 (1979).
241. M. Noda, N. Hirota, M. Sumitani, K. Yoshikara, J. Phys. Chem. **89**, 399 (1985).
242. H. Shizuka, M. Machii, Y. Higaki, M. Tanaka, I. Tanaka, J. Phys. Chem. **89**, 320 (1985).
243. P. Gütlich, Struct. Bond. (Berlin) **44**, 83 (1981).
244. S. Decurtins, P. Gütlich, K. M. Hasselbach, A. Hauser, H. Spiering, Inorg. Chem. **24**, 2174 (1985).
245. S. Decurtins, P. Gütlich, C. P. Köhler, H. Spiering, J. Chem. Soc., Chem. Commun. 430 (1985).
246. P. P. Zarnegar, D. G. Whitten, J. Am. Chem. Soc. **93**, 3776 (1971).
247. P. P. Zarnegar, C. R. Bock, D. G. Whitten, J. Am. Chem. Soc. **95**, 4367 (1973).
248. M. S. Wrighton, D. L. Morse, L. Pdungsap, J. Am. Chem. Soc. **97**, 2073 (1975).
249. R. A. Freitag., J. A. Mercer-Smith, D. G. Whitten, J. Am. Chem. Soc. **103**, 1226 (1981).
250. B. Eaton, J. A. King, K. P. C. Vollhardt, J. Am. Chem. Soc. **108**, 1359 (1986).
251. P. Haake, T. A. Hylton, J. Am. Chem. Soc. **84**, 3774 (1962).

252. S. H. Mastin, P. Haake, J. Chem. Soc., Chem. Commun. 202 (1970).
253. L. Moggi, G. Varani, N. Sabbatini, V. Balzani, Mol. Photochem. 3, 141 (1971).
254. P. R. Brookes, C. Masters, B. L. Show, J. Chem. Soc., A 3756 (1968).
255. P. R. Brookes, B. L. Show, J. Chem. Soc., Chem. Commun. 919 (1968).
256. A. W. Adamson, Adv. Chem. Ser. **49**, 237 (1965).
257. J. J. McGarvey, J. Wilson, J. Am. Chem. Soc. **97**, 2531 (1975).
258. P. J. Wagner, Top. Curr. Chem. **66**, 1 (1976).
259. D. G. Alway, K. W. Barnett, J. Organomet. Chem. **99**, C52 (1975).
260. M. C. Cimolino, N. J. Shirley, R. G. Linck, Inorg. Chem. **19**, 3291 (1980).
261. V. Sastri, C. H. Langford, J. Phys. Chem. **74**, 3945 (1970).
262. K. L. Stevenson, J. F. Verdieck, Mol. Photochem. **1**, 271 (1969).
263. N. A. P. Kane-Maguire, C. H. Langford, Can. J. Chem. **50**, 3381 (1972).
264. N. A. P. Kane-Maguire, B. Dunlop, C. H. Langford, J. Am. Chem. Soc. **93**, 6293 (1971).
265. K. L. Stevenson, J. Am. Chem. Soc. **94**, 6652 (1972).
266. M. Cusumano, G. Gugliemo, V. Ricevuto, S. Sostero, O. Traverso, T. J. Kemp, J. Chem. Soc., Dalton Trans. 302 (1981).
267. S. H. Goh, C. Y. Mok, J. Inorg. Nucl. Chem. **39**, 531 (1977).
268. B. Durham, S. R. Wilson, D. J. Hodgson, T. J. Meyer, J. Am. Chem. Soc. **102**, 600 (1980).
269. F. Benda, B. Hájek, Inorg. Chim. Acta **36**, L40 (1979).
270. L. H. Skibsted, Coord. Chem. Rev. **64**, 343 (1985).
271. H. Mäcke, V. Houlding, A. W. Adamson, J. Am. Chem. Soc. **102**, 6888 (1980).
272. N. Sabbatini, L. Moggi, G. Varani, Inorg. Chim. Acta **5**, 469 (1971).
273. E. V. Boldyreva, A. A. Sidelnikov, A. P. Tchupakhin, I. Z. Lakhov, V. V. Boldyrev, Dokl. Akad. Nauk SSSR **277**, 893 (1984).
274. A. D. Kirk, Coord. Chem. Rev. **39**, 225 (1981).
275. A. D. Kirk, J. Chem. Educ. **60**, 834 (1983).
276. E. Zinato, in Concepts of Inorganic Photochemistry, A. W. Adamson, P. D. Fleischauer (eds.), Wiley, New York, 1975, p. 143.
277. P. C. Ford, D. Wink, J. di Benedetto, Prog. Inorg. Chem. **30**, 213 (1983).
278. P. C. Ford, Coord. Chem. Rev. **44**, 61 (1982).
279. P. C. Ford, J. Chem. Educ. **60**, 829 (1983).
280. P. C. Ford, Rev. Chem. Intermediates **2**, 267 (1979).
281. P. C. Ford, R. E. Hintze, J. D. Petersen, in Concepts of Inorganic Photochemistry, A. W. Adamson, P. D. Fleischauer (eds.), Wiley, New York, 1975, p. 203.
282. M. Koyama, Y. Kanchiku, T. Fujinaga, Coord. Chem. Rev. **3**, 285 (1968).
283. F. Scandola, Org. Chem. **42/3**, 549 (1980).
284. L. G. Vanquickenborne, A. Ceulemans, D. Beyens, J. J. McGarvey, J. Phys. Chem. **86**, 494 (1982).
285. A. Vogler, in Concepts of Inorganic Photochemistry, A. W. Adamson, P. D. Fleischauer (eds.), Wiley, New York, 1975, p. 269.
286. M. A. Bergkamp, R. J. Watts, P. C. Ford, J. Am. Chem. Soc. **102**, 2627 (1980).
287. L. G. Vanquickenborne, A. Ceulemans, Coord. Chem. Rev. **48**, 157 (1983).
288. J. D. Petersen, P. C. Ford, J. Phys. Chem. **78**, 1144 (1974).
289. M. Talebinasab-Sarvari, A. Zanella, P. C. Ford, Inorg. Chem. **19**, 1835 (1980).
290. M. Nishizawa, P. C. Ford, Inorg. Chem. **20**, 294 (1981).
291. V. F. Manfrin, G. Varani, L, Moggi V. Balzani, Mol. Photochem. **1**, 387 (1969).
292. R. A. Pribush, C. M. Bruce, A. W. Adamson, J. Am. Chem. Soc. **96**, 3927 (1974).
293. C. H. Langford, C. P. J. Vuik, J. Am. Chem. Soc. **29**, 5409 (1976).
294. C. H. Langford, A. Y. S. Malkhasiah, J. Chem. Soc., Chem. Commun. 1210 (1982).
295. M. F. Manfrin, N. Sabbatini, L. Moggi, V. Balzani, M. W. Hosseini, J. M. Lehn, J. Chem. Soc., Chem. Commun. 555 (1984).

296. M. F. Manfrin, L. Moggi, V. Castelvetro, V. Balzani, M. W. Hosseini, J. M. Lehn, J. Am. Chem. Soc. **107**, 6888 (1985).
297. B. Dietrich, M. W. Hosseini, J. M. Lehn, R. B. Sessions, J. Am. Chem. Soc. **103**, 1282 (1981).
298. L. Moggi, F. Bolletta, V. Balzani, F. Scandola, J. Inorg. Nucl. Chem. **28**, 2589 (1966).
299. F. Peter, M. Groos, M. W. Hosseini, J. H. Lehn, J. Electroanal. Chem. **144**, 279 (1983).
300. A. W. Adamson, J. Inorg. Nucl. Chem. **13**, 275 (1960).
301. M. A. Bergkamp, J. Brannon, D. Magde, R. J. Watts, R. C. Ford, J. Am. Chem. Soc. **101**, 4549 (1979).
302. P. Riccieri, E. Zinato, Proc. XIVth ICCC, IUPAC, Toronto, Canada, 1972, p. 252.
303. P. Riccieri, E. Zinato, Inorg. Chem. Acta **52**, 133 (1981).
304. D. Strauss, P. C. Ford, J. Chem. Soc., Chem. Commun. 194 (1977).
305. P. Riccieri, E. Zinato, Inorg. Chim. Acta **7**, 117 (1973).
306. T. K. Toreman, B. S. Bonilha, D. G. Whitten, J. Phys. Chem. **86**, 3436 (1982).
307. M. M. Olken, A. B. Ellis, J. Am. Chem. Soc. **106**, 7468 (1984).
308. J. W. Johnson, A. J. Jacobson, Y. F. Brody, J. T. Lewandowski, Inorg. Chem. **23**, 3842 (1984).
309. M. S. Whittingham, A. J. Jacobson, Intercalation Chemistry, Academic Press, New York, 1982.
310. T. Iwamoto, J. Mol. Struct. **75**, 51 (1981).
311. M. B. Dines, M. Marocco, in Extended Linear Chain Compounds, Vol. 2, J. S. Miller (ed.), Plenum Press, New York, 1982, p. 1.
312. M. B. Dines, R. E. Cooksey, P. C. Griffith, R. H. Lane, Inorg. Chem. **22**, 1003 (1983).
313. G. J. Ferraudi, J. F. Endicott, J. R. Barber, J. Am. Chem. Soc. **97**, 6406 (1975).
314. T. L. Kelly, J. F. Endicott, J. Am. Chem. Soc. **94**, 1797 (1972).
315. T. L. Kelly, J. F. Endicott, J. Phys. Chem. **76**, 1937 (1972).
316. G. Malouf, P. C. Ford, J. Am. Chem. Soc. **96**, 601 (1974).
317. G. Malouf, P. C. Ford, J. Am. Chem. Soc. **99**, 7213 (1977).
318. P. C. Ford, De F. P. Rudd, R. Gaunder, H. Taube, J. Am. Chem. Soc. **90**, 1187 (1968).
319. P. C. Ford, G. Malouf, J. D. Petersen, V. A. Durante, ACS Adv. Chem. Ser. **150**, 187 (1976).
320. P. J. Giordano, M. S. Wrighton, Inorg. Chem. **16**, 160 (1977).
321. J. E. Figard, J. D. Petersen, Inorg. Chem. **17**, 1059 (1978).
322. M. S. Wrighton, H. B. Abrahamson, D. L. Morse, J. Am. Chem. Soc. **98**, 1105 (1976).
323. M. A. Bergkamp, R. J. Watts, P. C. Ford, Inorg. Chem. **20**, 1764 (1981).
324. A. W. Adamson, A. Vogler, I. Lantzke, J. Phys. Chem. **73**, 4183 (1969).
325. S. Ohno, Bull. Chem. Soc. Jpn. **40**, 1765 (1967).
326. R. E. Hintze, P. C. Ford, J. Am. Chem. Soc. **97**, 2664 (1975).
327. H. F. Wasgestian, Z. Phys. Chem. (Frankfurt am Main) **67**, 59 (1969).
328. R. Dannöhl-Fickler, H. Kelm, F. Wasgestian, J. Lumin. **10**, 103 (1975).
329. D. Sandrini, M. T. Gendolfi, L. Moggi, V. Balzani, J. Am. Chem. Soc. **100**, 1463 (1978).
330. A. W. Adamson, Comments Inorg. Chem. **1**, 33 (1981).
331. S. N. Chen, G. B. Porter, J. Am. Chem. Soc. **92**, 3196 (1970).
332. A. R. Gutierrez, A. W. Adamson, J. Phys. Chem. **82**, 902 (1978).
333. Y. S. Kang, F. Castelli, L. S. Forster, J. Phys. Chem. **83**, 2368 (1979)..
334. A. W. Adamson, A. Vogler, I. Lantzke, J. Phys. Chem. **77**, 127 (1973).
335. A. D. Kirk, K. C. Moss, J. G. Valentin, Can. J. Chem. **48**, 1524 (1971).
336. C. Kutal, A. W. Adamson, Inorg. Chem. **12**, 1990 (1973).
337. C. Kutal, A. W. Adamson, J. Am. Chem. Soc. **93**, 5581 (1971).
338. L. G. Vanquickenborne, A. Ceulemans, J. Am. Chem. Soc. **99**, 2208 (1977).
339. A. D. Kirk, L. A. Frederick, Inorg. Chem. **20**, 60 (1981).
340. L. G. Vanquickenborne, A Ceulemans, J. Am. Chem. Soc. **100**, 457 (1978).
341. L. G. Vanquickenborne, A. Ceulemans, Inorg. Chem. **18**, 897 (1979).

342. K. Angermann, R. Van Eldik, H. Kelm, F. Wasgestian, Inorg. Chem. **20**, 955 (1981).
343. K. Angermann, R. van Eldik, H. Kelm, F. Wasgestian, Inorg. Chim. Acta **49**, 247 (1981).
344. M. Talebinasab-Sarvari, P. C. Ford, Inorg. Chem. **19**, 2640 (1980).
345. K. F. Purcell, S. F. Clark, J. D. Petersen, Inorg. Chem. **19**, 2183 (1980).
346. L. H. Skibsted, D. Strauss, P. C. Ford, Inorg. Chem. **18**, 3171 (1979).
347. L. G. Vanquickenborne, A. Ceulemans, Inorg. Chem. **17**, 2730 (1978).
348. L. H. Skibsted, P. C. Ford, Inorg. Chem. **19**, 1828 (1980).
349. M. B. Rerek, P. S. Sheridan, Inorg. Chem. **19**, 2646 (1980).
350. J. D. Petersen, Inorg. Chem. **20**, 3123 (1981).
351. E. Zinato, R. D. Lindholm, A. W. Adamson, J. Am. Chem. Soc. **91**, 1076 (1969).
352. J. E. Martin, A. W. Adamson, Theor. Chim. Acta **20**, 119 (1971).
353. E. Zinato, P. Riccieri, A. W. Adamson, J. Am. Chem. Soc. **96**, 375 (1974).
354. S. C. Pyke, R. G. Linck, J. Am. Chem. Soc. **93**, 5281 (1971).
355. J. I. Zink, J. Am. Chem. Soc. **94**, 8039 (1972).
356. J. I. Zink, J. Am. Chem. Soc. **96**, 4464 (1974).
357. J. I. Zink, Mol. Photochem. **5**, 151 (1973).
358. M. Wrighton, H. B. Gray, G. S. Hammond, Mol. Photochem. **5**, 165 (1973).
359. C. Furlani, Theor. Chim. Acta **34**, 233 (1974).
360. M. J. Incorvia, J. I. Zink, Inorg. Chem. **13**, 2489 (1974).
361. P. Riccieri, E. Zinato, J. Am. Chem. Soc. **97**, 6071 (1975).
362. R. E. Wrigth, A. W. Adamson, Inorg. Chem. **16**, 3360 (1977).
363. C. F. C. Wong, A. D. Kirk, Inorg. Chem. **16**, 3148 (1977).
364. P. Riccieri, E. Zinato, personal communication.
365. L. G. Vanquickenborne, A. Ceulemans, Inorg. Chem. **20**, 110 (1981).
366. J. D. Petersen, F. P. Jakse, Inorg. Chem. **18**, 1818 (1979).
367. R. T. Walters, A. W. Adamson, Acta Chem. Scand., A **33**, 53 (1979).
368. C. H. Langford, B. R. Hollebone, IUPAC Coord. Chem. **20**, 57 (1980).
369. C. H. Langford, Acc. Chem. Res. **17**, 96 (1984).
370. B. R. Hollebone, C. H. Langford, N. Serpone, Coord. Chem. Rev. **39**, 181 (1981).
371. A. Devaquet, J. Am. Chem. Soc. **94**, 5626, 9102 (1971).
372. J. F. Endicott, Surv. Prog. Chem. **7**, 41 (1976).
373. A. Vogler, A. W. Adamson, J. Phys. Chem. **74**, 67 (1970).
374. A. W. Adamson, A. H. Sporer, J. Am. Chem. Soc. **80**, 3865 (1958).
375. A. W. Adamson, Discuss. Faraday Soc. **29**, 163 (1960).
376. C. M. Mitchel, G. F. A. Stone, J. Chem. Soc., Dalton Trans. 102 (1972).
377. W. H. Boon, M. D. Rausch, J. Chem. Soc., Chem. Commun. 397 (1977).
378. B. Kräutler, Helv. Chim. Acta **67**, 1053 (1984).
379. C. Gianotti, C. Fontaine, A. Chiaroni, C. Riche, J. Organomet. Chem. **113**, 57 (1976).
380. M. F. Lundmann, F. Wagestian, M. Dartiguenave, Y. Dartiguenave, Inorg. Chim. Acta **41**, 253 (1980).
381. K. J. Ivin, R. Jamieson, J. J. McGarvey, J. Am. Chem. Soc. **94**, 1763 (1972).
382. D. Kim, T. G. Spiro, J. Am. Chem. Soc. **108**, 2099 (1986).
383. E. W. Findsen, K. Alston, J. A. Shelnutt, M. R. Ondrias, J. Am. Chem. Soc. **108**, 4009 (1986).
384. M. F. Manfrin, D. Sandrini, A. Juris, M. T. Gandolfi, Inorg. Chem. **17**, 90 (1978).
385. Y. Kurauchi, K. Ogha, A. Yokoyama, S. Meriza, Bull. Chem. Soc. Jpn. **65**, 357 (1983).
386. A. L. Poznyak, V. Yu. Pavlovskii, Zh. Neorg. Khim. **26**, 539 (1981).
387. A. L. Poznyak, V. Yu. Pavlovskii, Z. Chem. **21**, 74 (1981).
388. J. M. Brown, J. A. Conneely, K. Mertis, J. Chem. Soc., Perkin Trans. 2. 905 (1974).
389. T. Shimidzu, T. Iyoda, K. Izaki, J. Phys. Chem. **89**, 642 (1985).
390. P. A. Lay, W. H. S. Sasse, Inorg. Chem. **23**, 4123 (1984).

391. S. H. Peterson, J. N. Demas, J. Am. Chem. Soc. **101**, 6571 (1979).
392. T. Akiyama, A. Sugimori, H. Hermann, Bull. Chem. Soc. Jpn. **46**, 1851, 1855 (1973).
393. J. L. Reed, H. D. Gafney, F. Basolo, J. Am. Chem. Soc. **96**, 1363 (1974).
394. J. L. Reed, F. Wang, F. Basolo, J. Am. Chem. Soc. **94**, 7173 (1972).
395. T. R. Weaver, F. Basolo, Inorg. Chem. **13**, 1535 (1974).
396. A. T. McPhail, G. R. Knox, C. G. Robertson, G. A. Sin, J. Chem. Soc., A 205 (1971).
397. M. S. Wrighton, D. S. Ginley, M. A. Schroeder, D. L. Morse, Pure Appl. Chem. **41**, 671 (1975).
398. M. S. Wrighton, Chem. Rev. **74**, 401 (1974).
399. H. Hennig, P. Thomas, R. Wagener, D. Rehorek, K. Jurdeczka, Z. Chem. **17**, 241 (1977).
400. L. Moggi, A. Juris, D. Sandrini, M. F. Manfrin, Rev. Chem. Intermediates **4**, 171 (1981).
401. J. Sýkora, Chem. Listy **76**, 1047 (1982).
402. R. G. Salomon, Tetrahedron **39**, 485 (1983).
403. G. G. Wubbels, Acc. Chem. Res. **16**, 285 (1983).
404. M. Julliard, M. Chanon, Chem. Rev. **83**, 425 (1983).
405. L. Moggi, A. Juris, D. Sandrini, M. F. Manfrin, Rev. Chem. Intermediates **5**, 107 (1984).
406. H. Hennig, D. Rehorek, R. D. Archer, Coord. Chem. Rev. **61**, 1 (1985).
407. C. Kutal, Coord. Chem. Rev. **64**, 191 (1985).
408. M. Schiavello (ed.), Photoelectrochemistry, Photocatalysis and Photoreactors, Reidel, Dordrecht, 1985.
409. E. Pelizetti, N. Serpone (eds.), Homogeneous and Heterogeneous Photocatalysis, Reidel, Dordrecht, 1986.
410. H. Kisch, H. Henning, EPA Newsletter **19**, 23 (1983).
411. M. J. Mirbach, EPA Newsletter **20**, 16 (1984).
412. M. Nakashima, S. Kida, Bull. Chem. Soc. Jpn. **55**, 806 (1984).
413. C. Kutal, P. Grutsch, Adv. Chem. Ser. **173**, 325 (1979).
414. J. Sýkora, Proc. 10th Conf. Coord. Chem., Smolenice–Bratislava, 1985, p. 387.
415. J. Sýkora, M. Pado, M. Jakubčová, J. Duník, Proc. 5th Symp. Photochem. Therm. React. Coord. Compounds, Veszprém, Hungary, 1985, p. 12.
416. J. Sýkora, J. Inf. Rec. Mater. **17**, 415 (1989).
417. J. Sýkora, E. Horváth, F. Diomedi-Camassei, I. Giannini, J. Gažo, Proc. XIXth ICCC, Prague, Czechoslovakia, 1978, p. 119a.
418. P. Bergamini, A. Maldotti, O. Sostero, O. Traverso, J. Sýkora, Inorg. Chim. Acta **85**, L15 (1984).
419. J. Sýkora, S. Sostero, O. Traverso, A. Maldotti, Abstracts of Papers XXIInd ICCC, Budapest, 1982, p. 329.
420. E. Horváth, J. Sýkora, J. Gažo, Z. Anorg. Allg. Chem. **442**, 235 (1978).
421. J. Sýkora, M. Jakubčová, Z. Cvengrošová, Coll. Czech. Chem. Commun. **47**, 2061 (1982).
422. J. Sýkora, M. Kureková, Chimika Chronika (New Series), Book of Abstracts, XXIVth ICCC, Athens, Greece, B4, 599 (1986).
423. P. Engelbrecht, Ph. Thomas, H. Hennig, J. Sýkora, Z. Chem. **26**, 137 (1986).
424. J. Sýkora in Photochemistry and Photophysics of Coordination Compounds, H. Yersin, A. Vogler (eds.), Springer-Verlag, Berlin, Heidelberg, 1987, p. 193.
425. B. V. Koryakin, T. S. Tshabiev, A. E. Shilov, Dokl. Akad. Nauk SSSR **229**, 128 (1976).
426. H. Arakawa, Y. Sugi, Chem. Lett. 1323 (1981).
427. K. Hatano, K. Usui, Y. Ishida, Bull. Chem. Soc. Jpn. **54**, 413 (1981).
428. H. Hennig, P. Scheibler, R. Wagener, D. Rehorek, Inorg. Chim. Acta **44**, 1231 (1980).
429. S. Luňák, P. Lederer, J. Vepřek-Šiška, Chem. List **81**, 1130 (1987).
430. A. P. Grutsch, C. Kutal, J. Am. Chem. Soc. **99**, 6460 (1977).
431. V. Balzani, F. Bolletta, M. Ciano, M. Maestri, J. Chem. Educ. **60**, 447 (1983).

432. V. Balzani, F. Bolletta, Comments Inorg. Chem. **2**, 211 (1983).
433. M. Grätzel (ed.), Energy Resources by Photochemistry and Catalysis, Academic Press, New York, 1983.
434. M. Anpo, T. Suzuki, Y. Kubokawa, F. Tanaka, S. Yamashita, J. Phys. Chem. **88**, 5778 (1984).
435. World Energy Resources 1985–2020 (Guildford, Surrey), IPC Science and Technology Press, (1977)
436. R. R. Hautala, R. Bruce King, Ch. Kutal (eds.), Solar Energy: Chemical Conversion and Storage, Humana Press, Clifton, NJ, 1979.
437. J. S. Connoly (ed.), Photochemical Conversion and Storage of Solar Energy, Academic Press, New York, 1981.
438. J. Rabani (ed.), Photochemical Conversion and Storage of Solar Energy, Weismann Press, Israel, 1982.
439. High-Level Expert Group Meeting Preparatory to the Fourth General Conference of UNIDO; International Forum on Technological Advances and Development, Tbilisi, USSR, 12–16 April 1983.
440. High-Level Expert Group Meeting Preparatory to the Fourth General Conference of UNIDO on Energy and Industrialization, Oslo, Norway, 29 Aug.–2 Sept. 1983.
441. G. Porter, M. D. Archer, Interdiscip. Sci. Rev. **1**, 119 (1976).
442. G. Tollin, J. Phys. Chem. **80**, 2274 (1976).
443. M. Almgren, Photochem. Photobiol. **27**, 603 (1978).
444. G. Porter, Proc. R. Soc. London, A. **362**, 281 (1978).
445. M. Calvin, Acc. Chem. Res. **11**, 369 (1978).
446. K. I. Zamaraev, V. N. Parmon, Russ. Chem. Rev. **49**, 695 (1980).
447. D. G. Whitten, Acc. Chem. Res. **13**, 83 (1980).
448. J. H. Fendler, J. Phys. Chem. **84**, 1485 (1980).
449. M. Grätzel, Acc. Chem. Res. **14**, 376 (1981).
450. J. Kiwi, K. Kalyanasundaram, M. Grätzel, Structure Bonding (Berlin) **49**, 37 (1982).
451. H. Gerischer, J. J. Katz, Light-Induced Charge Separation in Biology and Chemistry, Verlag Chemie, Weinheim, 1979.
452. M. Kirch, J. M. Lehn, J. P. Sauvage, Helv. Chim. Acta **62**, 1345 (1979).
453. K. Kalyanasundaram, Coord. Chem. Rev. **46**, 159 (1982).
454. Energy Supplies for Developing Countries — UNO — United Nations Conference on Trade and Development, Geneve, New York, 1980.
455. Energy Transition in the ECE Region, United Nations, New York, 1983.
456. D. J. Brinkvort, Solar Energy for Man, Mir, Moscow, 1976 (in Russian).
457. J. Kleczek, Solar Energy — an Introduction to Heliotechnics, Práce, Praha, 1981 (in Czech).
458. V. Silvestrini (ed.), Solar Energy Conversion by Photochemical and Photoelectrochemical Processes, Sogesta, Permanent School on Solar Energy Processes, 25 Sept. - 3 Dec. 1979.
459. D. O. Hall, W. Palz (eds.), Photochemical, Photoelectrochemical and Photobiological Processes, Series D, Vol. 1, Reidel, Dordrecht, 1981.
460. D. O. Hall, W. Palz, D. Pirrwitz (eds.), Photochemical, Photoelectrochemical and Photobiological Processes, Series D, Vol. 2, Reidel, Dordrecht, Boston, Lancaster, 1983.
461. C. Kutal, J. Chem. Educ. **60**, 880 (1982).
462. J. R. Bolton, Science **202**, 705 (1978).
463. N. Borsub, Shi-Ching Chang, C. Kutal, Inorg. Chem. **21**, 538 (1982).
464. S. W. Orchard, C. Kutal, Inorg. Chim. Acta **64**, L95, (1982).
465. C. Kutal, D. P. Schwendiman, P. Grutsch, Sol. Energy **19**, 651 (1977).
466. P. D. Grutsch, C. Kutal, J. Am. Chem. Soc. **108**, 3108 (1986).
467. N. Borsub, C. Kutal, J. Am. Chem. Soc. **106**, 4826 (1984).
468. K. Yasufuku, K. Takahashi, C. Kutal, Tetrahedron Lett. **25**, 4893 (1984).
469. R. R. Hautala, R. B. King, C. Kutal, in Ref. [436], p. 333.

470. Sakaki, I. Ikitaka, K. Ohkubo, Inorg. Chem. **23**, 198 (1984).
471. M. S. Wrighton, D. L. Morse, L. Pdungsap, J. Am. Chem. Soc. **97**, 2073 (1975).
472. D. P. Fisher, V. Piermattie, J. C. Dabrowiak, J. Am. Chem. Soc. **99**, 2811 (1977).
473. C. Kutal, Sci. Pap. Inst. Phys. Chem. Res. (Jpn.) **78**, 186 (1984).
474. H. Ikezawa, C. Kutal, K. Yasufuku, H. Yamazaki, J. Am. Chem. Soc. **108**, 1586 (1986).
475. A. J. Bard, Science **207**, 139 (1980).
476. A. W. Maverick, B. H. Gray, Pure Appl. Chem. **52**, 2339 (1980).
477. D. G. Whitten, J. C. Russel, R. H. Schmell, Tetrahedron **38**, 2455 (1982).
478. N. Sutin, C. Creutz, Pure Appl. Chem. **52**, 2727 (1980).
479. J. H. Fendler, J. Chem. Educ. **60**, 872 (1983).
480. J. H. Fendler, J. Phys. Chem. **89**, 2730 (1985).
481. E. Adar, Y. Degani, Z. Goren, I. Willner, J. Am. Chem. Soc. **108**, 4696 (1986).
482. N. J. Turro, M. Grätzel, A. M. Braun, Agnew. Chem., Int. Ed. **19**, 675 (1980).
483. P. A. Brugger, P. P. Infelta, A. M. Braun, M. Grätzel, J. Am. Chem. Soc. **103**, 320 (1981).
484. C. A. Evans, J. R. Bolton, Photochem. Photobiol. **30**, 697 (1979).
485. T. Matsuo, K. Takuma, Y. Tsusui, T. Nishigima, Coord. Chem. Rev. **10**, 195 (1980).
486. Y. Moroi, P. P. Infelta, M. Grätzel, J. Am. Chem. Soc. **101**, 573 (1979).
487. Y. Moroi, M. A. Braun, M. Grätzel, J. Am. Chem. Soc. **101**, 567 (1979).
488. I. Willner, J. W. Otvos, M. Calvin, J. Am. Chem. Soc. **103**, 3203 (1981).
489. I. Willner, J. M. Yang, J. W. Otvos, M. Calvin, J. Phys. Chem. **85**, 3277 (1981).
490. Y. Degani, I. Willner, J. Am. Chem. Soc. **105**, 6228 (1983).
491. I. Willner, C. Laane, J. W. Otvos, M. Calvin, ACS Symposium Series **177**, 71 (1982).
492. D. Mandler, Y. Degani, I. Willner, J. Phys. Chem. **88**, 4366 (1983).
493. C. A. Jones, L. E. Weaner, R. A. Mackay, J. Phys. Chem. **84**, 1495 (1980).
494. Y. Sudo, F. Toda, Nature (London) **279**, 808 (1979).
495. T. Matsuo, K. Itoh, K. Takuma, K. Hashimoto, T. Nagamura, Chem. Lett. 1009 (1980).
496. P. P. Infelta, M. Grätzel, J. H. Fendler, J. Am. Chem. Soc. **102**, 1497 (1980).
497. V. Balzani, A. Juris, F. Scandola, in Ref. [409], p. 1.
498. M. Maestri, M. Grätzel, Ber. Bunsenges. Phys. Chem. **81**, 504 (1977).
499. J. H. Fendler, P. Tundo, Acc. Chem. Res. **17**, 3 (1984).
500. K. I. Zamaraev, V. N. Parmon, Catal. Rev. Sci. Eng. **22**, 283 (1980).
501. V. N. Parmon, S. V. Lymar, K. I. Zamaraev, Proc. Indian Natl. Sci. Acad. **52A**, 848 (1986).
502. T. Matsuo, J. Photochem. **29**, 41 (1985).
503. J. M. Lehn, J. P. Sauvage, Nouv. J. Chim. **1**, 446 (1977).
504. C. V. Krishan, B. S. Brunschwig, C. Creutz, N. Sutin, J. Am. Chem. Soc. **107**, 2005 (1985).
505. J. R. Darwent, in Photogeneration of Hydrogen, A. Harriman, M. A. West (eds.), Academic Press, London, 1982, p. 23.
506. J. MacB. Harrowfield, A. J. Hertl, P. A. Lay, A. M. Sargeson, A. M. Bond, W. A. Mulac, J. C. Sullivan, J. Am. Chem. Soc. **105**, 5503 (1983).
507. C. O. Dietrich-Buchecker, J. P. Sauvage, J. Am. Chem. Soc. **106**, 3043 (1984).
508. J. C. Rodriquez-Ubis, B. Alpha, D. Plancherel, J. M. Lehn, Helv. Chim. Acta **67**, 2264 (1984).
509. J. M. Lehn, Science **227**, 849 (1985).
510. J. M. Lehn, in Frontiers of Chemistry (IUPAC), J. K. Laidler (ed.), Pergamon, Oxford, 1982, p. 265.
511. H. M. Colquhoun, S. M. Doughty, J. F. Stoddart, D. J. Williams, Angew. Chem., Int. Ed. **23**, 235 (1984).
512. H. M. Colquhoun, S. M. Doughty, J. M. Maud, J. F. Stoddart, D. J. Williams, J. B. Wolstenholme, Isr. J. Chem. **25**, 15 (1985).
513. F. Vögtle (ed.), Top. Curr. Chem. **98** (1981); **101** (1982).
514. D. J. Cram, S. Karbach, Y. H. Kim, L. Baczynskyj, G. W. J. Kalleymeyn, J. Am. Chem. Soc. **107**, 2575 (1985).

515. I. M. Tsvetkov, O. V. Gerasimov, S. V. Lymar, V. N. Parmon, in Ref. [501], p. 851.
516. M. Kaneko, N. Takabayashi, Y. Yamauchi, A. Yamada, Bull. Chem. Soc. Jpn. **57**, 156 (1984).
517. T. Ohsako, T. Sakamoto, T. Matsuo, Chem. Lett. 1675 (1983).
518. H. Nijs, J. J. Fripiat, H. van Damme, J. Phys. Chem. **87**, 255 (1983).
519. F. Bergaya D. Challal, J. J. Fripiat, H. van Damme, J. Photochem. **28**, 255 (1985).
520. O. Johansen, A. W. H. Mau, W. H. F. Sasse, Chem. Phys. Lett. **94**, 107, 113 (1983).
521. A. Edel, P. A. Marnot, J. P. Sauvage, Nouv. J. Chim. **8**, 495 (1984).
522. J. M. Lehn, J. P. Sauvage, R. Ziessel, Nouv. J. Chim. **5**, 291 (1981).
523. J. Koryta, Chem. Listy **75**, 785 (1981).
524. M. S. Wrighton, J. Chem. Educ. **60**, 877 (1983).
525. K. Chandrasekaran, D. G. Whitten, J. Am. Chem. Soc. **102**, 5119 (1980).
526. D. P. Rillema, W. J. Dressick, T. J. Meyer, J. Chem. Soc., Chem. Commun. 247 (1980).
527. B. F. Hoffman, P. D. Sima, J. Am. Chem. Soc. **105**, 1776 (1983).
528. A. J. Bard, A. B. Bocarsly, Fu-Ren F. Fan, E. G. Walton, M. S. Wrighton, J. Am. Chem. Soc. **102**, 3671 (1980).
529. C. M. Gronet, N. J. Lewis, Nature **300**, 733 (1982).
530. M. S. Wrighton, Acc. Chem. Res. **12**, 303 (1979).
531. A. Heller, Acc. Chem. Res. **14**, 154 [1981).
532. A. J. Nozik, Annu. Rev. Phys. Chem. **29**, 189 (1978).
533. W. J. Albery, Acc. Chem. Res. **15**, 142 (1982).
534. M. S. Wrighton, Chem. Eng. News **57**, 29 (1979).
535. K. I. Zamaraev (ed.), Photocatalytic Conversion of Solar Energy, Nauka, Novosibirsk, 1985 (in Russian).
536. J. M. Lehn, R. Ziessel, Proc. Natl. Acad. Sci. U.S.A. **79**, 701 (1982).
537. J. Hawecker, J. M. Lehn, R. Ziessel, J. Chem. Soc., Chem. Commun. 56 (1985).
538. M. Halmann, Nature (London) **275**, 115 (1978).
539. L. Willner, D. Mandler, A. Riklin, J. Chem. Soc., Chem. Commun. 1022 (1986).
540. R. Maidan, I. Willner, J. Am. Chem. Soc. **108**, 8100 (1986).
541. C. Kutal, M. A. Weber, G. Ferraudi, D. Geiger, Organometallics **4**, 2161 (1985).
542. M. Halmann, V. Katzir, E. Borgarello, J. Kiwi, Sol. Energy Mater. **10**, 85 (1984).
543. K. I. Zamaraev, V. N. Parmon, Usp. Khim. **49**, 1457 (1980); **52**, 1433 (1983).
544. U. A. Buslaev, A. T. Falkengof, V. S. Pervov, Koord. Khim. **8**, 867 (1982).
545. R. J. Crutchley, A. B. P. Lever, Inorg. Chem. **21**, 2276 (1982).
546. R. J. Crutchley, N. Kress, A. B. P. Lever, J. Am. Chem. Soc. **105**, 1170 (1983).
547. N. Kitamura,Y. Kawanishi, S. Tazuke, Chem. Phys. Lett. **97**, 103 (1983).
548. D. E. Morris, Y. Ohsawa, D. P. Segers, M. K. DeArmond, K. W. Hanck, Inorg. Chem. **23**, 3080 (1984).
549. V. Balzani, A. Juris, F. Barigelletti, P. Belser, A. von Zelewsky, Riken Q. **78**, 78 (1984).
550. W. M. Wacholtz, R. A. Auerbach, R. H. Schmehl, M. Ollino, W. R. Cherry, Inorg. Chem. **24**, 1758 (1985).
551. N. Serpone, G. Ponterini, M. A. Jamieson, F. Bolletta, M. Maestri, Coord. Chem. Rev. **50**, 209 (1983).
552. M. Nishizawa, T. M. Suzuki, S. Sprouse, R. J. Watts, P. C. Ford, Inorg. Chem. **23**, 1837 (1984).
553. A. Juris, P. Belser, F. Barigelletti, A. von Zelewsky, V. Balzani, Inorg. Chem. **25**, 256 (1986).
554. A. Harriman, G. Porter, M. C. Richoux, J. Chem. Soc., Faraday Trans. 2 **77**, 833 (1981).
555. H. B. Gray, A. W. Maverick, Science **214**, 1201 (1981).
556. V. Balzani, L. Moggi, Coord. Chem. Rev. **97**, 313 (1990).
557. E. A. Koerner von Gustorf, L. M. G. Leenders, I. Fischler, R. N. Perutz, Adv. Inorg. Chem. Radiochem. **19**, 65 (1978).
558. K. Sauer, Acc. Chem. Res. **13**, 248 (1980).

559. T. Kuwana, Anal. Chem. **35**, 1398 (1963).
560. J. M. Fitzgerald (ed.), Analytical Photochemistry and Photochemical Analysis, M. Dekker, New York, 1971.
561. M. C. Bradley (ed.), Chemical and Biochemical Applications of Lasers, Academic Press, New York, 1977.
562. J. H. Coleman, T. J. Marks, FR. DEMANDE 2, 408, 382 (Cl.BO1D59/34), Apparatus and Methods for Separation of U Isotopes.
563. H. S. Laver, in Developments in Polymer Stabilization 1, G. Scott (ed.), Applied Science, Barking, 1980, p. 163.
564. O. L. Chapman, Organic Photochemistry, M. Dekker, New York, 1967.
565. W. A. Noyes, G. S. Hammond, J. N. Pitts, Jr. (eds.), Advances in Photochemistry, John Wiley and Sons, New York (1967–present).
566. J. G. Calvert, J. N. Pitts, Jr., Photochemistry, John Wiley and Sons, New York, 1966.
567. J. Sýkora, J. Šima, O. Traverso, Proc. 9th Conf. Coordination Chemistry, Bratislava–Smolenice, 1983, p. 393.
568. J. C. Goan, C. H. Heuther, H. L. Podall, Inorg. Chem. **2**, 1078 (1963).
569. S. S. Minor, G. Witte, G. W. Everett, Inorg. Chem. **15**, 2052 (1976).
570. S. J. Lippard, B. J. Russ, Inorg. Chem. **6**, 1943 (1967).
571. R. L. Marks, S. E. Popielska, Inorg. Nucl. Chem. Lett. **10**, 885 (1974).
572. A. E. Nya, H. Mohan, Polyhedron **1**, 834 (1982).
573. R. P. Mitra, B. K. Sharma, H. Mohan, Can. J. Chem. **47**, 2317 (1969).
574. R. P. Mitra, H. Mohan, J. Inorg. Nucl. Chem. **36**, 3739 (1974).
575. W. Jakób, Z. Jakób, Rocz. Chem. **36**, 601 (1962).
576. W. Jakób, A. Samotus, Z. Stasicka, Rocz. Chem. **36**, 611 (1962).
577. W. Jakób, Z. Jakób, Rocz. Chem. **36**, 593 (1962).
578. S. I. Ali, Z. Murtaza, Polyhedron **4**, 821 (1985).
579. A. P. Pivovarov, Yu. V. Gak, T. N. Doronina, V. D. Makhaev, A. P. Borisov, Yu. G. Borodko, Izv. Akad. Nauk SSSR, Ser. Khim. 1207 (1981).
580. A. P. Pivovarov, Yu. V. Gak, Yu. M. Shulga, V. D. Makhaev, A. P. Borisov, Yu. G. Borodko, Izv. Akad. Nauk SSSR, Ser. Khim. 918 (1981).
581. R. Pierantozzi, G. L. Geoffroy, Inorg. Chem. **19**, 1821 (1980).
582. G. E. Bossard, D. C. Busby, M. Chang, A. George, S. D. A. Iske, J. Am. Chem. Soc. **102**, 1001 (1980).
583. A. A. Diamantis, J. Chatt, G. J. Leigh, G. A. Heath, J. Organomet. Chem. **84**, C11 (1975).
584. J. Chatt, A. A. Diamantis, G. A. Heath, N. E. Hooper, G. J. Leigh, J. Chem. Soc., Dalton Trans. 688 (1977).
585. P. C. Bevan, J. Chatt, R. A. Head, P. B. Hitchcock, G. J. Leigh, J. Chem. Soc., Chem. Commun. 509 (1976).
586. R. Ben-Shoshan, J. Chatt, W. Hussain, G. J. Leigh, J. Organomet. Chem. **112**, C9 (1976).
587. V. W. Day, T. A. George, S. D. A. Iske, J. Am. Chem. Soc. **97**, 4127 (1975).
588. A. M. Soares, W. P. Griffith, J. Chem. Soc., Dalton Trans. 1886 (1981).
589. M. A. Green, J. C. Huffman, K. G. Caulton, J. Am. Chem. Soc. **103**, 695 (1981).
590. D. A. Roberts, G. L. Geoffroy, J. Organomet. Chem. **214**, 221 (1981).
591. M. G. Bradley, D. A. Roberts, G. L. Geoffroy, J. Am. Chem. Soc. **103**, 379 (1981).
592. G. L. Miessler, G. Stuk, T. P. Smith, K. W. Given, M. C. Palazzotto, L. H. Pignolet, Inorg. Chem. **15**, 1982 (1976).
593. C. Parkanyi, J. H. Richards, J. Coord. Chem. **4**, 41 (1974).
594. R. N. Puri, R. O. Asplund, J. Coord. Chem. **11**, 73 (1981).
595. V. E. Stelmashok, S. A. Metskovskii, A. L. Poznyak, Zh. Neorg. Khim. **30**, 391 (1985).
596. I. Grenthe, E. Nordin, Inorg. Chem. **18**, 1869 (1979).
597. C. H. Langford, R. L. P. Sasselville, Can. J. Chem. **59**, 647 (1981).

598. S. Bagger, Acta Chem. Scand., A **34**, 63 (1980).
599. T. G. Hoon, C. Y. Mok, Inorg. Chim. Acta **62**, 231 (1982).
600. T. S. Roche, J. F. Endicott, J. Am. Chem. Soc. **94**, 8622 (1972).
601. H. Sugimoto, H. Hataoko, M. Mori, J. Chem. Soc., Chem. Commun. 1301 (1982).
602. V. E. Stelmashok, A. L. Poznyak, Koord. Khim. **6**, 144 (1980).
603. G. Ferraudi, S. Muralidharan, Inorg. Chem. **20**, 4262 (1981).
604. P. E. Hoggard, G. B. Porter, J. Am. Chem. Soc. **100**, 1457 (1978).
605. W. M. Wallace, P.E. Hoggard, Inorg. Chem. **19**, 2141 (1980).
606. W. M. Wallace, P. E. Hoggard, Inorg. Chem. **18**, 2934 (1979).
607. R. W. Callahan, T. J. Meyer, Inorg. Chem. **16**, 574 (1977).
608. B. Durham, L. J. Walsh, Ch. L. Carter, T. J. Meyer, Inorg. Chem. **19**, 860 (1980).
609. C. A. Bignozzi, C. Chiorboli, M. T. Indelli, M. A. Rampi Scandola, G. Varani, F. Scandola, J. Am. Chem. Soc. **108**, 7872 (1986).
610. P. G. Douglas, R. D. Feltman, H. G. Metzger, J. Am. Chem. Soc. **93**, 84 (1971).
611. K. W. Given, B. M. Mattson, M. F. Guiggan, G. L. Meissler, L. H. Pignolett, J. Am. Chem. Soc. **99**, 4855 (1977).
612. R. D. Gillard, J. D. Jesus de Pedrosa, L. R. M. Tipping, J. Chem. Soc., Chem. Commun. 58 (1977).
613. R. D. Gillard, J. D. Jesus de Pedrosa, J. Chem. Soc., Dalton Trans. 1895 (1984).
614. J. L. Reed, H. D. Gafney, F. Basolo, J. Am. Chem. Soc. **96**, 1363 (1974).
615. G. B. Kauffman, J. H. S. Tsai, M. H. Gubelmann, A. F. Williams, J. Chem. Soc., Dalton Trans. 1791 (1980).
616. G. L. Geoffroy, R. Pierantozzi, J. Am. Chem. Soc. **98**, 8054 (1976).
617. M. Cusumano, G. Guglielmo, V. Ricevuto, O. Traverso, T. J. Kemp, J. Chem. Soc., Chem. Commun. 775 (1979).
618. M. Cusumano, G. Guglielmo, V. Ricevuto, S. Sostero, O. Traverso, T. J. Kemp, J. Chem. Soc., Dalton Trans. 302 (1981).
619. N. W. Alcock, T. J. Kemp, F. L. Wimmer, J. Chem. Soc., Dalton Trans. 635 (1981).
620. N. W. Alcock, T. J. Kemp, E. L. Wimmer, O. Traverso, Inorg. Chim. Acta **44**, L245 (1980).
621. M. A. Khan, A. J. McAlees, Inorg. Chim. Acta **104**, 109 (1985).
622. D. M. Blake, R. Mersecchi, J. Chem. Soc., Chem. Commun. 1045 (1971).
623. D. M. Blake, C. J. Nyman, J. Am. Chem. Soc. **92**, 5359 (1970).
624. C. Bartocci, C. A. Bignozzi, A. Maldotti, F. Fagioli, Inorg. Chim. Acta **53**, L157 (1981).
625. C. A. Bignozzi, C. Bartocci, A. Maldotti, V. Carassiti, Inorg. Chim. Acta **62**, 187 (1982).
626. A. V. Babaeva, M. A. Mosyagina, Izv. Akad. Nauk SSSR **227** (1953).
627. H. C. Foley, R. H. Morris, T. S. Targos, G. L. Geoffroy, J. Am. Chem. Soc. **103**, 7337 (1981).
628. R. S. Hill, P. de Mayo, R. J. Puddephatt, Inorg. Chem. **21**, 3642 (1982).
629. I. Lifschitz, W. Froentjes, Z. Anorg. Chem. **224**, 173 (1935).
630. I. Lifschitz, W. Froentjes, Z. Anorg. Chem. **233**, 1 (1937).
631. O. Traverso, V. Carassiti, R. Portanova, P. A. Vigato, Inorg. Chim. Acta **9**, 227 (1974).
632. O. Traverso, R. Portanova, V. Carassiti, Inorg. Nucl. Chem. Lett. **10**, 771 (1974).
633. S. Sostero, O. Traverso, C. Bartocci, P. di Bernardo, L. Magon, V. Carassiti, Inorg. Chim. Acta **19**, 229 (1976).
634. G. Sbrignadello, G. Battiston, G.Tomat, O. Traverso, Inorg. Chim. Acta **24**, L43 (1977).
635. G. Sbrignadello, G. Tomat, G. Battiston, P. A. Vigato, O. Traverso, J. Inorg. Nucl. Chem. **40**, 1647 (1978).
636. G. M. Kramer, M. B. Dines, A. Kaldor, R. Hall, D. McClure, Inorg. Chem. **20**, 1412 (1981).
637. G. Buono-Core, K. Iwai, Y. L. Chow, T. Koyonagi, A. Kaji, J. I. Hayami, Can. J. Chem. **57**, 8 (1979).
638. J. Bartoň, E. Borsig, Complexes in Free-Radical Polymerization, Elsevier, Amsterdam – Veda, Bratislava, 1988.

639. C. H. Bamford, A. N. Ferrar, J. Chem. Soc., Faraday Trans. 1 **68**, 1243 (1972).
640. P. Natarajan, K. Chandrasekaran, M. Santappa, J. Polym. Sci., Polym. Lett. Ed. **144**, 455 (1976).
641. S. M. Aliwi, C. H. Bamford, J. Chem. Soc., Faraday Trans. 1 **71**, 1733 (1975).
642. N. Sakata, K. Takahashi, K. Nishihara, Makromol. Chem. **161**, 173 (1972).
643. F. Takemura, E. Morita, J. Asakura, JCS Japan Chem. Indust. Chem. 376 (1973).
644. T. Okimoto, M. Takahashi, Y. Inaki, K. Takemoto, Angew. Makromol. Chem. **38**, 81 (1974).
645. T. Okimoto, Y. Inaki, K. Takemoto, J. Macromol. Sci., Chem. **7**, 1537 (1973).
646. J. Bartoň, I. Leboc, I. Capek, J. Tkáč, Makromol. Chem., Rapid Commun. **1**, 7 (1980).
647. G. Scott (ed.), Developments in Polymer Stabilization, Part 1, Applied Sci. Publ., London, 1979.
648. Yu. L. Goldfarb, E. G. Ostapenko, V. B. Ivanov, A. F. Efremkin, V. L. Litvinov, Khim. Geterotsikl. Soedin. 1481 (1982).
649. H. O. Wirth, H. Andreas, Pure Appl. Chem. **49**, 627 (1977).
650. G. N. Prnezentseva, G. B. Zvegintseva, M. N. Volkotrub, Izv. Vyssh. Ucheb. Zaved., Khim. Tekhnol. **27**, 954 (1984).
651. N. S. Allen, Chem. Soc. Rev. **15**, 37 (1986).
652. R. P. Ranaweera, G. Scott, Eur. Polym. J. **12**, 591 (1976).
653. N. S. Allen, A. J. Chirinis-Padron, J. H. Appleyard, Eur. Polym. J. **21**, 101 (1985).
654. S. Al. Malaika, P. Desai, G. Scott, Plastics and Rubber Processing and Applications **5**, 15 (1985).
655. F. Gugumus, in Ref. [647], p. 261.
656. R. Chandra, P. S. Handa, Polym. Photochem. **3**, 391 (1983).
657. J. Avery, Int. J. Quantum Chem. **26**, 917 (1984).
658. N. S. Allen (ed.), Developments in Polymer Photochemistry, Vol. 1, Elsevier, Amsterdam, 1980, 222 pp.
659. N. S. Allen (ed.), Developments in Polymer Photochemistry, Vol. 2, Elsevier, Amsterdam, 1981, 278 pp.
660. N. S. Allen (ed.), Developments in Polymer Photochemistry, Vol. 3, Elsevier, Amsterdam, 1982, 350 pp.
661. G. Scott (ed.), Developments in Polymer Stabilisation, Vol. 6, Elsevier, Amsterdam, 1983, 340 pp.
662. G. Scott (ed.), Developments in Polymer Stabilisation, Vol. 7, Elsevier, Amsterdam, 1984, 308 pp.
663. G. Scott (ed.), Developments in Polymer Stabilisation, Vol. 5, Elsevier, Amsterdam, 1982, 237 pp.
664. N. Grassie (ed.), Developments in Polymer Degradation, Vol. 5, Elsevier, Amsterdam, 1984, 232 pp.
665. N. Grassie (ed.), Developments in Polymer Degradation, Vol. 6, Elsevier, Amsterdam, 1985, 264 pp.
666. N. Grassie (ed.), Developments in Polymer Degradation, Vol. 7, Elsevier, Amsterdam, 1987, 280 pp.
667. N. S. Allen, J. F. Rabek (eds.), New Trends in the Photochemistry of Polymers, Elsevier, Amsterdam, 1985, 314 pp.
668. A. Padua, Organic Photochemistry 5, M. Dekker, New York, 1981.
669. R. Roberts, R. P. Ouellette, M. M. Muradaz, R. F. Cozzens, P. N. Cheremisinoff, Applications of Photochemistry, Technomic, 1984.
670. Suwa Seikosha Co., Ltd, Jpn. Kokai Tokkyo Koho JP 60,107,030 (cit. from CA **103**, 224453 (1985)).
671. Suwa Seikosha Co., Ltd, Jpn. Kokai Tokkyo Koho JP 60,107,031 (cit. from CA **103**, 224454 (1985)).

672. D. M. Allen, J. Photogr. Sci. **24**, 61 (1976).
673. J. Malinowski, Photogr. Sci. Engng. **15**, 175 (1971).
674. J. F. Tanguay, S. L. Suib, Catal. Rev., Sci. Eng. **29**, 1 (1987).
675. F. S. Richardson, J. P. Riehl, Chem. Rev. **77**, 773 (1977).
676. B. Kazan, Displays 85, April 1985.
677. D. P. Hamblen, J. R. Clarke, IEEE Trans. Elect. Dev. **ED-20**, 1028 (1973).
678. A. T. Brault, G. R. Wilkes, T. O. Maier, Research Disclosure **145**, 38 (1976).
679. A. Adin, J. W. Boettcher, J. C. Fleming, U.S. 4,294,912 (13. 10. 1981).
680. H. Hennig, M. Benedix, R. Benedix, P. Thomas, Z. Anorg. Chem. **514**, 231 (1984).
681. H. Hennig, E. Hoyer, E. Lippmann, E. Nagorsnik, P. Thomas, M. Weissenfels, J. Signalaufzeichnungsm. **6**, 39 (1978).
682. M. Weissenfels, E. Lippman, J. Punkt, Z. Chem. **20**, 39 (1980).
683. F. R. Hartley, P. N. Vezey, Adv. Organomet. Chem. **15**, 189 (1977).
684. E. Klein, R. J. Kazlauskas, M. S. Wrighton, Organometallics **1**, 1338 (1982).
685. D. K. Liu, M. S. Wrighton, D. R. McKay, G. E. Maciel, Inorg. Chem. **23**, 212 (1984).
686. Yu. I. Ermakov, B. N. Kuznetsov, V. A. Zakharov, Catalysis by Supported Complexes, Elsevier, Amsterdam, 1981.
687. F. R. Hartley, Supported Metal Complexes, A New Generation of Catalysts, D. Reidel, Hingham, MA, 1985.
688. Y. Iwasawa, Tailored Metal Catalysts, D. Reidel, Hingham, MA, 1986.
689. A. L. Prignano, W. C. Trogler, J. Am. Chem. Soc. **109**, 3585 (1987).
690. A. Peter, L. J. Csányi, Acta Phys. Chem. (Szeged) **21**, 37 (1975).
691. A. Nemodruk, E. U. Bezrogova, Photochemical Reactions in Analytical Chemistry, Khimiya, Moscow, 1972 (in Russian).
692. C. E. Bricker, S. S. Schonberg, Anal. Chem. **30**, 922 (1958).
693. T. Kuwana, Electroanal. Chem. **1**, 197 (1967).
694. J. M. Fitzerald, D. E. Warren, Anal. Lett. **3**, 623 (1970).
695. J. L. Beck, J. M. Fizgerald, J. A. Bishop, Anal. Chim. Acta **51**, 935 (1970).
696. A. Péter, L. J. Csányi, Acta Chim. Acad. Sci. Hung. **100**, 163 (1979).
697. G. Almássy, E. Kovács, Magy. Kem. Foly. **60**, 182 (1954).
698. I. P. Harlamov, E. I. Dodyin, A. D. Mantsevich, Zh. Anal. Khim. **22**, 371 (1967).
699. G. Almássy, I. Dezső, Magy. Kem. Foly. **61**, 300 (1985).
700. J. M. Fitzgerald, J. L. Beck, Anal. Lett. **3**, 531 (1970).
701. N. Mataga, J. Mol. Struct. (Theochem) **135**, 279 (1986).
702. N. Mataga, in Biomolecules, C. Nagata (ed.), Japan Scientific Societies Press, Tokyo–Elsevier, Amsterdam, 1985, p. 127.
703. Y. Hirata, Y. Kanda, N. Mataga, J. Phys. Chem. **87**, 1659 (1983).
704. N. Mataga, Pure Appl. Chem. **56**, 1255 (1984).
705. V. Balzani, L. Moggi, F. Scandola, in Ref. [13], p. 1.
706. H. Kuhn, in Ref. [710], p. 411.
707. J. M. Lehn, Agnew. Chem., Int. Ed. **27**, 89 (1988).
708. M. S. Wrighton, Comments Inorg. Chem. **4**, 269 (1985).
709. S. Licht, V. Cammarata, M. S. Wrighton, Science **243**, 1176 (1989).
710. F. L. Carter (ed.), Molecular Electronic Devices II, M. Dekker, New York, 1987.